DPTO. QUÍMICA ORGÁNICA
FACULTAD DE QUÍMICA
UNIVERSIDAD DE SEVILLA

INSTITUTO DE
INVESTIGACIONES QUÍMICAS
CONSEJO SUPERIOR DE
INVESTIGACIONES CIENTÍFICAS

DYKAT and desymmetrization strategies for the synthesis of axially chiral heterobiaryls

Memoria presentada por el Licenciado
Antonio Romero Arenas
para optar al grado de Doctor en Química.

Sevilla, octubre 2019

DEPARTAMENTO DE QUÍMICA ORGÁNICA
FACULTAD DE QUÍMICA - UNIVERSIDAD DE SEVILLA

INSTITUTO DE INVESTIGACIONES QUÍMICAS.
CONSEJO SUPERIOR DE INVESTIGACIONES CIENTÍFICAS

VºBº El Director de la Tesis

Fdo. Dr. José María Lassaletta Simón
Profesor de Investigación del CSIC
Instituto de Investigaciones Químicas

VºBº La Directora de la Tesis

Fdo. Dra. Rosario Fernández Fernández,
Catedrática de Universidad
Departamento de Química Orgánica
Universidad de Sevilla

VºBº El director de la Tesis

Fdo. Abel Ros Laó
Contratado Ramón y Cajal
Departamento de Química Orgánica
Universidad de Sevilla

El presente trabajo ha sido realizado por el Licenciado Antonio Romero Arenas con un contrato predoctoral (BES-2014-070676) financiado por el proyecto del Ministerio de Economía y Competitividad “Sistemas Catalíticos y reactivos de nueva generación para aplicaciones en síntesis asimétrica” con referencia CTQ2013-48164-C2-1P; llevándose a cabo en el Grupo de Catálisis Asimétrica del Instituto de Investigaciones Químicas (IIQ) del Consejo Superior de Investigaciones Científicas (CSIC-US). Durante el desarrollo del mismo, ha contado con la supervisión del Dr. D. José María Lassaletta Simon, Profesor de Investigación del Instituto de Investigaciones Químicas (CSIC-US), la Dra. D.ª Rosario Fernández Fernández, Catedrática de Química Orgánica de la Universidad de Sevilla y el Dr. D. Abel Ros Laó, Investigador Ramón y Cajal de la Universidad de Sevilla.

1. Introduction

Chirality and its significance

Chirality is a geometrical property an object exhibits when it is not superimposable on its mirror image; in fact, etymologically the word "chirality" is derived from the Greek "χειρ (*kheir)*, "hand", in which we can observe this phenomenon.

From the mathematical point of view, an object is chiral if and only if it does not possess an inversion centre (i) or a plane of symmetry, i.e. no (Sn).[1] Molecules, being geometrical structures are subjected to this property, and it is most commonly present in those compounds bearing C(sp3) atoms with all different substituents. Since the stereogenic element, in this case, is a point, a centre; this kind of chirality can be classified as central or point chirality. Nonetheless, according to the previous definition, this molecular arrangement is not the only one leading to chiral properties,[1] and other stereogenic elements such as axis,[2] helixes[3] and planes[4] may originate chirality. Moreover, in addition to these chiral elements, enantiomorphism may also arise from

[1] (1) Wolf, C. *Dynamic Stereochemistry of Chiral Compounds*; The Royal Society of Chemistry, 2007. https://doi.org/10.1039/9781847558091.

[2] For reviews on axially chiral biaryls, see :a)R.Noyori, Angew.Chem.Int. Ed. 2002, 41,2008; Angew.Chem. 2002, 114,2108;b)P.Kocˇovsky´,Sˇ.Vy- skocˇil, M. Smrcˇina, Chem. Rev. 2003, 103,3213;c)G.Bringmann, A. J. Pri- ce Mortimer,P.A.Keller,M.J.Gresser,J.Garner,M.Breuning, Angew. Chem. Int. Ed. 2005, 44,5384; Angew.Chem. 2005, 117,5518;d)J.M. Brunel, Chem. Rev. 2005, 105,857;e)G.Ma, M. P. Sibi, Chem.Eur.J. 2015, 21,11644;f)J.Wencel-Delord, A. Panossian, F. R. Leroux,F.Colo- bert, Chem. Soc. Rev. 2015, 44,3418. (1) Lassaletta, J. M. *Atropisomerism and Axial Chirality*; WORLD SCIENTIFIC (EUROPE), 2019. https://doi.org/10.1142/q0192. For areview on axially chiral anilides, see: I. Takahashi, Y. Suzuki, O. Kita- gawa, Org. Prep. Proced. Int. 2014, 46,1. For reviews on axially chiral allenes, see:a)M.Ogasawara, Tetrahedron: Asymmetry 2009, 20,259;b)S.Yu, S. Ma, Angew.Chem. Int. Ed. 2012, 51,3074; Angew.Chem. 2012, 124,3128;c) R.K.Neff, D. E. Frantz, ACS Catal. 2014, 4,519 d) R.K.Neff, D. E. Frantz, Tetrahedron 2015, 71,7

[3] For reviews on helical chiral compounds, see: a) M. Gingras, Chem. Soc. Rev. 2013, 42,968;b)M.Gingras, G. F¦lix,R.Peresutti, Chem. Soc. Rev. 2013, 42,1007;c)M.Gingras, Chem. Soc. Rev. 2013, 42,1051;d)M.J. Narcis, N. Takenaka, Eur.J.Org. Chem. 2014,21; e) K. Tanaka, Y. Kimura, K. Murayama, Bull. Chem. Soc. Jpn. 2015, 88,375

[4] For reviews on planar chiral compounds, see: a)S.E.Gibson, J. D. Knight, Org.Biomol. Chem. 2003, 1,1256;b)G.C.Fu, Acc. Chem. Res. 2006, 39,853;c)D.Schaarschmidt, H. Lang, Organometallics 2013, 32, 5668;d)N.A.Butt, D. Liu, W. Zhang, Synlett 2014, 25,615;e)S.Arae, M. Ogasawara, Tetrahedron Lett. 2015, 56,1751.

directionality elements as in catenanes and rotaxanes,[5] which exhibit topological chirality (Figure 1).

Figure 1. Molecules displaying axial, helical and planar chirality.

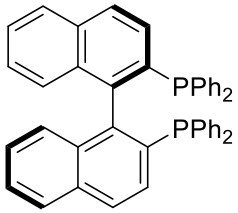

(R)-BINAP

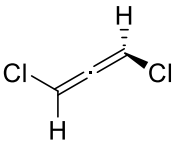

(*S*)-1,3-dichloroallene

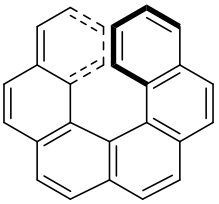

(*P*)-hexahelicene

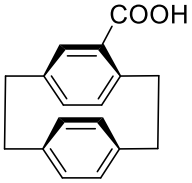

(*R*)-[2,2]paracyclophane-carboxylic acid

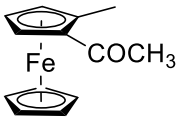

(*R*)-1-acetyl-2-methyl-ferrocene

On the other hand, asymmetric synthesis deals with the preparation of this kind of chiral compounds in a non-racemic manner, i.e. with the preferential formation of one enantiomer over the other, and it embodies one of the main topics in synthetic chemistry for two reasons: 1) the academic point of view including the expansion of chemical tools to access all the possible stereoisomers a compound may have and 2) the significance of the applications related to chiral substances.

In this regard, chiral compounds are present in natural products, materials and bioactive compounds such as drugs and agrochemicals. Furthermore, 65% of drugs are found as single enantiomers while only 7% corresponds to

[5] (1) Jamieson, E. M. G.; Goldup, S. M. Chirality Makes a Move. *Nat. Chem.* **2019**, *11* (9), 765–767. https://doi.org/10.1038/s41557-019-0320-z.
(1) Jamieson, E. M. G.; Modicom, F.; Goldup, S. M. Chirality in Rotaxanes and Catenanes. *Chem. Soc. Rev.* **2018**, *47* (14), 5266–5311. https://doi.org/10.1039/c8cs00097b.

racemates or mixture of diastereoisomers, [6] but the vast majority of synthetic methods relies on resolution technique. Thus, the development of new asymmetric methods to overcome the substantial cost of resolutions in terms of atom economy, time and resources, i.e., to fulfil Green Chemistry paradigms.[7]

The main interest in our research group is aligned with this aim, giving priority attention to the asymmetric synthesis of axially chiral heterobiaryls, which additionally is the main objective of this thesis.

Axially chiral heterobiaryls, as its very name indicates, exhibit chiral properties due to the presence of a chiral axis but in contrast to other compounds in this category, they also belong to another subclass of chiral molecules: they are atropisomers. First described by Richard Kuhn in 1933[8], atropisomer are enantiomers whose chirality arise from the restricted rotation around a single bond (the axis), and they can subsequently be isolated at room temperature. Since this property is closely related to a dynamic process and hence, to an energy barrier and time-dependant, the previous definition is rather vague and therefore, Ōki[9] later proposed this energy barrier should correspond to half-life of at least 1000 s (22 kcal·mol^{-1} at 27 °C) but still wholly arbitrary. "Isolation" is also relative as it may depend on the speed of the technique or the application of the compound. For instance, the stability of atropisomers is crucial in drug development when this kind of structures are present. [10]

In this vein, axially chiral biaryls and heterobiaryls have garnered an increasing interest due to their presence in natural products,[11] and their application in

---

[6] (1) Clayden, J.; Moran, W. J.; Edwards, P. J.; Laplante, S. R. The Challenge of Atropisomerism in Drug Discovery. *Angew. Chemie - Int. Ed.* **2009**, *48* (35), 6398–6401. https://doi.org/10.1002/anie.200901719.

[7] (1) Anastas, P.; Eghbali, N. Green Chemistry: Principles and Practice. *Chem. Soc. Rev.* **2010**, *39* (1), 301–312. https://doi.org/10.1039/b918763b.

[8] Kuhn, R. "Molekulare Asymmetrie" in Stereochemie. *Franz-Deutike (Red.), Leipzig-Wien* (1933).

[9] (1) Alkorta, I.; Elguero, J.; Roussel, C.; Vanthuyne, N.; Piras, P. *Atropisomerism and Axial Chirality in Heteroaromatic Compounds*; 2012; Vol. 105. https://doi.org/10.1016/B978-0-12-396530-1.00001-2.

(2) Ōki, M. Recent Advances in Atropisomerism. In *Topics in Stereochemistry*; John Wiley & Sons, Ltd, 2007; pp 1–81. https://doi.org/10.1002/9780470147238.ch1.

[10] (1) Clayden, J.; Moran, W. J.; Edwards, P. J.; Laplante, S. R. The Challenge of Atropisomerism in Drug Discovery. *Angew. Chemie - Int. Ed.* **2009**, *48* (35), 6398–6401. https://doi.org/10.1002/anie.200901719.

[11] L. Meca, D. Rˇ eha and Z. Havlas, J. Org. Chem., 2003, 68, 5677–5680.

different fields[12] such as drug discovery,[13] biologically active compound synthesis, materials[14,[15,16,17]] and catalysis (Figure 2).[18] Furthermore, many

---

3 G. Bringmann, C. Gu¨ nther, M. Ochse, O. Schupp and S. Tasler, Prog. Chem. Org. Nat. Prod., 2001, 82, 1–249.

a) G. Bringmann, C. Gìnther,M.Ochse, O. Schupp, S. Tasler in Progress in the ChemistryofOrganic Natural Products, Vol. 82 (Eds.:W.Herz,H. Falk, G. W. Kirby,R.E.Moore,),Springer,Berlin, 2001,pp. 1–129;b)P. Lloyd-Williams, E. Giralt, Chem.Soc. Rev. 2001, 30,145–157;c)M.C.Ko- zlowski, B. J. Morgan, E. C. Linton, Chem. Soc. Rev. 2009, 38,3193–3207; d) J. Clayden, W. J. Moran, P. J. Edwards, S. R. LaPlante, Angew. Chem.Int. Ed. 2009, 48,6398–6401; Angew.Chem. 2009, 121,6516–6520;e)G. Bringmann,M.Breuning, S. Tasler, Synthesis 1999,525–558;f)K. Tanaka, Chem. Asian J. 2009, 4,508–518;g)S.R.LaPlante, P. J. Edwards, L. D. Fader,A. Kakalian, O. Hucke, ChemMedChem 2011, 6,505–513; h) X. Fu, W. Fu, G. Liu, C. H. Senanayake, W. Tang, J. Am. Chem.Soc. 2014, 136,570–573. G. Bringmann,T.Gulder,T.A.M.Gulder,M.Breuning, Chem. Rev. 2011, 111,563–639

[12] a) J. L. Gustafson, D. Lim, S. J. Miller, Science 2010, 328, 1251–1255; b) I. Kania-Korwel, M. H. M. E. El-Komy, P. Veng-Pedersen, H.-J. Lehmler, Environ. Sci. Technol. 2010, 44, 2828–2835; c) D. Vizitiu, B. J. Halden, R. P. Lemieux, Chem. Commun. 1997, 1123–1124; d) B. A. Dreikorn, G. P. Jourdan, H. R. Hall, J. B. Deeter, N. J. Jones, J. Agric. Food Chem. 1990, 38, 549–552; e) A. Jamshidi, S. Hunter, S. Hazrati, S. Harrad, Environ. Sci. Technol. 2007, 41, 2153–2158; f) G. Bringmann, D. Menche, Acc. Chem. Res. 2001, 34, 615–624; g) J. Clayden, S. P. Fletcher, J. J. W. McDouall, S. J. M. Rowbottom, J. Am. Chem. Soc. 2009, 131, 5331–5343; h) R. D. Stipanovic, L. S. Puckhaber, J. Liu, A. A. Bell, J. Agric. Food Chem. 2009, 57, 566–571

[13] (1) Glunz, P. W. Recent Encounters with Atropisomerism in Drug Discovery. *Bioorganic Med. Chem. Lett.* **2018**, *28* (2), 53–60. https://doi.org/10.1016/j.bmcl.2017.11.050.

(1) Clayden, J.; Moran, W. J.; Edwards, P. J.; Laplante, S. R. The Challenge of Atropisomerism in Drug Discovery. *Angew. Chemie - Int. Ed.* **2009**, *48* (35), 6398–6401. https://doi.org/10.1002/anie.200901719.

(1) LaPlante, S. R.; Edwards, P. J.; Fader, L. D.; Jakalian, A.; Hucke, O. Revealing Atropisomer Axial Chirality in Drug Discovery. *ChemMedChem* **2011**, *6* (3), 505–513. https://doi.org/10.1002/cmdc.201000485.

[14] For example see: Y.-L. Wu, F. Ferroni, S. Pieraccini, W. Bernd Schweizer, B. B. Frank, G. Piero Spada and F. Diederich, Org. Biomol. Chem., 2012, 10, 8016.

[15] Cram, D. J. & Cram, J. M. Host–guest chemistry. Science 183, 803–809 (1974).

[16] Pu, L. Enantioselective fluorescent sensors: a tale of BINOL. Acc. Chem. Res. 45, 150–163 (2012).

[17] Sogah, G. D. Y. & Cram, D. J. Total chromatographic optical resolution of α-amino acid and ester salts through chiral recognition by a host covalently bound to polystyrene resin. J. Am. Chem. Soc. 98, 3038–3041 (1976).

[18] P. Kocovsky´ , S. Vyskocil and M. Smrcina, Chem. Rev., 2003, 103, 3213–3246; (b) Y. Chen, S. Yekta and A. K. Yudin, Chem. Rev., 2003, 103, 3155–3212; (c) J. M. Brunel, Chem. Rev., 2005, 105, 857–898; (d) M. Berthod, G. Mignani, G. Woodward and M. Lemaire, Chem. Rev., 2005, 105, 1801–1836.) C. Rosini, L. Franzini,A.Raffaelli, P. Salvadori, Synthesis 1992,503– 517;b)L.Pu, Chem. Rev. 1998, 98,2405–2494; c)

privilege ligands in metal catalysis present this kind of structures. For instance, Noyori hydrogenation, for which he shared the Nobel prize in 2011,[19] employs the axially chiral ligand BINAP.

M.McCarthy,P.J. Guiry, Tetrahedron 2001, 57,3809–3844; d) W.Tang, X. Zhang, Chem. Rev. 2003, 103,3029–3069;e)J.-H. Xie, Q.-L. Zhou, Acc. Chem. Res. 2008, 41,581–593; f) T.Akiyama, J. Itoh,K.Fuchibe, Adv. Synth. Catal. 2006, 348,999–1010; g) H.Shimizu, I. Nagasaki, T. Saito, Tetrahedron 2005, 61,5405–5432; h) T.Akiyama, Chem.Rev. 2007, 107,5744–5758; i) S. J. Connon, Angew.Chem.Int. Ed. 2006, 45,3909–3912; Angew. Chem. 2006, 118,4013–4016; j)Y.-M. Li, F.-Y.Kwong, W.-Y.Yu, A. S. C. Chan, Coord.Chem. Rev. 2007, 251,2119–2144;k)Y.Canac, R. Chauvin, Eur.J.Inorg. Chem. 2010,2325–2335; l) M.Terada, Chem. Commun. 2008,4097–4112; m) M. Terada, Synthesis 2010,1929–1982; n) A. Zamfir,S.Schenker,M.Freund, S. B. Tsogoeva, Org. Biomol.Chem. 2010, 8,5262–5276;o)M.Rueping, A. Kuenkel, I. Atodiresei, Chem. Soc. Rev. 2011, 40,4539–4549. D. S. Surry,S.L.Buchwald, Angew.Chem. Int. Ed. 2008, 47,6338–6361; Angew.Chem. 2008, 120,6438–6461. M. Yoshimura, S. Tanaka, M. Kitamura, TetrahedronLett. 2014, 55,3635– 3640

[19] (1) Noyori, R. Asymmetric Catalysis: Science and Opportunities (Nobel Lecture). *Angew. Chemie - Int. Ed.* **2002**, *41* (12), 2008–2022. https://doi.org/10.1002/1521-3773(20020617)41:12<2008::AID-ANIE2008>3.0.CO;2-4.

Figure 2. Axially chiral (hetero)biaryls in natural products and different applications.

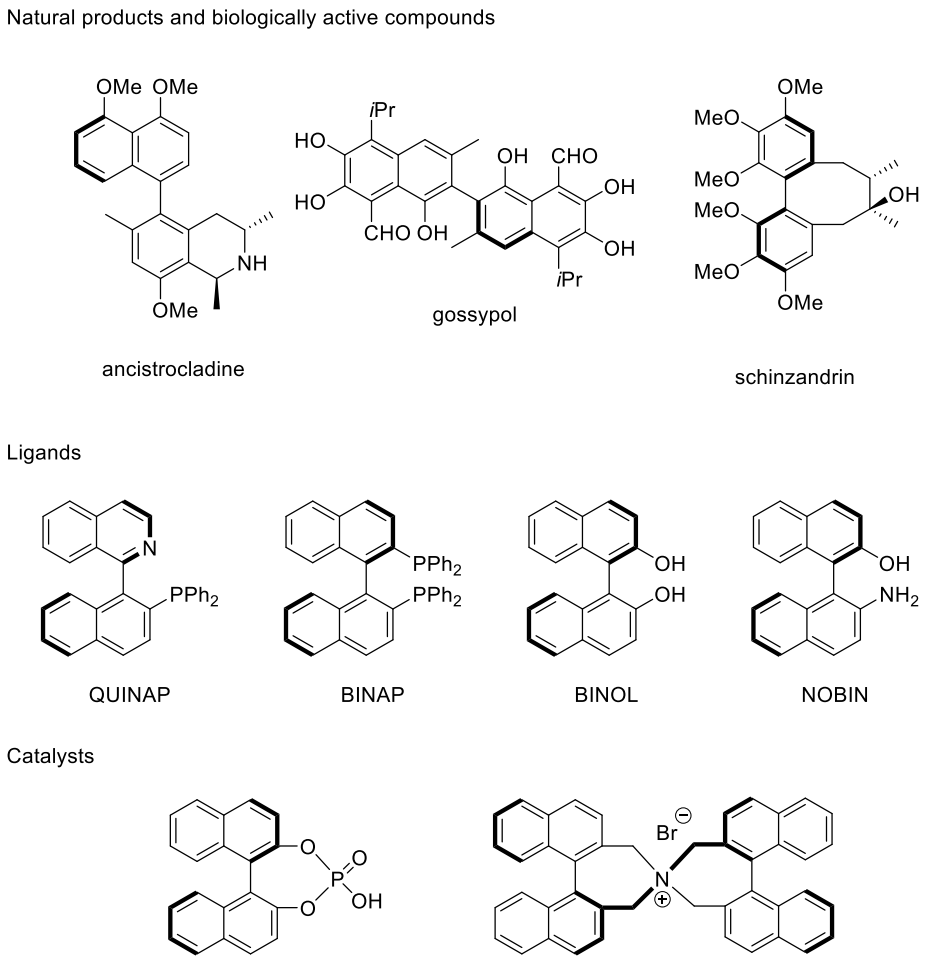

Strategies for the synthesis of axially chiral compounds

Due to the atropisomeric nature of axially chiral (hetero)biaryls, their chiral properties and therefore their further applications depend on the stability of the axis. Both electronic and steric factors determine the energy barrier associated with the rotation around the axis. Indeed, their most stable conformations are nor coplanar neither orthogonal as a balance of both effects.[1]

In this regard, the size and number of *ortho* substitutions influence the stabilisation of the axis. Thus, most of tri- or tetra-*ortho*-substituted biaryls are

stable unless some of these substitutions are the rather small MeO or F; whereas the stabilisation of 2,2'-disubstituted biaryls requires rather sterically hindering groups. Additionally, certain bridges, especially short ones, connecting both rings also destabilise the axis.[1]

By contrast, the influence of the *para*-substituents is related to electronic effects and may alter the rotational stability by up to 10%. Thus, electron-withdrawing groups at *para*-position stabilise rotational barriers while electron-donating groups exert the opposite effect. For instance, *p*-MeO increases the electron density at C1 or C1' positions and therefore, enhances out-of-plane bending providing a more straightforward pathway for the rotation. Moreover, the combination of both types of electro-modulating groups, for instance, *p*-Meo and *p*-NO2, at the different rings facilitate the conjugation of the system in a push-pull manner, lowering the energy barrier for the rotation.[1]

On the other hand, it is worth to notice that isomerisation may not be only accomplished by thermally overcoming the rotational barrier; other processes involving catalysis and photochemical processes may also lead to the same result.[1]

All these features have to be taken into account when designing a synthetic method to prepare axially chiral (hetero)biaryls. In this regard, methods leading to these compounds can be classified in two categories: those dealing with the synthesis of the scaffold and those concerning the functionalisation of (hetero)biaryls rendering a single stereoisomer (Scheme 0-1).

Scheme 0-1. Different approaches for the synthesis of axially chiral heterobiaryls

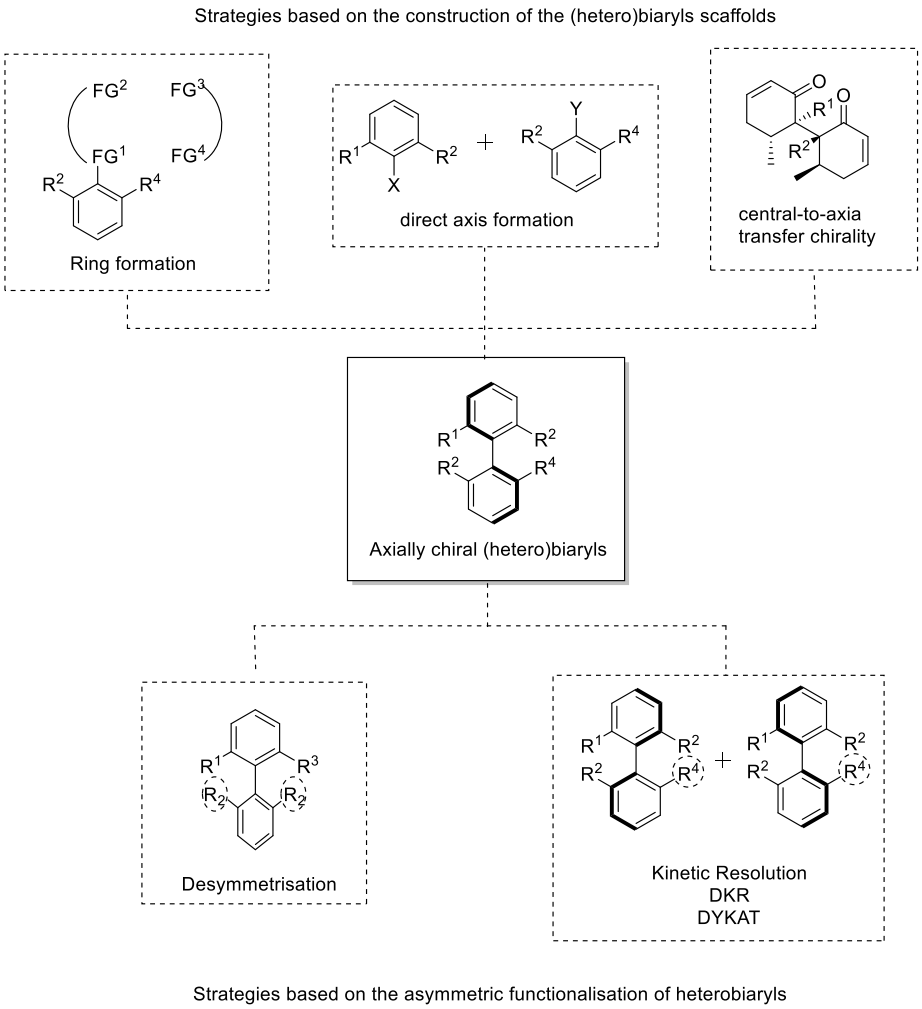

These strategies will be briefly depicted in the following section, paying more attention to desymmetrisation and deracemisation techniques as well as the synthesis of heterobiaryls in accordance to the main topic of this thesis.

Strategies based on the construction of the (hetero)biaryl scaffold

As we have mentioned, two main approaches can be envisioned for the synthesis of axially chiral (hetero)biaryls. The first one involves the construction of the biaryl skeleton from simpler structures, and this goal can be achieved by 3 distinct tactics:

1. Direct axis formation.
2. Ring formation
3. Central-to-Axial transfer chirality.

Direct axis formation via asymmetric cross-coupling reactions.

The most apparent approach to synthesise axially chiral heterobiaryls is the direct formation of the bond connecting both rings. In this regard, the powerful cross-coupling tools such as oxidative coupling and, especially Suzuki-Miyaura reaction, play a fundamental role in this strategy. Thus, in the last years, a significant progress has been made with important contributions by the groups of Bucwald,[20] Tang[21] and ours (Scheme 0-2).[22]

[20] J. Yin, and S. L. Buchwald, A catalytic asymmetric Suzuki coupling for the synthesis of axially chiral biaryl compounds, J. Am. Chem. Soc., 122, 12051-12052, (2000).
X. Shen, G. O. Jones, D. A. Watson, B.Bhayana, and S. L. Buchwald, Enantioselective synthesis of axially chiral biaryls by the Pd-catalyzed Suzuki-Miyaura reaction: Substrate ccope and quantum mechanical investigations, J. Am. Chem. Soc., 132, 11278-11287, (2010).

[21] W. Tang, N. D. Patel, G. Xu, X. Xu, J. Savoie, S. Ma, M.-H. Hao, S. Keshipeddy, A. G. Capacci, X. Wei, Y. Zhang, J. J. Gao, W. Li, S. Rodriguez, B. Z. Lu, N. K. Yee, and C. H. Senanayake, Efficient chiral monophosphorus ligands for asymmetric Suzuki-Miyaura coupling reactions, Org. Lett. 14, 2258-2262, (2012).
S. Rodriguez, B. Qu, N. Haddad, D. C. Reeves, W. Tang, H. Lee, D. Krishnamurthy, and C. H. Senanayake, Oxaphosphole-based monophosphorus ligands for Palladium-catalyzed amination reactions, Adv. Synth. Catal., 353, 533-537, (2011).
G. Xu, W. Fu, G. Liu, C. H. Senanayake, and W. Tang, Efficient syntheses of Korupensamines A, B and Michellamine B by asymmetric Suzuki-Miyaura coupling reactions, J. Am. Chem. Soc., 136, 570-573, (2014).

[22] A. Bermejo, A. Ros, R. Fernández, and J. M. Lassaletta, C2-symmetric bis-hydrazones as ligands in the asymmetric Suzuki-Miyaura cross-coupling, J. Am. Chem. Soc. 130, 15798-15799, (2008).
A. Ros, B. Estepa, A. Bermejo, E. ÃÅlvarez, R. FernÃ°ndez, and JosÃ© M. Lassaletta, Phosphino hydrazones as suitable ligands in the asymmetric Suzuki–Miyaura cross-coupling, J. Org. Chem., 77, 4740-4750, (2012).

Scheme 0-2. Selected examples of the synthesis of axially chiral biaryls by direct axis formation.

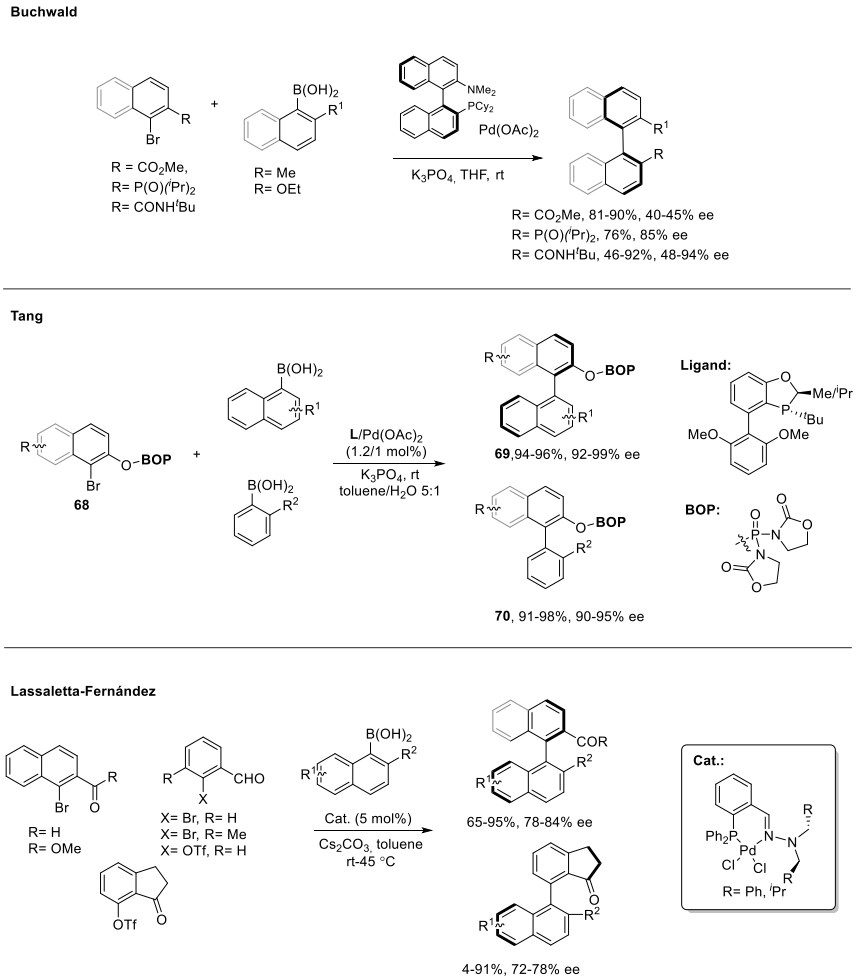

However, heterobiaryls synthesis through asymmetric bond formation (Scheme 0-3) is still a challenging task owing to the problems related to the nature of heteroaromatic rings, i.e., coordination of the substrate and the reduced reactivity or stability of the reagents. As an additional limitation, lone pairs at the heteroatom exert less steric hindrance than the corresponding C-H bond, and therefore, the axial stability of the products decreases.

Scheme 0-3. Axis disconnection for the synthesis of axially chiral heterobiaryls

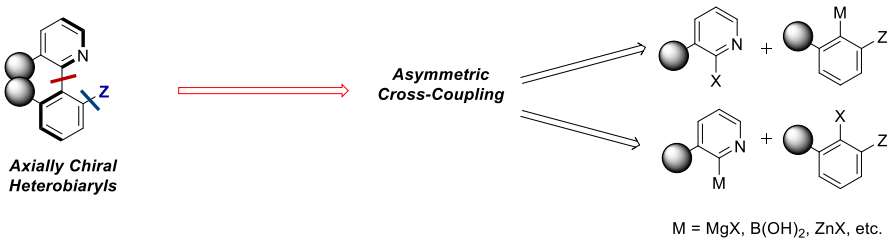

Consequently, reports on this topic are scarce, and only two publications are found in the literature. On the one hand, Sarandeses, Perez-Sotelo et al.[23] reported the first method concerning the asymmetric bond formation leading to heterobiaryls in 2013; however, poor selectivity values were obtained, perhaps due to the low configurational stability of the axis at 80 ºC.

Scheme 0-4. Sarandeses' synthesis of axially chiral heterobiaryls

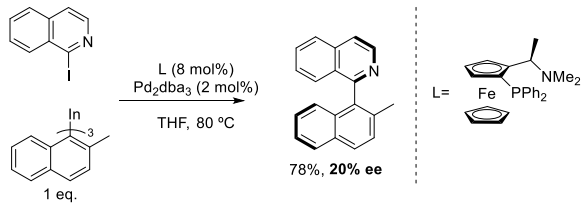

On the other, and more recently, Shi and co-workers[24] have overcome this limitation by using a bulky NHC ligand, affording the corresponding heterobiaryls in high yields and excellent enantioselectivities; but at any rate, the vast majority of the heterobiaryls did not bear the hetero atom at the "*ortho*" position.

[23] (1) Mosquera, Á.; Pena, M. A.; Pérez Sestelo, J.; Sarandeses, L. A. Synthesis of Axially Chiral 1,1'-Binaphthalenes by Palladium-Catalysed Cross-Coupling Reactions of Triorganoindium Reagents. *European J. Org. Chem.* **2013**, *2013* (13), 2555–2562. https://doi.org/10.1002/ejoc.201300042.

[24] (1) Shen, D.; Xu, Y.; Shi, S.-L. A Bulky Chiral N-Heterocyclic Carbene Palladium Catalyst Enables Highly Enantioselective Suzuki–Miyaura Cross-Coupling Reactions for the Synthesis of Biaryl Atropisomers. *J. Am. Chem. Soc.* **2019**, *141* (37), 14938–14945. https://doi.org/10.1021/jacs.9b08578.

Scheme 0-5. Synthesis of axially chiral heterobiaryls by Shi et. al

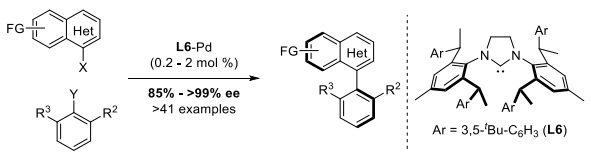

Axially chiral heterobiaryls through ring formation.

An alternative method for de novo synthesis of axially chiral (hetero)biaryls concerns the formation of one or the two cyclic moieties with concomitant generation of the axis. Thus, the key reaction to achieve this goal is [2+2+2] cycloaddition and can be carried out both in intra- and intermolecular manners.

A pioneering work in the asymmetric synthesis of these compounds was reported by Gutnov, Heller et al. [25,26] in a Co-catalysed cyclometrisation reaction leading to axially chiral 2-naphthylisoquinolines by the construction of the pyridine ring (Scheme 0-6).

Scheme 0-6. Synthesis of axially chiral 2-naphthylpyridines through [2+2+2] cycloaddition.

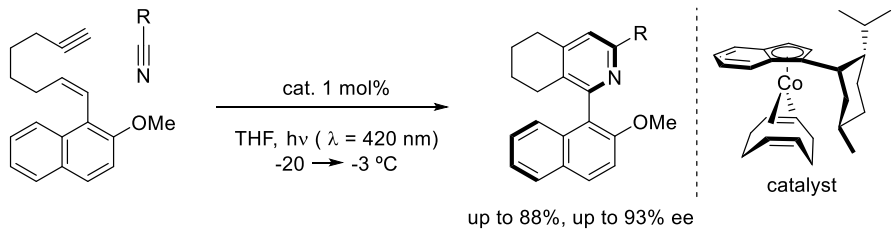

In a similar way, but using a Rh-based catalyst, Tanaka et al. developed a methodology in which aryl ring was build by [2+2+2] cycloaddition between

[25] A. Gutnov, B.e Heller, C. Fischer, H.-J. Drexler, A. Spannenberg, B. Sundermann, and C. Sundermann, Cobalt(I)-catalyzed asymmetric [2+2+2] cycloaddition of alkynes and nitriles: Synthesis of enantiomeri- cally enriched atropoisomers of 2-arylpyridines, Angew. Chem. Int. Ed. 43(29), 3795–3797, (2004).

[26] M. Hapke, K. Kral, C. Fischer, A. Spannenberg, A. Gutnov, D. Redkin, and B. Heller, Asymmetric synthesis of axially chiral 1-aryl-5,6,7,8- tetrahydroquinolines by cobalt-catalyzed [2+2+2] cycloaddition reaction of 1-aryl-1,7-octadiynes and nitriles, J. Org. Chem. 75(12), 3993–4003, (2010)

dyines and 1-alkynylisoquinoline affording the desired heterobiaryls in good yields and excellent enantioselectivities (Scheme 0-7).[27]

Scheme 0-7. Synthesis of axially chiral arylisoquinolines through [2+2+2] cycloaddition.

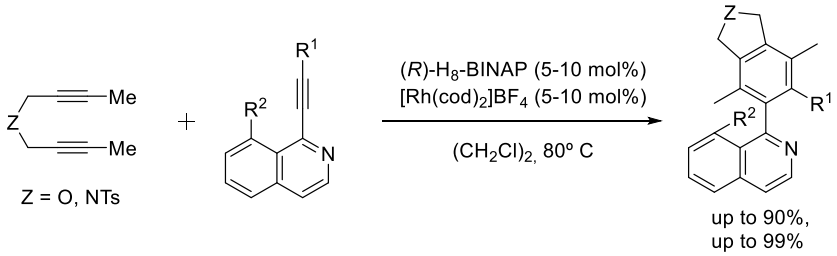

Central-to-axial chiral transfer

As complement to the previous strategies involving the direct or concomitant formation of the chiral axis, the synthesis of non-aromatic chiral (hetero)bicyclic structures involve as precursor moieties leading to axially chiral aromatic (hetero)biaryls also comprise an interesting approach for the synthesis of these compounds. As an example of this strategy, Li, Shi and co-workers[28] reported the synthesis of 3-(1-napthyl)-indoles in excellent enantioselectivities (82-94% ee) through an organocatalysed addition of naphthol to indole ring and subsequent rearomatisation of the latter (Scheme 0-8).

[27] N. Sakiyama, D. Hojo, K. Noguchi, and K. Tanaka, Enantioselective syn- thesis of axially chiral 1-arylisoquinolines by rhodium-catalyzed [2+2+2] cycloaddition, Chem. Eur. J. 17(5), 1428–1432, (2011).

[28] H.-H. Zhang, C.-S. Wang, C. Li, G.-J. Mei, Y. Li, and F. Shi, Design and enantioselective construction of axially chiral naphthyl–indole skeletons, Angew. Chem. Int. Ed. 56(1), 116–121, (2017).

Scheme 0-8. Synthesis of axially chiral naphthyl-indoles via central-to-axial chirality transfer.

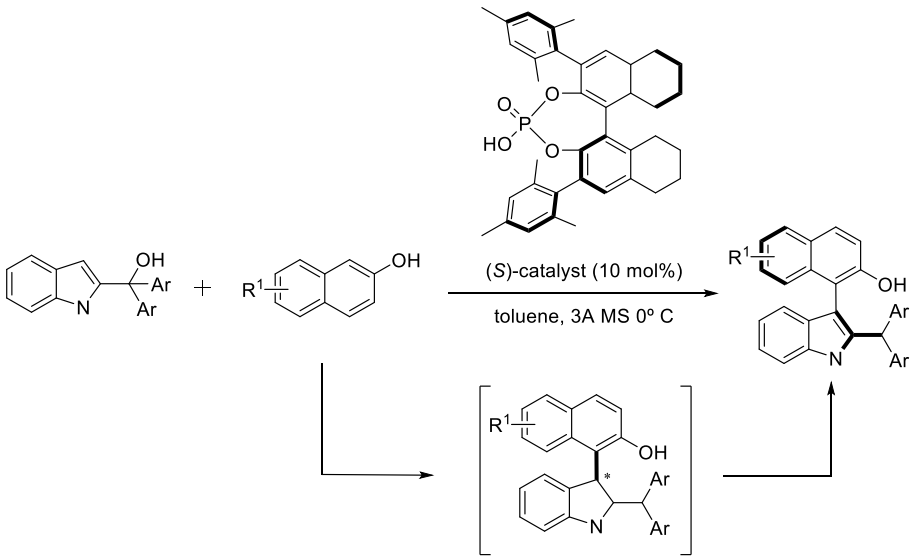

Asymmetric functionalisation as strategies for the synthesis of axially chiral (hetero)biaryls

So far, we have briefly exposed those methods concerning the generation of the whole biarylic structures from simpler substrates. However, there is another meaningful approach to access axially chiral (hetero)biaryls: the asymmetric transformation or derivatisation of (hetero)biaryls. Different strategies can be applied depending on the chirality of the heterobiaryls as starting materials, i.e., if they are racemic or achiral.

In this regard, methodologies leading to the preparation of one single stereoisomer from a racemate relies on a deracemisation process; however, two different but related approaches take advantage of this concept: KR, DKR and DYKAT.[29] By contrast, if the starting heterobiaryl is achiral, a desymmetrisation process is involved.

Desymmetrisation

According to the definition of chirality, (hetero)biaryls possessing a plane of symmetry are achiral; however, transformations leading to a reduction of

[29] (1) Faber, K. Non-Sequential Processes for the Transformation of a Racemate into a Single Stereoisomeric Product: Proposal for Stereochemical Classification. *Chem. - A Eur. J.* **2001**, *7* (23), 5004–5010. https://doi.org/10.1002/1521-3765(20011203)7:23<5004::AID-CHEM5004>3.0.CO;2-X.

their symmetry, i.e., the destruction of this plane (or the improper axis in case it applies), entails the introduction of chirality.

Scheme 0-9. Desymmetrisation

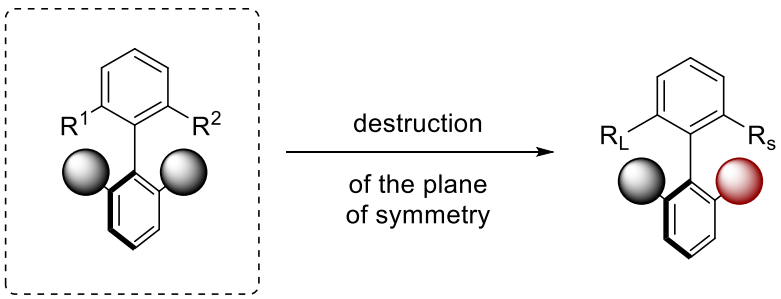

In this regard, two situations emerge depending on the stability of the axis. Thus, if the axis is labile, the asymmetric transformation would imply blocking the rotation around the axis so that the chiral product is configurationally stable. Due to this labile character of the starting material, the interconversion of both conformers is possible and the favoured reaction of one of them, with a chiral catalyst or reagent, leads to the asymmetric transformation of the (hetero)biaryl. According to this, the underlying strategy for this asymmetric transformation is closely related to DKR, being the only difference the lack of chirality in the starting material. These two strategies are frequently confused in the literature, and indeed, the seminal work of Miller[30] and co-workers on the atroposelctive bromination of biaryls clearly describes this situation.

In this methodology, 3-arylphenols having a low rotational barrier of ~ 7 kcal·mol-1, do not correspond to a chiral compound; instead, they preferably describe a conformational equilibrium of achiral compounds. Consequently, under the catalytic action of a peptide, one conformer is brominated faster than the other but the latter, is rapidly interconverted into the first. Hence, the brominated biaryl is obtained in high yields and enantioselectivities (Scheme 0-10.A).

[30] (1) Gustafson, J. L.; Lim, D.; Miller, S. J. Dynamic Kinetic Resolution of Biaryl Atropisomers via Peptide-Catalyzed Asymmetrie Bromination. *Science (80-.).* **2010**, *328* (5983), 1251–1255. https://doi.org/10.1126/science.1188403.

Scheme 0-10. Synthesis of axially chiral biaryls through desymmetrisation.

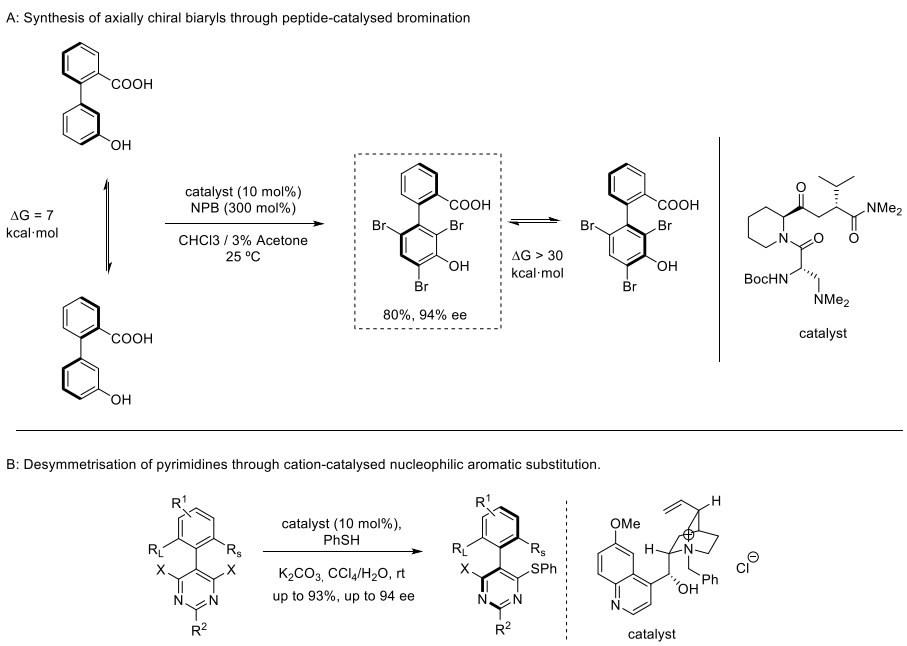

By contrast, prochiral configurationally stable (hetero)biaryls do not undergo any stereodynamic interconversion, and even though they could, the final conformer would be indistinguishable. Hence, the asymmetric induction in these cases relies on the preferential reaction on one face (*re* or *si*) over the other. One example of the desymmetrisation of configurationally stable heterobiarlys can be found in the report by Smith et al.[31] on the asymmetric synthesis of 5-aryl-pyrimidines. In this reaction, the symmetric chloro(bromo)pyrimidines undergo an organocatalysed nucleophilic aromatic substitution with thiophenol (Scheme 0-10.B)

Kinetic Resolution, Dynamic Kinetic Resolution and Dynamic Kinetic Asymmetric Transformation

Besides to symmetric but prochiral heterobiaryls previously described, asymmetric functionalisation or derivatisation can also be applied to racemic systems. In this case, a deracemisation process takes places rather than desymmetrisation, and two different strategies (DKR and DYKAT) aim to this goal.

[31] (1) Armstrong, R. J.; Smith, M. D. Catalytic Enantioselective Synthesis of Atropisomeric Biaryls: A Cation-Directed Nucleophilic Aromatic Substitution Reaction. *Angew. Chemie - Int. Ed.* **2014**, *53* (47), 12822–12826. https://doi.org/10.1002/anie.201408205.

Strictly speaking, deracemisation is a process describing the interconversion of one enantiomer into the other. Nevertheless, this is an endoergic process governed exclusively by the reduction of entropy and hence, difficult to accomplish. By contrast, coupling the racemisation process with a reaction, the enthalpy term associated with the transformation may overcome the entropy term related to the deracemisation and therefore, the product can be obtained as a single stereoisomer. Hence, deracemisation usually refers to the product of the reaction rather than the starting material. In this relation, Faber [et al.] suggest the following definition: "Deracemisation constitutes any process during which a racemate is transformed into a non-racemic product in 100% theoretical yield without intermediate separation of materials".

A closely related process is the Kinetic Resolution (KR). In this case, a racemate is set to react with a chiral catalyst or reagent, but both enantiomers react at different rates due to the formation of diastereomeric intermediates/transition states (Scheme 0-11). Thus, one enantiomer reacts faster than the other, and therefore, the product and the remaining starting material can be obtained as single enantiomers, though the yield of the reaction is limited to 50%.

Scheme 0-11. Dynamic Resolution

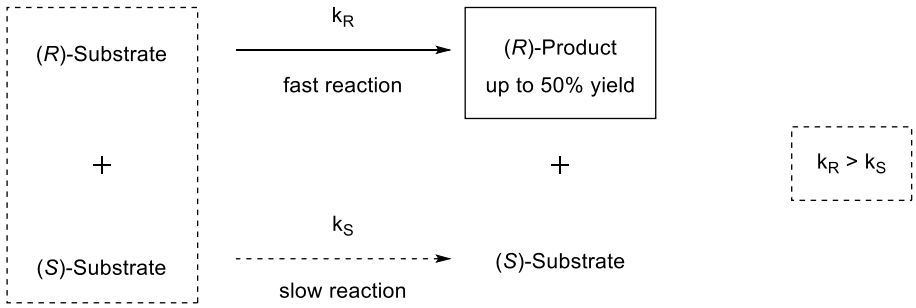

In the context of the synthesis of axially chiral heterobiaryls, Virgil, Stoltz et al. reported in 2013 a methodology involving the Kinetic Resolution of naphthylisoquinoline bromide through a cross-coupling reaction with diarylphosphines. Hence, kinetic resolution yields the exciting QUINAP-type products in excellent enantiomeric excesses, and so the bromide was recovered enantiomerically enriched (Scheme 0-11).[32] Nevertheless, by

[32] (1) Bhat, V.; Wang, S.; Stoltz, B. M.; Virgil, S. C. Asymmetric Synthesis of QUINAP via Dynamic Kinetic Resolution. *J. Am. Chem. Soc.* **2013**, *135* (45), 16829–16832. https://doi.org/10.1021/ja409383f.

changing the reaction conditions, the protocol could be adapted to a DYKAT process.

Scheme 0-12. Kinetic resolution of napthylisoquinolines for the synthesis of QUINAP and derivatives

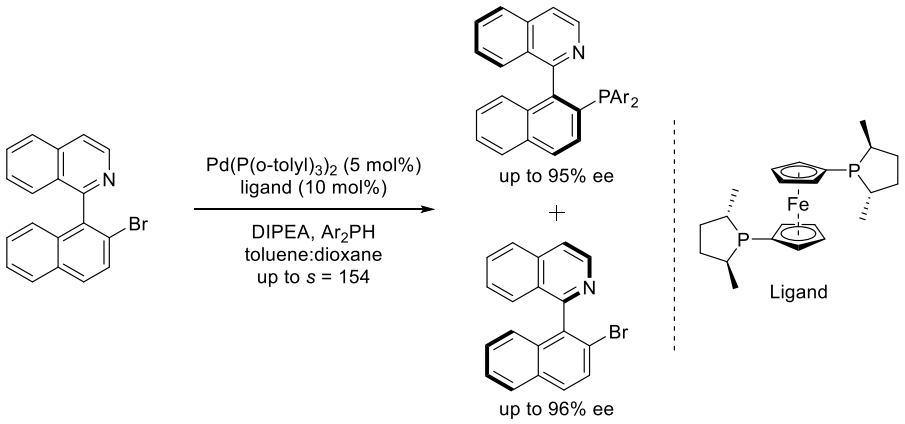

As we can see, the utility of kinetic resolution is restricted by the lack of interconversion between both enantiomers of the substrate. In this context, deracemisation processes, i.e. DKR and DYKAT, emerge as solutions to this limitation.

In this regard, Dynamic Kinetic Resolution (DKR) is a two-step process in which deracemisation is coupled with KR. Thus, in the DKR-based methodologies, one enantiomer undergoes the reaction with absolute configuration retention, whereas the other experiences an inversion before the asymmetric reaction takes place. Consequently, the whole racemate could be transformed into the product as a single enantiomer. Nevertheless, for this type of resolution to be successful, the rate of racemisation (K_{RI} and K_{SI}) must be at least higher than the slowest asymmetric reaction (KS) and ideally, higher than both asymmetric steps. On the other hand, it should be noted that the deracemisation step proceeds through an achiral transition state (Scheme 0-13).

Scheme 0-13. Dynamic Kinetic Resolution

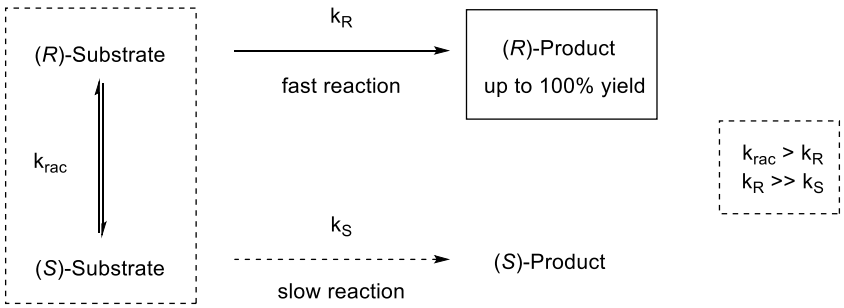

Thus, the hydrosilylation of arylpyridine-type ketones recently published by our group perfectly exemplifies this strategy (Scheme 0-14). Heterobiaryl ketones as tri-ortho-substituted platforms appear to be configurationally stable and hence, racemic. However, the opposite nature of pyridinic nitrogen and the carbon ketone results in an interaction between both groups. Consequently, the angles involved in the axial stability are widened, producing a distortion of the axis and, therefore promoting the labilisation of the axis with subsequent racemisation. Accordingly, a relatively low energy barrier of 22.1 Kcal·mol-1 for the naphthylisoquinoline ketone was calculated, providing a fast racemisation at THF reflux. The subsequent hydrosilylation/hydrolysis yields the corresponding alcohols with both axial and central chirality.[33]

Scheme 0-14. Dynamic Kinetic Resolution of naphthylisoquinoline ketones

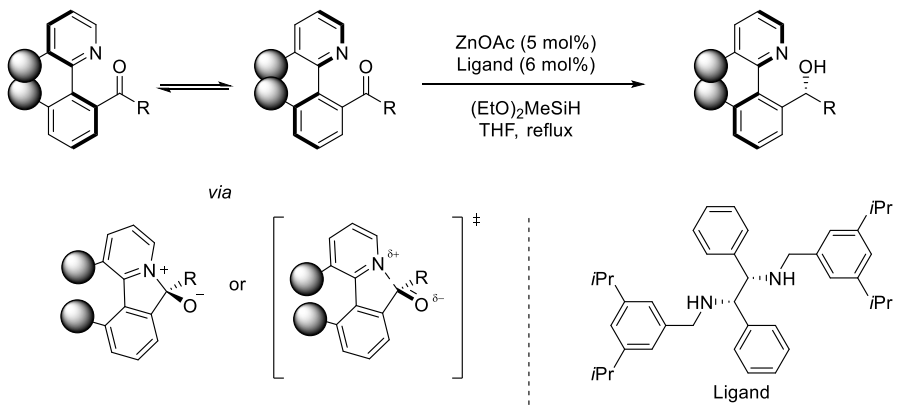

The other deracemisation strategy which deals with the transformation of a racemate into a product as a single enantiomer is the Dynamic Kinetic

[33] (1) Hornillos, V.; Carmona, J. A.; Ros, A.; Iglesias-Sigüenza, J.; López-Serrano, J.; Fernández, R.; Lassaletta, J. M. Dynamic Kinetic Resolution of Heterobiaryl Ketones by Zinc-Catalyzed Asymmetric Hydrosilylation. *Angew. Chemie - Int. Ed.* **2018**, *57* (14), 3777–3781. https://doi.org/10.1002/anie.201713200.

Asymmetric Transformation (DYKAT). However, the underlying mechanism is entirely different from that of DKR. In this case, the interconversion of the enantiomers is not the result of a racemisation process, but it proceeds through diastereomeric equilibration instead. Consequently, the equilibration rates of the stereoisomers are different, and the key intermediate of this process is chiral. [34] On the other hand, DYKAT methodologies can be classified into two subgroups.[35]

Scheme 0-15. Dynamic Kinetic Asymmetric Transformation

DYKAT type 1

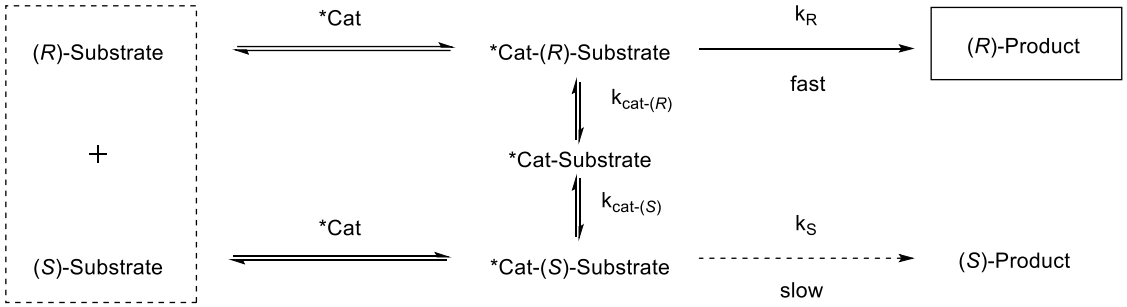

DYKAT type 2

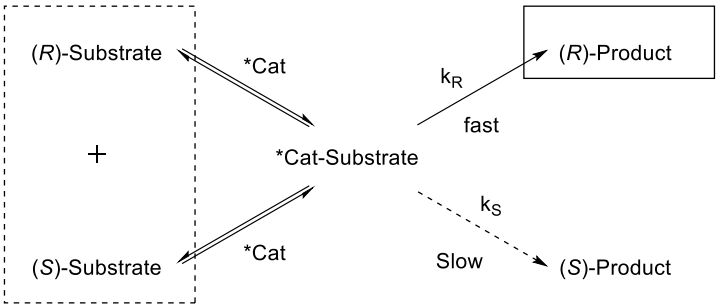

[34] Steinreiber, J.; Faber, K.; Griengl, H. De-Racemization of Enantiomers versus De-Epimerization of Diastereomers-Classification of Dynamic Kinetic Asymmetric Transformations (DYKAT). *Chem. - A Eur. J.* **2008**, *14* (27), 8060–8072. https://doi.org/10.1002/chem.200701643.

[35] DYKAT of racemic diastereomeric mixtures are also reported and hence, two other types of this kind of strategy emerge: DYKAT type III and DYKAT type IV. For further information, see reference 31.

For the DYKAT type I (Scheme 0-15), each enantiomer of the racemate interacts with a chiral catalyst forming diastereomeric complexes. If these species are not able to undergo an interconversion process, the situation would be similar to a KR. By contrast, if they do interconvert, a dynamic process similar to DKR evolves. However, the fact that the interconverting species are diastereoisomeric and hence, not energetically degenerated. Consequently, the population of both diastereomeric species is unequal and influence the selectivity of this kinetically controlled process.

In the case of DYKAT type II (Scheme 0-15), diastereomeric intermediates are not interconverting, but the equilibration between the racemate and the chiral intermediate may be unequal. Nevertheless, this is a desymmetrisation-type process, and hence, the selectivity of the product only depends on the asymmetric transformation step while the rate of the reaction depends on the formation of the chiral intermediate.

In this context, our group has successfully applied different DYKAT tactics to develop several methodologies for the synthesis of axially chiral heterobiaryls.

For instance, axially chiral arylisoquinolines and related compounds are challenging structures from an asymmetric synthesis of view. Indeed, previous attempts dealing with the direct formation of the axis results in a low enantioselection.[36] However, in 2013, we demonstrated for the first time that this kind of products could be efficiently prepared with moderate to excellent selectivities through DYKAT techniques. This procedure delivers the transformation of racemic triflates arylpyridines and isoquinolines *via* Suzuki-Miyaura reaction with aryl boroxines (Scheme 0-16).[37]

[36] (1) Mosquera, Á.; Pena, M. A.; Pérez Sestelo, J.; Sarandeses, L. A. Synthesis of Axially Chiral 1,1′-Binaphthalenes by Palladium-Catalysed Cross-Coupling Reactions of Triorganoindium Reagents. *European J. Org. Chem.* **2013**, *2013* (13), 2555–2562. https://doi.org/10.1002/ejoc.201300042.

[37] (1) Ros, A.; Estepa, B.; Ramírez-López, P.; Álvarez, E.; Fernández, R.; Lassaletta, J. M. Dynamic Kinetic Cross-Coupling Strategy for the Asymmetric Synthesis of Axially Chiral Heterobiaryls. *J. Am. Chem. Soc.* **2013**, *135* (42), 15730–15733. https://doi.org/10.1021/ja4087819.

Scheme 0-16. Dynamic Kinetic Asymmetric Suzuki-Miyaura reaction for the synthesis of axially chiral heterobiaryls.

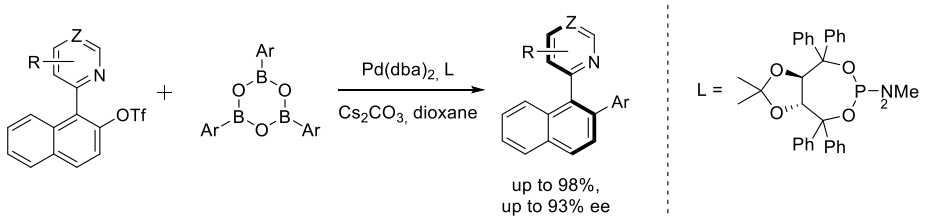

As a working hypothesis (Scheme 0-17), we thought the oxidative addition of triflates would lead to the formation of the corresponding diastereomeric palladacycles that would be able to undergo an epimerisation process. By isolating one oxidative addition intermediate, we proved the angles involved in the stability of the axis were widened, providing a pathway for the interconversion of diastereomeric species as a means of racemisation of the substrate as in Scheme 0-15 (DYKAT type I).

Scheme 0-17. Proposed mechanism for the DYKAT process involving the formation of palladacycles

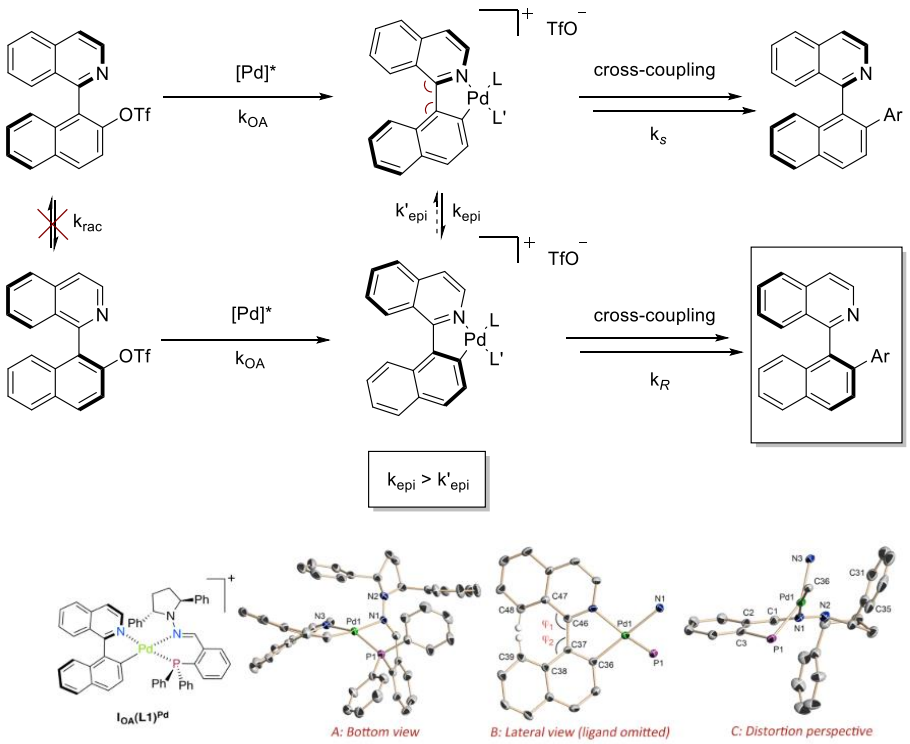

Given the outstanding results of this methodology, our group aimed to extend this DYKAT strategy to other transformations, and indeed, we applied other C-

C cross-coupling reactions to fulfil this goal[38]. Nevertheless, we then envisioned the combination of other C-X bond forming cross-coupling reactions with this dynamic approach would comprise elegant methods to prepare high valuable heterobiaryls.

In this connection, we proposed a methodology for the synthesis of QUINAP and derivatives through a dynamic kinetic C-P cross-coupling reaction.[39] Hence, the Pd-catalysed coupling between silylphosphines and the same triflates as above yield the desired products with excellent results (Scheme 0-18). This methodology, together with the previously mentioned from Virgil and Stoltz allow us to access to valuable QUINAP derivatives which will be used in one of our methodologies, presented in this work.

Scheme 0-18. Synthesis of BINAP and congeners through Dynamic Kinetic Asymmetric C-P cross coupling reaction

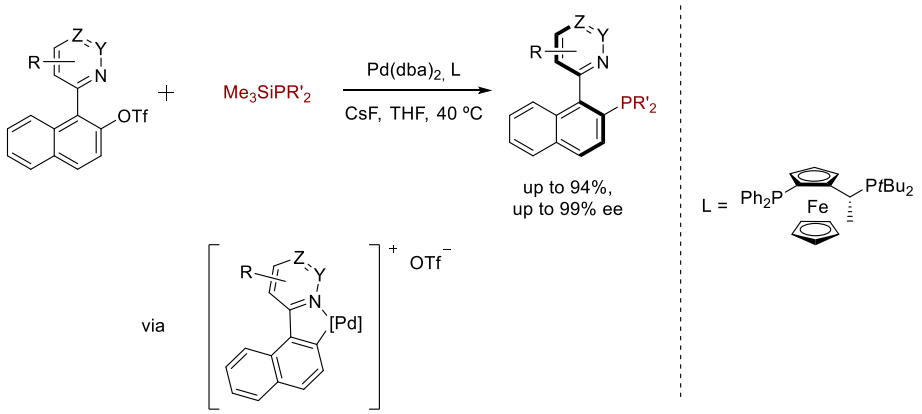

Considering the importance of heterobiaryls in different fields of the chemistry, new methods aiming to their development are required. In this

[38] (1) Hornillos, V.; Ros, A.; Ramírez-López, P.; Iglesias-Sigüenza, J.; Fernández, R.; Lassaletta, J. M. Synthesis of Axially Chiral Heterobiaryl Alkynes via Dynamic Kinetic Asymmetric Alkynylation. *Chem. Commun.* **2016**, *52* (98), 14121–14124. https://doi.org/10.1039/C6CC08997F.

(1) Carmona, J. A.; Hornillos, V.; Ramírez-López, P.; Ros, A.; Iglesias-Siguënza, J.; Gómez-Bengoa, E.; Fernández, R.; Lassaletta, J. M. Dynamic Kinetic Asymmetric Heck Reaction for the Simultaneous Generation of Central and Axial Chirality. *J. Am. Chem. Soc.* **2018**, *140* (35), 11067–11075. https://doi.org/10.1021/jacs.8b05819.

[39] (1) Ramírez-López, P.; Ros, A.; Estepa, B.; Fernández, R.; Fiser, B.; Gómez-Bengoa, E.; Lassaletta, J. M. A Dynamic Kinetic C–P Cross–Coupling for the Asymmetric Synthesis of Axially Chiral P,N Ligands. *ACS Catal.* **2016**, *6* (6), 3955–3964. https://doi.org/10.1021/acscatal.6b00784.

regard, our group has a great interest in this topic and we decided to further explore the asymmetric functionalisation of heterobiaryls to achieve this goal.

Hence, this thesis will have two chapters dealing with these approaches. In the chapter I, we will present a new methodology for the synthesis IAN-type amines through a Dynamic Kinetic Asymmetric Buchwald-Hartwig reaction. In the chapter II, we will develop an Ir(I)-catalalysed hydroarylation of vinyl ethers for the synthesis of heterobiaryls with bot axial and central chirality.

2. Dynamic Buchwald-Hartwig amination of heterobiaryls. Synthesis and applications of IAN-type amines.

Introduction

IAN-amine

As mentioned before, there exist many ligands of great importance in catalysis that are defined by their atropisomeric heterobiaryls nature. In this context, QUINAP[40], developed by Brown, is an outstanding representative. Since its advent, the other analogues (oxygen, sulphur and nitrogen) have been

[40] (1) Alcock, N. W.; Brown, J. M.; Hulmes, D. I. Synthesis and Resolution of 1-(2-Diphenylphosphino-1-Naphthyl)Isoquinoline; a P-N Chelating Ligand for Asymmetric Catalysis. *Tetrahedron: Asymmetry* **1993**, *4* (4), 743–756. https://doi.org/10.1016/S0957-4166(00)80183-4.

synthesised (Figure 3).[41,42] However, the lack of a general and efficient asymmetric methodology implies diastereomeric synthesis or resolution. [43]

[41] (1) Chelucci, G.; Bacchi, A.; Fabbri, D.; Saba, A.; Ulgheri, F. Enantiomerically Pure 1-(2-Methoxy-1-Naphthyl) and 1-(2-Methylthio-1-Naphthyl)Isoquinoline: Two New Axially Chiral NO and NS Ligands for Asymmetric Catalysis. *Tetrahedron Lett.* **1999**, *40* (3), 553–556. https://doi.org/10.1016/S0040-4039(98)02353-3.

[42] (a) Cortright, S. B.; Johnston, J. N. IAN-Amines: Direct Entry to a Chiral C2-Symmetric Zirconium(IV) β-Diketimine Complex. *Angew. Chemie Int. Ed.* **2002**, *41* (2), 345. https://doi.org/10.1002/1521-3773(20020118)41:2<345::AID-ANIE345>3.0.CO;2-U.

(b) Cortright, S. B.; Huffman, J. C.; Yoder, R. A.; Coalter, J. N.; Johnston, J. N. IAN Amines: Chiral C2 -Symmetric Zirconium(IV) Complexes from Readily Modified Axially Chiral C 1 -Symmetric β-Diketimines. *Organometallics* **2004**, *23* (10), 2238–2250. https://doi.org/10.1021/om049897p.

(c) Cortright, S. B.; Coalter, J. N.; Pink, M.; Johnston, J. N. A Remarkably Facile Zirconium(IV) → Aluminum(III) β-Diketiminate Transmetalation That Also Results in a More Active Olefin Polymerization Catalyst upon Activation. *Organometallics* **2004**, *23* (25), 5885–5888. https://doi.org/10.1021/om049364g.

(d) N. Johnston, J.; B. Cortright, S.; A. Yoder, R. Enantioenriched Axially Chiral B-Diketimines: Determination of the IAN-Amine Barrier to Atrop- Isomerization. *Heterocycles* **2004**, *62* (1), 223. https://doi.org/10.3987/COM-03-S(P)62.

(e) Luesse, S. B.; Counceller, C. M.; Wilt, J. C.; Perkins, B. R.; Johnston, J. N. A Preparation of Enantiomerically Enriched Axially Chiral β-Diketimines: Synthesis of (−)- and (+)-IAN Amine. *Org. Lett.* **2008**, *10* (12), 2445–2447. https://doi.org/10.1021/ol800728b.

[43] (1) Fache, F.; Schulz, E.; Tommasino, M. L.; Lemaire, M. Nitrogen-Containing Ligands for Asymmetric Homogeneous and Heterogeneous Catalysis. *Chem. Rev.* **2000**, *100* (6), 2159–2232. https://doi.org/10.1021/cr9902897.

(1) Togni, A.; Venanzi, L. M. Nitrogen Donors in Organometallic Chemistry and Homogeneous Catalysis. *Angew. Chemie Int. Ed. English* **1994**, *33* (5), 497–526. https://doi.org/10.1002/anie.199404971.

Figure 3. QUINAP and other heteroatom analogues.

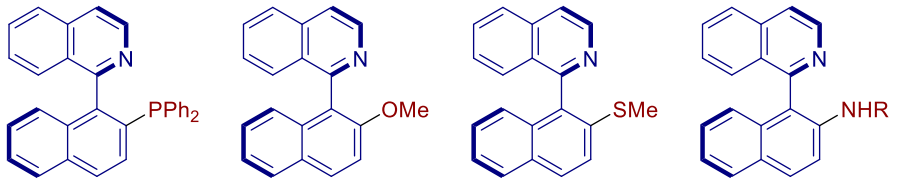

Brown 1993 **Chelucci 1999** **Johnston 2002**

Encouraged by good results on the Dynamic Kinetic C-P cross coupling for the synthesis of QUINAP ligands reported by our group,[44] we envisioned that similar strategy could be exploited and develop a DYKAT strategy for the synthesis of axially chiral *N,N*-diamines. In addition, the catalytic potential of these ligands is higher than the *N,O* and *N,S* ligands since many more applications have been reported for *N,N* containing ligands.[45]

These IAN-amines (Figure 4), as Johnston coined them after their synthesis, are derived from Isoquinoline and 2-Amino-Naphthalene; and they present a great potential in catalysis due to their intrinsic bidentate character. In fact, the two different nitrogen donor atoms (N(sp3) vs. N(sp2)) and the possibility of different substitution patterns provides a way to tuning the electronic,

[44] (1) Ramírez-López, P.; Ros, A.; Estepa, B.; Fernández, R.; Fiser, B.; Gómez-Bengoa, E.; Lassaletta, J. M. A Dynamic Kinetic C–P Cross–Coupling for the Asymmetric Synthesis of Axially Chiral P,N Ligands. *ACS Catal.* **2016**, *6* (6), 3955–3964. https://doi.org/10.1021/acscatal.6b00784.

[45] (1) Fache, F.; Schulz, E.; Tommasino, M. L.; Lemaire, M. Nitrogen-Containing Ligands for Asymmetric Homogeneous and Heterogeneous Catalysis. *Chem. Rev.* **2000**, *100* (6), 2159–2232. https://doi.org/10.1021/cr9902897.

steric and chelating properties of this ligands. Moreover, the application of *N,N*-ligands in (asymmetric) catalysis is far reported.[45]

Figure 4. Structure of IAN-type amines.

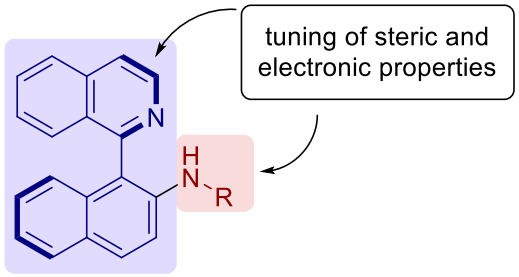

On the other hand, Johnston saw these compounds as formally β-diketimine class of ligands with a unique non-planar property. These β-diketimines are seen as complementary ligands to metallocenes of group IV and therefore, in addition to the IAN-amine synthesis, the preparation of a chiral C_2-symmetric Zr complex was also included in his report (Figure 5).[42a]

It is noteworthy that despite the racemic synthesis of the ligand, the Zr-IAN-amine complex was obtained as a single diastereoisomer. Attempting to prepare the dimethyl-Zr-IAN complex by reacting the bis(dimethylamido) complex with trimethylaluminium, the corresponding Al-IAN complex was obtained.[42c] In line to the ability of metallocenes to promote the polymerization of olefins, this kind of complexes were tested in the polymerization of ethylene exhibiting particularly substantial activity in the case of the Aluminium complex (Figure 5).[42a-c]

Figure 5. Zr(IV) and Al(III) IAN-amine complexes.

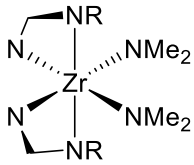

R = Me, Bn, Ph
X = NMe2, Cl, I

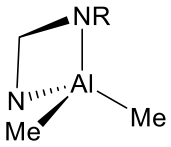

Regarding the chiral version, and therefore the application in asymmetric catalysis, the tetrahedral Zn(II) complex was also prepared in a similar fashion, and it was demonstrated to be the resting state of the catalytical asymmetric

addition of diethylzinc to benzaldehyde using (-)-Me-IAN as ligand. Hence, this is the first asymmetric catalytic application of IAN-type amines (Scheme 0-1).

Scheme 0-1. Application of Me-IAN ligand to the asymmetric addition of diethylzinc to benzaldehyde.

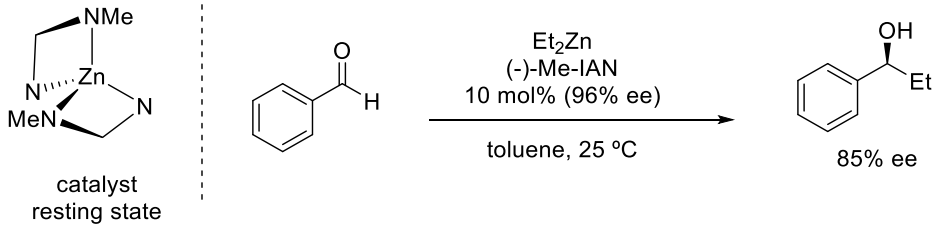

Notwithstanding, the potential of these amines is not only confined to the field of metallic catalysis, but of organocatalysis as well. In fact, amines are a typical structural feature of many organocatalysts (i.e. aminocatalysts, and hydrogen-bonding catalysis)[46] while pyridines are involved in Lewis-base catalysis.[47]

Despite all this potential, the applications of IAN-amines have not been further studied, probably owing to the unattractive method described so far, which requires the separation of diastereoisomers and subsequent deprotection. Thus, the synthetic methodology reported by Johnston relies on a diastereoselective version involving the disconnection of the axis.[42] Consequently, the synthesis consists of the coupling of the chiral naphthylamino fragment and isoquinoline moieties. First, the amine is prepared by either the Bucherer or the Buchwald-Hartwig reaction and, subsequently, the coupling is accomplished by means of a SNAr activating the isoquinoline with an Al-based Lewis acid (Scheme 0-2).

[46] (1) Bertelsen, S.; Jørgensen, K. A. Organocatalysis—after the Gold Rush. *Chem. Soc. Rev.* **2009**, *38* (8), 2178. https://doi.org/10.1039/b903816g.
(2) Erkkilä, A.; Majander, I.; Pihko, P. M. Iminium Catalysis. *Chem. Rev.* **2007**, *107* (12), 5416–5470. https://doi.org/10.1021/cr068388p.
(3) Doyle, A. G.; Jacobsen, E. N. Small-Molecule H-Bond Donors in Asymmetric Catalysis. *Chem. Rev.* **2007**, *107* (12), 5713–5743. https://doi.org/10.1021/cr068373r.
[47] (1) Denmark, S. E.; Beutner, G. L. Lewis Base Catalysis in Organic Synthesis. *Angew. Chemie Int. Ed.* **2008**, *47* (9), 1560–1638. https://doi.org/10.1002/anie.200604943.
(1) Spivey, A. C.; Arseniyadis, S. Nucleophilic Catalysis by 4-(Dialkylamino)Pyridines Revisited-The Search for Optimal Reactivity and Selectivity. *Angew. Chemie Int. Ed.* **2004**, *43* (41), 5436–5441. https://doi.org/10.1002/anie.200460373.

Scheme 0-2. Johnston's synthesis of IAN-amines

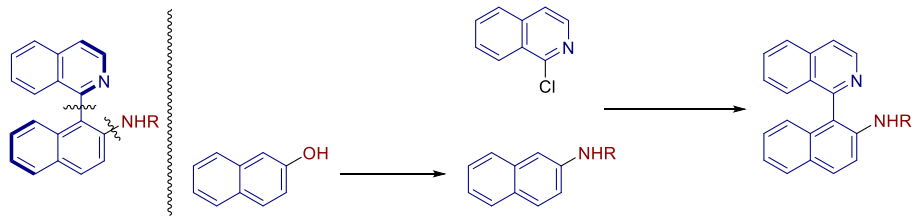

The main inconvenient of this methodology is the inherent lack of chiral induction and the enantiomers have to be resolved either by chiral chromatography or by resolution of diasteroisomers.

In view of this situation, we envisioned the application of the DYKAT strategy to solve this problem and develop a new and reliable method to prepare this IAN-amines. On the other hand, this strategy relies on the ability to find such a reaction that enables the formation of a C-N bond in such a way that isomerization of the axis is faster ($k_{epi} > k_{CN}$) (Scheme 0-3). Taking into consideration the similarity between P and N, we first thought to employ our methodology developed for the synthesis of QUINAP. That is to say, a palladium catalysed cross-coupling reaction utilizing silylamines as nucleophile.

Scheme 0-3. DYKAT strategy for the synthesis of IAN-type heterobiaryls.

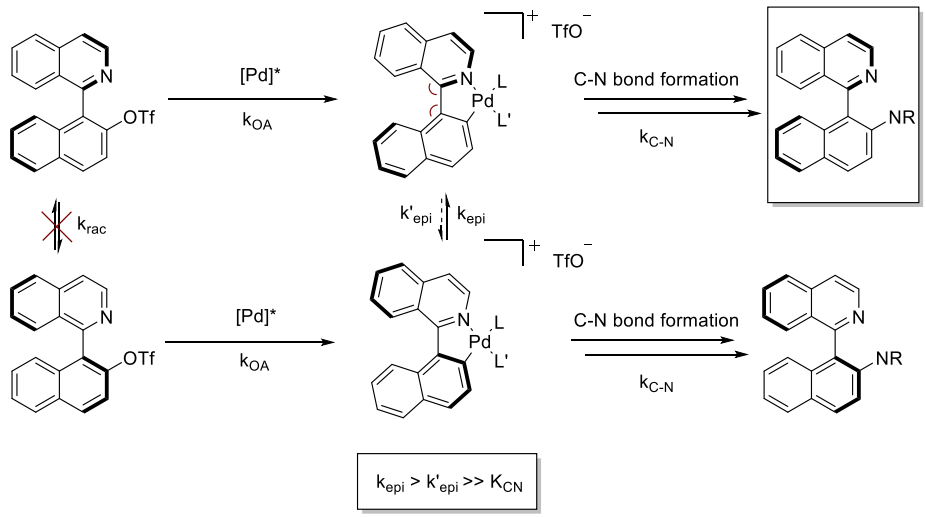

On the other hand, the use of silylamine reagents for the coupling reaction is not a new idea. Although it is not widely explored, there are reports on the

use of silylamines[48] and silyl-aldimines[49] as coupling partners of haloarenes. In fact, these compounds remind of the stannylamines[50] employed by Migita in the C-N cross-coupling before the Buchwald-Hartwig reaction was developed.[50]

Preliminary trials of this reaction with *N*-(trimethylsilyl)diphenylamine revealed a general lack of activity, even under the activation with F^- (Scheme 0-4). At first glance, the poor reactivity could be attributed to the partial N-Si

[48] (1) Smith, C. J.; Early, T. R.; Holmes, A. B.; Shute, R. E. Palladium Catalysed Cross-Coupling Reactions of Silylamines. *Chem. Commun.* **2004**, No. 17, 1976–1977. https://doi.org/10.1039/B406868H.
(2) Smith, C. J.; Tsang, M. W. S.; Holmes, A. B.; Danheiser, R. L.; Tester, J. W. Palladium Catalysed Aryl Amination Reactions in Supercritical Carbon Dioxide. *Org. Biomol. Chem.* **2005**, *3* (20), 3767. https://doi.org/10.1039/b509345g.
(3) Shimizu, K.; Minami, Y.; Goto, O.; Ikehira, H.; Hiyama, T. Silicon-Based C–N Cross-Coupling Reaction. *Chem. Lett.* **2014**, *43* (4), 438–440. https://doi.org/10.1246/cl.131075.
(4) Minami, Y.; Komiyama, T.; Shimizu, K.; Hiyama, T.; Goto, O.; Ikehira, H. Catalytic Carbon-Nitrogen Bond-Forming Cross-Coupling Using N-Trimethylsilylam
(5) Komiyama, T.; Minami, Y.; Hiyama, T. Recent Progress in the Cross-Coupling Reaction Using Triorganosilyl-Type Reagents. *Synlett* **2017**, *28* (15), 1873–1884. https://doi.org/10.1055/s-0036-1589008.
(6) Minami, Y.; Komiyama, T.; Shimizu, K.; Uno, S. I.; Hiyama, T.; Goto, O.; Ikehira, H. Nickel-Catalyzed N-Arylation Using N -Trimethylsilyl-Carbazole. *Synlett* **2017**, *28* (18), 2407–2410. https://doi.org/10.1055/s-0036-1588417.

[49] (1) Barluenga, J.; Aznar, F.; Valdés, C. N-Trialkylsilylimines as Coupling Partners for Pd-Catalyzed C-N Bond-Forming Reactions: One-Step Synthesis of Imines and Azadienes from Aryl and Alkenyl Bromides. *Angew. Chemie - Int. Ed.* **2004**, *43* (3), 343–345. https://doi.org/10.1002/anie.200352808.
(2) Candito, D. A.; Lautens, M. Palladium-Catalyzed Domino Direct Arylation/N-Arylation: Convenient Synthesis of Phenanthridines. *Angew. Chemie - Int. Ed.* **2009**, *48* (36), 6713–6716. https://doi.org/10.1002/anie.200902400.

[50] (1) Kosugi, M.; Kameyama, M.; Migita, T. Palladium-catalyzed aromatic amination of aryl bromides with *N,N*-di-ethylamino-tributyltin. *Chem. Lett.* **1983**, *12* (6), 927–928. https://doi.org/10.1246/cl.1983.927.
(b) Paul, F.; Patt, J.; Hartwig, J. F. Palladium-Catalyzed Formation of Carbon-Nitrogen Bonds. Reaction Intermediates and Catalyst Improvements in the Hetero Cross-Coupling of Aryl Halides and Tin Amides. *J. Am. Chem. Soc.* **1994**, *116* (13), 5969–5970. https://doi.org/10.1021/ja00092a058.
(3) Guram, A. S.; Buchwald, S. L. Palladium-Catalyzed Aromatic Aminations with in Situ Generated Aminostannanes. *J. Am. Chem. Soc.* **1994**, *116* (17), 7901–7902. https://doi.org/10.1021/ja00096a059.

double bond due to interaction of the nitrogen with the Si atom,[51] which would decrease its nucleophilic character. Nevertheless, it has been reported that reactivity of these silylamines in the C-N cross-couplings is in line with its low basicity, i.e., the less basic, the more reactive silylamines are. Therefore, this lack of reactivity might be ascribed to the steric hindrance exerted by the TMS and phenyl substituents on the amine.

*Scheme 0-4. Silylamine as amine surrogate for the C-N cross-coupling (**PR-684**).*

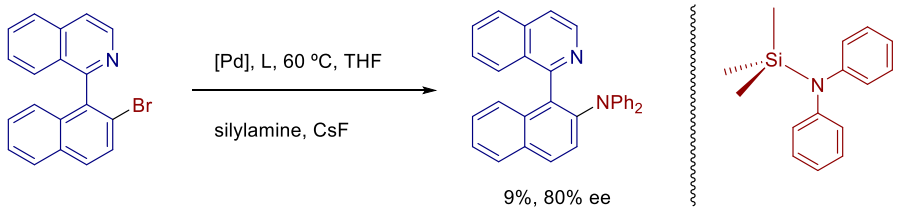

As we need a C-N cross-coupling reaction to achieve our goal, we decided to move towards the development of our methodology relying on the well described Buchwald-Hartwig reaction (Scheme 0-5).

Scheme 0-5. Working hypothesis for the synthesis of axially chiral NN-diamines

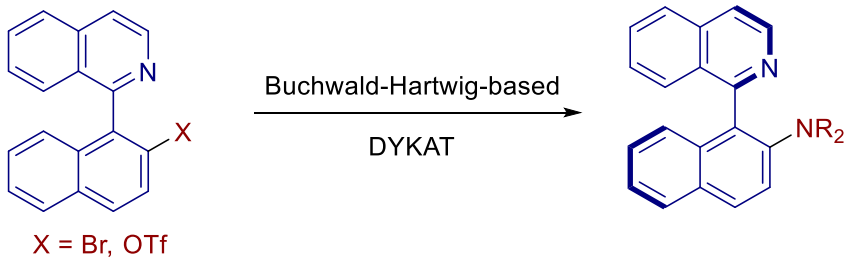

[51] (1) Ruhlandt-Senge, K.; Bartlett, R. A.; Olmstead, M. M.; Power, P. P. Silylamines with Pyramidal Coordination at Nitrogen. *Angew. Chemie Int. Ed. English* **1993**, *32* (3), 425–427. https://doi.org/10.1002/anie.199304251.

(2) Lehn, J. M.; Munsch, B. Nitrogen Inversion Barrier and Nature of the Si-N Bond in Silylamine: An Ab Initio SCF-LCAO-MO Study. *J. Chem. Soc. D Chem. Commun.* **1970**, No. 16, 994–996. https://doi.org/10.1039/C29700000994.

(3) Huber, G.; Schmidbaur, H. The Basicity of Silylamines and Alkylamines: An Equilibrium Study of the Competitive Borane Adduct Formation. *Zeitschrift fur Naturforsch. - Sect. B J. Chem. Sci.* **1998**, *53* (10), 1103–1108. https://doi.org/10.1515/znb-1998-1005.

The Buchwald-Hartwig reaction

The Buchwald-Hartwig reaction[52] represents one of the most powerful tools for chemist to achieve the formation of C(sp^2)-N bonds. This significance is due to the high generality of the reaction which affords the C-N forming products covering the whole spectrum of amines and derivatives with aryl (pseudo)halides as coupling partners. On the other hand, nitrogen is a key element in organic chemistry and C-N containing compounds are present in different fields: pharmaceuticals, agrochemicals, material science,[53] etc.

---

[52] Reviews: (1) Dorel, R.; Grugel, C. P.; Haydl, A. The Buchwald-Hartwig Amination after 25 Years. *Angew. Chemie Int. Ed.* **2019**. https://doi.org/10.1002/anie.201904795.

(3) Beletskaya, I. P.; Cheprakov, A. V. The Complementary Competitors: Palladium and Copper in C–N Cross-Coupling Reactions. *Organometallics* **2012**, *31* (22), 7753–7808. https://doi.org/10.1021/om300683c.

(4) Surry, D. S.; Buchwald, S. L. Dialkylbiaryl Phosphines in Pd-Catalyzed Amination: A User's Guide. *Chem. Sci.* **2011**, *2* (1), 27–50. https://doi.org/10.1039/C0SC00331J.

(7) Hartwig, J. F. Evolution of a Fourth Generation Catalyst for the Amination and Thioetherification of Aryl Halides. *Acc. Chem. Res.* **2008**, *41* (11), 1534–1544. https://doi.org/10.1021/ar800098p.

(8) Prim, D.; Campagne, J.-M.; Joseph, D.; Andrioletti, B. Palladium-Catalysed Reactions of Aryl Halides with Soft, Non-Organometallic Nucleophiles. *Tetrahedron* **2002**, *58* (11), 2041–2075. https://doi.org/10.1016/S0040-4020(02)00076-5.

(11) Hartwig, J. F. Approaches to Catalyst Discovery. New Carbon–Heteroatom and Carbon–Carbon Bond Formation. *Pure Appl. Chem.* **1999**, *71* (8), 1417–1423. https://doi.org/10.1351/pac199971081417.

(12) Yang, B. H.; Buchwald, S. L. Palladium-Catalyzed Amination of Aryl Halides and Sulfonates. *J. Organomet. Chem.* **1999**, *576* (1–2), 125–146. https://doi.org/10.1016/S0022-328X(98)01054-7.

(13) Hartwig, J. F. Transition Metal Catalyzed Synthesis of Arylamines and Aryl Ethers from Aryl Halides and Triflates: Scope and Mechanism. *Angew. Chemie - Int. Ed.* **1998**, *37* (15), 2046–2067. https://doi.org/10.1002/(SICI)1521-3773(19980817)37:15<2046::AID-ANIE2046>3.0.CO;2-L.

(14) Wolfe, J. P.; Wagaw, S.; Marcoux, J.-F.; Buchwald, S. L. Rational Development of Practical Catalysts for Aromatic Carbon−Nitrogen Bond Formation. *Acc. Chem. Res.* **1998**, *31* (12), 805–818. https://doi.org/10.1021/ar9600650.

(15) Hartwig, J. F. Carbon−Heteroatom Bond-Forming Reductive Eliminations of Amines, Ethers, and Sulfides. *Acc. Chem. Res.* **1998**, *31* (12), 852–860. https://doi.org/10.1021/ar970282g.

(17) Hartwig, J. F. Palladium-Catalyzed Amination of Aryl Halides: Mechanism and Rational Catalyst Design. *Synlett* **1997**, *1997* (4), 329–340. https://doi.org/10.1055/s-1997-789.

[53] (1) Zhao, H.; Tanjutco, C.; Thayumanavan, S. Design and Synthesis of Stable Triarylamines for Hole-Transport Applications. *Tetrahedron Lett.* **2001**, *42* (27), 4421–4424. https://doi.org/10.1016/S0040-4039(01)00702-X.

Hence, the Buchwald-Hartwig reaction along with its advances, has enormously contributed to these fields through its different applications.[54]

In this context, the Buchwald-Hartwig (B-H) reaction constitutes a major breakthrough in synthetic chemistry, since the previous reactions involving C(sp^2)-N bond formation were essentially based on S_NAr (via ipso substitution, $S_{RN}1$ or aryne formation)[55] and the Ullmann-Goldberg reaction.[56] Nevertheless, these methodologies were not efficient because they usually require activated substrates, stoichiometric amounts of Cu and/or harsh conditions; becoming not very suitable for many substrates diminishing the generality and applicability. Notwithstanding, the Ullmann-type reaction have evolved toward catalytic versions[57] which do not require such rough conditions, being still not as powerful as palladium-catalysed reactions though. In this regard, Ni-catalysed methodologies has also been developed.[58]

---

a) Shirota, Y. J. Mater. Chem. 2000, 10, 1. (b) Shirota, Y. J. Mater. Chem. 2005, 15,75

[54] 1) Ruiz-Castillo, P.; Buchwald, S. L. Applications of Palladium-Catalyzed C–N Cross-Coupling Reactions. *Chem. Rev.* **2016**, *116* (19), 12564–12649. https://doi.org/10.1021/acs.chemrev.6b00512

[55] (1) Razzuk, A.; Biehl, E. R. The Reaction of Various Methoxy-Substituted Haloarenes with Amines and Nitriles under Aryne-Forming Conditions. *J. Org. Chem.* **1987**, *52* (12), 2619–2622. https://doi.org/10.1021/jo00388a058.

(1) Razzuk, A.; Biehl, E. R. The Reaction of Various Methoxy-Substituted Haloarenes with Amines and Nitriles under Aryne-Forming Conditions. *J. Org. Chem.* **1987**, *52* (12), 2619–2622. https://doi.org/10.1021/jo00388a058.

(1) Bunnett, J. F. A General Conversion of Phenols to Anilines. *J. Org. Chem.* **1972**, *37* (22), 3570. https://doi.org/10.1021/jo00795a054.

[56] (1) Ullmann, F. Ueber Eine Neue Bildungsweise von Diphenylaminderivaten. *Berichte der Dtsch. Chem. Gesellschaft* **1903**, *36* (2), 2382–2384. https://doi.org/10.1002/cber.190303602174.

(1) Goldberg, I. Ueber Phenylirungen Bei Gegenwart von Kupfer Als Katalysator. *Berichte der Dtsch. Chem. Gesellschaft* **1906**, *39* (2), 1691–1692. https://doi.org/10.1002/cber.19060390298.

[57] (1) Monnier, F.; Taillefer, M. Catalytic C-C, C-N, and C-O Ullmann-Type Coupling Reactions. *Angew. Chemie - Int. Ed.* **2009**, *48* (38), 6954–6971. https://doi.org/10.1002/anie.200804497.

(1) Sambiagio, C.; Marsden, S. P.; Blacker, A. J.; McGowan, P. C. Copper Catalysed Ullmann Type Chemistry: From Mechanistic Aspects to Modern Development. *Chem. Soc. Rev.* **2014**, *43* (10), 3525–3550. https://doi.org/10.1039/c3cs60289c.

(1) Evano, G.; Blanchard, N.; Toumi, M. Copper-Mediated Coupling Reactions and Their Applications in Natural Products and Designed Biomolecules Synthesis. *Chem. Rev.* **2008**, *108* (8), 3054–3131. https://doi.org/10.1021/cr8002505.

[58] For a review, see: a) J. Bariwal, E. Van der Eycken, Chem. Soc. Rev. 2013, 42, 9283–9303. For selected examples of Ni-catalyzed C–N bond formation, see: b) M. Marín, R. J. Rama, M. C. Nicasio, Chem. Rec. 2016, 16, 1819–1832. c) C. M. Lavoie, M. Stradiotto,

In contrast to the much previously developed C-C bond cross-couplings, which was firstly reported in 1979[59], the C-N catalysed bond formation took longer time to be developed, in fact, it is the first catalysed hetero cross-coupling. This late development might be attributed to the less thermodynamic force leading to the products, making this kind of reaction more challenging relative to C-C counterpart. In fact, heteroatoms tend to be good donor ligands and hence, forms stable metal complexes preventing further reaction.

Migita's pioneering work and the Pd/P(o-tolyl)$_3$ catalytic system.

Based on the Stille-type reaction, the pioneering work on this hetero-coupling reaction is owed to Migita, who in 1983 reported the first Pd-catalysed amination of aryl bromides (Scheme 0-6. Eq. 1),[40] using toxic tin derivatives as nucleophiles. This fact, together with the small reaction scope probably made this coupling unattractive and thereby, this work was not referenced for over ten years.

ACS Catal. 2018, 8, 7228–7250. d) J. P. Tassone, E. V. England, P. M. MacQueen, M. J. Ferguson, M. Stradiotto, Angew. Chem. Int. Ed. 2019, 58, 2385–2489. e) E. B. Corcoran, M. T. Pirnot, S. Lin, S. D. Dreher, D. A. DiRocco, I. W. Davies, S. L. Buchwald, D. W. C. MacMillan, Science 2016, 353, 279– 283. f) E. M. Wiensch, J. Montgomery, Angew. Chem. Int. Ed. 2018, 57, 11045–11049. For selected examples using other transition metals, see: g) M. R. Brennan, D. Kim, A. R. Fout, Chem. Sci. 2014, 5, 4831–4839. h) M. Kim, S. Chang, Org. Lett. 2010, 12, 1640–1643.

[59] (1) Miyaura, N.; Yamada, K.; Suzuki, A. A New Stereospecific Cross-Coupling by the Palladium-Catalyzed Reaction of 1-Alkenylboranes with 1-Alkenyl or 1-Alkynyl Halides. *Tetrahedron Lett.* **1979**, *20* (36), 3437–3440. https://doi.org/10.1016/S0040-4039(01)95429-2.

(1) Bunnett, J. F.; Zahler, R. E. Aromatic Nucleophilic Substitution Reactions. *Chem. Rev.* **1951**, *49* (2), 273–412. https://doi.org/10.1021/cr60153a002.

(1) Heaney, H. The Benzyne and Related Intermediates. *Chem. Rev.* **1962**, *62* (2), 81–97. https://doi.org/10.1021/cr60216a001.

(1) Bunnett, J. F.; Hrutfiord, B. F. Cleavage of O-Halobenzophenones by Potassium Amide in Liquid Ammonia. *J. Org. Chem.* **1962**, *27* (12), 4152–4156. https://doi.org/10.1021/jo01059a009.

Scheme 0-6. First C-N cross-coupling reactions

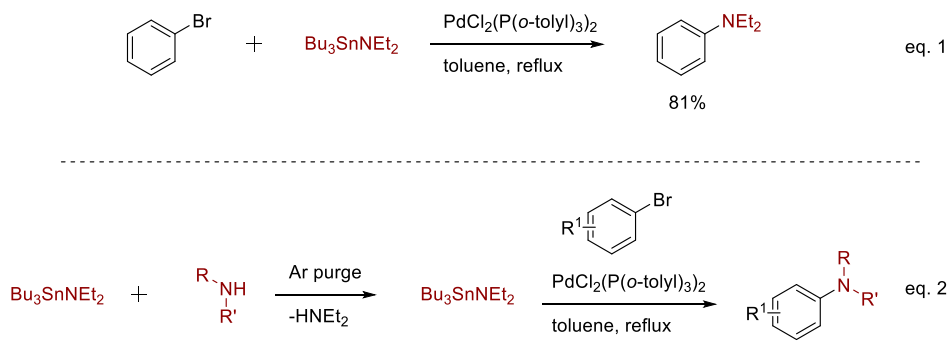

At this point, Hartwig and Buchwald independently were interested in this topic. On the one hand, Hartwig started to study the Migita's reaction mechanism;[50b] and on the other, Buchwald started to improve the methodology by generating the stannylamines *in situ*, affording a wider scope of products (Scheme 0-6. Eq. 2).[50c] These were the first steps towards the free-tin reaction, or what we actually call the Buchwald-Hartwig reaction.

In fact, the following year, in 1995, both authors reported their advances using free amines or amides as coupling partners (Scheme 0-7).[60]

[60] (1) Louie, J.; Hartwig, J. F. Palladium-Catalyzed Synthesis of Arylamines from Aryl Halides. Mechanistic Studies Lead to Coupling in the Absence of Tin Reagents. *Tetrahedron Lett.* **1995**, *36* (21), 3609–3612. https://doi.org/10.1016/0040-4039(95)00605-C.
(1) Guram, A. S.; Rennels, R. A.; Buchwald, S. L. A Simple Catalytic Method for the Conversion of Aryl Bromides to Arylamines. *Angew. Chemie Int. Ed. English* **1995**, *34* (12), 1348–1350. https://doi.org/10.1002/anie.199513481.

Scheme 0-7. First steps in the Buchwald-Hartwig reaction: C-N cross-coupling with free amines and proposed reaction mechanism

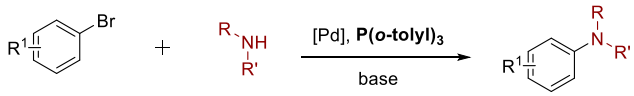

Migita reaction

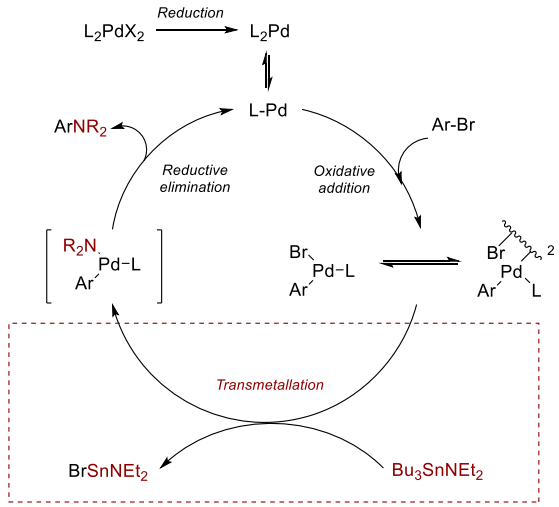

Buchwald-Hartwig Reaction

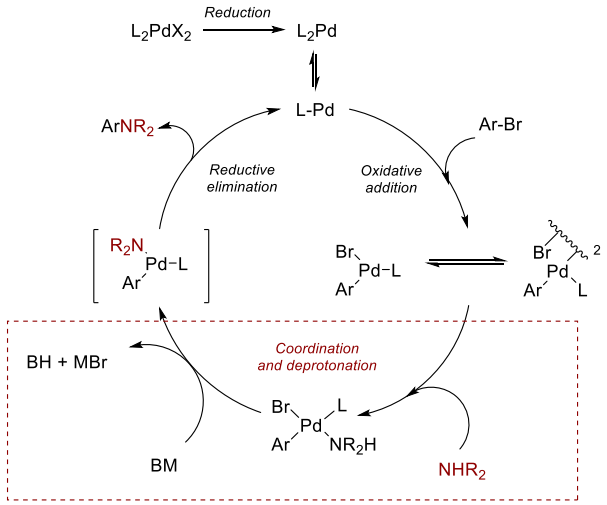

Regarding the mechanism in the reaction, it is proposed the transmetallation step in the Migita reaction is replaced by the coordination of the amine and subsequent deprotonation, as the acidity of the amine would be increased in this situation. In addition, kinetic and mechanistic studies carried out by

Hartwig seemed to point three coordinate palladium complexes as key intermediates in the cycle. The formation of 3-coordinated[61] species, facilitated by the steric hindrance of P(*o*-tolyl)$_3$, is responsible to favour the reductive elimination, which seems to be the rate determining step, over β-hydride elimination.[62]

Other mechanistic considerations studied by Hartwig revealed that the reductive elimination was also enhanced by the use of bulky and nucleophilic amines and electron-deficient aryl halide counterparts,[63] which is in accordance with the reported results.

However, these early years of the Buchwald-Hartwig reaction was characterized for several challenging problems to solve. For instance, the methodology was still confined to the use of aryl bromides. Besides, secondary and primary amines often underwent β-elimination reactions.[62] In fact, primary alkyl amines were only (moderately) affordable with electron-withdrawing or hindered *o*-substituted bromides.

Second generation catalysts: chelating ligands

Since the times of Migita's seminal work, the catalytic system was defined by the use of the bulky P(*o*-tolyl)$_3$ as the use of other ligands failed to provide good results. Not even chelating bis(phosphines) of the family of dppe were able to achieve this goal, which was not surprising according to the Hartwig's model of 3-coordinated species, at least with P(*o*-tolyl)$_3$.

Figure 6. Ligands of the family of dppe

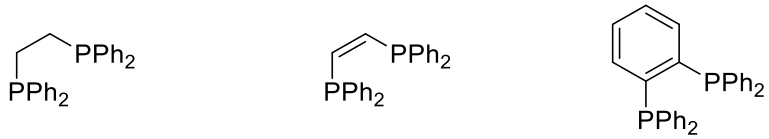

[61] (1) Driver, M. S.; Hartwig, J. F. A Rare, Low-Valent Alkylamido Complex, a Diphenylamido Complex, and Their Reductive Elimination of Amines by Three-Coordinate Intermediates. *J. Am. Chem. Soc.* **1995**, *117* (16), 4708–4709. https://doi.org/10.1021/ja00121a030.

[62] β-hydride elimination is only possible with alkyl amines.

[63] (1) Hartwig, J. F.; Richards, S.; Barañano, D.; Paul, F. Influences on the Relative Rates for C–N Bond-Forming Reductive Elimination and β-Hydrogen Elimination of Amides. A Case Study on the Origins of Competing Reduction in the Palladium-Catalyzed Amination of Aryl Halides. *J. Am. Chem. Soc.* **1996**, *118* (15), 3626–3633. https://doi.org/10.1021/ja954121o.

Nevertheless, Buchwald attempted to overcome this limited catalytic system and tried to accomplish the cross-coupling reaction in the presence of $Pd_2(dba)_3$ and BINAP as the ligand.[64] Importantly, the reaction not only took place, but also provided even better results than the Pd(0)/P(*o*-tolyl)$_3$ system. For instance, this new catalyst afforded better yields and the reaction could be performed at a lower temperature (around 20 °C lower) and even at a 0.05% catalyst loading. In addition, and most importantly, primary amines could be successfully cross-coupled with aryl bromides, both electron-donating and electron-withdrawing ones.

Scheme 0-8. Example of the improvement of the Buchwald-Hartwig amination using BINAP as the ligand.

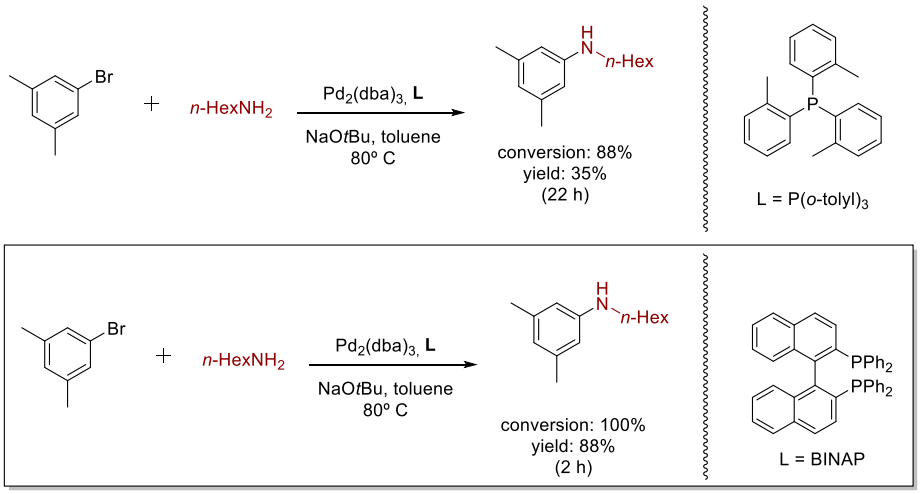

At this point, Buchwald suspected BINAP properties might be unique in contrast to other chelating bisphosphines (Scheme 0-8). On the other hand, the intermediate of the oxidative addition step could be synthesised and proved to be active in the catalytic cycle, proving that bis(phosphine) ligands are suitable ligands for the reaction and 4-coordinated species may be involved in the cycle. In fact, the existence of this kind of intermediates could be the reason why β-elimination was avoided, prevented by the saturation of the complex. The drop of this side-reaction accounts for the efficiency and broader scope of this system.

[64] (1) Wolfe, J. P.; Wagaw, S.; Buchwald, S. L. An Improved Catalyst System for Aromatic Carbon-Nitrogen Bond Formation: The Possible Involvement of Bis(Phosphine) Palladium Complexes as Key Intermediates. *J. Am. Chem. Soc.* **1996**, *118* (30), 7215–7216. https://doi.org/10.1021/ja9608306.

Scheme 0-9. Proposed mechanism for the Buchwald-Hartwig amination with chelating bisphosphines ligands

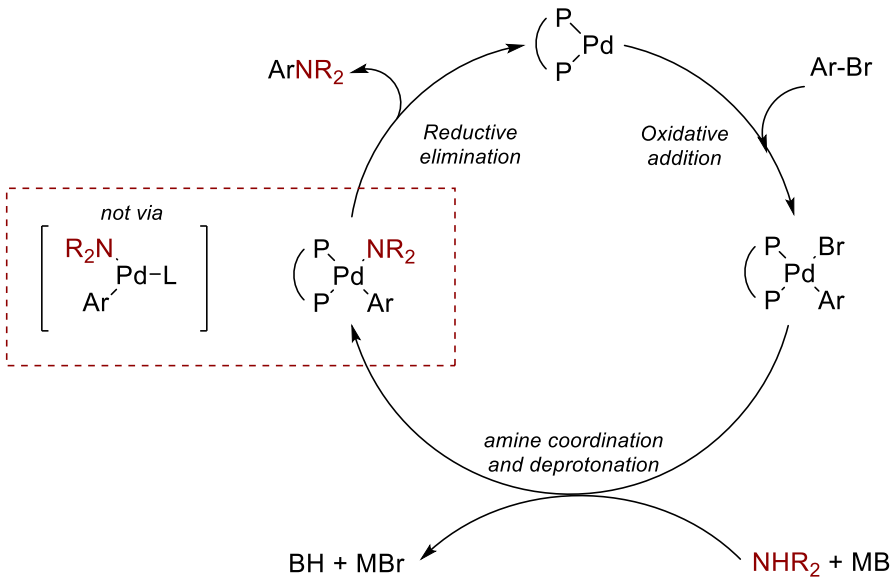

In summary, the use of BINAP as ligand marked a big step forward in the development of the reaction.

Simultaneously, in the same vein of Buchwald's finding, Hartwig studied the reactivity palladium amido complexes containing chelating bis(phosphines) as he also found that 4- and 3-coordinated monophosphine complexes could undergo reductive elimination in competition.[65] Most of ligands did not form stable complexes or yield the C-N bond forming products. The only exception he found was the case of DPPF which could be isolated and achieve the corresponding substituted amines upon heating (Scheme 0-10). In general terms, compared to first generation catalyst, (Pd/P(*o*-tolyl)$_3$), the yields were improved and the reaction could also be carried out effectively with aryl iodides. These substrates had been coupled using Pd(*o*-tolyl)$_3$, but special conditions were required and the results were poorer than those obtained with aryl bromides.[66] Besides, this DPPF/Pd catalytic system was also able to cross-couple primary aromatic and alkyl amines with electron-poor halides

[65] (1) Driver, M. S.; Hartwig, J. F. Carbon−Nitrogen-Bond-Forming Reductive Elimination of Arylamines from Palladium(II) Phosphine Complexes. J. Am. Chem. Soc. **1997**, 119 (*35*), 8232–8245. https://doi.org/10.1021/ja971057x.

[66] (1) Wolfe, J. P.; Buchwald, S. L. Palladium-Catalyzed Amination of Aryl Iodides. *J. Org. Chem.* **1996**, *61* (3), 1133–1135. https://doi.org/10.1021/jo951844h.

with excellent yields. As a limitation, the reaction did not proceed with secondary alkyl amines.[67]

Scheme 0-10. Amido complex isolation and application of DPPF as the ligand in the Buchwald-Hartwig reaction

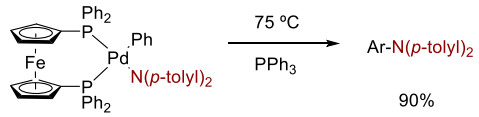

Hartwig's methodology based on the use of DPPF

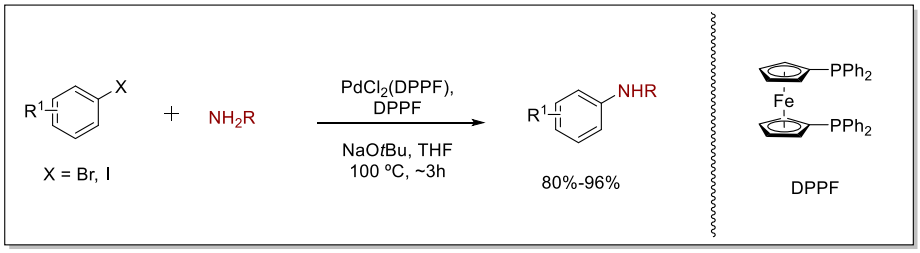

Buchwald's C-N cross-coupling reaction emplyoing BINAP as the ligand

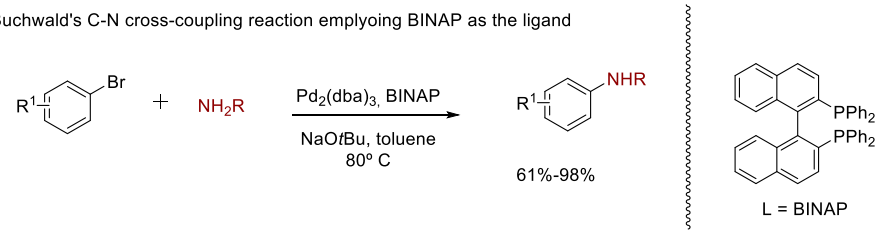

On the other hand, as DPPF is a smaller than P(*o*-tolyl)$_3$, the preference of reductive over β-elimination seems to be due to geometrical and coordination considerations rather than steric hindrance.

To sum up, these two ligands, DPPF and BINAP, represented the second generation of catalysts, and paved the way to the development of new systems based on chelating bis(phophine) ligands (Scheme 0-10).

Besides the already known problem of the C-N cross-coupling with secondary alkyl amines, there were other problems to solve yet. Hence, there were still room for improvement. For instance, the electrophiles were confined mainly to aryl bromides while reaction with the more convenient chlorides or

[67] (1) Driver, M. S.; Hartwig, J. F. A Second-Generation Catalyst for Aryl Halide Amination: Mixed Secondary Amines from Aryl Halides and Primary Amines Catalyzed by (DPPF)PdCl2. *J. Am. Chem. Soc.* **1996**, *118* (30), 7217–7218. https://doi.org/10.1021/ja960937t.

pseudohalides remained underdeveloped, despite the use of the latter in the Stille and Suzuki-Miyaura reaction.[68]

In this regard, Hartwig found that both ligands (DPPF and BINAP) catalyse the reaction of amines with triflates while P(*o*-tolyl)$_3$ was ineffective in this transformation. Thus, anilines were very well tolerated substrates, moderate to good yields were obtained with primary and cyclic secondarly amines while alkyl aryl amines gave worse results than the coupling with halides counterparts.[69]

In the search of more active and cheaper bidentate bis(phosphine) ligands, the family of Xantphos, firstly developed for the rhodium-catalysed hydroformylation, [70] emerged as an alternative system to BINAP which years after their synthesis were used by van Leeuwen[71] and Buchwald[72] itself in the C-N amination.

To further improve the substrate scope and selectivity, new catalysts had to be developed and such a task required mechanistic information.

As we have mentioned, Hartwig performed several studies involving the reaction mechanism with monodentate and chelating phosphines; and synthetic amido complexes.[65]

First, it was found that the reaction mechanism involving monophosphines such as P(*o*-tolyl)$_3$ could take place with 4-coordinated species in the presence of high concentration of phosphine, in addition to the 3-coordinated 14

---

[68] (12) Echavarren, A. M.; Stille, J. K. J. Am. Chem. Soc. 1987, 109, 5478-5486. (13) Oh-e, T.; Miyaura, N.; Suzuki, A. J. Org. Chem. 1993, 58, 2201. (14) Ritter, K. Synthesis 1993, 735

[69] (1) Louie, J.; Driver, M. S.; Hamann, B. C.; Hartwig, J. F. Palladium-Catalyzed Amination of Aryl Triflates and Importance of Triflate Addition Rate. *J. Org. Chem.* **1997**, *62* (5), 1268–1273. https://doi.org/10.1021/jo961930x.

[70] (1) Kranenburg, M.; van der Burgt, Y. E. M.; Kamer, P. C. J.; van Leeuwen, P. W. N. M.; Goubitz, K.; Fraanje, J. New Diphosphine Ligands Based on Heterocyclic Aromatics Inducing Very High Regioselectivity in Rhodium-Catalyzed Hydroformylation: Effect of the Bite Angle. *Organometallics* **1995**, *14* (6), 3081–3089. https://doi.org/10.1021/om00006a057.

[71] (1) Guari, Y.; van Es, D. S.; Reek, J. N. H.; Kamer, P. C. J.; van Leeuwen, P. W. N. M. An Efficient, Palladium-Catalysed, Amination of Aryl Bromides. *Tetrahedron Lett.* **1999**, *40* (19), 3789–3790. https://doi.org/10.1016/S0040-4039(99)00527-4.

[72] (1) Sadighi, J. P.; Harris, M. C.; Buchwald, S. L. A Highly Active Palladium Catalyst System for the Arylation of Anilines. *Tetrahedron Lett.* **1998**, *39* (30), 5327–5330. https://doi.org/10.1016/S0040-4039(98)00988-5.

electrons species mechanism depicted before. In addition, this 3-coordinated species are also responsible for the β-elimination reaction.[73]

By contrast, chelating phosphines was proven to follow a mechanism involving 4-coordinated species, preventing β-elimination side-reaction.

To obtain further insight into the impact of the properties of these and other promising chelating ligands in the amination reaction, Hartwig performed a variation of the three main properties of this kind of ligands and studied their activity and selectivity in the amination reaction. Thus, perturbing the electronic, the steric properties and the bite angle, he obtained surprising results:[74]

In sharp contrast to what is expected from a reaction that is governed by the rate of the reductive elimination, the best selectivities, i.e. the highest amine:arene ratios, were achieved with electron rich, not too bulky phosphines with small bite angles. This finding would indicate oxidative addition step would be play a more important role in the reaction.

In line with this, Hartwig also found that the aforementioned chelating phosphines formed a 2-ligated palladium complex as the resting state of the catalytic system. Hence, the rate determining step would be the oxidative addition. However, the dissociation of one ligand is required for such step and therefore, a good catalyst design would also facilitate this.

Taking this into consideration and the great activity of chelating ligands, an electron-rich phosphine would enhance the rate of the oxidative addition and a bulky enough phosphine would also facilitate the dissociation of the resting state. Therefore, Hartwig's group tested the ability of dialkylphosphino chelating ligands such as D^{t}BPF, among others to catalyse the amination of different aryl halides, including chlorides, and tosylates.[75]

---

[73] (1) Hartwig, J. F. Directly-Observed β-Hydrogen Elimination of a Late Transition Metal Amido Complex and Unusual Fate of Imine Byproducts. *J. Am. Chem. Soc.* **1996**, *118* (29), 7010–7011. https://doi.org/10.1021/ja961439n.

[74] (1) Hamann, B. C.; Hartwig, J. F. Systematic Variation of Bidentate Ligands Used in Aryl Halide Amination. Unexpected Effects of Steric, Electronic, and Geometric Perturbations. *J. Am. Chem. Soc.* **1998**, *120* (15), 3694–3703. https://doi.org/10.1021/ja9721881.

[75] (1) Hamann, B. C.; Hartwig, J. F. Sterically Hindered Chelating Alkyl Phosphines Provide Large Rate Accelerations in Palladium-Catalyzed Amination of Aryl Iodides, Bromides, and Chlorides, and the First Amination of Aryl Tosylates. *J. Am. Chem. Soc.* **1998**, *120* (29), 7369–7370. https://doi.org/10.1021/ja981318i.

These catalysts showed a very good catalytic activity and selectivity. In addition, the amination of unactivated chlorides[76] was achieved for the first time as well as the use of tosylates in this kind of reaction.

Third generation catalysts: bulky and biphenyl-based phosphines

As for Buchwald, he also found by NMR measurements that oxidative addition was the determining step for the BINAP/Pd(0) system, so his laboratory aimed to design new catalysts to enhance this step and additionally, overcome the poor reactivity of aryl chlorides, due to its relative inertness toward oxidative addition. Based on a previous work,[77] he envisioned the synthesis of an electron rich dialkyl phosphino-biphenyl-amine ligand to achieve this goal (Figure 7).[78]

Figure 7. Electron-rich phosphino-biphenyl ligand developed by Buchwald

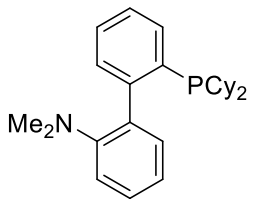

This ligand gave excellent results in the amination of chlorides and bromides, which was active even at room temperature.

Nevertheless, for the case of the aryl chlorides, only the very activated 4-chlorobenzonitrile underwent the reaction at room temperature so, further investigations of this third new generation of ligands needed to be accomplished.

In this context, Buchwald wondered whether the use of a bulkier substitution on the phosphine would improve the activity and if the amine group was necessary for the catalysis. Indeed, the activity of the catalyst improved with

---

[76] (1) Beller, M.; Riermeier, T. H.; Reisinger, C. P.; Herrmann, W. A. First Palladium-Catalyzed Aminations of Aryl Chlorides. *Tetrahedron Lett.* **1997**, *38* (12), 2073–2074. https://doi.org/10.1016/S0040-4039(97)00289-X.

[77] (1) Marcoux, J.-F.; Wagaw, S.; Buchwald, S. L. Palladium-Catalyzed Amination of Aryl Bromides: Use of Phosphinoether Ligands for the Efficient Coupling of Acyclic Secondary Amines. *J. Org. Chem.* **1997**, *62* (6), 1568–1569. https://doi.org/10.1021/jo9622946.

[78] (1) Old, D. W.; Wolfe, J. P.; Buchwald, S. L. A Highly Active Catalyst for Palladium-Catalyzed Cross-Coupling Reactions: Room-Temperature Suzuki Couplings and Amination of Unactivated Aryl Chlorides. *J. Am. Chem. Soc* **1998**, *120* (37), 9722–9723. https://doi.org/https://doi.org/10.1021/ja982250+

t-butyl substitution on the phosphine, presumably due to an enhance of the reductive elimination step. On the other hand, the amine was found not to be an essential substitution and the deaminated ligands proved to be sexcellent ligands for the reaction. Thus, the reaction could be performed at room temperature using aryl chlorides with secondary and primary alkyl amines, although the latter required *o*-substitution at the aryl chloride counterpart.[79]

In the search for a more general catalysts that overcome the limitations of this ligand, Buchwad's group also prepared other biphenyl-derived phosphines (5, 6).[80]

Figure 8. Some biphenyl phosphines ligands developed by Buchwald's group

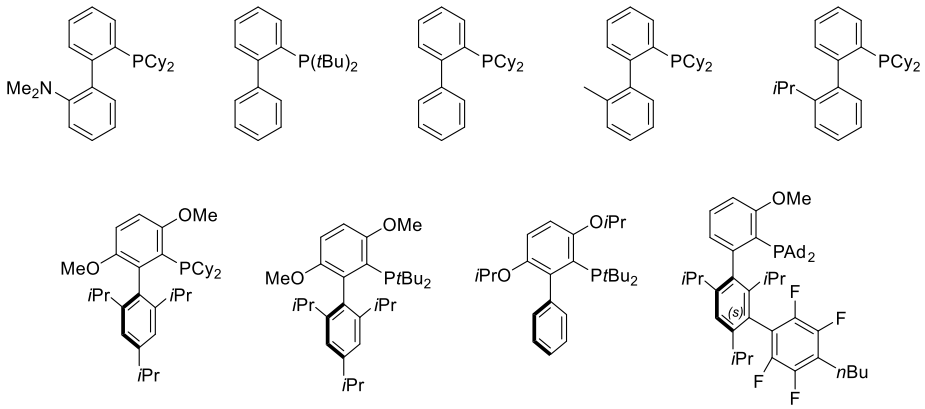

The use of this small family of ligands afforded the use of bromides, chlorides and triflates of different nautre, even chloropyridines were suitable substrates. Additionally, a good combination of these catalysts could also tolerate base-sensitive functionalities such as methyl esters, ketones, nitriles, etc.

Mechanistically, this kind of ligands may function as P(*o*-tolyl)$_3$, as it seems to follow a three-coordinated mechanism, although some interaction between the second phenyl ring may occur. The main improvements lie in the unique steric and electronic properties of the ligand that affect different points at the

[79] (1) Wolfe, J. P.; Buchwald, S. L. A Highly Active Catalyst for the Room-Temperature Amination and Suzuki Coupling of Aryl Chlorides. *Angew. Chemie - Int. Ed.* **1999**, *38* (16), 2413–2416. https://doi.org/10.1002/(SICI)1521-3773(19990816)38:16<2413::AID-ANIE2413>3.0.CO;2-H.

[80] (1) Wolfe, J. P.; Tomori, H.; Sadighi, J. P.; Yin, J.; Buchwald, S. L. Simple, Efficient Catalyst System for the Palladium-Catalyzed Amination of Aryl Chlorides, Bromides, and Triflates. *J. Org. Chem.* **2000**, *65* (4), 1158–1174. https://doi.org/10.1021/jo991699y.

catalytic cycle. Hence, the electron rich phosphine enhances the oxidative addition which is even affordable for aryl chlorides. On the other hand, the formation of the Pd-N bond is facilitated by the formation of a monophosphine palladium complex and the steric hindrance would enhance the reductive elimination step.

In these systems, the rate determining step seems to be the Pd-N bond formation or the reductive elimination, depending on the amine. Thus, for the more acidic anilines, the slowest step would be the reductive elimination, whereas for aliphatic amines, it would be the formation of the amido complex.

Nevertheless, the Buchwald-type family of ligands, i.e. dialkyl biphenyl monophosphines, proved to be more powerful and were furtherly expanded over the years,[81] making the reaction even more versatile. For instance, recently the use of 12 has allowed for the use of an organic base, DBU, in the Buchwald-Hartwig reaction.[82]

On the other hand, biphenyl phosphines were not the only family of bulky monophosphines that were applied to the amination reaction.

Josiphos ligands

Despite all these advancements in the catalytic C-N coupling reaction and almost every combination of substrates has been covered, the coupling of some of them were still partially solved and a more active and general catalyst

---

[81] (1) Fors, B. P.; Dooleweerdt, K.; Zeng, Q.; Buchwald, S. L. An Efficient System for the Pd-Catalyzed Cross-Coupling of Amides and Aryl Chlorides. *Tetrahedron* **2009**, *65* (33), 6576–6583. https://doi.org/10.1016/j.tet.2009.04.096.

(1) Huang, X.; Anderson, K. W.; Zim, D.; Jiang, L.; Klapars, A.; Buchwald, S. L. Expanding Pd-Catalyzed C-N Bond-Forming Processes: The First Amidation of Aryl Sulfonates, Aqueous Amination, and Complementarity with Cu-Catalyzed Reactions. *J. Am. Chem. Soc.* **2003**, *125* (22), 6653–6655. https://doi.org/10.1021/ja035483w.

(2) Maiti, D.; Fors, B. P.; Henderson, J. L.; Nakamura, Y.; Buchwald, S. L. Palladium-Catalyzed Coupling of Functionalized Primary and Secondary Amines with Aryl and Heteroaryl Halides: Two Ligands Suffice in Most Cases. *Chem. Sci.* **2011**, *2* (1), 57–68. https://doi.org/10.1039/c0sc00330a.

(3) Fors, B. P.; Watson, D. A.; Biscoe, M. R.; Buchwald, S. L. A Highly Active Catalyst for Pd-Catalyzed Amination Reactions: Cross-Coupling Reactions Using Aryl Mesylates and the Highly Selective Monoarylation of Primary Amines Using Aryl Chlorides. *J. Am. Chem. Soc.* **2008**, *130* (41), 13552–13554. https://doi.org/10.1021/ja8055358.

[82] (1) Dennis, J. M.; White, N. A.; Liu, R. Y.; Buchwald, S. L. Breaking the Base Barrier: An Electron-Deficient Palladium Catalyst Enables the Use of a Common Soluble Base in C–N Coupling. *J. Am. Chem. Soc.* **2018**, *140* (13), 4721–4725. https://doi.org/10.1021/jacs.8b01696.

would be desirable. In this regard chlorides halides, which are the cheapest and therefore, the most interesting halides are the less reactive and primary amines keep on giving some trouble of selectivity. In addition, some heterocycle halides are more challenging substrates due to the coordination properties arising from the heteroatom. Hence, a catalytic system that could deal with all these problems is desirable.

At this juncture, Hartwig[83] reasoned which features could enhance the activity and the robustness of the catalytic system and which features could be behind of its deactivation. He envisioned that desirable properties would be long lifetimes, steric hindrance, strong donation and tight binding in a chelating way.

Thus, he performed a series of experiments with this kind of inactivated and/or challenging substrates so as to find a better catalyst.

First, if the catalyst needed to be long-lived, the deactivation must be avoided and the possible route for such a process had to be accounted. Hence, his group studied the stability of [Pd(P*t*Bu$_3$)$_2$] and the corresponding three-coordinate OA Pd(II) complex, [Pd(P*t*Bu3)(tolyl)(Br)], in the presence of pyridine and benzylamine. On the one hand, Pd(0) complex remained unreacted. On the other, Pd(II) did react with both pyridine and benzylamine which displaced the ligand and added to the 4th coordination vacancy, forming 4-coordinated Pd(II) species, despite the basicity of the alkyl phosphine. Thus, the formation of complexes with pyridine or primary amines could be the reason of the slower rates of amination of this kind of substrates, since they do not catalyse the reaction.

A possible solution to this problem would be a chelating bis(phosphine) to prevent the replacement and dissociation; and still possesses high steric hindrance and strong electron donation to keep high activity. Nevertheless, the use of bis(phosphines) may evolve other problems: the possible formation of polymeric structures, a change in the denticity to κ^1, and the formation of Pd(0)L2 complexes. Thus, κ^1 mode of coordination makes the ligand be more prone to substitution, and the formation of PdL2 complexes may slow down the oxidative addition as ligand dissociation is necessary prior to this step.

[83] (1) Shen, Q.; Shekhar, S.; Stambuli, J. P.; Hartwig, J. F. Highly Reactive, General, and Long-Lived Catalysts for Coupling Heteroaryl and Aryl Chlorides with Primary Nitrogen Nucleophiles. *Angew. Chemie - Int. Ed.* **2005**, *44* (9), 1371–1375. https://doi.org/10.1002/anie.200462629.

Therefore, the chelating ligand should be very rigid in order to avoid these possibilities.

In this context, Josiphos ligand CyPF-*t*Bu was an excellent candidate as it fulfils all this requirement. Thus, its catalytic activity was tested with the challenging aryl and pyridyl chlorides with primary amines.

Figure 9. Josiphos ligand CyPF-tBu

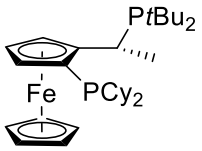

The performance and selectivity for the monoarylation of this new catalytic system was extraordinary, achieving very high activity (at ppm scale) exceeding those of the previous catalysts for at least 2 orders of magnitude. In addition, it could catalyse the amidation of chloropyridines for the first time and showed an excellent functional group tolerance. For instance, protic functionalities such as -OH, were well tolerated despite the use of LiHMDS as base. In this regard, softer bases make this system be less effective than others.

NHC ligands

In the context of the search of new catalyst to improve the catalytic C-N bond formation allowing for the preparation of amines from aryl chlorides and the use of primary alkyl amines without side problems of selectivity or β-elimination, the use and/or design of new ligands is of critical importance.

With the appearance of NHC ligands in the scenario of catalytic reactions, this kind of ligands attracted the attention of Nolan and applied them in C-C cross couplings of such as Kumada's and Suzuki's with aryl chlorides,[84] so he wondered whether they would catalyse the amination of aryl chlorides too.

The appealing features of this ligands rely on the fact that they form very stable metal complexes, so no excess of ligand is required, preventing the formation of polyligated species that may deactivate the catalyst. Besides, their stereoelectronic properties are very attractive for C-N couplings for three reasons. First, their good electron donor ability points to favour the oxidative addition of challenging substrates such as chlorides. Second, the 2,5-substituion pattern make them sterically demanding. And last but not least,

[84] Zhang, C.; Huang, J.; Trudell, M. L.; Nolan, S. P. J. Org. Chem. **1999**, 64, 3804-3805

from the different substitution of the parent imidazolium salts, modulation of this properties is possible.

Thus, the use of IPrHCl salt allowed for the *in situ* formation of the palladium catalyst, affording the coupling reaction of primary and secondary amines with chlorides, bromides and iodides with excellent yields.[85]

Figure 10. Imidazolium salts as NHC precursors

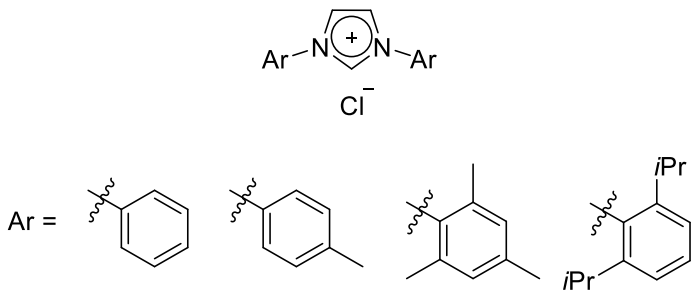

Subsequently, Hartwig used a similar ligand to perform the C-N catalytic reaction.[86] Thus, the corresponding dihydroimidazoline NHC from Figure 11 showed excellent catalytic properties, achieving the coupling reaction with aryl chlorides with different amines with low catalytic loadings and even at room temperature. The arylation of primary alkyl amines were poor though. Remarkably, the reaction was also successful with pyridyl chlorides, which usually give poor results presumably owing to their ability to replace phosphines, inhibiting the catalyst. The stability of the NCH carbene complexes seems to be a key role for coupling of these pyridyl chlorides at room temperature.

Figure 11. Dihydroimidazolium salt as precursor of NHC ligand

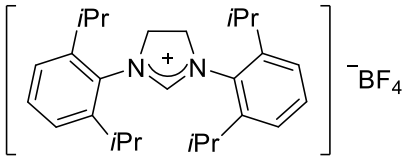

[85] (1) Huang, J.; Grasa, G.; Nolan, S. P. General and Efficient Catalytic Amination of Aryl Chlorides Using a Palladium/Bulky Nucleophilic Carbene System. *Org. Lett.* **1999**, *1* (8), 1307–1309. https://doi.org/10.1021/ol990987d.

[86] (1) Stauffer, S. R.; Lee, S.; Stambuli, J. P.; Hauck, S. I.; Hartwig, J. F. High Turnover Number and Rapid, Room-Temperature Amination of Chloroarenes Using Saturated Carbene Ligands. *Org. Lett.* **2000**, *2* (10), 1423–1426. https://doi.org/10.1021/ol005751k.

Further development of NHC-based catalysts relied on the precatalyst modification rather than the ligand design itself. With these variations, different improvements such as broader scope, use of pseudohalides, lower temperature and reaction times were achieved.

Figure 12. Selected NHC-based precatalysts

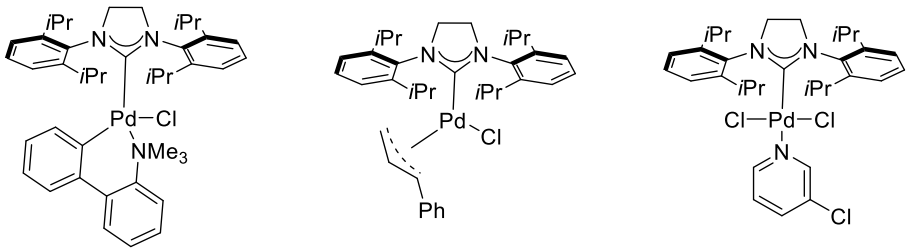

Other important features and considerations of the Buchwald-Hartwig reaction.

Other N-containing substrates beyond amines

So far, we have focused on the historical development of the reaction as well as the mechanistic implications of each new catalytic system. Along with the improvement of the ligands, a broader scope of coupling partners has been achieved, encompassing different halides and pseudahalides; and different types of amines.

On the other hand, the application of this methodology to other N-containing coupling partners have been obviated for simplification and a better understanding of the improvements over the years.

Notwithstanding, achievements for this kind of substrates will be shortly discussed in this section.

Thus, there exist other N-containing functionalities that could be act as substrates for the C-N cross-coupling reaction. For instance, the direct arylation of amides, sulphonamides, imines, etc. could be interesting from the synthetic point of view, achieving more direct synthesis of target molecules and besides, some of this groups could be seen as protecting groups, paving the way to the synthesis primary aryl amines.

The main issue concerning this kind of functionalities is the rather acidic character of the N and the reductive C-N bond formation is usually facilitated by nucleophilic amines. In addition, the presence of other coordinating atoms may interfere in the coordination chemistry and hence the catalytic cycle.

Nevertheless, Buchwald-Hartwig methodologies have expanded, providing direct access to this kind of molecules.

Hence, the coupling of carbamate could be first achieved with P(*t*Bu)$_3$ as ligand and using NaOPh as the base.[87]

Although the analogous amidation reaction had been previously reported in an intramolecular fashion since the early years of the reaction,[112,88] the intermolecular version had been unsuccesfull except for the previous coupling of carbamate. It was Buchwald who uncovered Xantphos/Pd(OAc)$_2$ system could accomplish such a task. Therefore, not only amides and lactams,[89] but carbamates and sulphonamides could also be coupled with aryl halides and triflates.[90] In this regard, carbamates and amides seemed to have the same reactivity while sulphonamides were more inert.

Afterwards, the catalytic system for substituted amide formation has been improved so that the limitations could be overcome, for instance, biphenyl-backboned alkylphosphine tBuBrettPhos ligand performed the reaction with excellent yields even with *o*-substituted aryl chlorides.[91]

The sulfonyl analogous of lactams, the sultams were later synthesised applying the Buchwald-Hartwig amination based on the XantPhos system previously used for the coupling with sulphonamides.[92]

---

[87] (1) Hartwig, J. F.; Kawatsura, M.; Hauck, S. I.; Shaughnessy, K. H.; Alcazar-Roman, L. M. Room-Temperature Palladium-Catalyzed Amination of Aryl Bromides and Chlorides and Extended Scope of Aromatic C−N Bond Formation with a Commercial Ligand. *J. Org. Chem.* **1999**, *64* (15), 5575–5580. https://doi.org/10.1021/jo990408i.

[88] (1) Yang, B. H.; Buchwald, S. L. The Development of Efficient Protocols for the Palladium-Catalyzed Cyclization Reactions of Secondary Amides and Carbamates. *Org. Lett.* **1999**, *1* (1), 35–38. https://doi.org/10.1021/ol9905351.

[89] (1) Shakespeare, W. C. Palladium-Catalyzed Coupling of Lactams with Bromobenzenes. *Tetrahedron Lett.* **1999**, *40* (11), 2035–2038. https://doi.org/10.1016/S0040-4039(99)00086-6.

[90] (1) Yin, J.; Buchwald, S. L. Palladium-Catalyzed Intermolecular Coupling of Aryl Halides and Amides. *Org. Lett.* **2000**, *2* (8), 1101–1104. https://doi.org/10.1021/ol005654r.

(1) Yin, J.; Buchwald, S. L. Pd-Catalyzed Intermolecular Amidation of Aryl Halides: The Discovery That Xantphos Can Be Trans-Chelating in a Palladium Complex. *J. Am. Chem. Soc.* **2002**, *124* (21), 6043–6048. https://doi.org/10.1021/ja012610k.

[91] (1) Fors, B. P.; Dooleweerdt, K.; Zeng, Q.; Buchwald, S. L. An Efficient System for the Pd-Catalyzed Cross-Coupling of Amides and Aryl Chlorides. *Tetrahedron* **2009**, *65* (33), 6576–6583. https://doi.org/10.1016/j.tet.2009.04.096.

[92] (1) Steinhuebel, D.; Palucki, M.; Askin, D.; Dolling, U. Synthesis of N-Arylated Sultams: Palladium- and Copper-Catalyzed Cross Coupling of Aryl Halides with 1,4-

Another related family of compounds are ureas, which could also be first coupled by Beletskaya using the same ligand, Xantphos. Thereby, symmetrical, and unsymmetrical *N,N*'-phenyl ureas could be obtained with this catalyst and activated aryl bromides.[93]

Other N-containing substrates that have been successfully coupled are hydrazones,[94] providing a way to access to indoles, *via* Fischer synthesis utilizing BINAP or Xantphos as ligand, the latter providing better results though.

Ammonia equivalents

Despite the great advances accomplished in the amine coupling reaction for the synthesis of different substituted arylamines, the coupling of ammonia to afford the parent anilines was a problem that was not resolved yet. However, this issue could be surrounded by coupling amines that were prone to be deprotected later on.

In response to this problem, several ammonia surrogates have been used.

For instance, several alkylamines can be viewed as protecting groups. This would be the case of allyl-, diallyl- or benzylamino groups, for example. Therefore, these masked amines have been conveniently coupled and subsequently deprotected.[95]

Butane and 1,3-Propanesultams. *Tetrahedron Lett.* **2004**, *45* (16), 3305–3307. https://doi.org/10.1016/j.tetlet.2004.02.081.

[93] (1) Artamkina, G. A.; Sergeev, A. G.; Beletskaya, I. P. Palladium-Catalyzed Reaction of Aryl Halides with Ureas. *Tetrahedron Lett.* **2001**, *42* (26), 4381–4384. https://doi.org/10.1016/S0040-4039(01)00716-X.

[94] (1) Wagaw, S.; Yang, B. H.; Buchwald, S. L. A Palladium-Catalyzed Strategy for the Preparation of Indoles: A Novel Entry into the Fischer Indole Synthesis. *J. Am. Chem. Soc.* **1998**, *120* (26), 6621–6622. https://doi.org/10.1021/ja981045r.

(1) Wagaw, S.; Yang, B. H.; Buchwald, S. L. A Palladium-Catalyzed Method for the Preparation of Indoles via the Fischer Indole Synthesis. *J. Am. Chem. Soc.* **1999**, *121* (44), 10251–10263. https://doi.org/10.1021/ja992077x.

[95] (1) Jaime-Figueroa, S.; Liu, Y.; Muchowski, J. M.; Putman, D. G. Allyl Amines as Ammonia Equivalents in the Preparation of Anilines and Heteroarylamines. *Tetrahedron Lett.* **1998**, *39* (11), 1313–1316. https://doi.org/10.1016/S0040-4039(97)10877-2.

(1) Prim, D.; Campagne, J.-M.; Joseph, D.; Andrioletti, B. Palladium-Catalysed Reactions of Aryl Halides with Soft, Non-Organometallic Nucleophiles. *Tetrahedron* **2002**, *58* (11), 2041–2075. https://doi.org/10.1016/S0040-4020(02)00076-5.

Among this kind of surrogates, we can find benzophenone imine. This ammonia equivalent is very interesting since it is expected to be a very convenient nucleophile in the reaction because it cannot undergo β-elimination. Additionally, this protecting group can be easily removed under different conditions. Hence, Buchwald's group could couple this imine with different halides and triflates using the BINAP/$Pd(OAc)_2$ catalytic system with excellent results.[96]

Subsequently, Hartwig studied the reaction of different aryl bromides with N(sp^2) containing coupling partners, i.e., pyrroles and the aforementioned imine.[97] $Pd(OAc)_2$/DPPF was a competitive catalytic system for this goal. Additionally, studies on the C-N reductive elimination revealed that this step required higher temperature for pyrroles and the rates were similar in the case of imine and anilines, showing that nucleophilicity of the amine plays an important role. In order to favour the reductive elimination when arylating pyrrole containing substrates, the use of the electron donor and bulky P(*t*Bu)$_3$ afforded the reaction using milder conditions.[98]

On the other hand, Hartwig's group also used lithium bis(trimethylsilyl)amide as coupling partner in a catalytic system defined by $Pd(dba)_2$ and P(*t*Bu)$_3$.[99] Other phosphines or even NHC-based ligands were ineffective or inferior for this transformation. The reaction could be performed under mild conditions with *m*- and *p*- substituted chlorides and bromides. Nevertheless, *o*-aryl halides, which usually are good electrophiles in the Buchwald-Hartwig reaction were ineffective due to the steric hindrance it exerts over the bulky bis(trimethylsilyl)amide. In the same line, the lower yields obtained when

[96] (1) Wolfe, J. P.; Åhman, J.; Sadighi, J. P.; Singer, R. A.; Buchwald, S. L. An Ammonia Equivalent for the Palladium-Catalyzed Amination of Aryl Halides and Triflates. *Tetrahedron Lett.* **1997**, *38* (36), 6367–6370. https://doi.org/10.1016/S0040-4039(97)01465-2.

[97] (1) Mann, G.; Hartwig, J. F.; Driver, M. S.; Fernández-Rivas, C. Palladium-Catalyzed C–N(Sp 2) Bond Formation: N -Arylation of Aromatic and Unsaturated Nitrogen and the Reductive Elimination Chemistry of Palladium Azolyl and Methyleneamido Complexes. *J. Am. Chem. Soc.* **1998**, *120* (4), 827–828. https://doi.org/10.1021/ja973524g.

[98] (1) Hartwig, J. F.; Kawatsura, M.; Hauck, S. I.; Shaughnessy, K. H.; Alcazar-Roman, L. M. Room-Temperature Palladium-Catalyzed Amination of Aryl Bromides and Chlorides and Extended Scope of Aromatic C–N Bond Formation with a Commercial Ligand. *J. Org. Chem.* **1999**, *64* (15), 5575–5580. https://doi.org/10.1021/jo990408i.

[99] (1) Lee, S.; Jørgensen, M.; Hartwig, J. F. Palladium-Catalyzed Synthesis of Arylamines from Aryl Halides and Lithium Bis(Trimethylsilyl)Amide as an Ammonia Equivalent. *Org. Lett.* **2001**, *3* (17), 2729–2732. https://doi.org/10.1021/ol016333y.

using the parent silylamine could be attributed to steric factors, since the amine would need to coordinate palladium and then, the approach of the base would abstract the proton in a very hindered situation to form the amido complex.

Similarly, these results are in line with our first attempts to use silylamines as coupling partners.

By contrast, Buchwald overcame the problem of the *o*-substituted aryl halides by using a less hindered silylamide. Thus, if the reaction was performed using triphenylsilylamine, which only bears one bulky silyl group, in the presence of LiHMDS, the desired products were obtained with excellent yields.[100]

Ammonia

Despite primary aryl amines are interesting target molecules, the synthesis of these products relying on the Buchald-Hartwig reaction is confined to the use of ammonia equivalents for different reasons.

First, ammonia can displace phosphine ligands, form bridged structures and deactivate the catalyst.[83] Second, the reductive elimination of Ar-Pd-NH_2 was unknown. And third, a problem of selectivity may arise due the reactivity of the primary amine products. Hence, the direct amination of aryl halides was unreported at the time.

However, after finding Josiphos was an excellent ligand for the C-N cross couplings with chlorides and primary amines, Hartwig tested this ligand in the direct amination of aryl halides.[101] Thus, the reaction afforded good to excellent yields with bromides, the coupling was also effective with aryl chlorides or iodide but the scope on this substrates were not studied, though. By contrast, triflate underwent hydrolysis under these conditions. With this methodology, *o*-aryl substrates could also be aminated, which could not be achieved by using $KN(SiMe_3)_2$. It was also noted that the control of concentration and excess of ammonia is key to achieve good activity and selectivity.

Additionally, the reaction could also be accomplished with $LiNH_2$,[66] which is solid and hence, might be more convenient from an operative point of view.

---

[100] (1) Huang, X.; Buchwald, S. L. New Ammonia Equivalents for the Pd-Catalyzed Amination of Aryl Halides. *Org. Lett.* **2001**, *3* (21), 3417–3419. https://doi.org/10.1021/ol0166808.

[101] (1) Shen, Q.; Hartwig, J. F. Palladium-Catalyzed Coupling of Ammonia and Lithium Amide with Aryl Halides. *J. Am. Chem. Soc.* **2006**, *128* (31), 10028–10029. https://doi.org/10.1021/ja064005t.

Again, the products were obtained in moderate to excellent yields although the selectivity was a little bit lower than that using ammonia. Besides, the parent amido complex Pd(L)(*p*-MeOPh)(NH_2) could be synthesised and for the first time, this kind of complex underwent reductive elimination.

In 2009, an improved version of this catalyst was achieved by replacing the Pd source from Pd(II), difficult to reduce in the absence of β-hydrogens, to Pd(P(*o*-tolyl)$_3$)$_2$. By contrast, Pd(dba)$_2$ is avoided due to the potential tight binding of dba. Thus, the scope of the reaction could be extended to chlorides, iodides and for the first time, to tosylates. Even base-sensitive functionalities were tolerated.

In the meantime, Buchwald demonstrated that biaryl monophosphines could also carried out the arylation of ammonia,[102] not only to achieve anilines but to prepare symmetrical and unsymmetrical secondary and tertiary amines selectively starting from bromides and chlorides of different nature.

The selectivity was achieved by careful selecting the ligand substitution and the unsymmetrical amines were obtained in sequential reactions whenever ammonia excess is removed and the reaction volume was reduced. Addition of a second ligand is required in these cases too.

Additionally, in an effort to make this methodology easier, Hartwig envisioned the use of ammonium salts, as solid, stable source of ammonia for the synthesis of primary amines.[103] After the screening of the previous reported ligands for the arylation of ammonia, it was found that Josiphos/Pd[P(*o*-tolyl)$_3$]$_2$ was the best system to accomplish such a goal. Bromides and chlorides aryls were suitable substrates although the latter exhibited a higher selectivity to form primary amines. In addition, the methodology could be extended to volatile amines such as methyl and ethylamine, which are not common substrates because of this.

[102] (1) Surry, D. S.; Buchwald, S. L. Selective Palladium-Catalyzed Arylation of Ammonia: Synthesis of Anilines as Well as Symmetrical and Unsymmetrical Di- and Triarylamines. *J. Am. Chem. Soc.* **2007**, *129* (34), 10354–10355. https://doi.org/10.1021/ja074681a.

[103] (1) Green, R. A.; Hartwig, J. F. Palladium-Catalyzed Amination of Aryl Chlorides and Bromides with Ammonium Salts. *Org. Lett.* **2014**, *16* (17), 4388–4391. https://doi.org/10.1021/ol501739g.

On the other hand, the use of the P,N-ligand MorDalPhos, allowed for the amination of some aryl chlorides at room temperature for the first time.[104]

Among other catalysts that have proven active in the arylation of ammonia, we can find Pd-NHC[105] and heteroarylphosphines.[106]

Base effect and functional group tolerance

Considering that we aimed to develop a methodology in which triflates and nonaflates can be employed as the electrophile partner, the base tolerance of these substrates is mandatory.

We have seen in some catalytic systems, the reaction turnover determining step is the formation of the amido complex, i.e., the coordination and deprotonation of the amine. It is not surprising that the acid/base properties of the amine and the base play an important role.

On the other hand, it is generally accepted that the formation of the amido complex occurs after deprotonation of the corresponding amino complex, as this coordination would enhance the acidity of the amine. Moreover, the most widely used base for the C-N cross-coupling is NaO*t*Bu, which is not basic enough to deprotonate amines by itself.

Notwithstanding, other unconsidered mechanisms and species may occur and, in this context, Hartwig studied the possible intermediacy of alkoxo complexes in the formation of the amido counterpart. Thus, Hartwig could prepared the corresponding alkoxo complex by substitution of an OA intermediate with NaOtBu, although it decomposes at room temperature within hours. As a consequence, the homocoupling product, biphenyl and the hydrodehalogenated arene was obtained, but no ether formation was observed.

---

[104] (1) Lundgren, R. J.; Peters, B. D.; Alsabeh, P. G.; Stradiotto, M. A P,N-Ligand for Palladium-Catalyzed Ammonia Arylation: Coupling of Deactivated Aryl Chlorides, Chemoselective Arylations, and Room Temperature Reactions. *Angew. Chemie Int. Ed.* **2010**, *49* (24), 4071–4074. https://doi.org/10.1002/anie.201000526.

[105] (1) Lombardi, C.; Day, J.; Chandrasoma, N.; Mitchell, D.; Rodriguez, M. J.; Farmer, J. L.; Organ, M. G. Selective Cross-Coupling of (Hetero)Aryl Halides with Ammonia To Produce Primary Arylamines Using Pd-NHC Complexes. *Organometallics* **2017**, *36* (2), 251–254. https://doi.org/10.1021/acs.organomet.6b00830.

[106] (1) Schulz, T.; Torborg, C.; Enthaler, S.; Schäffner, B.; Dumrath, A.; Spannenberg, A.; Neumann, H.; Börner, A.; Beller, M. A General Palladium-Catalyzed Animation of Aryl Halides with Ammonia. *Chem. - A Eur. J.* **2009**, *15* (18), 4528–4533. https://doi.org/10.1002/chem.200802678.

Scheme 0-11. Substitution of an oxidative addition intermediate and subsequent formation of an alkoxo-Pd(II) complex

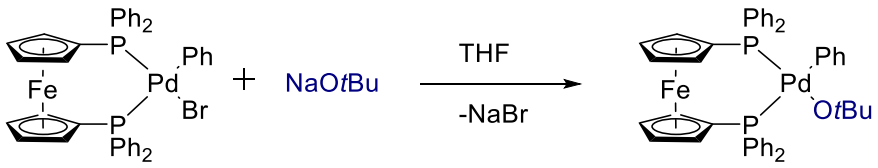

On the other hand, it was found hydroxo palladium complexes react with amines to form amido species.[107] Taking this into account, alkoxo complexes could be involved the formation of the amido complexes in the catalytic cycle, since they can be potentially present in the reaction media. Thus, this complex reacts with both ditolylamine and aniline to afford the amido complex, which upon heating underwent reductive elimination of the corresponding amine.

By contrast, the alkoxo complexes bearing electron poor aryls were much more reactive and did undergo reductive elimination of the ether upon formation, paving the way to the catalytic Buchwald-Hartwig C-O cross-coupling.[108]

[107] (1) Driver, M. S.; Hartwig, J. F. General N-H Activation of Primary Alkylamines by a Late Transition-Metal Complex. *J. Am. Chem. Soc.* **1996**, *118* (17), 4206–4207. https://doi.org/10.1021/ja954129y.

[108] (1) Mann, G.; Hartwig, J. F. Palladium Alkoxides: Potential Intermediacy in Catalytic Amination, Reductive Elimination of Ethers, and Catalytic Etheration. Comments on Alcohol Elimination from Ir(III). *J. Am. Chem. Soc.* **1996**, *118* (51), 13109–13110. https://doi.org/10.1021/ja963273w.

Scheme 0-12. Reactivity of Pd(II)-alkoxo complexes

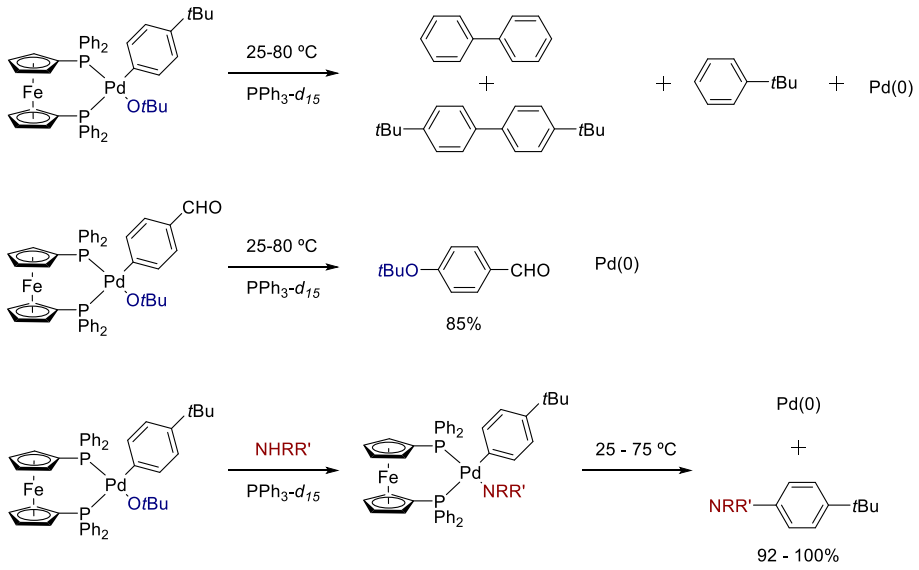

On the other hand, alkoxo complexes may form in other points of the catalytic cycle. Moreover, if these species are involved in the turnover limiting step, both the nature and concentration could affect the rate of the reaction. In this regard, Hartwig also found that concurrent mechanisms may appear for the amination of aryl chlorides catalysed by P(*t*Bu)$_3$/Pd where the rate determining step is the oxidative addition. Thus, a pathway would involve oxidative addition to monoligated palladium-phosphine complex and the other, to the alkoxo/phosphino complex.[109] More importantly, the formation of anionic alkoxo complexes may play an important role when Pd(dba)$_2$ is used as precatalyst, promoving its displacement.[110]

Another important base commonly used in the Buchwald-Hartwig amination is Cs_2CO_3. The most important feature is its weaker basicity, which could be convenient in those reactions with base-sensitive functionalities.

Despite the widely use of these bases, their air sensibility and poor solubility in organic solvents may become a drawback. For instance, if the

[109] (1) Shekhar, S.; Hartwig, J. F. Effects of Bases and Halides on the Amination of Chloroarenes Catalyzed by Pd(P t Bu 3) 2. *Organometallics* **2007**, *26* (2), 340–351. https://doi.org/10.1021/om0607548.

[110] (1) Alcazar-Roman, L. M.; Hartwig, J. F. Mechanism of Aryl Chloride Amination: Base-Induced Oxidative Addition. *J. Am. Chem. Soc.* **2001**, *123* (51), 12905–12906. https://doi.org/10.1021/ja016491k.

deprotonation occurs at the base surface, the structure and size of insoluble bases may have an important role in the reaction rate.[111]

Thus, the use of air-stable, soluble and weak organic bases is desirable and recent works on the Buchwald-Hartwig amination have dealt with this. For instance, Buchwald has recently reported a C-N coupling using DBU employing AlPhos as ligand, as we have previously mentioned.[82]

Coupling of chiral amines

It is worth to mention that the Buchwald-Hartwig amination cannot be carried out in an asymmetric fashion as it deals with the formation of C(sp2)-N bonds; however, chiral amines could in principle employed as coupling partners.

In this regard, after studying the intramolecular amination and amidation reaction of aryl bromides,[112] Buchwald tried to expand the scope of the reaction by using α-chiral amines. The reaction catalysed by the Pd/ P(*o*-tolyl)$_3$ system afforded the desired chiral cyclic amines without erosion of the optical purity. By contrast, the attempt to apply this protocol to the intermolecular coupling with chiral amines resulted in partial or total racemisation of the stereocenter. However, the application of chelating bis(phosphines) such as BINAP solved the problem and the amines were obtained with complete enantiorretention. This significative difference between the catalysts is due to the differences in the reaction mechanism.[113]

As we have seen, the reaction with bulky monosphosphines involves three-coordinated species bearing only one ligand. As a consequence, β-elimination can take place with the subsequent imine formation. The change of coordination mode from π to σ and vice versa is a route for imine faces to exchange and racemate after insertion into the Pd-H bond.

---

[111] (1) Meyers, C.; Maes, B. U. W.; Loones, K. T. J.; Bal, G.; Lemière, G. L. F.; Dommisse, R. A. Study of a New Rate Increasing "Base Effect" in the Palladium-Catalyzed Amination of Aryl Iodides. *J. Org. Chem.* **2004**, *69* (18), 6010–6017. https://doi.org/10.1021/jo049774e.

[112] (1) Wolfe, J. P.; Rennels, R. A.; Buchwald, S. L. Intramolecular Palladium-Catalyzed Aryl Amination and Aryl Amidation. *Tetrahedron* **1996**, *52* (21), 7525–7546. https://doi.org/10.1016/0040-4020(96)00266-9.

[113] (1) Wagaw, S.; Rennels, R. A.; Buchwald, S. L. Palladium-Catalyzed Coupling of Optically Active Amines with Aryl Bromides. *J. Am. Chem. Soc.* **1997**, *119* (36), 8451–8458. https://doi.org/10.1021/ja971583o.

Scheme 0-13. Isomerisation of α-chiral amines through β-elimination

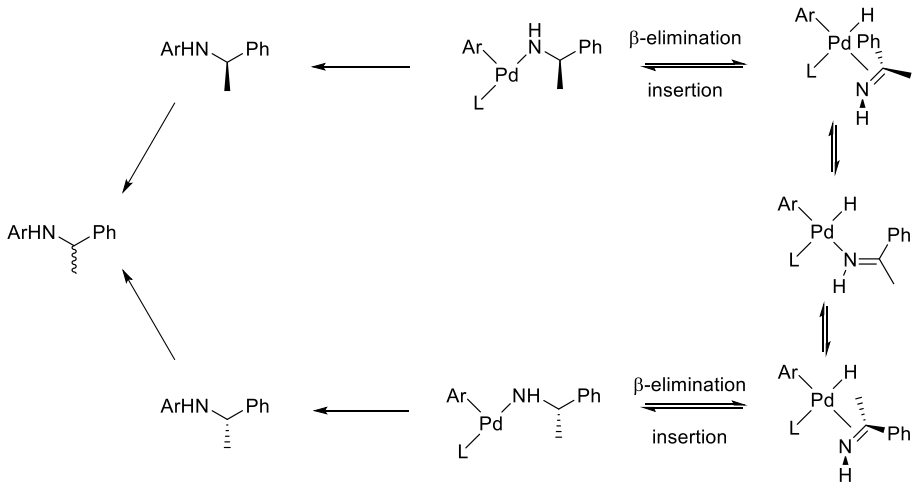

On the other hand, chelating bis(phosphines) remain coordinated during the catalytic cycle and hence, β-elimination is decreased although not fully supressed. The key fact is even though β-elimination is possible, the steric hindrance of the complex may prevent the change of the coordination mode of the imine from π to σ. If this process is not allowed, there is not a pathway for the racemisation of the amine.

Scheme 0-14. Prevention isomerisation of α-chiral amines by using chelating bisphosphines

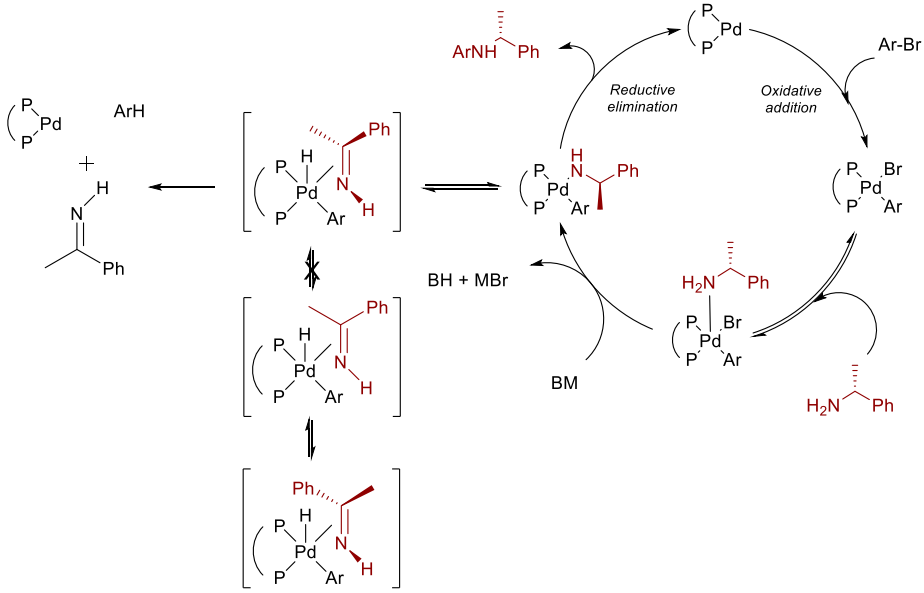

Regarding the intramolecular reaction, the β-elimination is not favoured when a 5- or 6-member metallacycles are formed. Therefore, P(*o*-tolyl)$_3$ is a good ligand in this case.

Objective

As it has been mentioned during the memory, our group is interested in the synthesis of axially chiral heterobiaryls. In this regard, DYKAT strategies have been a fundamental approach to achieve this goal. Thus, we have reported several asymmetric protocols for the asymmetric preparation of this kind of compounds via different cross-couplings reactions (Figure 13).[44,114,117]

Figure 13. Examples of DYKAT strategies for the synthesis of axially chiral heterobiaryls developed in our group.

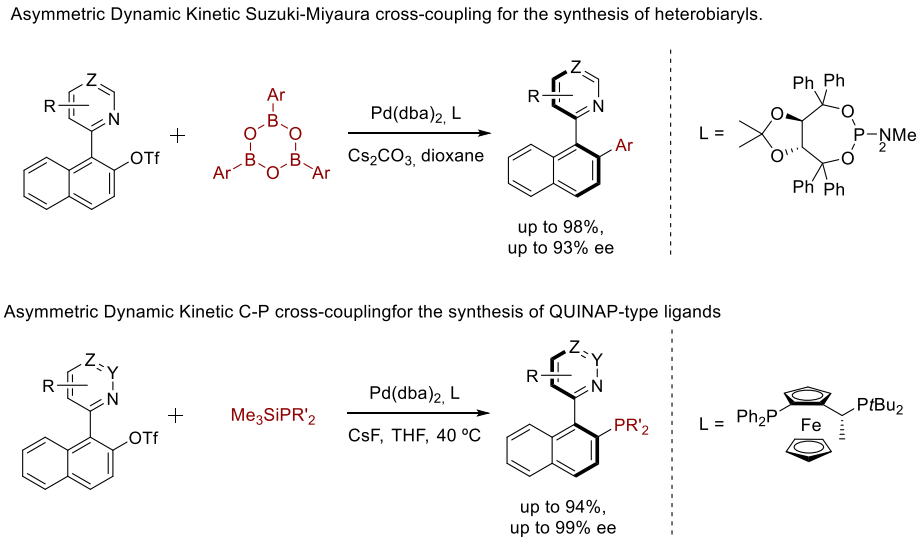

On the other hand, IAN-type amines are a family of compounds with great potential in catalysis; However, these applications have not been exploited probably due to the lack of a general and reliable method to prepare them. In this regard, they have only been accessible by resolution techniques and diastereomeric methods.[42]

[114] (1) Hornillos, V.; Ros, A.; Ramírez-López, P.; Iglesias-Sigüenza, J.; Fernández, R.; Lassaletta, J. M. Synthesis of Axially Chiral Heterobiaryl Alkynes via Dynamic Kinetic Asymmetric Alkynylation. *Chem. Commun.* **2016**, *52* (98), 14121–14124. https://doi.org/10.1039/C6CC08997F.

(1) Carmona, J. A.; Hornillos, V.; Ramírez-López, P.; Ros, A.; Iglesias-Siguënza, J.; Gómez-Bengoa, E.; Fernández, R.; Lassaletta, J. M. Dynamic Kinetic Asymmetric Heck Reaction for the Simultaneous Generation of Central and Axial Chirality. *J. Am. Chem. Soc.* **2018**, *140* (35), 11067–11075. https://doi.org/10.1021/jacs.8b05819.

Figure 14. IAN-type amine

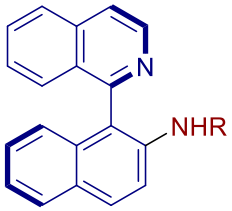

Considering the analogy of this type of compounds and QUINAP, and our previous work on their synthesis through a Dynamic Kinetic Asymmetric C-P[44] cross-coupling, we envisioned a similar strategy could be employed to solve this problem (Figure 15).

In this regard, initial attempts to achieve this DYKAT using silylamines were unsuccessful so we decided to explore the Buchwald-Hartwig amination as a strategy to develop this new methodology.

Figure 15. Working hypothesis on the Dynamic Kinetic Buchwald-Hartwig amination for the synthesis of axially chiral IAN-type amines.

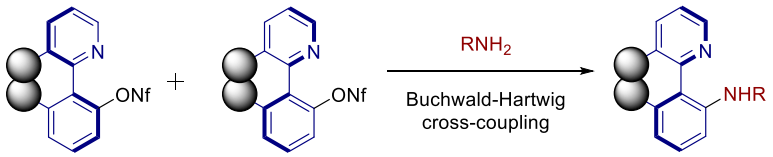

Thus, the objective of this chapter is the development of a new Dynamic Kinetic Asymmetric Buchwald amination for the synthesis of axially chiral IAN-type amines.

Results and discussion

Optimization of the reaction conditions

Model reaction

Inspired by the previous works on the synthesis of heterobiaryls based on C-C and C-P cross-couplings accomplished in our group, and after the unsuccesful attempts using silylamines as coupling partners for the synthesis of axially chiral *N,N*-diamines, we decided to explore the Buchwald-Hartwig amination to achieve this goal. Thus, we decided to start our investigations selecting the cross-coupling between aniline and a naphthylisoquinoline electrophile as the model reaction.

Since nonaflates are less prone to hydrolysis than triflates[115] we chose them as the starting material for the reaction. Thus, we set the amination of the napthylisoquinoline nonaflate (±)-**1A** with aniline as the model reaction keeping the rest of the conditions: anhydrous toluene at 60 °C, NaO*t*Bu as the base, $Pd(dba)_2$ 10 mol % and 12 mol % of the ligand under study (Scheme 0-15).

Scheme 0-15. Model reaction

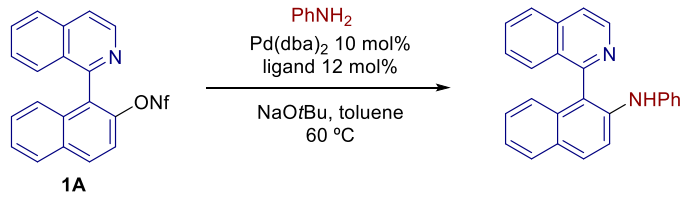

Ligand screening

For this study we chose different families of ligands (Table 1). First, we tested some hydrazone-based ones (**L1**-**L2)** previously designed in our research group and two phosphoramidite ligands such as TADDOL derivative **L3** which had been successful ligand in asymmetric Suzuki-Miyaura reactions. While the hydrazones were applied to classic versions of the coupling[116], TADDOL

[115] (1) Högermeier, J.; Reissig, H. U. Nine Times Fluoride Can Be Good for Your Syntheses. Not Just Cheaper: Nonafluorobutanesulfonates as Intermediates for Transition Metal-Catalyzed Reactions. *Adv. Synth. Catal.* **2009**, *351* (17), 2747–2763. https://doi.org/10.1002/adsc.200900566.

[116] (a) Ros, A.; Estepa, B.; Bermejo, A.; Álvarez, E.; Fernández, R.; Lassaletta, J. M. Phosphino Hydrazones as Suitable Ligands in the Asymmetric Suzuki–Miyaura Cross-Coupling. *J. Org. Chem.* **2012**, *77* (10), 4740–4750. https://doi.org/10.1021/jo300548z.

derivative **L3** was succesfully utilized to pursue dynamic kinetic resolution/transformation strategies.[117] However, the activity of all these ligands in the amination was low although in the case of **L2** the enantiomeric excess was moderate.

On the other hand, ferrocene-based ligands have been proved to be excellent ligands in the Buchwald-Hartwig reaction and, they also were suitable ligands for the previously reported C-P cross-coupling reactions.[44] Thus, we decided to check if some of these ligands would have a better performance. Then, we tested several ligands of the Josiphos family (**L5**-**L9**) and Taniaphos ligand **L10**. In general terms, a rise in the yield and in the selectivity was observed, obtaining up to 60 % yield and 67% ee when **L5** was used.

However, despite these promising results we needed further improvement, so we studied the performance of other ligands. Phosphine-based ligands featuring axial chirality play a special role in asymmetric catalysis and, as a matter of fact, BINAP comprises a very important system in the Buchwald-Hartwig reaction. In this vein, our next option was the selection of different common and commercially available chiral P,P and P,O ligands (**L11-L13**). Unfortunately, we did not make any progress since the yields (18% – 61%) were moderate and the enantioselectivies rather poor (4% ee – 34% ee).

However, the use of the less accessible P,N-ligand QUINAP **L14a**, for which our research group have developed a synthetic methodology,[118] made a quantum leap in the enantioselectivity (87% ee) although the yield was still moderate (45%).

(b) Bermejo, A.; Ros, A.; Fernández, R.; Lassaletta, J. M. C 2 -Symmetric Bis-Hydrazones as Ligands in the Asymmetric Suzuki−Miyaura Cross-Coupling. *J. Am. Chem. Soc.* **2008**, *130* (47), 15798–15799. https://doi.org/10.1021/ja8074693.

[117] Ros, A.; Estepa, B.; Ramírez-López, P.; Álvarez, E.; Fernández, R.; Lassaletta, J. M. Dynamic Kinetic Cross-Coupling Strategy for the Asymmetric Synthesis of Axially Chiral Heterobiaryls. *J. Am. Chem. Soc.* **2013**, *135* (42), 15730–15733. https://doi.org/10.1021/ja4087819.

[118] Ramírez-López, P.; Ros, A.; Estepa, B.; Fernández, R.; Fiser, B.; Gómez-Bengoa, E.; Lassaletta, J. M. A Dynamic Kinetic C–P Cross–Coupling for the Asymmetric Synthesis of Axially Chiral P,N Ligands. *ACS Catal.* **2016**, *6* (6), 3955–3964. https://doi.org/10.1021/acscatal.6b00784.

Table 1. Ligand screening

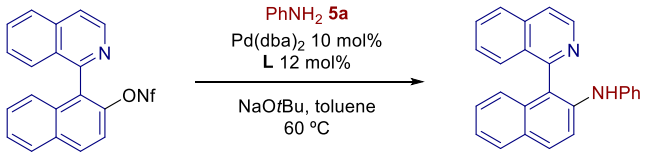

1A **6Aa**

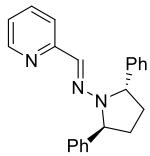

L1: 0%

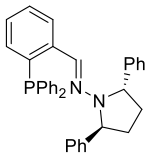

L2: 17%, 72% ee

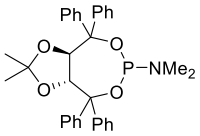

L3: 8%, 8% ee

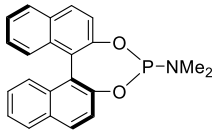

L4: 0%, 0% ee

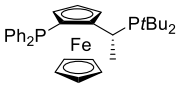

L5: 60%, 67% ee

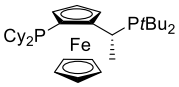

L6: 28%, 44% ee

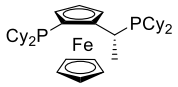

L7: 31%, 39% ee

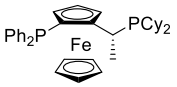

L8: 42%, 16% ee

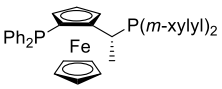

L9: 47%, 58% ee

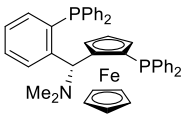

L10: 76%, 44% ee

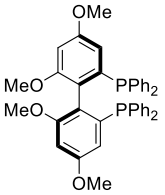

L11: 76%, 44% ee

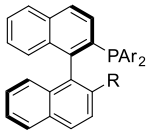

L12: R = PPh_2; 61%, 19% ee
L13: R = OMe; 18%, 34% ee

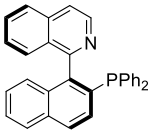

L14a: 45%, 87%

This result was noteworthy for two reasons: 1) QUINAP showed a bad performance on the aforementioned C-P cross-coupling, closely related to this project; and 2) as a consequence of the former project, our group has a large family of QUINAP-type ligands ready to be tested.

On the other hand, we also wanted to check the reactivity of other naphthylisoquinoline electrophiles that had been previously used in other related projects in the group. Thus, the model reaction carried out under the same conditions using naphthylisoquinoline bromide (±)-**3A** provided excellent results, increasing the yield and the enantioselectivity up to 95% and 89% ee (Table 2, entry 1).

With this remarkable result in hands, we speculated whether the use of the other different QUINAP-type ligand (**L14b**-**L14g**) would improve the reaction (Table 2).

All the ligands showed excellent activity except for the case of those featuring alkyl-substitutions or the quinazoline scaffold (**L14e**-**L14g**), especially with ligand **L14e** containing bulky *i*Bu substituents (Table 2, entry 10).[119] However, even though much of these ligands gave reactions with almost quantitative yield, unfortunately none of them could perform the reaction with better selectivity. Taking this into account, we kept the QUINAP (**L14a**) as the best ligand for the reaction. Indeed, by using this ligand the reaction could be carried out at 50 ^{o}C obtaining a slightly higher ee value (Table 2, entry 2).

On the other hand, the good enantioselectivity leaves room for solving the yield issues, mainly when they are due to hydrolysis of the starting materials **2A** or **1A**; or due to reduction of **3A**. Additionally, there were other variables unoptimized.

[119] Ligands of the family of QUINAP bearing alkyl substituents at phosphorous are not common ligands in catalysis. These very bulky ligands may prevent the efficient coordination to the metal centres.

Table 2. Optimisation

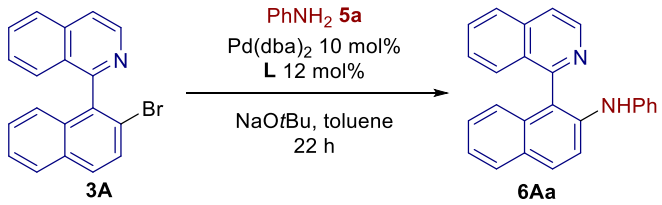

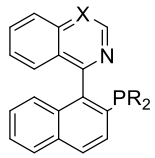

(*S*)-**L14b**: X = C, R = (*p*-OMe-C_6H_4)
(*S*)-**L14c**: X = C, R = (*p*-Me-C_6H_4)
(*S*)-**L14d**: X = C, R = (*p*-F-C_6H_4)
(*R*)-**L14e**: X = C, R = *i*Bu
(*R*)-**L14f**: X = C, R = Cy
(*S*)-**L14g**: X = N, R = Ph

Entry	Base	T (°C)	L	Yield (%)	ee[b] (%)
1[d]	NaO*t*Bu	60	(*S*)-**L14a**	95	89
2	NaO*t*Bu	50	(*S*)-**L14a**	90	91
3	NaO*t*Bu	60	(*S*)-**L14b**[f]	99	84
4	NaO*t*Bu	60	(*S*)-**L14c**[g]	98	77
5	NaO*t*Bu	60	(*S*)-**L14d**	98	61
6	NaO*t*Bu	60	(*R*)-**L14e**	26	50
7	NaO*t*Bu	60	(*R*)-**L14f**	77	68
8	NaO*t*Bu	60	(*S*)-**L14g**[h]	78	20

[a] Reactions conditions: 0.1 mmol scale in toluene (2 mL), 2 equiv. of **5a**, 2 equiv. of base. [b] Determined by chiral HPLC analysis. [c] t: 48 h. [d] t: 17h. [f] 98% ee. [g] 96% ee. [h] 99% ee.

Reaction parameters optimisation

Base optimization

One of the main problems we must solve is the moderate yield when naphthylisoquinoline nonaflate (±)-**1A** and triflate (±)-**2A** is used as the electrophile in the model reaction, as base-assisted side-reactions such as hydrolysis of sulphonate take place. For this reason, and despite nonaflate is robust enough in this regard, we decided to replace NaO*t*Bu for a weaker base.

*Table 3. Base optimization for nonaflate **1A***

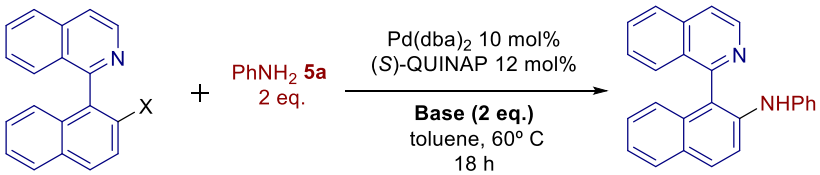

1A, X = ONf
2A, X = OTf

6Aa

Entry	X	Base	Yield (%)[b]	ee (%)[c]
1	ONf	NaO*t*Bu	45	87
2	**ONf[d]**	**Cs_2CO_3**	**99**	**88**
3	OTf[e]	Cs_2CO_3	81	92
4	ONf[f]	K_2CO_3	42	-
5	OTf[g]	Cs_2CO_3	84	90
6	ONf	LiO*t*Bu	44	89

[a] Reactions were performed at 60 °C on a 0.1 mmol scale using anhydrous toluene (2 mL/0.1 mmol substrate). [b] Isolated yield. [c] Determined by HPLC on chiral stationary. [d] Reaction was stopped and analyzed after 20 h. [e] Reaction was carried out at 50 °C with $Pd(dba)_2$ 7.5 mol% and (*S*)-QUINAP 10% for 48h. f The reaction was carried out using *rac*-BINAP as the ligand. [g] The reaction was carried out at 50 °C.

This way, the weaker Cs_2CO_3 was tested in the model reaction affording a better result (Table 3). Another experiment was carried out using K_2CO_3 with similar conditions (using *rac*-BINAP instead of (*S*)-QUINAP)[120], but its lower solubility in organic solvents achieves only 42% after 48h. When LiO*t*Bu, which is a more soluble base than its sodium counterpart, a poorer result is achieved as expected.

We also wanted to test the robustness and performance of the triflate derivative (±)-**2A** as starting material since triflates are the most common pseudohalide in cross-coupling reactions. This way, we carried out a control experiment using *rac*-BINAP and Cs_2CO_3 as the base affording nearly quantitative yield with just traces of hydrolysis. From this emerges the fact that triflates are also suitable substrates for this reaction. This way, we carried out the reaction with the chiral ligand (*S*)-QUINAP and the result was in accordance with what we expected: 84%, and a selectivity of 90% ee at 50 °C in order to avoid hydrolysis.

In addition, other weak organic bases were also tested but, Unfortunately, none of these organic bases (DMAP, DABCO, DIPEA, DBU and 2,6-lutidine) worked and the starting material was recovered. These results were not surprising since the use of soluble organic bases is rare in the Buchwald-Hartwig amination. In fact, the use of DBU as the base has been achieved recently, as we pointed out in the introduction.[82]

Regarding the use of the bromide naphthylisoquinoline electrophile **3A**, hydrolysis is not any issue but picking the best base is mandatory for a perfect optimization of the reaction. In this case, the main side reaction is the

[120] Due to the high price of (S)-QUINAP we decided to perform some experiments with *rac*-BINAP as it showed a better performance in terms of activity.

debromination of the starting material. Thus, the careful selection of the base could balance the reaction toward reductive elimination.

In this regard, we decided to study the behaviour of the alkaline metal *tert*-butoxides in the reaction using **3A** as the electrophile (Table 4). However, the mild Cs_2CO_3 was not a suitable base for this electrophile. Hence, the base of choice for **3A** is NaO*t*Bu. Additionally, NaO*t*Bu not only functions as a base, but as a Br^- scavenger too. In the case of **3A**, this is a key feature after oxidative addition for the reaction to proceed, as will be explained later.

*Table 4. Base optimization for Bromide **3A***

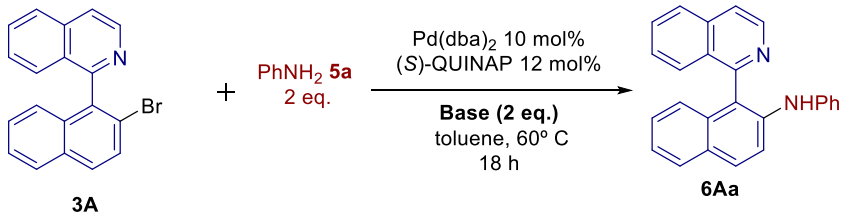

Entry	Base	Yield (%)[b]	ee (%)[c]
1	LiO*t*Bu	46	87
2	**NaO*t*Bu**	**95**	**89**
3	KO*t*Bu	90	85
4	NaO*t*Bu (4 equiv)	95	89
5	Cs_2CO_3	82	89

Solvent screening

Considering the solubility of the base plays an important role in the reaction regarding other side-processes, we decided to study the effect of the solvent attending at their nature. Thus, ethers and low polar solvents such as toluene (Table 5, entries 1-5), which indeed is the best solvent, are competent for this reaction. By contrast, protic and aprotic polar solvents make the reaction achieve poor results (Table 5, entries 6-8); while chlorinated solvents seem to promote the hydrodehalogenation, in case of reaction. In short, toluene, which is one of the prototypical solvents for the Buchwald-Hartwig reaction, gave the best results. In this regard, the low solubility of NaBr in this solvent may accelerate the reaction enhancing the scavenger ability of NaO*t*Bu. Nevertheless, THF have shown it can provide good results as well.

Table 5. Solvent screening.

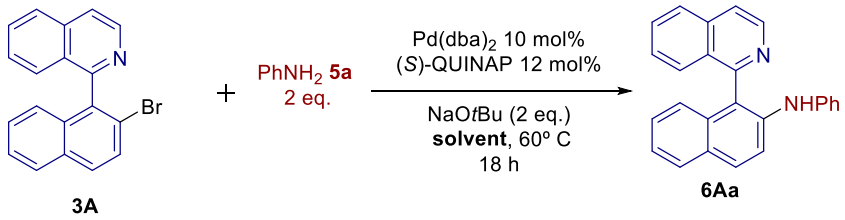

Entry	Solvent	Yield (%)[b]	ee (%)[c]
1	Toluene	**95**	**89**
2	$PhCF_3$	93	88
3	Dioxane	59	86.5
4	DME	62	88
5	THF	78	89
6	*t*BuOH	38	88
7	DMSO	-	-
8	DMF	27	5

[a] Reactions were performed at 60 °C on a 0.1 mmol scale using anhydrous solvents (2 mL/0.1 mmol substrate). [b] Isolated yield. [c] Determined by HPLC on chiral stationary phases.

Palladium source and catalytic loading

With the idea of decreasing the catalyst loading from the economical point of view, and to see the influence in the reaction performance; we also considered the metal source and its loading, concentration, etc (Table 6). In this line, we focused just on palladium catalysts although it is worth noting nickel is an alternative metal for the Buchwald-Hartwig reaction.

If we decrease the loading below 10 mol% the reaction proceeds with lower conversion although the selectivity can be hold close to 90% (Table 6, entries 1-3). On the other hand, from doubling the amount of the ligand, we can rule out the deactivation of the catalyst by the formation of 2:1 ligand to metal complexes (Table 6, entries 1 and 4). Thus, a 1:1 stoichiometry is postulated for the catalytic system.

Table 6. Palladium source and catalyst loading

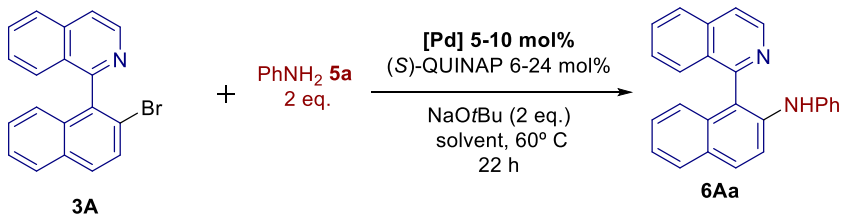

Entry	Pd source	L	Yield (%)[b]	ee (%)[c]
1	**$Pd(dba)_2$ (10% mol)**	**12 mol%**	**99**	**89**
2	$Pd(dba)_2$ (7.5% mol)	10 mol%	93	87
3	$Pd(dba)_2$ (5% mol)	6 mol%	78	89
4	**$Pd(dba)_2$ (10% mol)**	**24 mol%**	**99**	**88**
5	$Pd_2(dba)_3$ (5 %mol)	12 mol%	79	89
6	$PdCl_2$ (10% mol)	12 mol%	23	81
7	$Pd(OAc)_2$ (10% mol)	12 mol%	34	80

[a] Reactions were performed at 60 °C on a 0.1 mmol scale using anhydrous toluene (2 mL/0.1 mmol substrate). [b] Isolated yield. [c] Determined by HPLC on chiral stationary phases.

From these control experiments we can conclude that Pd(0) are better sources than Pd(II) salts, despite both oxidation states are commonly used in the amination reaction. Presumably, the lower yields afforded with Pd(II) salts (Table 6, entries 6 and 7) are related to the fact that they need to be reduced to Pd(0) to generate the catalytically active species.

Concentration

Another important variable to take into account is the concentration of the reagents, since it could modify the kinetics and equilibria of the reaction. Besides, our system fully relies on the electrophile and therefore, they might behave in a completely different manner when changing these parameters.

First, the Buchwald-Hartwig reaction with nonaflate seems to be quite sensitive to concentration: when the reaction is performed at double concentration the activity and selectivity are compromised significantly (Table 7, entries 1-2). It is worth noting that when doing this, the concentration of the base is risen too, and it is more likely that other side reactions like hydrolysis take place.

On the other hand, when the reaction is carried out with bromide naphthylisoquinoline **3A** (Table 7, entries 3-7), the enantioselectivities of the product are just slightly affected by the concentration of the starting material, the base or even longer reaction times. Regarding the yield, the result remains nearly unaltered when the concentration from 0.05 M to 0.1 M was changed in stark contrast to nonaflate **1A**. However, raising the concentration to 0.2 M results in a significant drop of the yield, even though the enantioselectivity is basically maintained. It is worth to notice that the reaction is heterogenous and doubling the concentration may result in worse agitation, accounting for the lower yield.

Table 7. Concentration optimization.

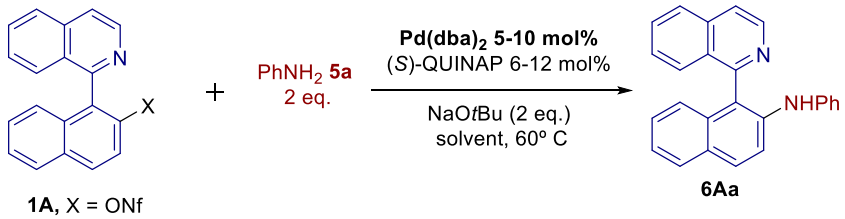

1A, X = ONf
3A, X = Br

6Aa

Entry	X	Base	C (M)	Yield (%)[b]	ee (%)[c]
1	**ONf**[d]	**Cs_2CO_3**	**0.05**	**99**	**88**
2	ONf[d]	Cs_2CO_3	0.1	77	76
3	**Br**	**NaO*t*Bu**	**0.05**	**99**	**89**
4	**Br**	**NaO*t*Bu**	**0.1**	**95**	**89**
5	Br[e]	NaO*t*Bu	0.1	90	88
6	Br[e]	NaO*t*Bu (3 equiv)	0.1	91	89
7	Br[e]	NaO*t*Bu (3 equiv)	0.2	43	86

[a] Reactions were performed for 18 h at 60 °C on a 0.1 mmol scale using anhydrous toluene, $Pd(dba)_2$ 10 mol% and (*S*)-QUINAP 12%. [b] Isolated yield. [c] Determined by HPLC on chiral stationary phases. [d] Reaction time was 22 h using $Pd(dba)_2$ 10 mol% and (*S*)-QUINAP 12%. [e] Reaction time was 45 h using $Pd(dba)_2$ 5 mol% and (*S*)-QUINAP 6%.

Temperature

Temperature is a key parameter in asymmetric catalysis since it concerns not only the conversion but the selectivity too. Generally, enantioselectivities decrease with increasing temperature in most asymmetric catalytic reactions because both energy barriers associated to diastereomeric intermediates are easier to overcome. Taking this into account, it is important to keep the reaction at mild temperatures, trying to keep it as low as possible without compromising the reaction time.

As expected, when the reaction with the nonaflate **1A** is carried out at lower temperatures (Table 8, entries 1-3) the enantioselectivity increases to 91% but a drop in the yield to 64% was observed. E.g., even though the temperature is lowered by just 10 °C, the yield drops by 10% and we just take an advantage of 2% ee in return.

On the other hand, the bromide **3A** behaves in a similar fashion, but we note a subtle difference in reactivity when compared to nonaflate: at similar temperature, similar yields are observed but with shorter reaction times (Table 8, entries 6 vs. 2). Thus, bromide seems to have a better chemical performance when used in this reaction, in line with the general Buchwald-Hartwig reaction. Another feature to highlight is the fact that classical

Buchwald-Hartwig aminations normally proceed at higher temperatures while our system works at mild conditions, making a turning point for its application to our methodology. A possible explanation for that is the oxidative addition step is facilitated by the formation of a 5-membered palladacycle assisted by the previous coordination of isoquinolinic nitrogen.

Table 8. Reaction temperature optimisation.

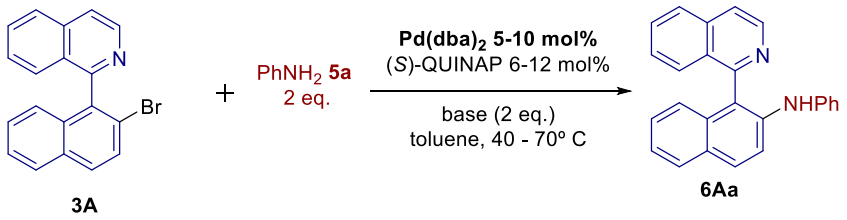

Entry	X	Base	t (h)	T (ºC)	Yield (%)	ee (%)
1	**NfO**	**Cs_2CO_3**	**20**	**60**	**99**	**88**
2	NfO[b]	Cs_2CO_3	48	50	89	89
3	NfO[b]	Cs_2CO_3	71	40	64	91
4	Br	NaO*t*Bu	~15	70	97	85
5	**Br**	**NaO*t*Bu**	**21**	**60**	**99**	**86**
6	**Br**	**NaO*t*Bu**	**21**	**50**	**90**	**89**
7	Br[b]	NaO*t*Bu	21	40	57	89

[a] Reactions were performed on a 0.1 mmol scale using anhydrous toluene, $Pd(dba)_2$ 10 mol% and (S)-QUINAP 12%. [b] $Pd(dba)_2$ 5 mol% and (S)-QUINAP 6 mol% were used.

From these optimization studies we can sum up that the best electrophile for the reaction are those bearing bromide as the "leaving group". This higher reactivity permits to lower the temperature from 60 ºC of standard conditions to 50º C, which could translate to increased selectivities. Nevertheless, if necessary, the reaction could also be carried out using nonaflate **1A** and Cs_2CO_3 as the base, although longer reaction times would be required.

Scope and particularities

With the optimised conditions in hands, we decided to explore the scope of the reaction.

Scheme 0-16. General procedure for enantioselective amination of heterobiaryls.

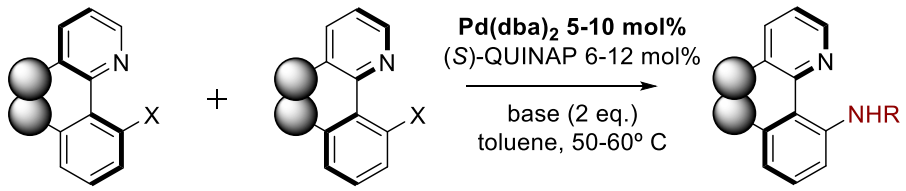

On the one hand, we selected different amines regarding its electronic and stereochemical properties in order to study the scope of the reaction. First, we can distinguish 2 main groups: aryl and alkyl amines, whose biggest difference lies in the stronger basicity and the presence of β-hydrogens for the latter (Figure 16).

On the other, the study of the reaction scope must go beyond the model substrate **A** and other napthylisoquinoline-like electrophiles have to be considered. In this regard, 1-(4-methoxinaphthyl)isoquinoline **C**, 2-napthyl-3-picoline **D**, 1-(*o*-totyl)isoquinoline **E**, 4-naphthylquinazoline **F** and 1-(1-naphth-1-yl)phthalazine **G** bromides and nonaflates were regarded (Figure 16.A).

Figure 16. Selected heterobiaryls and amines for the amination reaction.

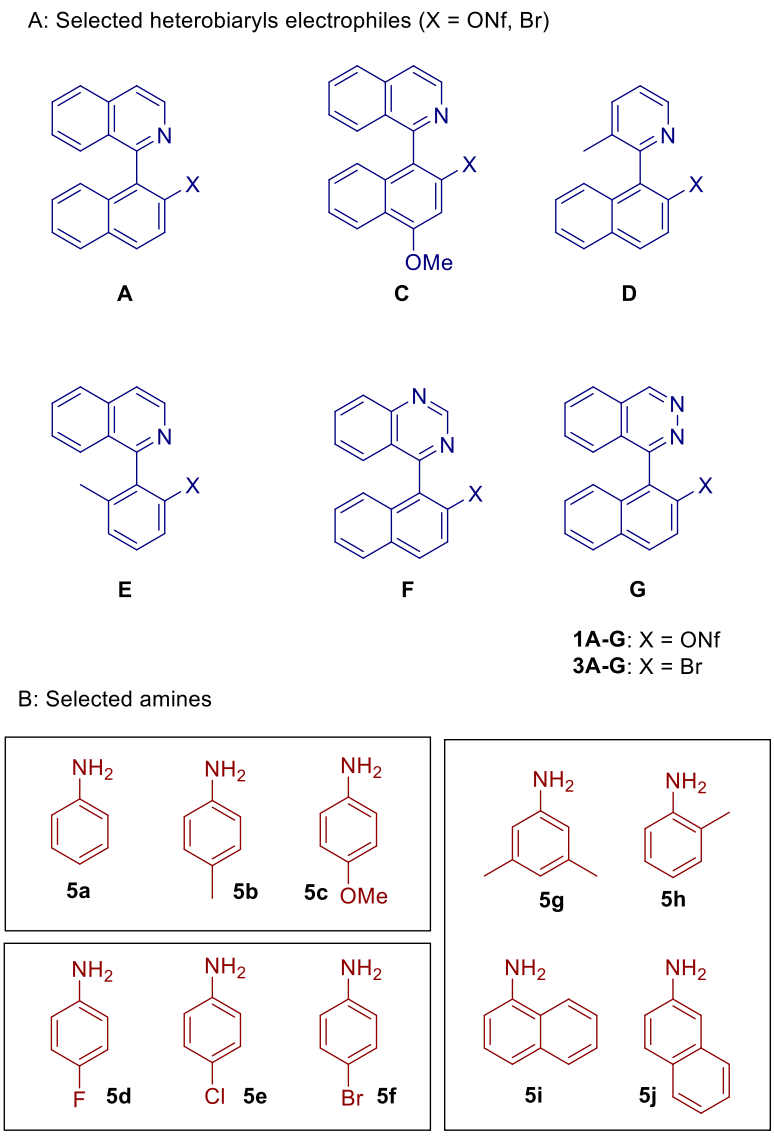

Aryl amines

Once we have selected a number of primary arylamines to study the reaction scope, we can classify them into: 1) electron-rich, 2) electron-poor and 3) amines with diverse steric hindrance patterns.

To begin with, the amination of the model substrate **3A** (Table 9) afforded the corresponding amines at 50 °C with neutral, electron rich amines and even strained amines with excellent yields (over 88%) and enantioselectivies (over 90% ee). Among these aryl amines, just (*R*)-**6Aj** was obtained with a slightly

poorer result (81%, 88% ee), presumably due to a combination of steric hindrance and low basicity.

In the same vein, electron-poor anilines (**5d-5f**) required higher temperatures to improve their yield. In fact, the reaction with these substrates were carried out at 60 ^{o}C in order not to compromise the selectivity by further temperature increase. However, despite this energetic aid, the yields were not as high as the previous cases, although they were still moderate (74%-64%).

In this group, the exception was given by (*R*)-**6Ad** (Table 9) with a yield of 99% and 92% ee. The explanation for this singularity is based on the fact that despite the remarkable electronegativity of fluorine, its resonance effect on the aromatic ring is still capable to balance it out. Consequently, its basic properties are rather in line with aniline instead of its halogen-derivative counterparts.

Table 9. Reaction scope for series A.

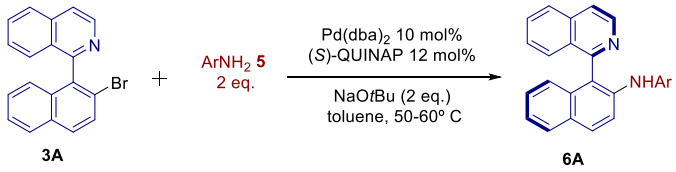

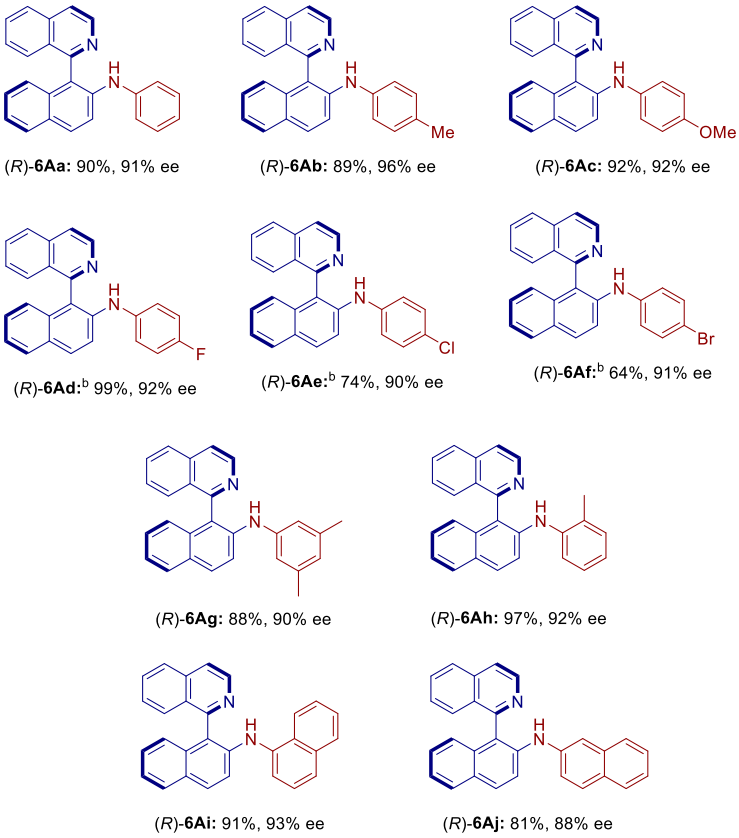

[a] Reactions performed on a 0.1 mmol scale using anhydrous toluene (2 mL), 2 equiv. of **5**, 2 equiv. of NaO*t*Bu at 50 °C for a period of time of 22-48 h (see experimental part). Ee's determined by chiral HPLC analysis. [b] The reaction was carried out at 60 °C.

As for the series **D** (Table 10), all the reactions were carried out at 50 °C, affording good to excellent results regarding the yields and enantioselectivities (around 90% ee for all cases). Here, it is worth to notice that 4-halo-anilines did not need a higher temperature to achieve similar results compared to series **A**. Longer reaction times were applied so as to

balance out the lower temperature, though. At any rate, the trend keeps on being similar for these electron-poor amines (including 2-naphthylamine).

In addition, the crystallization of the products (*R*)-**6Df** and (*R*)-**6Dl** produced an enantioenrichement of the products, affording full enantiopurity (99% ee). On the other hand, the crystals of (*R*)-**6Df** had X-ray quality and the subsequent analysis revealed the configuration of the axis was R_a. Thus, the absolute configuration of these products was assigned assuming the reaction proceeds with similar pathways in all cases.

Table 10. Reaction scope for series D.

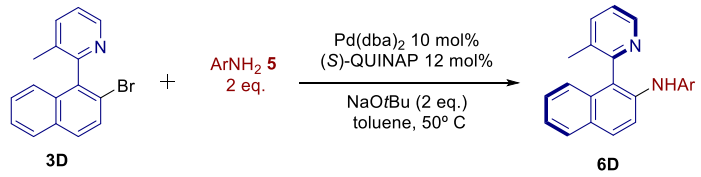

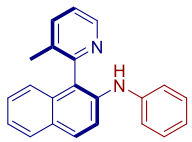

(*S*)-**6Da:**[b] 84%, 89% ee

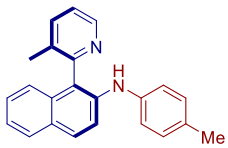

(*S*)-**6Db:**[b] 98%, 90% ee

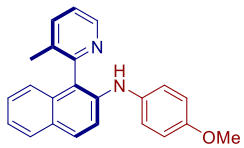

(*S*)-**6Dc:**[b] 78%, 91% ee

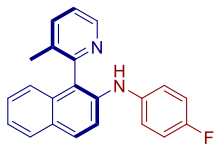

(*S*)-**6Dd:**[b] 89%, 92% ee

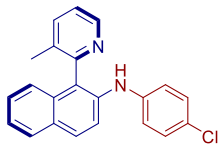

(*R*)-**6De:** 83%, 93% ee

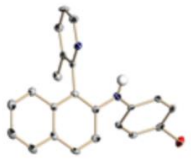

(*R*)-**6Df:** 67%, 89% ee[c]

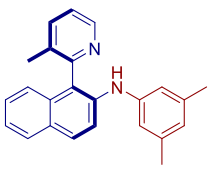

(*S*)-**6Dg:**[b] 97%, 88% ee

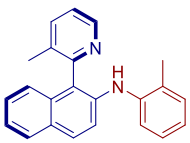

(*R*)-**6Dh:** 94%, 90% ee

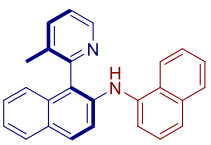

(*S*)-**6Di:**[b] 94%, 92% ee

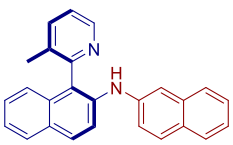

(*S*)-**6Dj:**[b] 83%, 86% ee

[a] Reactions performed on a 0.1 mmol scale using anhydrous toluene (2 mL), 2 equiv. of **5**, 2 equiv. of NaO*t*Bu at 50 °C for a period of time of 22-48 h (see experimental part). Ee's determined by chiral HPLC analysis. [b] (*R*)-**L14a** was used. [c] > 99% ee after crystallisation.

On the other hand, series **E** (Table 11) required both longer reaction times (48 h) and higher temperature (60 °C) for all the substrates. In view of this, we did not try the synthesis of IAN-type amines with deactivated 4-halo-anilines. Nevertheless, all the synthesised amines were obtained with satisfactory yields (>93%) and enantioselectivity (>88% ee).

Table 11. Reaction scope for series E.

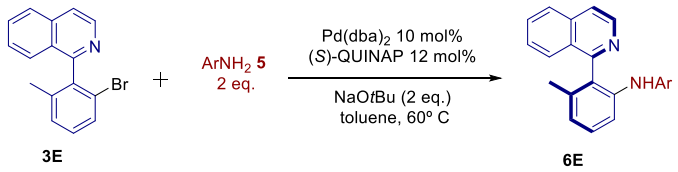

3E **6E**

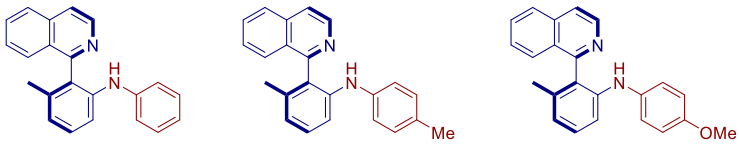

(*R*)-**6Ea:** 93%, 90% ee (*R*)-**6Eb:** 98%, 90% ee (*R*)-**6Ec:** 94%, 91% ee

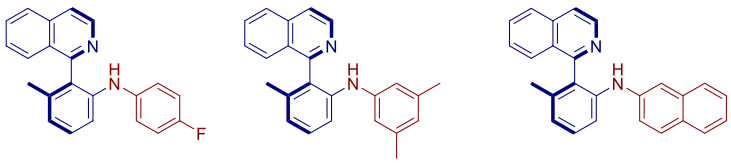

(*R*)-**6Ed:** 95%, 91% ee (*R*)-**6Eg:** 97%, 88% ee (*R*)-**6Cj:** 72%, 91% ee

[a] Reactions performed on a 0.1 mmol scale using anhydrous toluene (2 mL), 2 equiv. of **5**, 2 equiv. of NaO*t*Bu at 50 °C for a period of time of 22-48 h (see experimental part). Ee's determined by chiral HPLC analysis.

Apparently, the reactivity of both bromides **3E** and **3D** should be similar, since they have similar steric hindrance at the "*ortho*" positions, and both rings are aromatic. However, when examined in detail, the electronic properties of the active rings, 6-tolyl for **3E** and naphthyl for **3D**, are completely different. Thus, the naphthalene fragment (**3D**) is electronically poor and therefore the reductive elimination should be faster.

Aliphatic amines

Regarding the alkyl amines (**5k-q**), these present some differences compared to aniline derivatives. The alkyl amines are more basic, present α protons capable to undergo β elimination and in some cases, and are bulkier (three-dimensional distribution).

As we have seen, anilines are good amines to perform this Dynamic Kinetic Buchwald-Hartwig amination, particularly, electron-rich or relatively basic ones. Therefore, we expected primary alkyl amines, with a basicity of an order of magnitude 4 times higher, would be even better substrates for this reaction. By contrast, the amination gave lower yields when standard conditions were applied. Indeed, a further optimization was required for this kind of amines. Just as we chose anilines as the model amine before, now we selected benzylamine and bromide **3D** to carry out this study.

Table 12. Optimization process for alkyl amines.

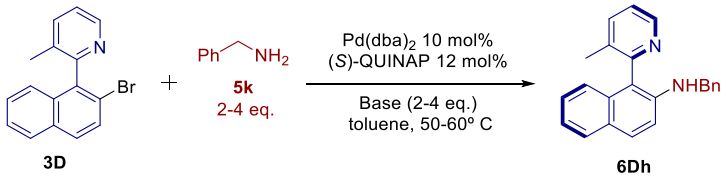

Entry	NaO*t*Bu (equiv.)	Benzylamine (equiv.)	T (°C)	t (h)	Yield (%)[b]	ee (%)[c]
1	2	2	50	47	13	96
2	2	2	60	66	20	93
3	2	2 (distilled)	50	48	35	93
4	2	2 (distilled)	60	60	58	92
5	4	4 (distilled)	60	70	95	93

[a] Reactions were performed on a 0.1 mmol scale using anhydrous toluene, $Pd(dba)_2$ 10 mol% and (*S*)-QUINAP 12%. [b] Isolated yield. [c] Determined by HPLC on chiral stationary phases.

As we can see, the previous standard conditions shown in Table 12, entry 1; gave a low yield for the amination while the enantioselectivity was kept. Hence, the first thing we attempted was a rise in temperature and a longer reaction time (Table 12, entry 2). However, this change did not translate to a great improvement in the yield and the selectivity was slightly reduced by 3 points. On the other hand, the amines were used as they were purchased and some of them were reagents that could have been stored in our laboratory for years. In this regard, it is well known that amines may undergo oxidation reactions and we wonder if the presumed impurities of benzylamine could interfere with the catalytic cycle. Thus, we carried out the reaction with freshly distilled benzylamine (Table 12, entry 3 and 4) and the reaction was almost 3 times more efficient compared to the previous experiment. Next, we performed the reaction with the double amount of both base and benzylamine. In this case, the reaction gave an excellent yield of 95% and the enantioselectivity was kept at 93% ee (Table 12, entry 5).

To sum up, alkylamines required longer reaction times and a higher amount of base and the amine itself. These forcing conditions may be required due to the higher basicity of these amines, and therefore, less acidity of the corresponding Pd(II)-amino adduct. In this regard, coordination to the Pd(II) could be facilitated but the subsequent deprotonation would be more difficult compared to anilines.

Next step in our research was the selection of different alkyl amines so as to study the reaction scope with these nucleophiles (Figure 17).

Figure 17. Selected alkyl amines

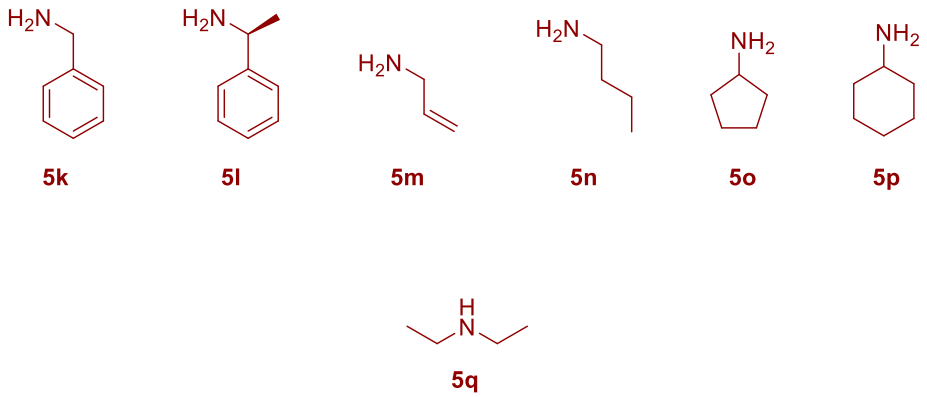

5k **5l** **5m** **5n** **5o** **5p**

5q

The reaction with neither the simplest and prototypical *n*-butylamine **5n** nor small cyclopentylamine **5o** succeed. By contrast, the bigger cyclohexylamine **5p** did react giving moderate yields but good selectivity (Table 13). On the other hand, allyl-like amines were also suitable nucleophiles for this reaction. In this regard, benzylamine **5k** afforded the best results among the alkylamines.

As a curiosity, and considering the benzylamine **5k** afforded the best results, the amination with the chiral amine **5l** was considered to check if there could be a matching or mismatching effect. Unfortunately, only the formation of traces of the product were obtained, allegedly owing to the increased steric hindrance, although a mismatch effect could be accounted. In the case of allylamine **5m**, the reaction required 10 equivalents due to its lower boiling point and therefore, its lower effective concentration.

Unfortunate but not surprisingly, the reaction with bulky amines such as *t*butylamine and adamantylamine was unsuccessful.

Table 13. Scope for alkyl amines.

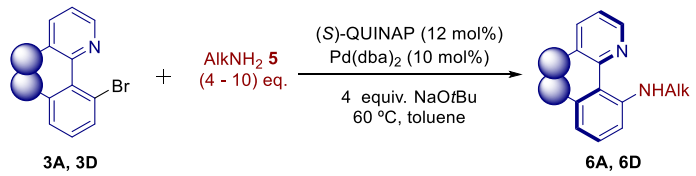

3A, 3D **6A, 6D**

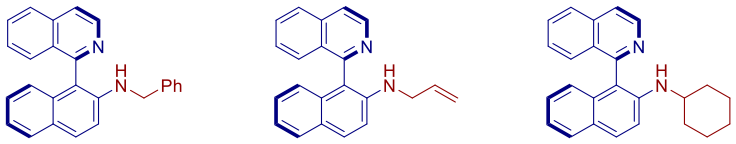

(*R*)-**6Ak:** 86%, 86% ee (*R*)-**6Am:**[b] 61%, 88% ee (*R*)-**6Ap:** 63%, 91% ee

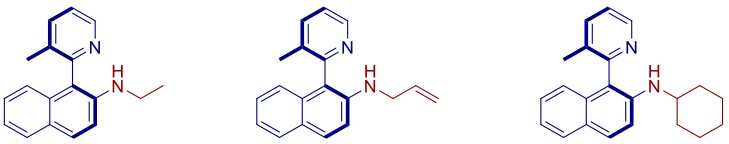

(*S*)-**6Dk:**[c] 94%, 93% ee (*S*)-**6Dm:**[b,c] 59%, 92% ee (*S*)-**6Dp:**[c] 60%, 91% ee

[a] Reactions performed on a 0.1 mmol scale using anhydrous toluene (2 mL), 2 equiv. of **5**, 2 equiv. of NaO*t*Bu at 60 °C for a period of time of 22-48 h (see experimental part). Ee's determined by chiral HPLC analysis. [b] 4 equiv. of NaO*t*Bu and 10 equiv. of **5** were used. [c] (*R*)-**L14a** was used.

Additionally, we also wanted to check the performance of secondary amines and diethylamine **5q** was chosen as a model for the reaction. However, this attempt was unsuccessful and the starting material was recovered. This lack of reactivity can be rationalized in terms of steric hindrance around the palladium centre. As we will see in the section related to the reaction mechanism, the opening of the palladacycle is difficult to achieve by simple coordination of the aniline. In this regard, bulkier secondary amines are even more hampered in such a task. Considering this, no additional secondary amine was tested.

Other heterobiaryl substrates

As we mentioned at the beginning of this section, the methodology was extended to other heterobiaryl electrophiles, thus, 4-naphthylquinazoline **F**, 1-naphthylphthalazine **G**, and 1-(4-methoxynaphthyl)isoquinoline **C** bromides and nonaflates were regarded.

First, the model reaction carried out with 4-naphthylquinazoline bromide **3F** was complete but a poor enantioselectivity was obtained (7% ee). Similarly, and **1F** underwent the reaction affording the product in 52%, 25% ee (**6Fa**). Thus, although the reaction proceeds well in terms of conversion, the lack of

selectivity makes us rule out this heterobiaryls for the scope of the reaction. On the other hand, this low chiral induction may be explained by the much lower basicity of the quinazoline not forming efficiently the palladacycle which is mandatory for the DYKAT process.

In the case of 1-naphthylphthalazine **1G**, a similar situation is found. The reaction took place with moderate yield and selectivity (**6Ga**: 80%, 61% ee). In this case, the basicity of the diazine cycle is between that of the quinazoline and the isoquinoline. Hence, the formation of the DYKAT active palladacycle occurs but not as efficiently as isoquinoline.

In addition, these heterocycles have an additional nitrogen that can coordinate to the palladium.

As for the 1-(4-methoxynaptht**h**yl)isoquinoline **3C**, the reaction proceeded with moderate yield and good enantioselectivity (**6Ca:** 52%, 82% ee), as it is expected for a isoquinoline-based electrophile (Table 14). However, in an attempt to improve the yield by increasing the reaction time, we noted an erosion of the enantiopurity of the product. Thus, when monitoring the reaction at 24h and 48 h approximately, the optical purity of the products was 77% and 73% ee respectively. Similarly, a longer reaction time of almost 3 days afforded the product with just 66% ee.

In this case, a push-pull effect can be account for this racemisation process. Thus, the methoxy group in the naphthyl group donates electrons toward the electron-poor isoquinoline making the axis have a partially double bond character, facilitating the atropisomerisation (Scheme 0-17).

*Scheme 0-17. Push-pull effect in **6Ca***

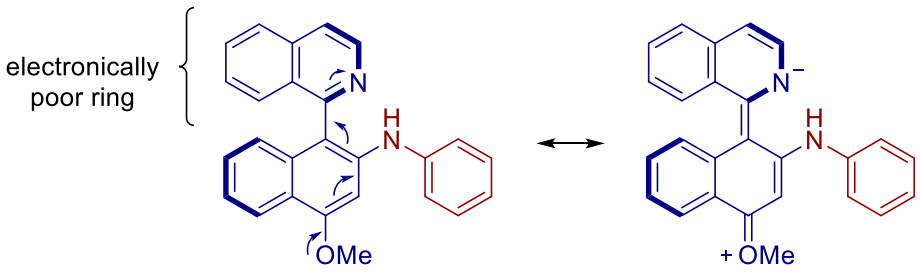

On the other hand, we also wondered if chloride heterobiaryls could be good substrates for this reaction, as it is usually the worse kind of electrophile in the Buchwald-Hartwig reaction. In order to prove this, we performed the reaction with naphthylisoquinoline chloride **4A** under standard conditions and the product was obtained satisfactorily (92%, 89% ee).

Table 14. Amination products of other heterobiaryls with aniline

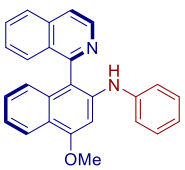

(*R*)-**6Ca:** 52%, 82% ee

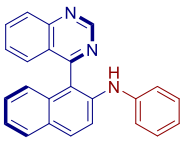

(*R*)-**6Fa:** 52%, 25% ee

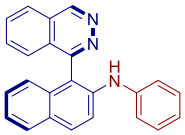

(*R*)-**6Ga:** 80%, 61% ee

Chemoselectivity

As we have previously exposed, the methodology has been applied to the cross-coupling of different heterobiaryl systems with 4-haloanilines (**5d-f**).

Here, it is worth to notice the selectivity of the reaction for the cross-coupling instead of the homo-coupling of 4-haloanilines. In this regard, heterobiaryls (pseudo)halides undergo oxidative addition preferentially over 4-haloanilines. This is in accordance with our hypothesis, in which the isoquinoline nitrogen assists this step by coordination to palladium.

IAN amine synthesis

As it was mentioned before in the introduction, one of the aims of this project is the synthesis of the free IAN-amine itself, not only its substituted derivatives. For this purpose, the shortest route to achieve this goal is the direct cross-coupling with ammonia.

As we have seen in the introduction, several procedures have been published concerning this transformation[101,102,121] although the use of high pressure, ammonia solutions or specific/selective ligands reduces the applicability to our catalytic system. Therefore, we preferred to attempt the synthesis of the free IAN through the coupling with ammonia subrogates.

In this regard, typical ammonia equivalents that can be found in the literature could be benzophenone imine,[96,97] carbamates[87,90] and silylamines[48*,99,100]. Among these reagents we tried the coupling reaction with the imine, NH_2Boc

[121] (1) Klinkenberg, J. L.; Hartwig, J. F. Catalytic Organometallic Reactions of Ammonia. *Angew. Chemie Int. Ed.* **2011**, *50* (1), 86–95. https://doi.org/10.1002/anie.201002354.
(1) Aubin, Y.; Fischmeister, C.; Thomas, C. M.; Renaud, J.-L. Direct Amination of Aryl Halides with Ammonia. *Chem. Soc. Rev.* **2010**, *39* (11), 4130. https://doi.org/10.1039/c003692g.

and ammonium sulphate.[103] Unfortunately, even though we carried out these reactions under harsher conditions, the reactions did not afford the products.

Figure 18. Amine surrogates for the synthesis of IAN-amine.

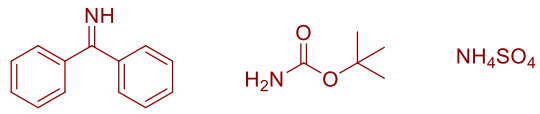

It is worth to notice that in the case of benzophenone imine, the reaction took place in the racemic version using BINAP, which are a common ligand for this amination. On the other hand, the character of the carbamate is rather acidic, and in fact, the amido group is less coordinating due to the delocalisation of the lone pair of the nitrogen. Then, it would not be surprising that poor coordination to the Pd centre ends up in no reaction.

Regarding the use of ammonia[122] or ammonium salt, this is a difficult coupling partner for several reasons: it forms stable complexes that will not undergo reductive elimination.[123] Besides, the product, as a primary amine, may also react to give secondary amines. Literature shows that fine selection of conditions and ligands are required. In this context, Josiphos[124] CyPF-*t*Bu (Figure 9) and the alkyl P,N MorDalPhos[125] forms suitable catalysts for this transformation. Unfortunately, we have proven that Josiphos ligands (Table 1) do not form good catalytic systems in the context of the DYKAT process for our heterobiaryls. On the other hand, QUINAP is far to mimic the properties

[122] Aubin, Y.; Fischmeister, C. C.; Thomas, C. M.; Renaud, J.-L. Direct Amination of Aryl Halides with Ammonia. *Chem. Soc. Rev* **2010**, *39*, 4130–4145. https://doi.org/10.1039/c003692g.

[123] Klinkenberg, J. L.; Hartwig, J. F. Slow Reductive Elimination from Arylpalladium Parent Amido Complexes. *J. AM. CHEM. SOC* **2010**, *132*, 11830–11833. https://doi.org/10.1021/ja1023404.

(b) Dorel, R.; Grugel, C. P.; Haydl, A. The Buchwald-Hartwig Amination after 25 Years. *Angew. Chemie Int. Ed.* **2019**. https://doi.org/10.1002/a

[124] Green, R. A.; Hartwig, J. F. Palladium-Catalyzed Amination of Aryl Chlorides and Bromides with Ammonium Salts. *Org. Lett.* **2014**, *16* (17), 4388–4391. https://doi.org/10.1021/ol501739g.

(b) Shen, Q.; Hartwig, J. F. Palladium-Catalyzed Coupling of Ammonia and Lithium Amide with Aryl Halides. *J. Am. Chem. Soc.* **2006**, *128* (31), 10028–10029. https://doi.org/10.1021/ja064005t.

[125] Lundgren, R. J.; Peters, B. D.; Alsabeh, P. G.; Stradiotto, M. A P,N-Ligand for Palladium-Catalyzed Ammonia Arylation: Coupling of Deactivated Aryl Chlorides, Chemoselective Arylations, and Room Temperature Reactions. *Angew. Chemie - Int. Ed.* **2010**, *49* (24), 4071–4074. https://doi.org/10.1002/anie.201000526.

of MorDalPhos and it is known that aryl phosphines are bad ligands as electron rich ligands are preferred when ammonia is the nucleophile.[124]

Another alternative to achieve the primary free amine is by means of silylamides[48*,99,100] as nucleophiles. However, we started this project studying the amination with this kind of reagents, with no results. This is not surprising since the best ligands for these nucleophiles are bulky electron-rich ones.[126]

Deprotection of amines to achieve free IAN.

If we have a better look at our scope, we find that some amines can be considered as masked free IANs. Thus, allyl, benzyl and *p*-methoxyphenyl (PMP) are removable protecting groups. Taking this into consideration, we aimed to find conditions to achieve this goal.

Deprotection of PMP

The first attempt to deprotect the amine was by means of the *p*-methoxhyphenyl (PMP) group removal by using oxidant conditions. These conditions turn the PMP group into a benzoquinone-like ring whose further hydrolysis would release the free amine.

Scheme 0-18. Deprotection of PMP group with CAN.

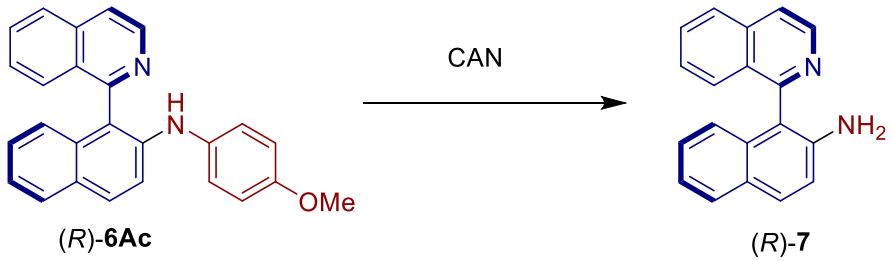

(*R*)-**6Ac** (*R*)-**7**

The first attempt of this kind of deprotection was carried out following the classical procedure using CAN.[127] After consumption of the protected amine, a new organic compound is formed but the ^{1}H-NMR analysis showed the formation of another product that did not correspond with free IAN-amine

[126] Huang, X.; Buchwald, S. L. New Ammonia Equivalents for the Pd-Catalyzed Amination of Aryl Halides. *J. Organomet. Chem* **1998**, *37*, 1144–1157. https://doi.org/10.1021/ol0166808.

[127] (1) P. G. M.; Greene, T. W. *Greene's Protective Groups in Organic Synthesis*; John Wiley & Sons, Inc.: Hoboken, NJ, USA, 2007; Vol. 9. https://doi.org/10.1002/9780470053485.ch2.book

However, other milder conditions can be utilized. Thus, we used periodic acid or TCCA[128] and the deprotection of the amine could be observed in both cases. However, the isolation of the product was not possible.

Thus, despite different conditions have been tested, the oxidative cleavage of this group could not be successfully achieved.

Deprotection of benzyl group

On the other hand, benzylamine **6Ak** is another suitable substrate to liberate IAN amine. The classical procedure to do so is the hydrogenolysis of the benzyl group under palladium on carbon catalyst with different hydrogen sources. We carried out the reaction with ammonium formate[129,130] or hydrogen gas[130] at different temperatures and using different solvents but none of them worked. In this regard, the reaction may not take place because of the coordination of the isoquinoline nitrogen or even the formation of chelates that may prevent the reaction.

Scheme 0-19. Deprotection of benzyl group

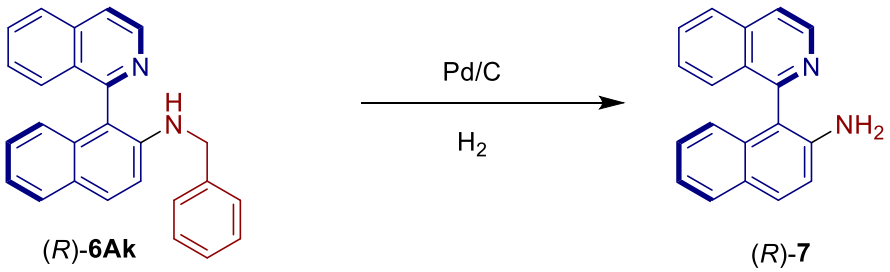

(*R*)-**6Ak** (*R*)-**7**

Deprotection of allyl group

For the deprotection of allyl from an amino group, there are a wider range of procedures. From the aforementioned hydrogenolysis to a number of metal-catalysed homogenous reactions.

---

[128] (b) Verkade, J. M. M.; van Hemert, L. J. C.; Quaedflieg, P. J. L. M.; Alsters, P. L.; van Delft, F. L.; Rutjes, F. P. J. T. Mild and Efficient Deprotection of the Amine Protecting P-Methoxyphenyl (PMP) Group. *Tetrahedron Lett.* **2006**, *47* (46), 8109–8113. https://doi.org/10.1016/j.tetlet.2006.09.044.

[129] Hoarau, C.; Couture, A.; Deniau, E.; Grandclaudon, P. A Convenient Synthesis of Alkyl- and Dialkylphenanthren-9-Ylamines. *Synthesis (Stuttg).* **2004**, *2001* (10), 1462–1470. https://doi.org/10.1055/s-2001-16090.

[130] Wuts, P. G. M.; Greene, T. W. *Greene's Protective Groups in Organic Synthesis*; John Wiley & Sons, Inc.: Hoboken, NJ, USA, 2007; Vol. 9.

As in the previous case, allyl group can be removed by hydrogenolysis due to their common "allylic" nature, and in the same vein, the hydrogenolysis did not work.

Owing to this lack of reactivity, we decided to test other methods. Thus, we performed a battery of reactions to pursue the deprotection. Contrary to the previous method, these reactions make use of homogenous catalysts based on Ni, Pd and Ru.

The first attempt was carried out using the Ogasawara's methodology[131] consisting of a Ni-based catalytic cleavage with DIBAL in toluene. This reaction seems to proceed *via* hydroalumination-elimination mechanism.[132] Nevertheless, the reaction did not occur.

Figure 19. Ni-Catalysed deprotection of allylamine with DIBAL

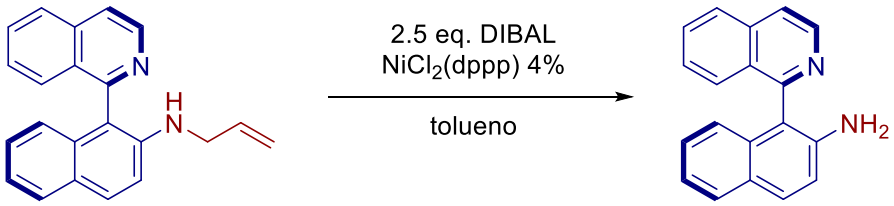

(*R*)-**6Am** (*R*)-**7**

On the other hand, the most common routes to achieve allylic cleavage by means of metal catalysis are: 1) The isomerization of the double bond that gives a product prone to hydrolysis (Grubbs' catalyst is a very suitable for this reaction). 2) the formation of a π-metal complex (typically with Pd), and a posterior extrusion of the allyl group using a scavenger that reacts with it.

Thus, we first tried the cleavage applying the first strategy using mild conditions in water described by Cadierno and Gimeno.[133] However, the use of the Ru(IV)-based catalytic system did not work.

---

[131] Taniguchi, T.; Ogasawara, K. Facile and Specific Nickel-Catalyzed de-N-Allylation. *Tetrahedron Lett.* **1998**, *39* (26), 4679–4682. https://doi.org/10.1016/S0040-4039(98)00876-4.

[132] Taniguchi, T.; Ogasawara, K. Extremely Facile and Selective Nickel-Catalyzed Allyl Ether Cleavage. *Angew. Chemie Int. Ed.* **1998**, *37* (8), 1136–1137. https://doi.org/10.1002/(SICI)1521-3773(19980504)37:8<1136::AID-ANIE1136>3.0.CO;2-Z.

[133] Cadierno, V.; García-Garrido, S. E.; Gimeno, J.; Nebra, N. Ru(Iv)-Catalyzed Isomerization of Allylamines in Water: A Highly Efficient Procedure for the

As we failed in this attempt, we moved towards trying the deprotection *via* formation of a π-complex with Pd and different scavengers such as PMHS,[134] $PhSO_2Na$/CSA,[135] *N,N'*-dimethylbarbituric acid.

Figure 20. Pd-catalysed deprotection of allyl-IAN.

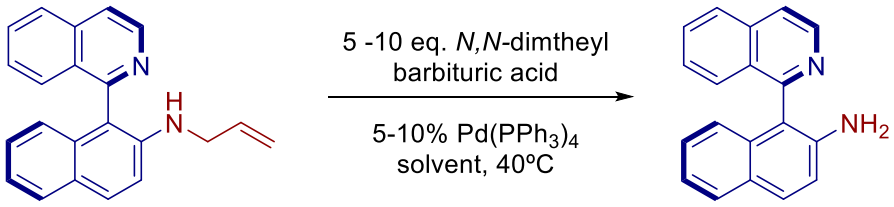

(*R*)-**6Am** (*R*)-**7**

Among these methods, the last one gave the best results regarding yield (86%) and with almost no erosion of the enantiopurity (88% ee → 86% ee). By contrast, the other two reactions ended up with a racemisation of the product although it is obtained with good or complete yield in the reaction with PMHS. As we have mentioned, these IAN amines are sensitive to acidic conditions since they promote the lability of the axis. Thus, it is not surprising that in these procedures where CSA or Zn^{2+} are utilized, the products have lost their optical purity. Furthermore, the starting material can undergo the same process. In fact, this is the case for the reaction with PMHS.

Intrigued by this unexpected result, we then decided to study the racemisation process of this kind of products.

Deprotection of N-Allylic Amines. *Chem. Commun.* **2005**, No. 32, 4086. https://doi.org/10.1039/b506788j.

[134] Chandrasekhar, S.; Raji Reddy, C.; Jagadeeshwar Rao, R. Facile and Selective Cleavage of Allyl Ethers, Amines and Esters Using Polymethylhydrosiloxane–ZnCl 2 /Pd(PPh 3) 4. *Tetrahedron* **2001**, *57* (16), 3435–3438. https://doi.org/10.1016/S0040-4020(01)00187-9.

[135] Barluenga, J.; Gómez, A.; Santamaría, J.; Tomás, M. Regioselective Synthesis of 4,6,7-Trisubstituted Benzofurans from Furfural Imines and Nonheteroatom Stabilized Alkynylcarbene Complexes. *J. Am. Chem. Soc.* **2009**, *131* (41), 14628–14629. https://doi.org/10.1021/ja9063712.

Scheme 0-20. Racemisation of IAN under acidic conditions.

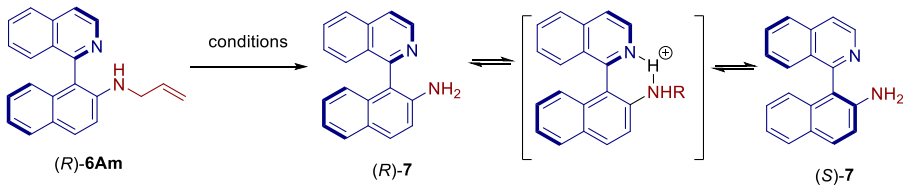

Racemisation studies

As we have just mentioned, during the deprotection of the corresponding secondary substituted amines in order to prepare free IAN itself, we observed that some procedures achieved this aim with a significative drop in the enantio-retention of the products.

In this regard, despite the racemisation of IAN-type amines may occur thermally, other routes may promote the widening of the angles involved in the axial stability facilitating this loss of enantiopurity.

In relation to the thermal racemisation, temperature is a key variable for our methodology: its influence goes beyond activity and selectivity of the reaction, and it might affect the optical purity of the product after the bond formation event, due to its atropisomeric and dynamic nature. Thus, even though the product is obtained with total enantiopurity, if allowed in solution it could racemise as time goes by. The rate at which this racemisation process occurs depends on the temperature.

In order to have an approximate idea of the racemisation energy barrier we monitored the enantiopurity of the compound (*R*)-**6Aa** (91%ee) in solution at different temperatures after 48 h (Figure 21).

*Figure 21. Thermal racemisation of (*R*)-**6Aa**.*

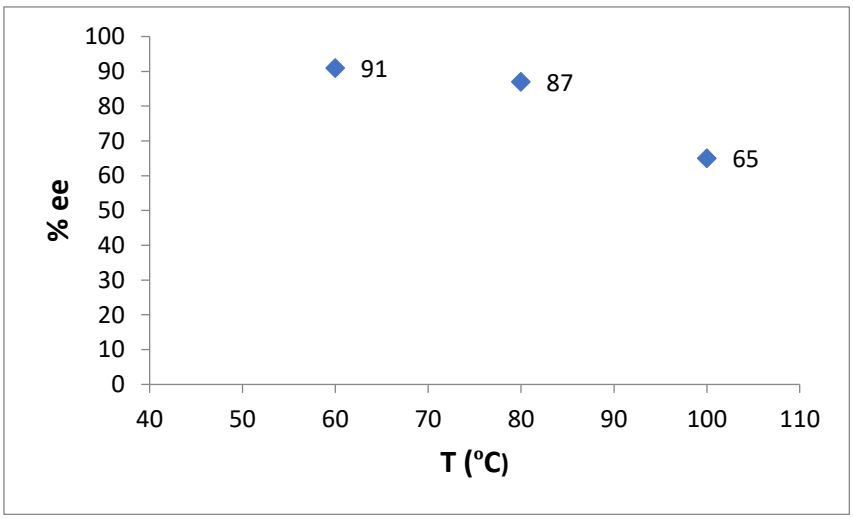

From this series of experiments, we can conclude that under standard reaction conditions (60 °C) the racemisation of the axis is too slow to be noticed and therefore, the enantiomeric excesses are reliable. Conversely, the axis stability is partially lost when raising the temperature, i.e., at 80 °C the loss of enantiopurity is noticeable (it decreased by 4% ee) and at 100 °C the racemisation process takes over and the optical purity drops to 65% ee.

On the other hand, the atropisomerisation barriers for some IAN-type amines has been measured experimentally and for others, $\Delta H^{\ddagger}$ has been computationally calculated[136].

Accordingly, the lowest $\Delta H^{\ddagger}$ for the racemisation of **6Aa** is calculated to be of 33.9 kcal/mol[136], since the heterobiaryls has two different ways of doing so, i.e., adopting a *syn*- or *anti*- conformations. The most accessible pathway corresponds to the latter, given that the amine non-bonding electron pair exerts less steric hindrance than the corresponding hydrogen at position 8.

[136] N. Johnston, J.; B. Cortright, S.; A. Yoder, R. Enantioenriched Axially Chiral B-Diketimines: Determination of the IAN-Amine Barrier to Atrop- Isomerization. *Heterocycles* **2004**, *62* (1), 223–227.

Scheme 0-21. Atropisomerisation process for IAN-amines

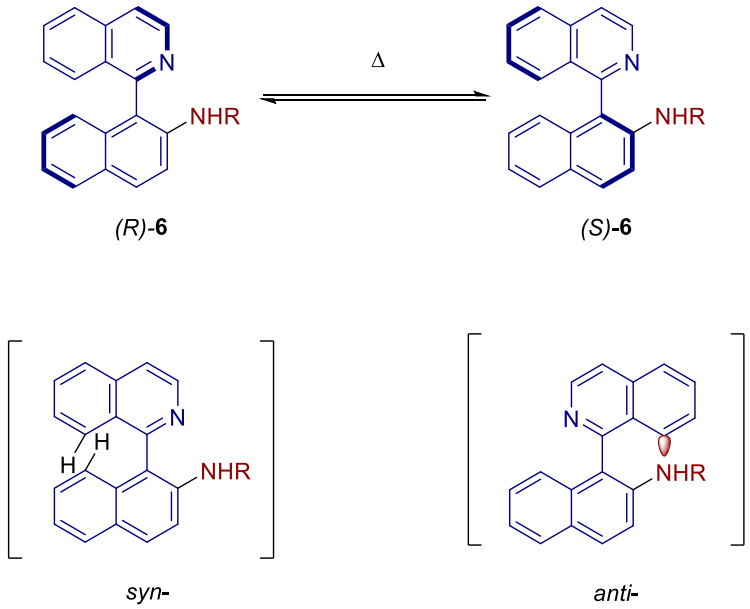

Surprisingly, this Ph-IAN **6Aa** has a lower barrier if compare to other secondary amines such as Me-IAN ($\Delta H^{\ddagger}$ = 36.2 kcal/mol) or the free amine IAN itself (experimental $\Delta H^{\ddagger}$ = 35.3 kcal/mol).[136] This could be explained by the fact that the electronegativity of the nitrogen in Ph-IAN is increased by the second aryl substitution. This way, a contraction of the non-bonding electron pair of the nitrogen would be produced. On the other hand, experimental calculations of some of these IAN-type amines show a $\Delta G^{\ddagger}$ ~ 30 Kcal/mol.[136] Thus, the magnitude of this atropisomerisation barrier implies a half-life of around 6 days at 70 ^{o}C, which seems to be in agreement with our experiments.

On the other hand, although there are not direct measured data of the atropisomerisation process for other heterobiaryls[137], Johnston could

[137] (a) Alcock, N. W.; Brown, J. M.; Hulmes, D. I. Synthesis and Resolution of 1-(2-Diphenylphosphino-1-Naphthyl)Isoquinoline; a P-N Chelating Ligand for Asymmetric Catalysis. *Tetrahedron: Asymmetry* **1993**, *4* (4), 743–756.
(b) Tucker, S. C.; Brown, J. M.; Oakes, J.; Thornthwaite, D. Resolution and Coupling of 1-(2'-Hydroxy-1'-Naphthyl)Isoquinolines. *Tetrahedron* **2001**, *57* (13), 2545–2554.
(c) Chelucci, G.; Bacchi, A.; Fabbri, D.; Saba, A.; Ulgheri, F. Enantiomerically Pure 1-(2-Methoxy-1-Naphthyl) and 1-(2-Methylthio-1-Naphthyl)Isoquinoline: Two New Axially Chiral NO and NS Ligands for Asymmetric Catalysis. *Tetrahedron Lett.* **1999**, *40* (3), 553–556.

estimate their energetic order on the basis of its 2'-substitution:[136] -PPh_2 ~ -SMe > -NR^1R^2 >> OH.

Considering other mechanisms for the racemisation of IAN, we have seen that most of the deprotection methods we tried for the preparation of free IAN involves the use of acidic reagents that can act as a proton source. Therefore, this proton might mediate the atropisomerisation of IAN through a six-member ring *via* its interaction with both nitrogens (Figure 22). Besides, the very small size of hydrogen nucleus would make this process even easier. Nevertheless, this racemisation could be avoid by rapid and careful work-up.

Figure 22. Acid mediated racemisation of IAN-type amines

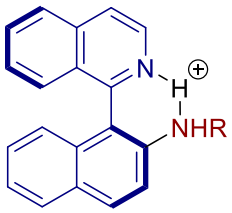

Reaction mechanism

Once the scope of this methodology has been studied, we decided to study the reaction mechanism aiming to prove our initial hypothesis on the DYKAT process as well as the limitations of this protocol. Thus, we decided to conduct some mechanistic insights by the isolation of some intermediate and experiments with them.

Scheme 0-22. Proposed Buchwald-Hartwig amination mechanism with a P,N-chelating ligand

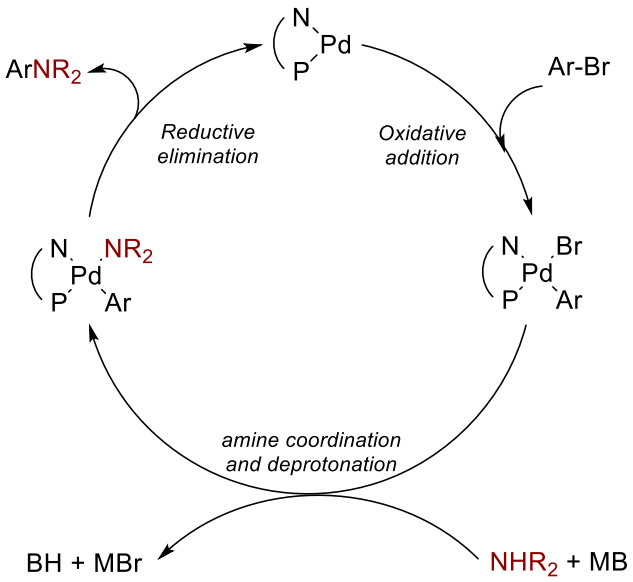

First, our proposal is based on a classic Buchwald-Hartwig mechanism (Scheme 0-22). However, this must be coupled to the Dynamic Asymmetric Transformation paradigms, so it must fulfil the following requirements:[138]

1. Two enantiomeric species react with a chiral catalyst resulting in two diastereomeric complexes.
2. These complexes are in equilibrium with each other through a chiral intermediate or TS. These complexes may have different populations depending on the rates of formation and/or interconversion.
3. The bond-forming event must be slower than the epimerisation of the complex.
4. One of these diasterosiomers must react in a faster manner providing the enantiomeric process.

Applying these concepts to the Buchwald-Hartwig cycle, the catalytic process would look as follow:

[138] Faber, K. Non-Sequential Processes for the Transformation of a Racemate into a Single Stereoisomeric Product: Proposal for Stereochemical Classification. *Chem. - A Eur. J.* **2001**, *7* (23), 5004–5010. https://doi.org/10.1002/1521-3765(20011203)7:23<5004::AID-CHEM5004>3.0.CO;2-X.

Scheme 0-23. Dynamic Kinetic Asymmetric Amination proposed mechanism.

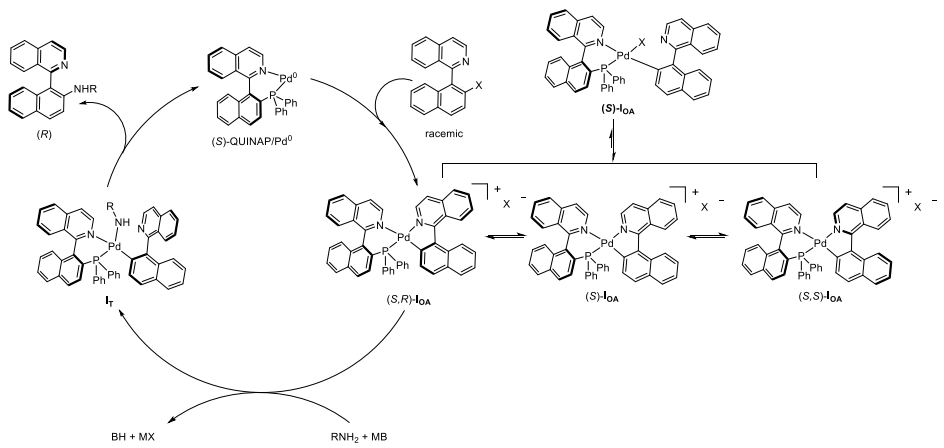

As we see, the key points on the cycle are the oxidative addition to form the palladacycle, the coordination of the amine, the deprotonation to form the amido complex and the reductive elimination step.

On the other hand, the most important step regarding the DYKAT process is the oxidative addition, since the epimerisation process occurs upon this step. This can only happen here as it is the only step in which the palladacycle is formed, and it induces the widening of the angles involved in the stability of the axis. By contrast, the eventual coordination of the amine (or the base) would release the isoquinoline moiety, stabilizing the axis.

Isolation of OA intermediate of naphthylisoquinoline triflate and X-ray analysis

Thus, our first aim is the preparation, isolation and analysis of the oxidative addition intermediate with the corresponding naphthylisoquinoline electrophile. Due to the different behaviour of triflate and bromide substrates we will study each case separately.

First, the formation of the oxidative addition intermediate (OAI) was performed considering the real system, i.e., the isoquinoline electrophile, Pd(0) and the same ligand as in the methodology, (*S*)-QUINAP. As a source of palladium, we first use [Pd(cod)(CH_2SiMe_3)$_2$] as our group did in the Suzuki-Miyaura reaction,[117] although the reaction did not proceed. Fortunately, the use of cyclopentadienyl allyl palladium gave the expected product (Scheme 0-24, more details in the experimental part) that could be crystallised and analysed by X-ray diffraction.

*Scheme 0-24. Preparation of the Oxidative Addition Intermediate from naphthylisoquinoline triflate **2A***

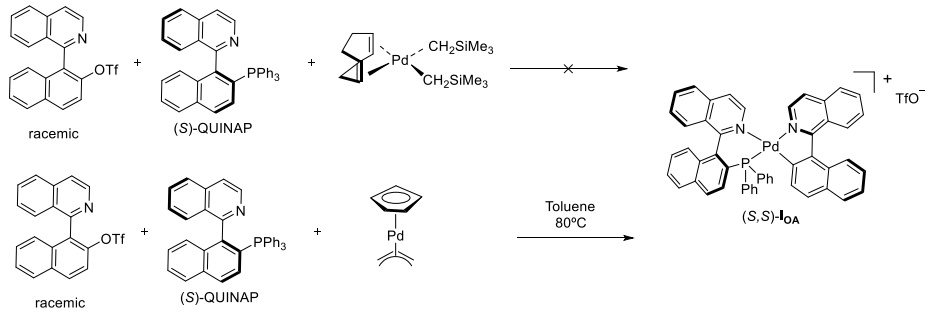

The X-ray analysis of this structure (Figure 23) reveals some interesting features. The most important is the widening of the angles involved in the axial stability of the substrate (127.6º and 125.0º instead of ideal 120º). Besides, we can notice an elongation of the Pd-N(1) (2.141 Å) if compared to Pd-N(2) (2.098 Å) due to the higher *trans* influence of the aryl fragment with respect to the phosphine. The complex also showed a deviation from the ideal square-planar geometry consisting in a torsion angle of 23.1° between the P−Pd−N(1) and the C(50)−Pd−N(2) planes.

Figure 23. X-ray analysis of (OAI)(OTf)

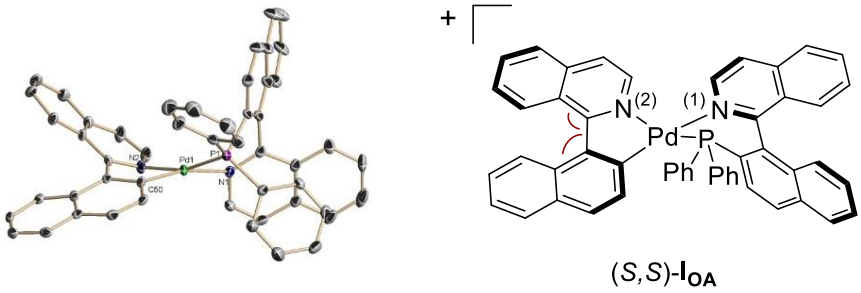

[a] Ph groups in the phosphine and OTf^- omitted.

Thus, the crystallyzation of the (OAI)+(OTf)- showed that one of the two diasteroisomers is more stable, and the interesting point is the fact that the axial configuration of the substrate is opposed to that of the product. Despite this initial contradiction, these results are in accordance to the Curtin-Hammett Principle, for which the less stable diasteromeric species could have a lower transition state energy for the rate-determining step (Figure 24). In addition, the lower energy difference observed by the NMR experiments allows for the interconversion of the more stable diasteroisomer to the catalytically active one. Furthermore, this process is in accordance to the

DYKAT process, in which the epimerisation must be faster than the enantiomerically determining step.[138]

Figure 24. Representation of the Curtin-Hammett principle and epimerisation equilibrium.

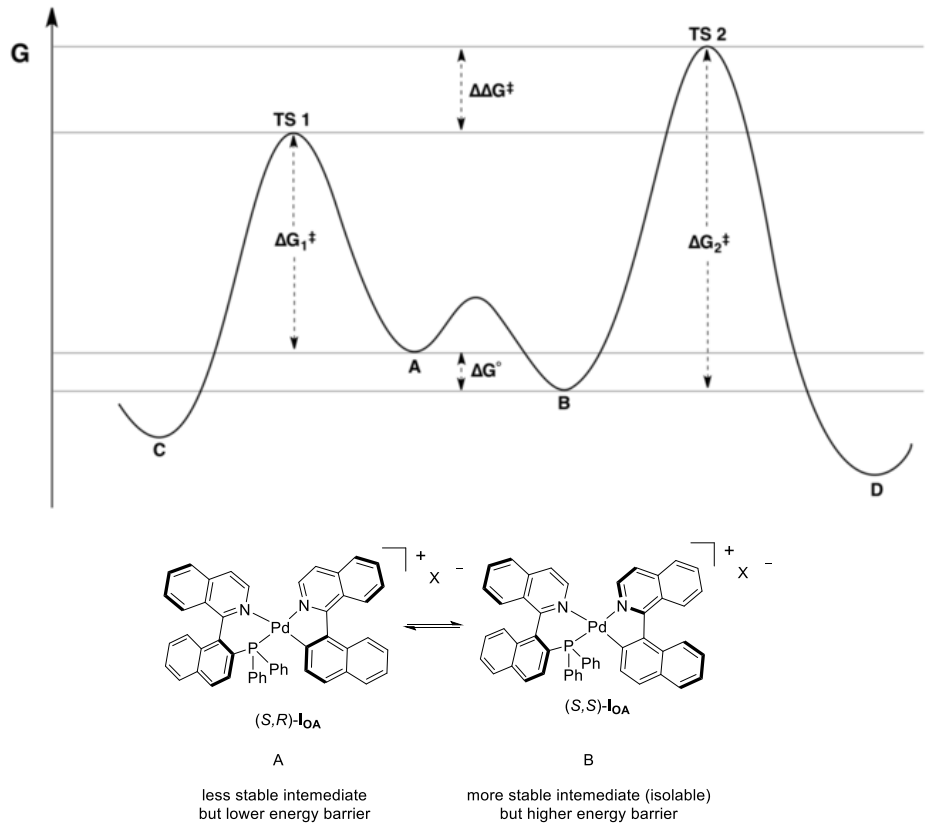

Thus, when triflate (±)-**2A** is the substrate, a tetracoordinated cationic complex is formed upon oxidative addition, due to the poor coordinating properties of the anion. The examination by ^{1}H and ^{31}P-NMR of this complex revealed the presence of a single species, which could suggest that one of the diasteroisomers in equilibrium is more stable or the epimerisation process is very fast in an NMR time scale. (Scheme 0-23).

In order to confirm this hypothesis, we examined the dynamic behaviour of the complex at different temperatures. Lowering it down to -78 ^{o}C resulted in a shift of some signals and the sharpening and widening of others, owing to the reduced mobility of aryl groups of the ligand. However, this observation is in sharp contrast to our expectations. According to our hypothesis, 2 sets of signals might arise in the case of an equilibrium between the 2 diastereomeric species. This does not mean the equilibrium does not exist, it indicates the species undergo an epimerisation process which is very fast at the NMR time

scale, even at low temperature, and an “average” compound is observed (Figure 25).

Figure 25. “Average” compound observed in NMR as a consequence of the rapid interconversion of diastereoisomers.

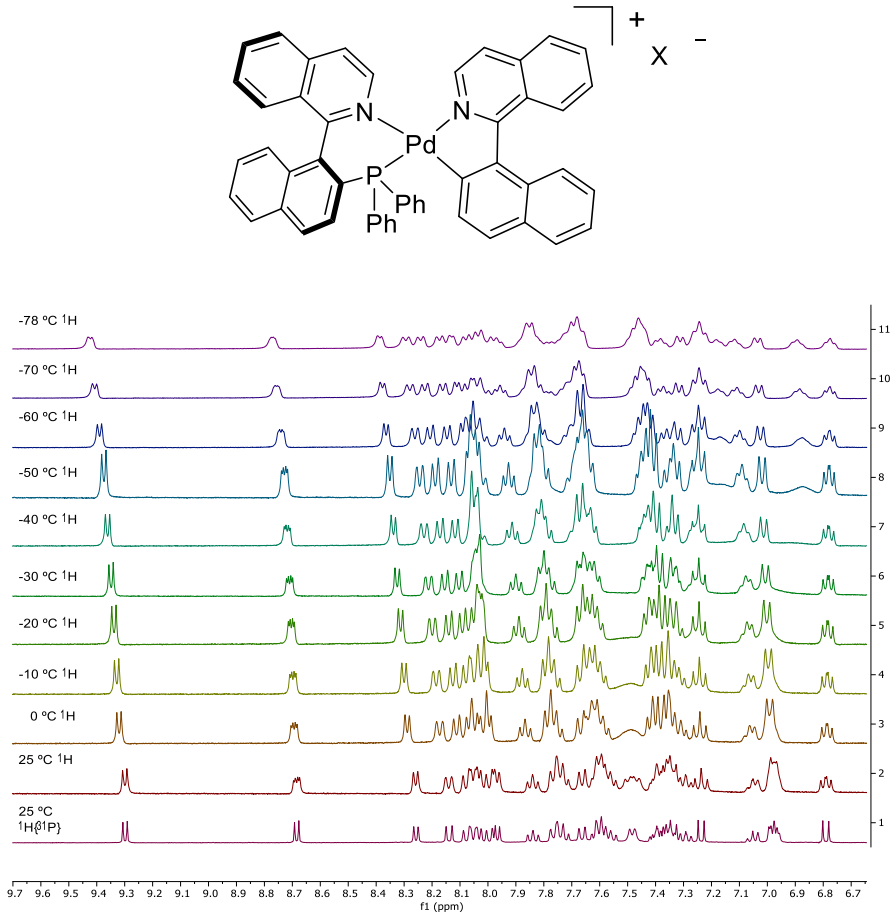

On the other hand, the crystallyzation of the (OAI)+(OTf)- showed that one of the two diasteroisomers is more stable, and the interesting point is the fact that the axial configuration of the substrate is opposed to that of the product. Despite this initial contradiction, these results are in accordance to the Curtin-Hammett Principle, for which the less stable diasteromeric species could have a lower transition state energy for the rate-determining step (Figure 24). In addition, the lower energy difference observed by the NMR experiments allows for the interconversion of the more stable diasteroisomer to the catalytically active one. Furthermore, this process is in accordance to the DYKAT process, in which the epimerisation must be faster than the enantiomerically determining step.[138]

Isolation of OA intermediate naphthylisoquinoline bromide and X-ray analysis

As we have already successfully prepared the OAI for the triflate we used the same procedure for the synthesis of the oxidative addition intermediate of naphthylisoquinoline bromide **3A** (Scheme 0-25). As a result of the reaction, a red-brown solid was formed and the crude was analysed by NMR after washing with pentane.

*Scheme 0-25. Preparation of the oxidative addition intermediate from naphthylisoquinoline bromide **3A**.*

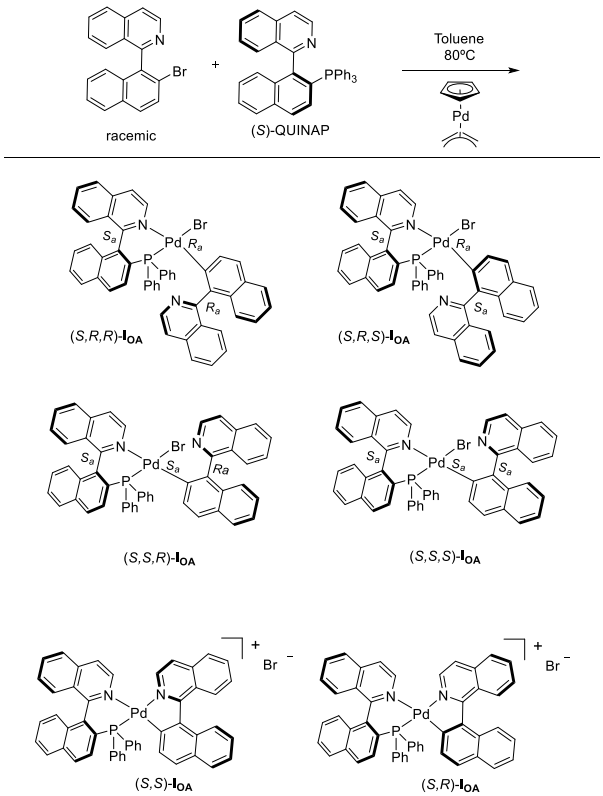

In doing so, we found a completely unexpected result. First, although we expected a different complex to (OAI)(OTf), we did not only find one signal, but several ones. The main reason of this complex mixture relies on the fact that a new axis (Pd-C bond) is generated upon coordination of bromide and therefore 4 distinct diasteroisomers can account for. In addition, a detail inspection of the spectrum reveals the presence of a species that can be assigned to a cationic palladacycles (OAI)(Br). Furthermore, the extraction of the crude with toluene allowed for a more defined spectrum, with an increased amount of the cationic complex.

Figure 26. ^{31}P NMR of OAI-Br.

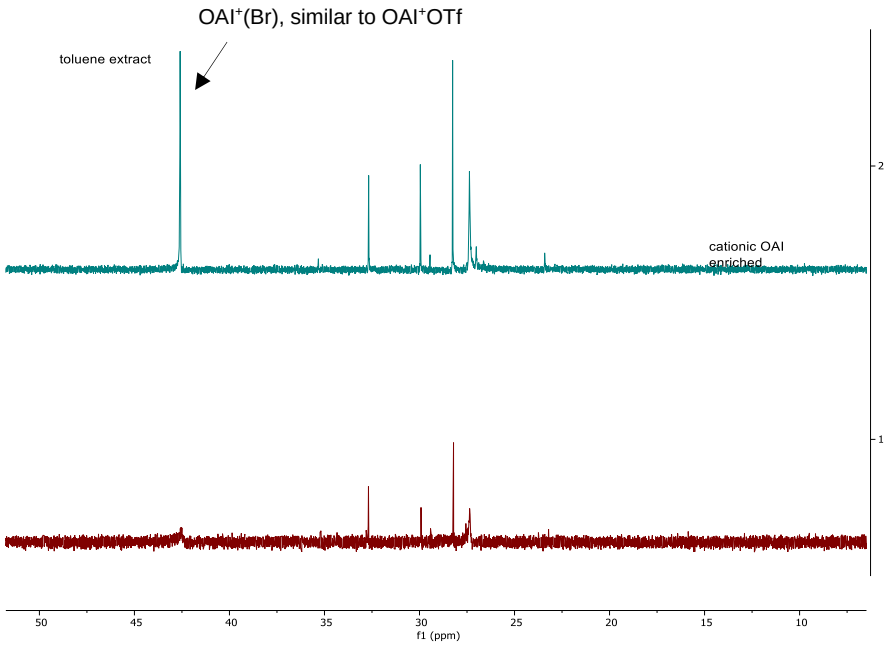

On the other hand, the crystallisation of the mixture allowed for the isolation of one of the neutral complexes, the one with the same axial configuration (R_a) as the product. Less importantly, this diastereoisomer also had R_a configuration on the C-M bond. In this structure the only one Pd-N bond is even longer (2.185 Å) than those in the (OAI)(OTf). However, we cannot compare neutral with cationic complexes although there exist a the strong *trans* influence exerted by the phenyl ligand (Figure 27). Besides, the complex is almost perfectly planar with a slight deviation corresponding to a torsion of 0.65º between the planes of P-Pd-N and C-Pd-Br.

Figure 27. X-ray analysis of OAI-Br.

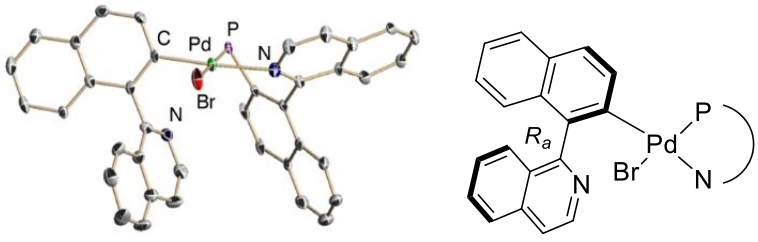

[a] Ph groups in the phosphine omitted.

This complex seems to be far stable, and the ligand exchange must be a slow process since the analysis by NMR of the crystals showed a simplified spectrum in which the cationic species is missed. This is not surprising since the long reaction time (over 2 days) and moderate temperature (80 ^{o}C) not only promotes the formation of the complex, but the lability of the ligands too.

Figure 28. OAI-Br ^{1}H NMR.

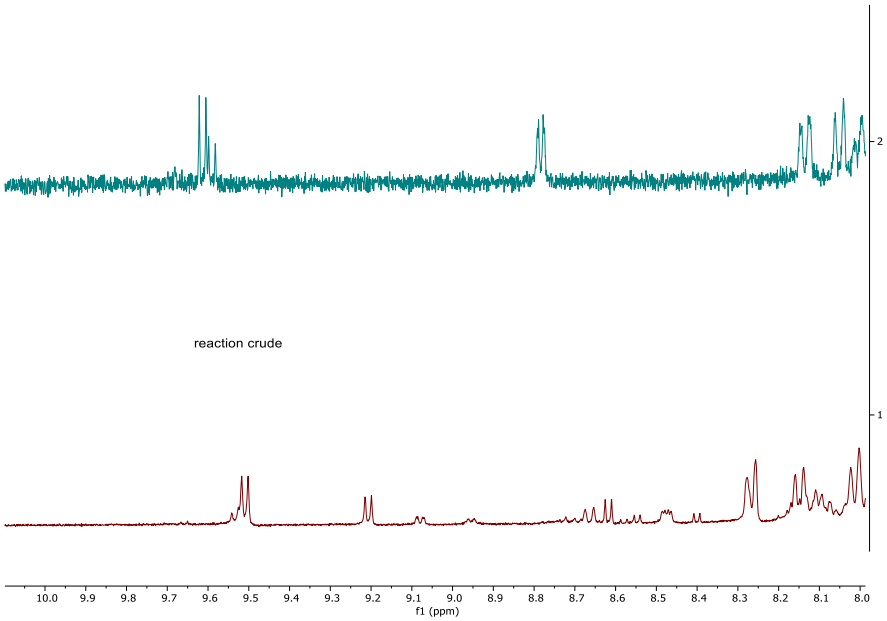

Titration with aniline and coupling experiments

Once we analysed the dynamic aspects concerning the axial chirality of our system, we wondered which would be the rate-determing step. First, we undertook studies on the oxidative addition step and then, we wanted to search on the coordination of the amine and deprotonation steps.

Hence, we carried out a titration of the cationic (OAI)(OTf) complex with aniline, which did not achieve any perturbation of the complex, even with a large excess of the amine (20 eq., Scheme 0-26). This lack of reactivity in the presence of the nucleophile, even though the reaction mixture was heated up (70^{o} C overnight) and despite the cationic nature of the complex; seems to indicate the formation of the amine-Pd complex might be the turnover determining step (Scheme 0-26).

Scheme 0-26. Titration of (OAI)+(OTf)- with aniline.

On the other hand, the base has a fundamental role in this step since the addition of Cs_2CO_3 to the NMR tube made the reaction starts even at room temperature. Therefore, the aperture of the palladacycle does not occur by the simple presence of the amine and the formation of the amido complex should be assisted by the base somehow.

Additionally, we also performed the stoichiometric reaction with (OAI)(OTf) at the standard conditions (50 ^{o}C, 7h) providing similar results to the catalytic reaction (57%, 74% ee).

Due to this stability and the lack of reactivity of the cationic (OAI)(OTf) complex, it is not very likely aniline replaces the bromide in this neutral complex and undergo the following steps of the cycle, despite it has the same configuration as the product.

However, the cationic (OAI)(Br) might follow the same steps than the (OTf) counterpart. Moreover, even though the interconversion between the neutral and cationic bromide complexes is slow, the process could be sped up in the presence of the base due to its dual role. Stated another way, NaOtBu would act as a Br- scavenger, promoting all the complexes to collapse into the corresponding cationic (OAI)(OtBu) which will have the same fate as (OAI)(OTf).

Titration of (OAI)(OTf) with NaOtBu

On the other hand, we also wanted to study if the palladacycle could be opened by the action of a strong nucleophile such as NaO*t*Bu under strictly anhydrous conditions. The addition of 1 equivalent of this base to the (OAI)(OTf) had no effect on the complex. However, when the base was added in excess, 2 species can be detected by ^{31}P NMR at expense of the (OAI)(OTf) (Figure 29). These 2 presumedly diastereoisomers (32.2 and 29.8 ppm) evolve and become a single species (26.4 ppm). Hence, the reaction with NaO*t*Bu could open the palladacycle and 2 diasteroisomers were formed in a close to 1:1 ratio. This is not surprising since we expected a rapid isomerization between the two almost degenerate diastereomeric palladacycles. On the other hand, we would have expected 4 species due to the additional axis generated (C-Pd) upon the dissociation of the isoquinoline and its two possible relative orientations regarding the complex plane. However, the diastereomeric nature of the intermediate in solution may direct the attack of the base towards the opening of the complex from only one direction, in a stereoselective manner.

Next, the reaction did not stop after the coordination of the NaO*t*Bu and kept on evolving toward the formation of a single species. On the other hand, this species and that which is achieved after stochiometric Buchwald-Hartwig reaction with the (OAI)(OTf) show similar chemical shifts (^{31}P NMR signals at 26.4 and 26.2 ppm respectively) indicating the formation of a Pd(0) complex. According to this, we would expect the reductive elimination of tBuO – naphthylisoquinoline product, but it was not observed. At any rate, it has been reported that alkoxo complexes may undergo decomposition providing products from reactions such as homocoupling, arene reduction, and even aryl exchange from the phosphine.[108]

Figure 29. Titration of (OAI)(OTf) with NaOtBu.

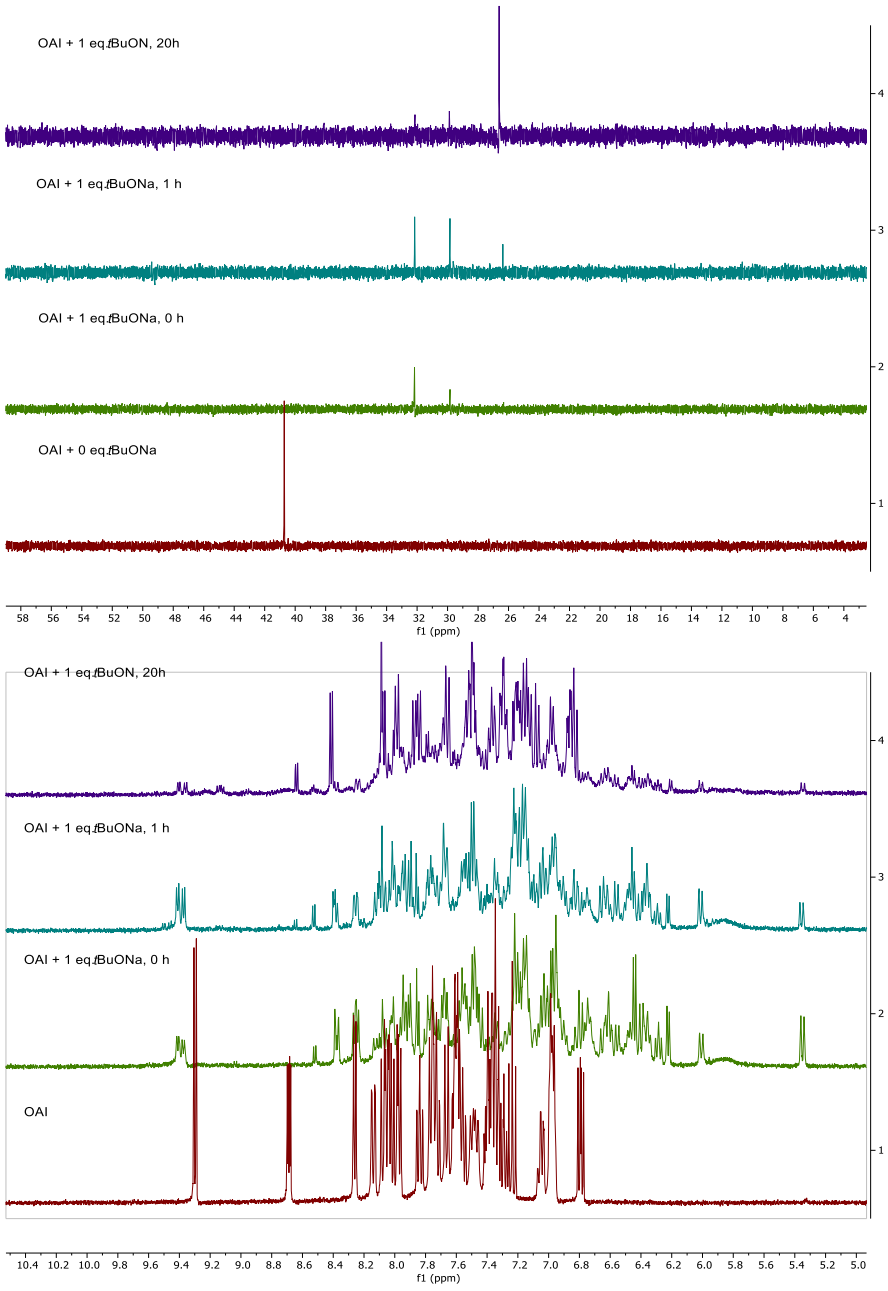

This experiment demonstrates that the base-mediated opening of the palladacycle is possible at room temperature and base-palladium complexes might be potential intermediates in the reaction.

Titration of OAI-Br with NaOtBu

In view of these results, we also wanted to check the reactivity of the mixture of bromide complexes upon oxidative addition in the presence of NaO*t*Bu; reaction which was monitored by NMR in THF-d8. Thus, the mixture immediately reacted with the base affording a ^{1}H NMR spectra with signals very similar to those of the reaction of (OAI)(OTf) with NaO*t*Bu (around 9.1 and 8.4 ppm).

Figure 30. Titration of OAI-Br with NaOtBu.

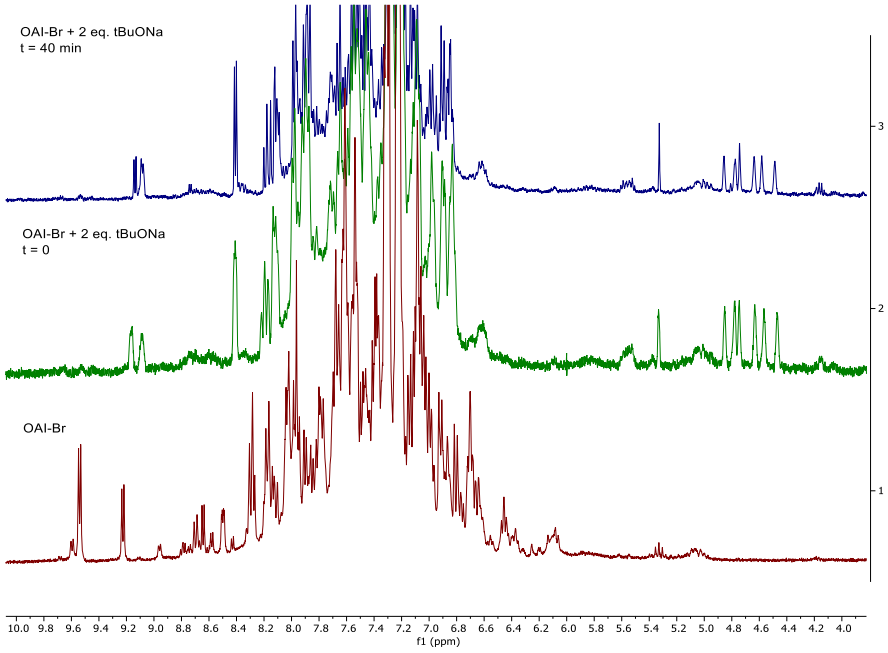

By contrast, the ^{31}P NMR spectra showed a more complex situation (Figure 30): The system was not simplified and several new signals appeared, although 2 of them were very similar to those found in the case of (OAI)(OTf). Nevertheless, these two signals (32.7 ppm and 30.0 ppm) evolved in different ratios, contrary to the case of (OAI)(Br), which reached 1:1. Additionally, this mixture did not evolve into the putative Pd(0) complex, at least during the monitoring time.

Figure 31. Titration of OAI-Br with NaOtBu. ^{31}P NMR

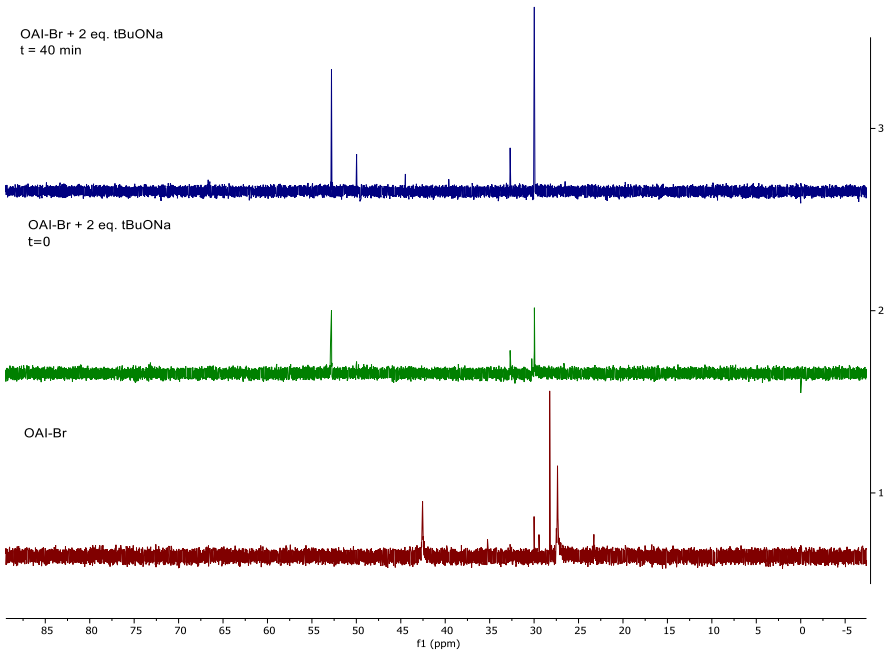

Thus, it is proven that the reaction of the oxidative addition intermediates of the bromide naphthylisoquinoline with NaOtBu occurs. However, the lack of a simple spectrum might be due to a number of reasons. First, the starting mixture was composed for several type of complexes in different ratios. Therefore, different reactivity is expected. Second, due to the different non-degenerated diastereomeric relations between the starting species, the products may appear in different ratios.

Titration with PPh_3

Considering that the palladacycle opening was not possible using aniline (20 equiv.) as the nucleophile, and with the idea in mind of analysing this "transmetallation step", we decided to carry out this study with a more nucleophile compound like PPh_3. In addition, these experiments could reveal which is the more labile position of the complex and hence, where the attack of the amine would take place.

Thus, we conducted a titration with triphenylphosphine in a solution of the (OAI)(OTf) complex affording the formation of major diphosphino palladium adduct. The ^{31}P NMR spectrum uncovered an AB system in which the $J_{P\text{-}P}$ = 373 Hz indicated the relative positions of the phosphines corresponded to a trans

disposition.[139] At first sight, the regiochemistry of this substitution could be surprising if we take into consideration the strong trans effect exerted by the naphthyl ring to the QUINAP isoquinoline. However, the substrate moiety is strained due to the formation of the 5-membered palladacycle and therefore, the substitution of the substrate isoquinoline results in an energy release making the reaction kinetically favoured.

Scheme 0-27. Titration of (OAI)(OTf) with PPh_3

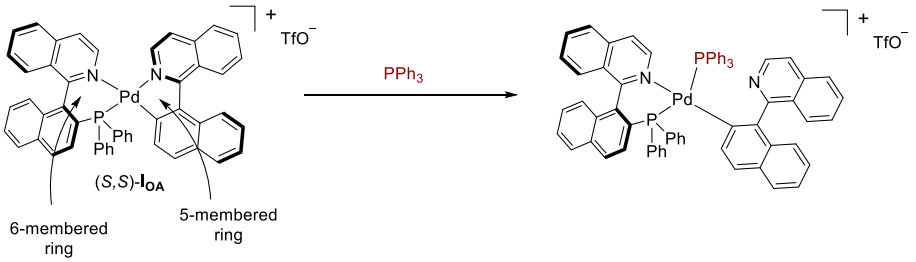

In addition to this adduct, other species appeared providing different signals that cannot be easily assigned due to the number of geometries, stereoisomers, etc. that might arise. These resonances become more obvious when an excess of triphenylphosphine is added and then free phosphine appears at -5.3 ppm as a broad signal upon 2.5 equivalents.

On the other hand, inspecting the ^{1}H NMR spectrum we found that the resonances corresponding to one of the isoquinoline rings (3H) is shielded which can be interpreted as the unbinding of the nitrogen and replacement by the phosphine.

[139] $J_{trans} \sim 360$, $J_{cis} \sim 50$.

Figure 32. Titration of (OAI)(OTf) with PPh_3. ^1H NMR.

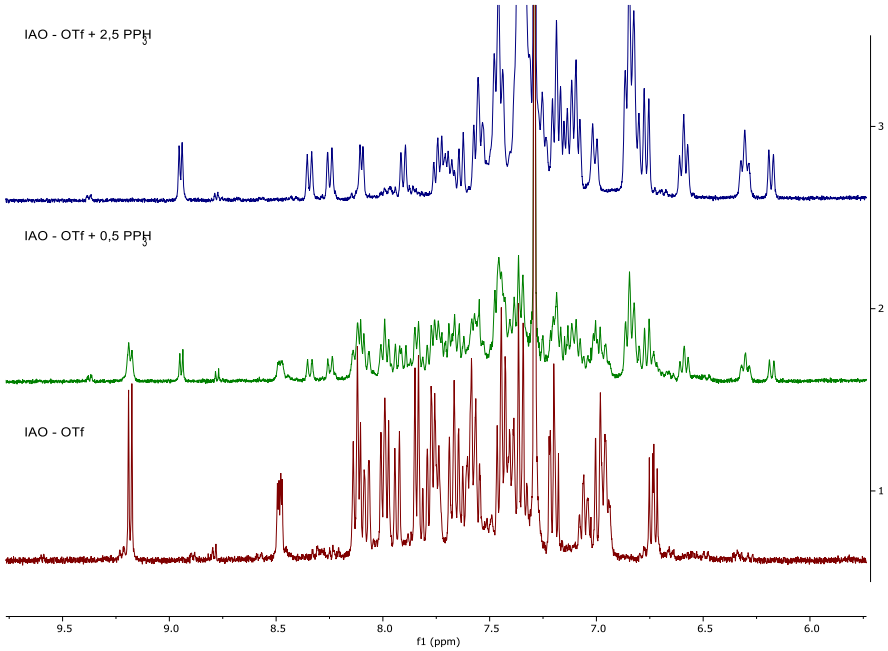

Figure 33. Titration of (OAI)(OTf) with PPh3. ^{31}P NMR.

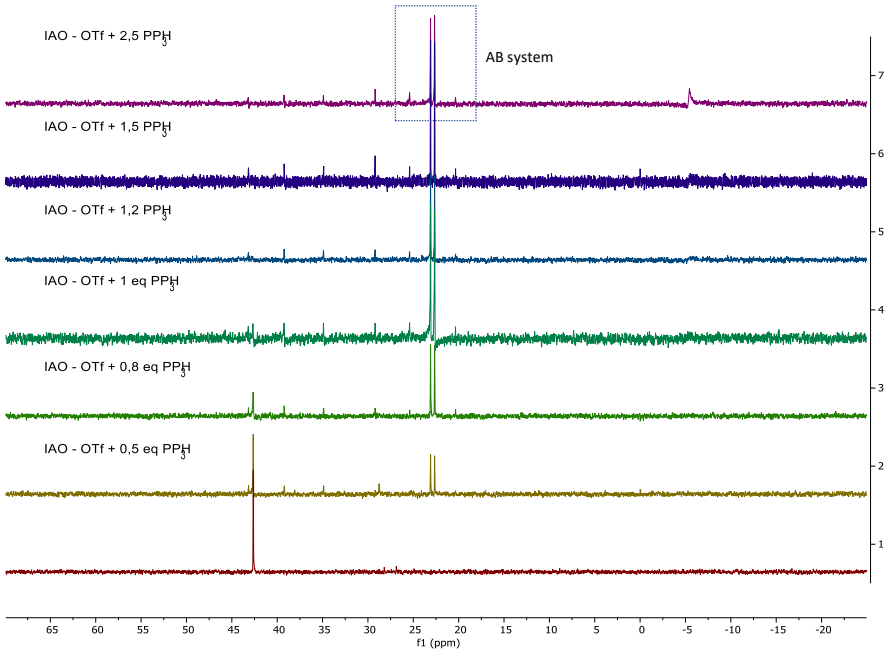

Reaction monitoring

In order to reveal more details concerning the turnover limiting step we conducted the reaction of (OAI)(OTf) with aniline with similar conditions to those of the catalytic reaction, i.e., 20 eq of both amine and base.

The reaction was first carried out at 50 ^{o}C and was monitored by ^{1}H and ^{31}P NMR for over 24 h. This experiment showed the consumption of the oxidative addition intermediate could be complete after ~7h, and the analysis of the product is in accordance to the methodology (57%, 74% ee). However, the heterogenous character of the reaction and the temperature close to the boiling point of the solvent made the NMR acquisition poor, so this is just a vague estimation. On the other hand, when the same reaction was carried out at 40 ^{o}C a better resolution was obtained although around 30 h were necessary for the reaction to be completed (Figure 34).

Figure 34. Reaction monitoring of (OAI)(OTf) with aniline by 1H and 31P NMR at 40 ^{o}C

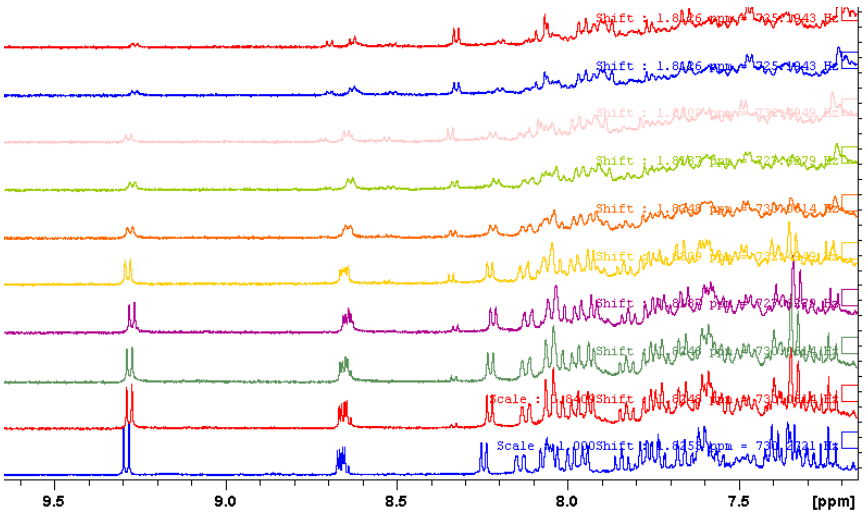

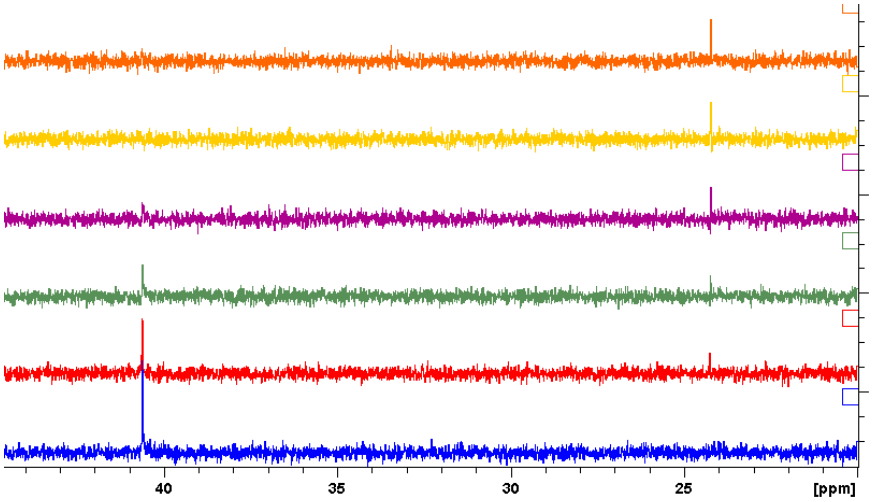

In both cases we observe the consumption of (OAI)(OTf) and the formation of another palladium complex, which could presumably be assigned to a Pd(0)/(*S*)-QUINAP complex, as the reaction goes by. These 2 complexes were the only Pd-species that could be detected. By contrast, the putative amido-complex resulted from coordination and deprotonation of the amine, was not observed. This lack of the amido complex points to the fact that it is not the resting state and the reductive elimination is fast. In other words, the formation of the amido complex seems to be turning limiting step.

Proposed mechanism

With all this information in hand, a general mechanism for the Dynamic Kinetic Asymmetric amination of heterobiaryls can be proposed (Scheme 0-28). However, some differences are found when triflate or bromide are used as the coupling partner.

Scheme 0-28. Proposed reaction mechanism

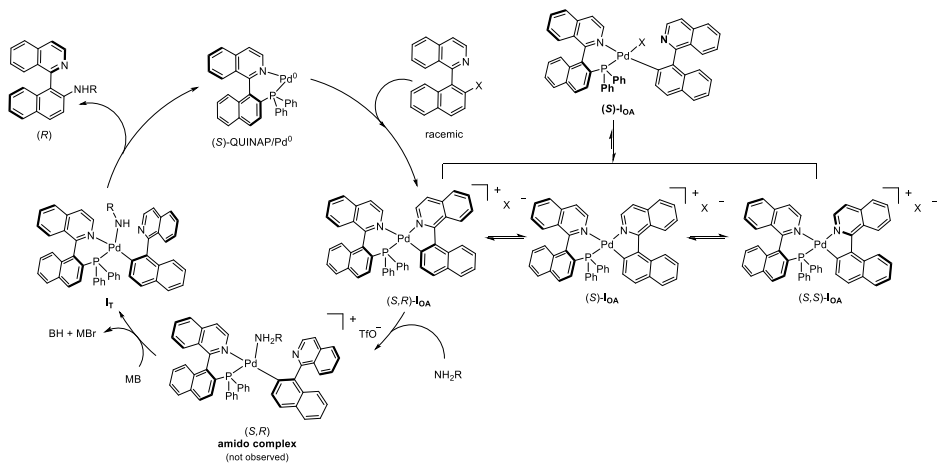

Thus, when triflate heterobiaryls undergo the oxidative addition step, the racemisation of the axis occurs through a rapid epimerisation equilibrium of the palladacycle. Then, the most unstable complex undergoes the next step of the cycle according to the Curtin-Hammett principle, since the other diasteroisomer is stable enough to be isolated.

On the other hand, the rate of reaction accomplished with the (OAI)(OTf) is comparable to the catalytic procedure, so oxidative addition is unlikely to be the rate limiting step. In addition, we have previously seen that the coupling reaction with **4A** chloride with aniline gave excellent results, supporting this idea.

Thus, the resting state of the reaction mechanism must be some step concerning the "transmetallation". This is so, because the reaction of the (OAI)(OTf) with the rest of the reagents evolves in the product and no species between oxidative addition and reductive elimination can be detected by ^{31}P NMR. Hence, the lack of a more stable intermediate implies the species we have at the beginning of the reaction is indeed the resting state.

Unfortunately, the details involved in the "transmetallation" remain unclear. It seems fair to say that amines are too basic to be deprotonated by the base without activation by the metal. Furthermore, the formation of the amido complex by means of an alkoxo complex cannot be rule out. At any rate, the formation of the amido complex is mandatory.

On the other hand, according to the trans influence exerted by naphthyl ring, the most labile position of the (OAI) would be occupied by isoquinolinic nitrogen of QUINAP. By contrast, we have seen that substitution occurs trans

to the phosphine although this may happen as a consequence of a rapid reorganization process.

In case this reorganization is required, this process could happen after deprotonation, since free p orbitals of the amido-ligand would facilitate this isomerization[140]. As a result, the amide/amine would end up in the substrate's nitrogen position, liberating the isoquinoline moiety and hence, making the configuration of the axis fixed. In other words, this is the stereodetermining step of the reaction.

Once the amide and the aryl are in cis configuration, the reductive elimination would lead to the product, a Pd(0) complex, and the catalytic cycle is closed.

On the other hand, the synthetic conditions when using bromide are slightly different, possibly due to the different nature of the anion generated upon oxidative addition. This may translate to some distinct reaction pathways and/or particularities, such as the different optimal base.

Thus, in the same vein of the triflate, we conducted the isolation of the (OAI)(Br) and some stoichiometric reactions.

In the case of bromide heterobiaryls, the catalytic cycle starts following the same steps, i.e., the substitution of ligands and oxidative addition. We will not consider the effect of dba on oxidative addition for simplification; despite it may reduce the rate of the step.

As we have seen, upon this step the formation of a mixture of palladium species takes place. Thus, diastereomeric cationic species are formed but the corresponding neutral palladacycle too. The reason for this is the fact that anionic ligands such as bromide coordinates preferentially to the metal rather than neutral ligands such as isoquinoline.

At any rate, these species are found in equilibrium, and the broad signals on in the ^{31}P NMR spectra accounts for that. Hence, this entails a way for the labilisation of the axis. However, it is unclear if the process only happens by means of bromide-isoquinoline-bromide exchange or it may compete with the epimerisation of the neutral complex itself like in the case of (OAI)(OTf). Since the epimerisation of neutral palladium complexes seems to be slow, it is more likely this process happens via cationic complexes. In this regard, NaO*t*Bu may

[140] Sunesson, Y.; Limé, E.; Nilsson Lill, S. O.; Meadows, R. E.; Norrby, P.-O. Role of the Base in Buchwald–Hartwig Amination. *J. Org. Chem.* **2014**, *79* (24), 11961–11969. https://doi.org/10.1021/jo501817m.

have a key role, as it would provoke the precipitation of NaBr and subsequently, the formation of the neutral palladacycle (OAI)(OtBu).

The next step is the coordination / deprotonation of the amine which would happen in a similar fashion to that of triflate natphtylisoquinoline. Similarly, the formation of the amido complex would be the rate-determining step and the subsequent redutive elimination would afford the amination product.

Conclusions

In summary, in this chapter a new methodology for the synthesis of IAN type amines have been developed through a DYKAT-based Buchwald-Hartwig amination. In this regard, we have prepared a family of this axially chiral *N,N*-diamines in high yields and good to excellent enantioselectivities employing different racemic heterobiaryls as the starting materials. Reaction worked in a very efficient manner with different primary arylamines contaning electron donating and electron withdrawing groups, while primary alkyl amines required longer reaction times, the use of more equivalents and showed a limited reaction scope.

In addition, the isolation of the oxidative addition intermediates and reactivity studies of these have been carried out, supporting the proposed idea in which the chiral axis is labilised by the formation of 5-membered palladacycles.

Experimental section

General information

^{1}H NMR spectra were recorded at 300 MHz, 400 MHz or 500 MHz; ^{13}C NMR spectra were recorded at 75 MHz, 100 MHz or 125 MHz with the solvent peak used as the internal reference (7.26 and 77.2 ppm for ^{1}H and ^{13C} respectively for $CDCl_3$; 5.32 and 53.8 ppm for ^{1}H and ^{13C} respectively for CD_2Cl_2; and 3.58 and 1.73 ppm for ^{1}H THF-d_8); Column chromatography was performed on silica gel (Merck Kieselgel 60). Analytical and preparative TLC was performed on aluminum backed plates (1.5 × 5 cm) pre-coated (0.25 mm) with silica gel (Merck, Silica Gel 60 F_{254}). Compounds were visualized by exposure to UV light or by dipping the plates in a solution of 5% $(NH_4)_2Mo_7O_{24}{\cdot}4\ H_2O$ in 95% EtOH (w/v) or followed by heating.

Anhydrous 1,4-dioxane and THF were obtained by distillation from sodium using benzophenone as indicator. $Pd(dba)_2$ and ligands **L4-L13** were purchased from Aldrich and used without any further purification.

Ligands **L1**,[141] **L2**,[116] and **L3**,[117,142] **L14**[44]nonaflates (±)**-1A,F** and triflates **(±)-2A**[143] and **(±)-2B**,[144] 1-napththylisoquinoline,[145] 3-methyl-2-(naphthalen-1-yl)pyridine[144] and 1-(*o*-tolyl)isoquinoline[146] were synthesized according to literature procedures.

---

[141] Álvarez-Casao, Y., Estepa, B.; Monge, D.; Ros, A.; Iglesias-Sigüenza, J.; Álvarez, E.; Fernández, R.; Lassaletta, J. *M. Tetrahedron*, **2016**, *72*, 5184–5190.

[142] a) Ros, A; Estepa, B; Ramírez-López, P; Álvarez, E; Fernández, R; Lassaletta, J. M. *J. Am. Chem. Soc*. **2013**, *135*, 15730-15733. b) Alexakis, A.; Burton, J.; Vastra, J.; Benhaim, C.; Fournioux, X.; van den Heuvel, A.; Levêque, J.-M.; Mazeé, F.; Rosset, S. *Eur. J. Org. Chem.* **2000** , 4011-4027.

[143] Lim, C. W.; Tissot, O.; Mattison, A.; Hooper, M. W.; Brown, J. M.; Cowley, A. R.; Hulmes, D. I.; Blacker, A. J. *Org. Process Res. Dev.*, **2003**, *7*, 379–384.

[144] Connolly, D. J.; Lacey, P. M.; McCarthy, M.;. Saunders, C. P.; Carroll, A-M.; Goddard, R.; Guiry, P. J. *J. Org. Chem.* **2004**, *69*, 6572–6589.

[145] Yang, C.-H.; Tai, C.-C.; Huang, Y.-T.; Sun, I.-W. *Tetrahedron* **2005**, *61*, 4857-4861.

[146] Doherty, S.; Knight, J. G.; McGrady, J. P.; Ferguson, A. M.; Ward, N. A. B.; Harrington, R. W.; Clegg, W. *Adv. Synth. Catal.* **2010**, *352*, 201-211.

Synthesis of bromides (±)-3A,D-E and chloride (±)-4A.

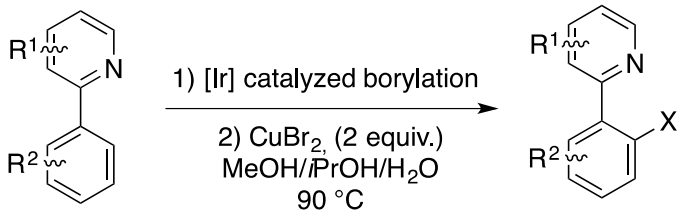

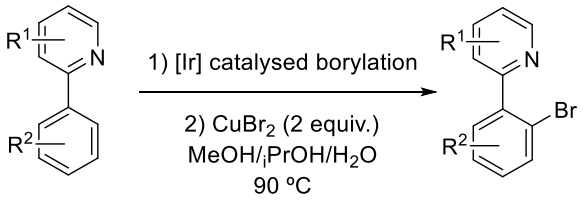

Following the described procedure for the directed borylation reaction,[147] a dried Schlenk tube was charged with the corresponding arylisoquinoline and B_2pin_2 (1.2 eq.), [Ir(□-OMe)(cod)]$_2$ (1 mol%) precatalyst and *N*,*N*-Dibenzyl-*N*'-(pyridin-2-ylmethylene)hydrazine (2 mol%) as the ligand. THF (2 mL/mmol substrate) and pinacolborane (HBpin; 5 mol%) were added and the mixture was stirred at 70 °C until consumption of the starting material (TLC monitoring). The mixture was dissolved in a 3:2 MeOH/*i*-PrOH mixture (19 mL/mmol substrate), treated with a solution of $CuBr_2$ (2.0 eq.) in H_2O (9.5 mL/mmol substrate), and stirred overnight at 90 °C.[148] The mixture was cooled to rt, neutralized (aq. NH_3), and extracted with EtOAc. The combined organic layer was washed with a saturated solution of EDTA, dried ($MgSO_4$,) filtered, concentrated, and the residue was purified by column chromatography (*n*-hexane/EtOAc or CH_2Cl_2/EtOAc mixtures). Starting material, solvent used for chromatography, yields, and characterization data for products **3A-C** are as follows:

[147] Ros, A.; Estepa, B.; López-Rodríguez, R.; Álvarez, E.; Fernández, R.; Lassaletta, J. M. *Angew. Chem., Int. Ed*. **2011**, *50*, 11724-11728.

[148] Pais, V. F.; Alcaide, M. M.; López-Rodríguez, R.; Collado, D.; Nájera, F.; Pérez-Inestrosa, E.; Álvarez, E.;. Lassaletta, J. M.; Fernández, R.; Ros, A.; Pischel, U. *Chem. Eur. J.* **2015**, *21*, 15369-15376.

*1-(2-Bromonaphthalen-1-yl)isoquinoline (±)-**3A**.*

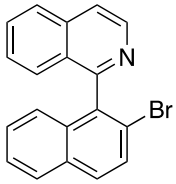

Following the general procedure from 1-napththylisoquinoline (5 mmol, 1.28 g), flash chromatography (20:1 CH_2Cl_2/EtOAc) afforded (±)-**3A** (870 mg, 52%) as a light yellow solid. Spectroscopic and physical data matched those reported in the literature.[142a]

*2-(2-Bromonaphthalen-1-yl)-3-methylpyridine (±)-**3D**.*

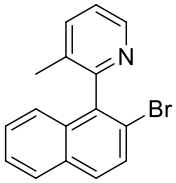

Following the general procedure from 3-methyl-2-(naphthalen-1-yl)pyridine (5 mmol, 1.27 mg), flash chromatography (5:1 *n*-hexane/EtOAc) afforded (±)-**3D** (740 mg, 50%) as a light yellow amorphous solid. ^{1}H NMR (400 MHz, $CDCl_3$) δ 8.65 (ddd, 1H, *J* = 4.8, 1.6 and 0.6 Hz), 7.87 (d, 1H, *J* = 8.2 Hz), 7.78 (d, 1H, *J* = 8.7 Hz), 7.72 (d, 1H, *J* = 8.8 Hz), 7.70 (ddd, 1H, *J* = 7.7, 1.6 and 0.8 Hz), 7.49 (ddd, 1H, *J* = 8.2, 6.9 and 1.2 Hz), 7.38 (ddd, 1H, *J* = 8.4, 7.2 and 1.1 Hz), 7.34 (dd, 1H, *J* = 7.9 and 5.0 Hz), 7.14 (ddt, 1H, *J* = 8.4, 1.1 and 0.7 Hz), 2.04 (s, 3H). ^{13}C NMR (100 MHz, $CDCl_3$) δ 157.6, 147.3, 138.2, 137.9, 133.2, 132.6, 129.9, 129.8, 128.3, 127.4, 126.3, 125.5, 123.2, 121.0, 18.6. HRMS (EI) calcd. for $C_{16}H_{12}BrN$ (M^+) 297.0153. Found 297.0157.

*1-(2-Bromo-6-methylphenyl)isoquinoline (±)-**3E**.*

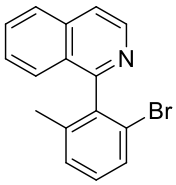

Following the general procedure from 1-(*o*-tolyl)isoquinoline (3 mmol, 675 mg), flash chromatography (3:1 *n*-hexane/EtOAc) gave the borylation product (340 mg, 33%) which was used in the second step of the general procedure to afford product (±)-**3E** (150 mg, 50%) as a light yellow amorphous solid after flash chromatography (20:1 CH_2Cl_2/EtOAc). ^{1}H NMR (500 MHz, $CDCl_3$) δ 8.66 (d, 1H, *J* = 5.7 Hz), 7.92 (d, 1H, *J* = 8.2 Hz), 7.79-7.68 (m, 2H), 7.56 (d, 1H, *J* = 7.8 Hz), 7.54-7.48 (m, 2H), 7.30 (d, 1H, *J* = 7.5 Hz), 7.28-7.23 (m, 1H), 1.97 (s, 3H). ^{13}C NMR (100 MHz, $CDCl_3$) δ 160.3, 142.6, 139.5, 139.3, 136.5, 130.5, 130.2, 129.8, 129.3, 127.7, 127.2, 126.5, 123.6, 120.5, 20.5. HRMS (EI) calcd. for $C_{16}H_{12}BrN$ (M^+) 297.0153. Found 297.0159.

*1-(2-Chloronaphthalen-1-yl)isoquinoline (±)-**4A**.*

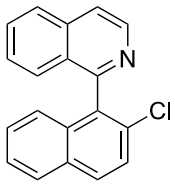

Following the general procedure from 1-napththylisoquinoline (2.35 mmol, 600 mg) and using $CuCl_2$ (2.0 equiv.) instead of $CuBr_2$, flash chromatography (*n*-hexane/EtOAc 4:1) afforded (±)**-4A** (325 mg, 65%) as a white amorphous solid. ^{1}H NMR (400 MHz, $CDCl_3$) δ 8.80 (d, 1H, *J* = 5.8 Hz,), 7.95-7.90 (m, 3H), 7.79 (dd, 1H, *J* = 5.8 Hz and 0.5Hz), 7.68-7.63 (m, 2H), 7.50-7.45 (m, 2H), 7.39 (ddd, 1H, *J* = 8.1 Hz, 6.8 Hz and 1.1 Hz), 7.31 (ddd, 1H, *J* = 8.3 Hz, 6.8 Hz and 1.2 Hz), 7.13 (dd, 1H, *J* = 8.4 Hz and 0.7 Hz). ^{13}C NMR (100 MHz, $CDCl_3$) δ 157.9, 142.6, 136.3, 134.4, 133.6, 132.0, 131.4, 130.4, 130.0, 128.0, 128.0, 127.6, 127.2, 127.1, 127.0, 126.7, 126.1, 125.7, 120.7. HRMS (EI) calcd. for $C_{19}H_{12}NCl$ (M^+) 289.0658. Found 289.0656.

Dynamic Kinetic Asymmetric C-N Cross–Coupling employing QUINAP ligand L14a.

*From heterobiaryl sulfonates***:** A dried Schlenk tube was charged with the corresponding nonaflate (±)**-1A** or triflate (±)**-2A** (0.1 mmol), $Pd(dba)_2$ (10 mol%, 5.75 mg), **L14a** (12 mol%, 5.3 mg) and Cs_2CO_3 (0.2 mmol, 65 mg). After three cycles of vacuum-argon, dry toluene (2 mL) and amine **5** (0.2 mmol) were sequentially added.[149] The mixture was stirred at 50-60 °C until consumption of the starting material (TLC monitoring), filtered through celite (CH_2Cl_2), concentrated to dryness and purified by flash chromatography on silica gel.

*From heterobiaryl bromides***:** A dried Schlenk tube was charged with bromide (±)**-3A-C** (0.1 mmol), $Pd(dba)_2$ (10 mol%, 5.75 mg), **L14a** (12 mol%, 5.3 mg) and NaO*t*Bu (0.2 mmol, 19.2 mg). After three cycles of vacuum-argon, dry toluene (2 mL) and then the corresponding amine **5** (0.2 mmol) were added.[149] The mixture was stirred at 50-60 °C until consumption of the starting material (TLC monitoring), filtered through celite, concentrated to dryness and purified by flash chromatography on silica gel.

Note: The racemic products were prepared by heating (80 °C) a mixture of the corresponding starting nonaflate (±)**-1A-B** or bromide (±)**-3E** *(0.1 mmol),*

[149] Solid amines **5** were added at the beginning together with the rest of the solids.

Cs_2CO_3 (0.2 mmol) and amine (0.2 mmol) in toluene (2 mL), using (±)-BINAP (12 mol%)/$Pd(dba)_2$ (10 mol%) as the catalyst.

Starting materials yields, solvent used for chromatography, and characterization data for products **6A-C** are as follows:

*(R)-1-(Isoquinolin-1-yl)-N-phenylnaphthalen-2-amine **6Aa**.*

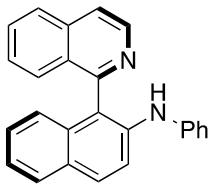

Following the general procedure from (±)-**3A** and **5a** (28 h, 50 °C, (*S*)-**L14a**), flash chromatography (50:1→10:1 CH_2Cl_2/EtOAc) afforded (*R*)-**6Aa** (31 mg, 90%) as a light yellow foam. $[\alpha]^{20}_D$ –187.0 (*c* 0.55, $CHCl_3$) for 91 % ee. ^{1}H NMR (400 MHz, $CDCl_3$): 8.78 (d, 1H, *J* = 5.8 Hz), 7.93 (d, 1H, *J* = 8.3 Hz), 7.88 (d, 1H, *J* = 9.0 Hz), 7.83 (d, 1H, *J* = 8.0 Hz), 7.78 (dd, 1H, *J* = 5.7 and 0.6 Hz), 7.68 (ddd, 1H, *J* = 8.2, 6.9 and 1.2 Hz), 7.71 (d, 1H, *J* = 9.0 Hz), 7.60 (dd, 1H, *J* = 8.5 and 0.8 Hz), 7.39 (ddd, 1H, *J* = 8.4, 7.0 and 1.2 Hz), 7.30 (ddd, 1H, *J* = 8.1, 6.9 and 1.2 Hz), 7.23-7.16 (m, 3H), 7.02-6.97 (m, 2H), 6.95-6.91 (m, 1H), 6.88 (t, 1H, *J* = 7.3 Hz), 6.05 (s, 1H). ^{13}C NMR (100 MHz, $CDCl_3$): δ 158.6, 143.1, 142.9, 139.4, 136.9, 134.0, 130.7, 129.7, 129.4, 129.3, 128.6, 128.2, 127.8, 127.5, 127.2, 126.7, 124.9, 123.5, 121.9, 121.4, 120.7, 119.1, 118.8. HRMS (ESI) calcd. for $C_{25}H_{19}N_2$ (M + H^+) 347.1543. Found 347.1537. HPLC (IA column, 85:15 *n*-hexane/*i*-PrOH, T= 30°C, 0.5 mL/min): t_R 18.56 min (major) and 22.77 min (minor).

*Note: The reaction could be carried out at 2 mmol scale following the general procedure A using (±)-**1A** as the starting material, to get (R)-**6Aa** in 87% yield (600 mg) and 90% ee.*

*(R)-1-(Isoquinolin-1-yl)-N-(p-tolyl)naphthalen-2-amine **6Ab**.*

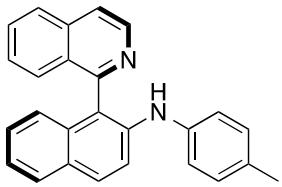

Following the general procedure from (±)-**3A** and **5b** (28 h, 50 °C, (*S*)-**L14a**), flash chromatography (50:1→10:1 CH_2Cl_2/EtOAc) afforded (*R*)-**6Ab** (32 mg, 89%) as a light yellow foam. $[\alpha]^{20}_D$ –95.0 (*c* 0.5, $CHCl_3$) for 96 % ee. ^{1}H NMR (400 MHz, $CDCl_3$): 8.77 (d, 1H *J* = 5.8 Hz), 7.93 (d, 1H, *J* = 8.3 Hz), 7.85 (d, 1H, *J* = 9.0 Hz), 7.81 (d, 1H, *J* = 8.0 Hz), 7.77 (d, 1H, *J* = 5.7 Hz), 7.68 (t, 1H, *J* = 7.6 Hz), 7.65-7.59 (m, 2H), 7.42-7.36 (m, 1H), 7.29-7.24 (m, 1H), 7.18 (t, 1H, *J* = 7.6 Hz), 7.04-6.99 (m, 2H), 6.96-6.88 (m, 3H), 5.89 (s, 1H), 2.26 (s, 3H). ^{13}C NMR (100 MHz, $CDCl_3$): δ 158.7, 143.2, 140.2, 140.2, 136.9, 134.1, 131.4, 130.7, 129.9, 129.7, 129.1, 128.7,

128.1, 127.8, 127.5, 127.2, 126.7, 124.8, 123.2, 120.8, 120.7, 119.8, 119.5, 20.8. HRMS (ESI) calcd. for $C_{26}H_{21}N_2$ (M + H^+) 361.1699. Found 361.1693. HPLC (IA column, 85:15 *n*-hexane/*i*-PrOH, T= 30°C, 0.5 mL/min): t_R 21.62 min (major) and 31.95 min (minor).

(R)-1-(Isoquinolin-1-yl)-N-(4-methoxyphenyl)naphthalen-2-amine ***6Ac****.*

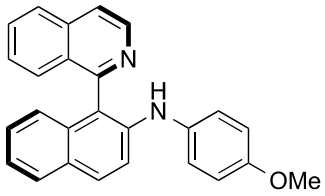

Following the general procedure from (±)-**3A** and **5c** (28 h, 50 °C, (*S*)-**L14a**), flash chromatography (10:1 Toluene/EtOAc) afforded (*R*)-**6Ac** (34 mg, 90%) as a light yellow foam. $[\alpha]^{20}_D$ −105.0 (*c* 0.52, $CHCl_3$) for 92 % ee. ^{1}H NMR (400 MHz, $CDCl_3$): δ 8.78 (d, 1H, *J* = 5.7 Hz), 7.94 (d, 1H, *J* = 8.3 Hz), 7.83 (d, 1H, *J* = 9.1 Hz), 7.80 (m, 2H), 7.70 (ddd, 1H, *J* = 8.0, 6.9 and 1.1 Hz), 7.64 (d, 1H, *J* = 8.3 Hz), 7.49 (d, 1H, *J* = 9.1 Hz), 7.42 (ddd, 1H, *J* = 8.2, 7.0 and 1.0 Hz), 7.28-7.22 (m, 1H), 7.18 (ddd, 1H, *J* = 8.2, 6.9 and 1.3 Hz), 7.03-6.95 (m, 2H), 6.88 (d, 1H, *J* = 8.4 Hz), 6.82-6.75 (m, 2H), 5.76 (br s, 1H), 3.75 (s, 3H). ^{13}C NMR (100 MHz, $CDCl_3$): δ 158.6, 155.6, 142.8, 141.4, 137.1, 135.7, 134.0, 131.0, 129.9, 128.7, 128.7, 128.2, 127.9, 127.7, 127.2, 126.8, 124.5, 123.0, 123.0, 120.8, 119.1, 117.8, 114.7, 55.7. HRMS (ESI) calcd. for $C_{26}H_{21}N_2O$ (M + H^+) 377.1648. Found 377.1641. HPLC (IA column, 70:30 *n*-hexane/*i*-PrOH, T= 30 °C, 0.5 mL/min): t_R 10.13 min (major) and 24.45 min (minor).

(R)-N-(4-Fluorophenyl)-1-(isoquinolin-1-yl)naphthalen-2-amine ***6Ad****.*

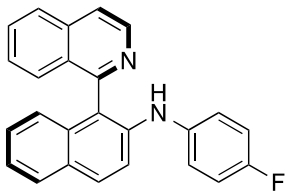

Following the general procedure from (±)-**3A** and **5d** (22 h, 60 °C, (*S*)-**L14a**), flash chromatography (50:1 CH_2Cl_2→CH_2Cl_2/EtOAc) afforded (*R*)-**6Ad** (36 mg, 99%) as a light yellow foam. $[\alpha]^{20}_D$ −58.6 (*c* 0.5, $CHCl_3$) for 92 % ee. ^{1}H NMR (400 MHz, $CDCl_3$): 8.77 (d, 1H, *J* = 5.8 Hz), 7.94 (d, 1H, *J* = 8.3 Hz), 7.86 (d, 1H, *J* = 9.1 Hz,), 7.82 (d, 1H, *J* = 7.9 Hz), 7.78 (dd, 1H, *J* = 5.8 and 0.7 Hz), 7.69 (ddd, 1H, *J* = 8.2, 6.9 and 1.2 Hz), 7.60 (dd, 1H, *J* = 8.5 and 0.9 Hz), 7.55 (d, 1H, *J*=9.0 Hz), 7.40 (ddd, 1H, *J* = 8.4, 7.0 and 1.2 Hz), 7.28 (ddd, 1H, *J* = 8.1, 6.9 and 1.3 Hz), 7.19 (ddd, 1H, *J* = 8.4, 6.9 and 1.4 Hz), 7.00-6.94 (m, 2H), 6.93-6.86 (m, 3H), 5.88 (br s, 1H). ^{13}C NMR (100 MHz, $CDCl_3$): δ 158.5, 158.4 (d, 2C, $^1J_{C\text{-}F}$ = 241 Hz), 143.1, 140.1, 138.8 (d, 2C, $^4J_{C\text{-}F}$ = 2 Hz), 136.9, 134.0, 130.8, 129.8, 129.1, 128.6, 128.2, 127.8, 127.4, 127.2, 126.8, 124.8, 123.4, 121.5 (d, 2C, $^3J_{C\text{-}F}$ = 7 Hz), 121.0, 120.7, 118.2, 115.9 (d, 2C, $^2J_{C\text{-}F}$ = 23 Hz). ^{19}F NMR (377 MHz, $CDCl_3$) δ −121.53. HRMS (ESI)

calcd. for $C_{25}H_{18}FN_2$ ($M + H^+$) 365.1449. Found 365.1442. HPLC (IA column, 85:15 *n*-hexane:*i*-PrOH, T= 30 °C, 0.5 mL/min): t_R 20.90 min (major) and 28.19 min (minor).

(R)-N-(4-Chlorophenyl)-1-(isoquinolin-1-yl)naphthalen-2-amine ***6Ae****.*

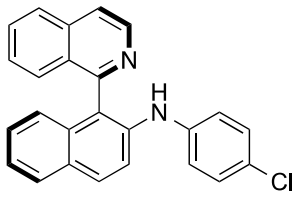

Following the general procedure from (±)-**3A** and **5e** (48 h, 60 °C, (*S*)-**L14a**), two sequential flash chromatographies (50:1→10:1 CH_2Cl_2/EtOAc and 5:1 *n*-hexane/EtOAc) afforded (*R*)-**6Ae** (28 mg, 74%) as a light yellow foam. $[\alpha]^{20}_D$ –106.1 (*c* 0.51, $CHCl_3$) for 90 % ee. ^{1}H NMR (400 MHz, $CDCl_3$): δ 8.76 (d, 1H, *J* = 5.7 Hz), 7.93 (d, 1H, *J* = 8.3 Hz), 7.89 (d, 1H, *J* = 9.0 Hz), 7.84 (d, 1H, *J* = 8.0 Hz), 7.78 (dd, 1H, *J* = 5.7 and 0.7 Hz), 7.68 (ddd, 1H, *J* = 8.2, 6.9 and 1.2 Hz), 7.63 (d, 1H, *J* = 9.0 Hz), 7.57 (dd, 1H, *J* = 8.5 and 0.9 Hz), 7.39 (ddd, 1H, *J* = 8.4, 7.0 and 1.2 Hz), 7.31 (ddd, 1H, *J* = 8.0, 6.9 and 1.2 Hz,), 7.20 (ddd, 1H, *J* = 8.4, 6.9 and 1.3 Hz), 7.14-7.10 (m, 2H), 6.93 (d, 1H, *J* = 9.1 Hz), 6.91-6.87 (m, 2H), 6.02 (s, 1H). ^{13}C NMR (100 MHz, $CDCl_3$): δ 158.4, 143.1, 141.7, 138.9, 136.9, 133.9, 130.8, 129.9, 129.6, 129.3, 128.6, 128.2, 127.8, 127.4, 127.2, 126.9, 126.0, 125.0, 123.9, 122.6, 120.8, 119.7, 119.1. HRMS (ESI) calcd. for $C_{25}H_{18}ClN_2$ ($M + H^+$) 381.1153. Found 381.1149. HPLC (AD-H column, 80:20 *n*-hexane/*i*-PrOH, T = 30 °C, 0.5 mL/min): t_R 21.65 min (major) and 29.32 min (minor).

(R)-N-(4-Bromophenyl)-1-(isoquinolin-1-yl)naphthalen-2-amine ***6Af****.*

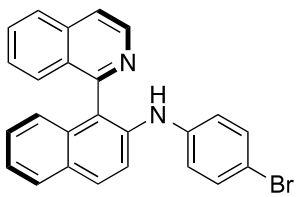

Following the general procedure from (±)-**3A** and **5f** (48 h, 60 °C, (*S*)-**L14a**), two sequential flash chromatographies (50:1→10:1 CH_2Cl_2/EtOAc and 5:1 *n*-hexane/EtOAc) afforded (*R*)-**6Af** (27 mg, 64%) as a light yellow foam. $[\alpha]^{20}_D$ –100.0 (*c* 0.48, $CHCl_3$) for 91 % ee. ^{1}H NMR (400 MHz, $CDCl_3$): δ 8.76 (d, 1H, *J* = 5.7 Hz), 7.93 (d, 1H, *J* = 8.3 Hz), 7.89 (d, 1H, *J* = 9.1 Hz), 7.84 (d, 1H, *J* = 8.0 Hz), 7.78 (dd, 1H, *J* = 5.8 and 0.8 Hz), 7.68 (ddd, 1H, *J* = 8.2, 6.9 and 1.1 Hz), 7.64 (d, 1H, *J* = 9.0 Hz), 7.56 (ddd, 1H, *J* = 8.5, 2.0 and 0.9 Hz), 7.38 (ddd, 1H, *J* = 8.4, 7.0 and 1.1 Hz), 7.31 (ddd, 1H, *J* = 8.1, 6.9 and 1.1 Hz), 7.28-7.23 (m, 2H), 7.20 (ddd, 1H, *J* = 8.4, 6.9 and 1.4 Hz), 6.93 (dd, 1H, *J* = 8.5 and 1.0 Hz), 6.87-6.82 (m, 2H), 6.02 (s, 1H). ^{13}C NMR (100 MHz, $CDCl_3$) δ 158.3, 143.0, 142.2, 138.7, 136.8, 133.9, 132.1, 130.8, 129.8, 129.6, 128.5, 128.2, 127.8, 127.3, 127.2, 126.8, 125.0, 123.9, 122.9, 120.8, 119.9, 119.2, 113.1. HRMS (ESI) calcd. for $C_{25}H_{18}BrN_2$ (M +

H^+) 425.0648. Found 425.0643. HPLC (AD-H column, *n*-hexane/*i*-PrOH 80:20, T = 30 °C, 0.5 mL/min): t_R 24.22 min (major) and 32.47 min (minor).

(R)-N-(3,5-dimethylphenyl)-1-(isoquinolin-1-yl)naphthalen-2-amine ***6Ag****.*

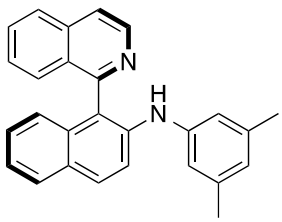

Following the general procedure from (±)-**3A** and **5g** (28 h, 50 °C, (*S*)-**L14a**), flash chromatography (50:1 CH_2Cl_2→CH_2Cl_2/EtOAc) afforded (*R*)-**6Ag** (33 mg, 88%) as a light yellow foam. $[\alpha]^{20}_D$ –180.0 (*c* 0.52, $CHCl_3$) for 90 % ee. ^{1}H NMR (400 MHz, $CDCl_3$): δ 8.77 (d, 1H, *J* = 5.7 Hz), 7.92 (d, 1H, *J* = 8.2 Hz), 7.88 (d, 1H, *J* = 9.0 Hz), 7.83 (d, 1H, *J* = 8.0 Hz), 7.77 (d, 1H, *J* = 5.7 Hz), 7.73 (d, 1H, *J* = 9.0 Hz), 7.70-7.65 (m, 1H), 7.62 (d, 1H, *J* = 8.5 Hz), 7.41-7.37 (m, 1H), 7.31-7.27 (m, 1H), 7.21-7.17 (m, 1H), 6.92 (d, 1H, *J* = 8.5 Hz), 6.64 (s, 2H), 6.55 (s, 1H), 5.97 (br s, 1H), 2.21 (s, 6H). ^{13}C NMR (100 MHz, $CDCl_3$): δ 158.7, 143.1, 142.8, 139.6, 139.0, 136.9, 134.0, 130.7, 129.6, 129.2, 128.7, 128.1, 127.8, 127.6, 127.1, 126.7, 124.9, 123.4, 123.3, 121.6, 120.6, 119.3, 116.6, 21.4. HRMS (ESI) calcd. for $C_{27}H_{23}N_2$ (M + H^+) 375.1856. Found 375.1850. HPLC (IA column, 85:15 *n*-hexane/*i*-PrOH, T = 30 °C, 0.5 mL/min): t_R 14.40 min (minor) and 17.24 min (major).

(R)-1-(isoquinolin-1-yl)-N-(o-tolyl)naphthalen-2-amine ***6Ah****.*

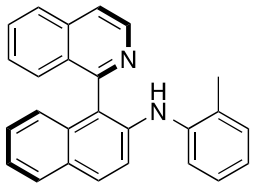

Following the general procedure from (±)-**3A** and **5h** (30 h, 50 °C, (*S*)-**L14a**), flash chromatography (50:1 CH_2Cl_2→CH_2Cl_2/EtOAc) afforded (*R*)-**6Ah** (35 mg, 97%) as a light yellow foam. $[\alpha]^{20}_D$ –80.4 (*c* 0.5, $CHCl_3$) for 92 % ee. ^{1}H NMR (400 MHz, $CDCl_3$): □ 8.79 (d, 1H, *J* = 5.8 Hz), 7.93 (d, 1H, *J* = 8.3 Hz), 7.87 (d, 1H, *J* = 9.0 Hz), 7.83 (d, 1H, *J* = 8.0 Hz), 7.78 (d, 1H, *J* = 5.7 Hz), 7.69 (ddd, 1H, *J* = 8.2, 6.9 and 1.0 Hz), 7.64 (d, 1H, *J* = 8.5 Hz), 7.53 (d, 1H, *J* = 9.0 Hz), 7.40 (ddd, 1H, *J* = 8.3, 7.0 and 1.1 Hz), 7.32-7.26 (m, 1H), 7.26-7.18 (m, 2H), 7.13-7.07 (m, 2H), 6.98 (d, 1H, *J* = 8.5 Hz), 6.91-6.85 (m, 1H), 5.97 (br s, 1H), 2.03 (s, 3H). ^{13}C NMR (100 MHz, $CDCl_3$): δ 158.7, 143.0, 140.9, 140.1, 136.9, 134.0, 130.9, 130.7, 129.7, 129.0, 128.8, 128.7, 128.1, 127.7, 127.6, 127.2, 126.8, 126.7, 124.9, 123.3, 122.1, 120.9 120.7, 119.1, 118.8, 17.9. HRMS (ESI) calcd. for $C_{26}H_{21}N_2$ (M + H^+) 361.1699. Found 361.1692. HPLC (AD-H column, 80:20 *n*-hexane/*i*-PrOH, T = 30 °C, 0.5 mL/min): t_R 18.02 min (major) and 22.33 min (minor).

(R)-N-(1-(isoquinolin-1-yl)naphthalen-2-yl)naphthalen-1-amine ***6Ai****.*

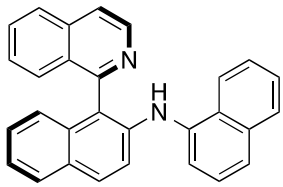

Following the general procedure from (±)-**3A** and **5i** (30 h, 50 °C, (*S*)-**L14a**), flash chromatography (50:1 CH_2Cl_2→CH_2Cl_2/EtOAc) afforded (*R*)-**6Ai** (36 mg, 91%) as a light yellow foam. $[\alpha]^{20}_D$ +4.8 (*c* 0.5, $CHCl_3$) for 93 % ee. ^{1}H NMR (400MHz, $CDCl_3$): 8.84 (d, 1H, *J* = 5.7 Hz), 7.95-7.91 (m, 1H), 7.90-7.86 (m, 1H), 7.83 (d, 2H, *J* = 9.0 Hz), 7.81-7.77 (m, 2H), 7.75 (dd, 1H, *J* = 8.5 and 0.9 Hz), 7.72-7.67 (m, 1H), 7.52 (dd, 1H, *J* = 7.4 and 1.6 Hz), 7.49 (d, 1H, *J* = 9.1 Hz), 7.47-7.41 (m, 2H), 7.41-7.35 (m, 3H), 7.30 (ddd, 1H, *J* = 8.0, 6.9 and 1.2 Hz), 7.23 (ddd, 1H, *J* = 8.3, 6.9 and 1.4 Hz), 7.00 (d, 1H, *J* = 8.5 Hz), 6.45 (br s, 1H). ^{13}C NMR (100 MHz, $CDCl_3$): δ 158.6, 143.1, 141.0, 138.5, 137.0, 134.7, 134.0, 130.8, 129.8, 129,0, 128.7, 128.5, 128.2, 128.1, 127.8, 127.5, 127.2, 126.7, 126.2, 126.0, 125.8, 124.8, 123.3, 123.2, 122.0, 120.8, 120.7, 118.9, 116.7. HRMS (ESI) calcd. for $C_{29}H_{21}N_2$ (M + H^+) 397.1699. Found 397.1691. HPLC (AD-H column, 80:20 *n*-hexane/*i*-PrOH, T = 30 °C, 0.5 mL/min): t_R 18.66 min (minor) and 22.33 min (major).

(R)-1-(isoquinolin-1-yl)-N-(naphthalen-2-yl)naphthalen-2-amine ***6Aj****.*

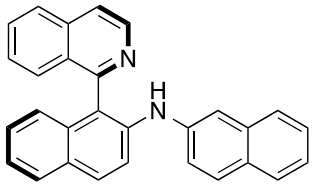

Following the general procedure from (±)-**3A** and **5j** (30 h, 50 °C, (*S*)-**L14a**), flash chromatography (CH_2Cl_2→10:1 CH_2Cl_2/EtOAc) afforded (*R*)-**6Aj** (32 mg, 81%) as a light yellow foam. $[\alpha]^{20}_D$ –96.0 (*c* 0.5, $CHCl_3$) for 88 % ee. ^{1}H NMR (400 MHz, $CDCl_3$): 8.81 (d, 1H, *J* = 5.7 Hz), 7.93 (m, 2H), 7.88 (d, 1H, *J* = 8.1 Hz), 7.84 (s, 1H), 7.83-7.77 (m, 1H), 7.73-7.64 (m, 4H), 7.62 (d, 1H, *J* = 8.2 Hz), 7.44-7.21 (m, 6H), 7.14 (dd, 1H, *J* = 8.8 and 1.9 Hz), 7.00 (d, 1H, *J* = 8.5 Hz), 6.29 (s, 1H). ^{13}C NMR (100 MHz, $CDCl_3$): δ 158.5, 143.1, 140.6, 139.2, 136.9, 134.6, 134.0, 130.7, 129.8, 129.6, 129.4, 129.1, 128.6, 128.2, 127.8, 127.7, 127.4, 127.1, 126.8, 126.6, 126.5, 125.0, 123.7, 123.7, 122.6, 120.7, 120.6, 119.4, 112.8. HRMS (ESI) calcd. for $C_{29}H_{21}N_2$ (M + H^+) 397.1699. Found 397.1692. HPLC (AD-H column, 80:20 *n*-hexane/*i*-PrOH, T = 30 °C, 0.5 mL/min): t_R 27.71 min (major) and 31.31 min (minor).

(R)-N-benzyl-1-(isoquinolin-1-yl)naphthalen-2-amine ***6Ak****.*

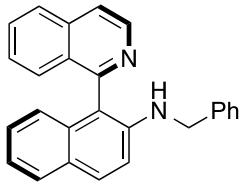

Following the general procedure from (±)-**3A** and **5k** (72 h, 60 °C, (*S*)-**L14a**, 4 equiv. of **5k** and 4 equiv. of NaO*t*Bu), flash chromatography (50:1→10:1 CH_2Cl_2/EtOAc) afforded (*R*)-**6Ak** (31 mg, 86%) as a light yellow foam. $[\alpha]^{20}_D$ −12.7 (*c* 0.5, $CHCl_3$) for 86 % ee. ^{1}H NMR (400 MHz, $CDCl_3$): 8.78 (d, 1H, *J* = 5.7 Hz), 7.98-7.91 (m, 1H), 7.82 (d, 1H, *J* = 9.1 Hz), 7.79-7.73 (m, 2H), 7.71 (ddd, 1H, *J* = 8.2, 6.9 and 1.1 Hz), 7.58 (d, 1H, *J* = 7.9 Hz), 7.42 (ddd, 1H, *J* = 8.2, 7.0 and 1.0 Hz), 7.25-7.10 (m, 8H), 6.81 (d, 1H, *J* = 8.3 Hz), 4.42 (d, 2H, *J*=3.9 Hz), 4.26-4.21(m, 1H). ^{13}C NMR (100 MHz, $CDCl_3$): δ 158.9, 143.9, 143.5, 139.7, 137.0, 133.9, 130.7, 130.2, 128.8, 128.7, 128.1, 127.7, 127.4, 127.2, 127.1, 127.0, 127.0, 126.7, 124.0, 122.0, 120.6, 116.4, 115.0, 48.0. HRMS (ESI) calcd. for $C_{26}H_{21}N_2$ (M + H^+) 361.1699. Found 361.1685. HPLC (IA column, 85:15 *n*-hexane/*i*-PrOH, T = 30 °C, 0.5 mL/min): t_R 23.27 min (major) and 29.96 min (minor).

(R)-N-cyclohexyl-1-(isoquinolin-1-yl)naphthalen-2-amine ***6Ap****.*

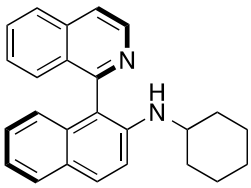

Following the general procedure from (±)-**3A** and **5p** (72 h, 60 °C, (*S*)-**L14a**, 4 equiv. of **5p** and 4 equiv. of NaO*t*Bu), flash chromatography (50:1→10:1 CH_2Cl_2/EtOAc) afforded (*R*)-**6Ap** (22 mg, 63%) as a light yellow foam. $[\alpha]^{20}_D$ +21.6 (*c* 0.5, $CHCl_3$) for 91% ee. ^{1}H NMR (400 MHz, $CDCl_3$): 8.77 (d, 1H, *J* = 5.7 Hz), 7.94 (d, 1H, *J* = 8.3 Hz), 7.85 (d, 1H, *J* = 8.9 Hz), 7.78-7.73 (m, 2H), 7.69 (ddd, 1H, *J* = 8.2, 6.9 and 1.2 Hz), 7.54 (dd, 1H, *J* = 8.5 and 1.0 Hz), 7.39 (ddd, 1H, *J* = 8.3, 6.9 and 1.2 Hz), 7.26 (d, 1H, *J* = 9.0 Hz), 7.15 (ddd, 1H, *J* = 8.0, 6.8 and 1.4 Hz), 7.10 (ddd, 1H, *J* = 8.3, 6.8 and 1.6 Hz), 6.76-6.73 (m, 1H), 3.50 (br s, 1H), 3.45-3.35 (m, 1H), 1.97 (m, 1H) 1.86 (m, 1H), 1.69-1.47 (m, 3H), 1.37-1.19 (m, 2H), 1.12-0.91 (m, 2H), 0.92-0.77 (m, 1H). ^{13}C NMR (100 MHz, $CDCl_3$): δ 159.1, 143.6, 143.5, 136.9, 134.2, 130.6, 130.0, 128.7, 128.0, 127.8, 127.6, 127.2, 127.1, 126.5, 123.9, 121.8, 120.4, 116.4, 115.4, 52.2, 33.9, 33.6, 25.9, 25.0, 24.9. HRMS (ESI) calcd. for $C_{25}H_{25}N_2$ (M + H^+) 353.2012. Found 353.2005.

HPLC (AD-H column, 90:10 *n*-hexane:*i*-PrOH, T = 30 °C, 0.5 mL/min): t_R 25.43 min (minor) and 39.39 min (major).

(R)-N-cyclohexyl-1-(isoquinolin-1-yl)naphthalen-2-amine ***6Am****.*

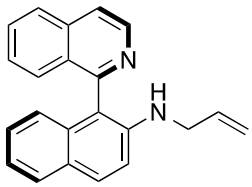

Following the general procedure from (±)-**3A** and **5m** (48 h, 60 °C, (*S*)-**L14a**, 10 equiv. of **5m** and 4 equiv. of NaO*t*Bu), flash chromatography (50:1→10:1 CH_2Cl_2/EtOAc) afforded (*R*)-**6Am** (19 mg, 61%) as a light yellow viscous oil. $[\alpha]^{20}_D$ –40.2 (*c* 0.5, $CHCl_3$) for 88 % ee. ^{1}H NMR (400 MHz, $CDCl_3$): 8.77 (d, 1H, *J* = 5.7 Hz), 7.94 (d, 1H, *J* = 8.3 Hz), 7.88 (d, 1H, *J* = 9.1 Hz), 7.74-7.81 (m, 2H), 7.70 (ddd, 1H, *J* = 8.2, 6.8 and 1.3 Hz), 7.54 (d, 1H, *J* = 8.5 Hz), 7.40 (ddd, 1H, *J* = 8.3, 6.8 and 0.9 Hz), 7.21 (d, 1H, *J* = 9.1 Hz), 7.19-7.15 (m, 1H), 7.12 (ddd, 1H, *J* = 8.3, 6.8 and 1.6 Hz), 6.78 (d, 1H, *J* = 8.3 Hz), 5.88-5.76 (m, 1H), 5.14 (dd, 1H, *J* = 17.2 and 1.5 Hz), 5.04 (dd, 1H, *J* = 10.3 and 1.2 Hz), 3.83 (br s, 2H). ^{13}C NMR (100 MHz, $CDCl_3$): δ 158.9, 143.9, 143.4, 137.0, 136.0, 133.9, 130.7, 130.1, 128.7, 128.1, 127.7, 127.7, 127.3, 127.2, 126.6, 123.9, 121.9, 120.5, 116.2, 116.0, 114.4, 46.44. HRMS (ESI) calcd. for $C_{22}H_{19}N_2$ ($M + H^+$) 311.1543. Found 311.1541. HPLC (AS-H column, 97:3 *n*-hexane/*i*-PrOH, T= 30 °C, 0.5 mL/min): t_R 27.65 min (major) and 30.45 min (minor).

(S)-1-(3-methylpyridin-2-yl)-N-phenylnaphthalen-2-amine ***6Da****.*

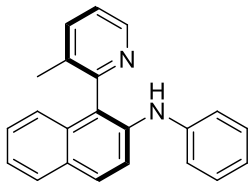

Following the general procedure from (±)-**3D** and **5a** (26 h, 50 °C, (*R*)-**L14a**), flash chromatography (85:15→70:30 *n*-hexane/EtOAc) afforded (*S*)-**6Da** (26 mg, 84%) as a beige foam. $[\alpha]^{20}_D$ +347.3 (*c* 0.5, $CHCl_3$) for 89 % ee. ^{1}H NMR (400 MHz, $CDCl_3$): δ 8.67 (d, 1H, *J* = 4.3 Hz), 7.79 (m, 2H), 7.68 (d, 1H, *J* = 7.6 Hz), 7.63 (d, 1H, *J* = 9.0 Hz), 7.34-7.26 (m, 3H), 7.26-7.18 (m, 2H), 7.07 (dd, 1H, *J* = 6.1 and 3.4 Hz), 7.01 (d, 2H, *J* = 7.9 Hz), 6.90 (t, 1H, *J* = 7.3 Hz), 5.88 (br s, 1H), 2.04 (s, 3H). ^{13}C NMR (100 MHz, $CDCl_3$): δ 156.3, 148.0, 143.2, 138.7, 138.4, 134.3, 129.6, 129.4, 129.2, 128.3, 126.8, 124.1, 123.7, 123.6, 122.9, 121.3, 119.3, 118.4, 19.0. HRMS (ESI) calcd. for $C_{22}H_{19}N_2$ ($M + H^+$) 311.1543. Found 311.1536. HPLC (AD-H column,

95:5 *n*-hexane/*i*-PrOH, T = 30 °C, 0.5 mL/min): t_R 35.57 min (minor) and 35.59 min (major).

(S)-1-(3-methylpyridin-2-yl)-N-(p-tolyl)naphthalen-2-amine ***6Db****.*

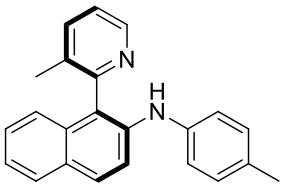

Following the general procedure from (±)-**3D** and **5b** (44 h, 40 °C, (*R*)-**L14a**), flash chromatography (50:1→10:1 CH_2Cl_2/EtOAc) afforded (*S*)-**6Db** (32 mg, 98%) as a white foam. $[\alpha]^{20}_D$ +374.9 (*c* 0.5, $CHCl_3$) for 90 % ee. ^{1}H NMR (400 MHz, $CDCl_3$): δ 8.70 (d, 1H, *J* = 3.8 Hz), 7.83-7.74 (m, 2H), 7.69 (dd, 1H, *J* = 7.7 and 0.8 Hz), 7.59 (d, 1H, *J* = 9.0 Hz), 7.34-7.27 (m, 3H), 7.12-7.03 (m, 3H), 7.01-6.94 (m, 2H), 5.78 (br s, 1H), 2.30 (s, 3H), 2.07 (s, 3H). ^{13}C NMR (100 MHz, $CDCl_3$): δ 156.3, 148.1, 140.4, 139.1, 138.7, 134.3, 133.0, 131.2, 129.9, 129.3, 129.1, 128.3, 126.8, 124.0, 123.3, 122.9, 122.6, 119.3, 118.7, 20.8, 19.0. HRMS (ESI) calcd. for $C_{23}H_{21}N_2$ (M + H^+) 325.1699. Found 325.1695. HPLC (IA column, 85:15 *n*-hexane/*i*-PrOH, T = 30 °C, 0.5 mL/min): t_R 19.77 min (minor) and 21.82 min (major).

(S)-N-(4-methoxyphenyl)-1-(3-methylpyridin-2-yl)naphthalen-2-amine ***6Dc****.*

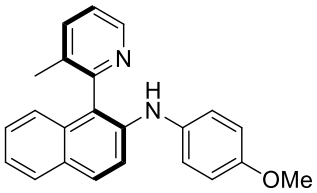

Following the general procedure from (±)-**3D** and **5c** (41 h, 50 °C, (*R*)-**L14a**), purification by preparative TLC (7:3 Et_2O/*n*-hexane) afforded (*S*)-**6Dc** (26 mg, 78%) as a pale yellow foam. $[\alpha]^{20}_D$ +91.9 (*c* 0.5, $CHCl_3$) for 91 % ee. ^{1}H NMR (400 MHz, $CDCl_3$): δ 8.69 (dd, 1H, *J* = 4.8 and 1.1 Hz), 7.78-7.75 (m, 1H), 7.74 (d, 1H, *J* = 8.7 Hz), 7.71 (ddd, 1H, *J* = 7.7, 1.6 and 0.7 Hz), 7.43 (d, 1H, *J* = 9.0 Hz), 7.33-7.23 (m, 3H), 7.04-7.02 (m, 1H), 7.03 (d, 2H, *J* = 8.9 Hz), 6.83 (d, 2H, *J* = 8.9 Hz), 5.60 (br s, 1H), 3.78 (s, 3H), 2.08 (s, 3H). ^{13}C NMR (100 MHz, $CDCl_3$): δ 156.3, 155.5, 148.2, 140.2, 138.7, 136.0, 134.4, 133.0, 129.2, 128.9, 128.3, 126.8, 123.8, 123.0, 122.9, 122.6, 121.2, 117.7, 114.8, 55.7, 19.0. HRMS (ESI) calcd. for $C_{23}H_{21}N_2O$ (M + H+) 341.1648. Found 341.1648. HPLC (AD-H column, 90:10 *n*-hexane/*i*-PrOH, T = 30 °C, 0.5 mL/min): t_R 33.71 min (minor) and 37.11 min (major).

(S)-N-(4-fluorophenyl)-1-(3-methylpyridin-2-yl)naphthalen-2-amine ***6Dd****.*

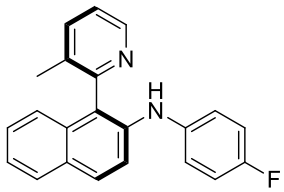

Following the general procedure from (±)-**3D** and **5d** (44 h, 50 °C, (*R*)-**L14a**), flash chromatography (50:1→10:1 CH_2Cl_2/EtOAc) afforded (*S*)-**6Dd** (29 mg, 89%) as white foam. $[\alpha]^{20}_D$ +207.7 (*c* 0.5, $CHCl_3$) for 92 % ee. ^{1}H NMR (400 MHz, $CDCl_3$): δ 8.68 (d, 1H, *J* = 4.6 Hz), 7.78 (d, 2H, *J* = 8.8 Hz), 7.71 (d, 1H, *J* = 7.8 Hz), 7.48 (d, 1H, *J* = 9.0 Hz), 7.34-7.27 (m, 3H), 7.08-7.03 (m, 1H), 7.03-6.90 (m, 4H), 5.76 (br s, 1H), 2.06 (s, 3H). ^{13}C NMR (100 MHz, $CDCl_3$): δ 158.3 (d, 1C, $^1J_{C\text{-}F}$ = 240 Hz), 156.2, 148.1, 139.1 (d, 1C, $^4J_{C\text{-}F}$ = 2 Hz), 139.1, 138.8, 134.3, 132.9, 129.3, 128.3, 126.9, 124.0, 123.5, 123.0, 122.8, 121.1 (d, 2C, $^3J_{C\text{-}F}$ = 8 Hz), 118.4, 116.1 (d, 2C, $^2J_{C\text{-}F}$ = 23 Hz), 19.0. ^{19}F NMR (377 MHz, $CDCl_3$): δ −121.8. HRMS (ESI) calcd. for $C_{22}H_{18}FN_2$ (M + H^+) 329.1449. Found 329.1442. HPLC (IA column, 90:10 *n*-hexane/*i*-PrOH, T = 30 °C, 0.5 mL/min): t_R 21.06 min (minor) and 23.69 min (major).

(R)-N-(4-chlorophenyl)-1-(3-methylpyridin-2-yl)naphthalen-2-amine ***6De****.*

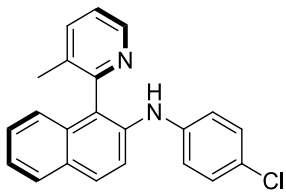

Following the general procedure from (±)-**3D** and **5e** (72 h, 50 °C, (*S*)-**L14a**), two sequential flash chromatographies (50:1→10:1 CH_2Cl_2/EtOAc and 85:15 *n*-hexane/EtOAc) afforded (*R*)-**6De** (29 mg, 83%) as a white foam. $[\alpha]^{20}_D$ −359.7 (*c* 0.5, $CHCl_3$) for 93 % ee. ^{1}H NMR (400 MHz, $CDCl_3$): □ 8.67 (d, 1H, *J* = 4.7 Hz), 7.85-7.78 (m, 2H), 7.70 (d, 1H, *J* = 7.6 Hz), 7.57 (d, 1H, *J* = 8.9 Hz), 7.37-7.28 (m, 3H), 7.17 (d, 2H, *J* = 8.5 Hz), 7.11-7.05 (m, 1H), 6.93 (d, 2H, *J* = 8.5 Hz), 5.88 (br s, 1H), 2.03 (s, 3H). ^{13}C NMR (100 MHz, $CDCl_3$): δ 156.1, 148.0 142.0, 138.7, 137.9, 134.2, 132.9, 129.8, 129.3, 129.3, 128.3, 126.9, 125.7, 124.4, 124.2, 123.9, 123.0, 119.3, 119.3, 119.2, 19.0. HRMS (ESI) calcd. for $C_{22}H_{18}ClN_2$ (M + H^+) 345.1153. Found 345.1149. HPLC (AD-H column, 90:10 *n*-hexane/*i*-PrOH, T = 30 °C, 0.5 mL/min): t_R min 29.03 (major) and min 34.82 (minor).

(R)-N-(4-bromophenyl)-1-(3-methylpyridin-2-yl)naphthalen-2-amine ***6Df****.*

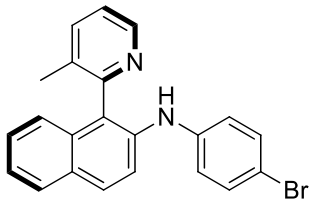

Following the general procedure from (±)-**3D** and **5f** (72 h, 50 °C, (*S*)-**L14a**), two sequential flash chromatographies (50:1→10:1 CH_2Cl_2/EtOAc and 4:1 *n*-hexane/EtOAc) afforded (*R*)-**6Df** (26 mg, 67%) as a white foam. X-ray quality crystals (colorless prisms) were obtained by slow diffusion of *n*-hexane into a solution of (*R*)-**6Df** in CH_2Cl_2. M. p. 115-117 °C. $[\alpha]^{20}_D$ –352.7 (*c* 0.5, $CHCl_3$) for 89 % ee. ^{1}H NMR (400 MHz, $CDCl_3$): 8.64 (d, 1H, *J* = 3.8 Hz), 7.84 -7.78 (m, 2H), 7.71-7.67 (m, 1H), 7.56 (d, 1H, *J* = 9.0 Hz), 7.37-7.27 (m, 5H), 7.12-7.06 (m, 1H), 6.89-6.84 (m, 2H), 5.99 (br s, 1H), 2.03 (s, 3H). ^{13}C NMR (100 MHz, $CDCl_3$): δ 156.0, 147.9, 142.6, 138.7, 137.7, 134.2, 132.9, 132.2, 129.9, 129.3, 128.3, 126.9, 124.7, 124.2, 124.0, 123.0, 119.5, 119.4, 112.8, 19.0. HRMS (ESI) calcd. for $C_{22}H_{18}BrN_2$ ($M + H^+$) 389.0648. Found 389.0643. HPLC (AD-H column, 90/10 *n*-hexane:*i*-PrOH, T = 30 °C, 0.5 mL/min): t_R 30.35 min (major) and 36.39 min (minor).

(S)-N-(3,5-dimethylphenyl)-1-(3-methylpyridin-2-yl)naphthalen-2-amine ***6Dg****.*

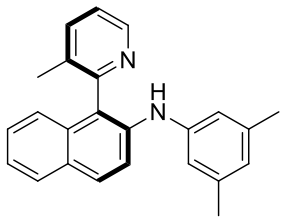

Following the general procedure from (±)-**3D** and **5g** (44 h, 50 °C, (*R*)-**L14a**), flash chromatography (50:1→10:1 CH_2Cl_2/EtOAc) afforded (*S*)-**6Dg** (33 mg, 97%) as a white foam. $[\alpha]^{20}_D$ +333.6 (*c* 0.5, $CHCl_3$) for 88 % ee. ^{1}H NMR (400MHz, $CDCl_3$): δ 8.68 (d, 1H, *J* = 4.8 Hz), 7.83-7.76 (m, 2H), 7.68 (d, 1H, *J* = 7.7 Hz), 7.64 (d, 1H, *J* = 9.0 Hz), 7.31-7.28 (m, 3H), 7.09-7.03 (m, 1H), 6.66 (s, 2H), 6.57 (s, 1H), 5.79 (br s, 1H), 2.24 (s, 6H), 2.05 (s, 3H). ^{13}C NMR (100 MHz, $CDCl_3$): δ 156.3, 148.0, 143.0, 139.1, 138.6, 138.5, 134.3, 132.1, 129.4, 129.1, 128.2, 126.7, 124.0, 123.4, 123.4, 123.1, 122.8, 119.4, 116.1, 21.5, 19.0. HRMS (ESI) calcd. for $C_{24}H_{23}N_2$ ($M + H^+$) 339.1856. Found 339.1848. HPLC (IA column, 85:15 *n*-hexane/*i*-PrOH, T = 30 °C, 0.5 mL/min): t_R 17.80 min (major) and 21.03 min (minor).

(R)-1-(3-methylpyridin-2-yl)-N-(o-tolyl)naphthalen-2-amine ***6Dh****.*

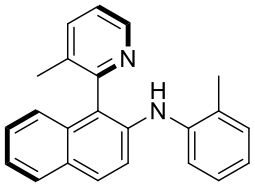

Following the general procedure from (±)-**3D** and **5h** (71 h, 50 °C, (*S*)-**L14a**), flash chromatography (50:1→25:1 CH_2Cl_2/EtOAc) afforded (*R*)-**6Dh** (30 mg, 94%) as a white foam. $[\alpha]^{20}_D$ –150.3 (*c* 0.2, $CHCl_3$) for 90 % ee. ^{1}H NMR (400 MHz, $CDCl_3$): δ 8.73 (d, 1H, *J* = 4.4 Hz), 7.83 (d, 1H, *J* = 9.3 Hz), 7.82 (d, 1H, *J* = 8.8 Hz), 7.73 (d, 1H, *J* = 7.5 Hz), 7.52 (d, 1H, *J* = 8.9 Hz), 7.38-7.31 (m, 3H), 7.30-7.26 (m, 1H), 7.20-7.12 (m, 3H), 6.93 (t, 1H, *J* = 7.3 Hz), 5.85 (br s, 1H), 2.13 (s, 3H), 2.10 (s, 3H). ^{13}C NMR (100 MHz, $CDCl_3$): δ 156.4, 147.9, 141.3, 139.0, 138.8, 134.3, 132.9, 131.0, 129.3, 129.2, 128.3, 126.8, 126.8, 124.0, 123.3, 122.9, 122.8, 121.8, 119.1, 118.4, 19.0, 17.9. HRMS (ESI) calcd. for $C_{23}H_{21}N_2$ (M + H^+) 325.1699. Found 325.1694. HPLC (AD-H column, 90:10 *n*-hexane/*i*-PrOH, T = 30 °C, 0.5 mL/min): t_R 20.10 min (minor) and 21.47 min (major).

(S)-N-(1-(3-methylpyridin-2-yl)naphthalen-2-yl)naphthalen-1-amine ***6Di****.*

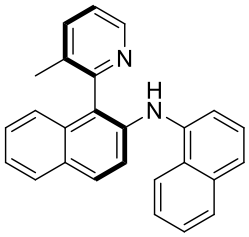

Following the general procedure from (±)-**3D** and **5i** (64 h, 50 °C, (*R*)-**L14a**), flash chromatography (50:1→25:1 CH_2Cl_2/EtOAc) afforded (*S*)-**6Di** (34 mg, 94%) as a light yellow foam. $[\alpha]^{20}_D$ +75.0 (*c* 0.5, $CHCl_3$) for 92 % ee. ^{1}H NMR (400 MHz, $CDCl_3$): δ 8.74 (dd, 1H, *J* = 4.9 and 1.1 Hz), 7.91 (dd, 1H, *J* = 8.2 and 0.9 Hz), 7.85-7.77 (m, 2H), 7.75 (d, 1H, *J* = 9.1 Hz), 7.70 (ddd, 1H, *J* = 7.8, 1.7 and 0.8 Hz), 7.53 (m, 1H), 7.47 (ddd, 1H, *J* = 8.2, 6.8 and 1.5 Hz), 7.43 (d, 1H, *J* = 9.1 Hz), 7.45-7.39 (m, 1H), 7.38-7.34 (m, 2H), 7.34-7.28 (m, 3H), 7.14-7.10 (m, 1H), 6.30 (br s, 1H), 2.14 (s, 3H). ^{13}C NMR (100 MHz, $CDCl_3$): δ 156.3, 148.2, 139.9, 138.9, 134.8, 134.4, 132.9, 129.3, 129.2, 128.6, 128.4, 127.9, 126.9, 126.3, 126.1, 125.8, 124.0, 123.4, 123.0, 122.9, 122.6, 121.9, 119.2, 115.8, 19.2. HRMS (ESI) calcd. for $C_{26}H_{21}N_2$ (M + H+) 361.1699. Found 361.1692. HPLC (IA column, 85:15 *n*-hexane/*i*-PrOH, T = 30 °C, 0.5 mL/min): t_R 16.22 min (major) and 20.31 min (minor).

(S)-1-(3-methylpyridin-2-yl)-N-(naphthalen-2-yl)naphthalen-2-amine ***6Dj****.*

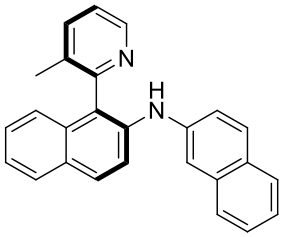

Following the general procedure from (±)-**3D** and **5j** (45 h, 50 °C, (*R*)-**L14a**), flash chromatography (50:1→10:1 CH_2Cl_2/EtOAc) afforded (*S*)-**6Dj** (30 mg, 83%) as a white foam. $[\alpha]^{20}_D$ +222.5 (*c* 0.5, $CHCl_3$) for 86 % ee. ^{1}H NMR (400 MHz, $CDCl_3$): δ 8.70 (dd, 1H, *J* = 4.8 and 1.2 Hz), 7.89-7.81 (m, 1H), 7.85 (d, 1H, *J* = 9.1 Hz), 7.73 (d, 1H, *J* = 8.9 Hz), 7.73-7.71 (m, 1H), 7.70 (d, 1H, *J* = 8.5 Hz), 7.69 (ddd, 1H, *J* = 7.8, 1.6 and 0.7 Hz), 7.62 (d, 1H, *J* = 8.1 Hz), 7.42-7.38 (m, 2H), 7.37-7.30 (m, 2H), 7.34 (d, 1H, *J* = 5.6 Hz), 7.30-7.26 (m, 1H), 7.15 (dd, 1H, *J* = 8.8 and 2.2 Hz), 7.13-7.08 (m, 1H), 6.07 (br s, 1H), 2.07 (s, 3H). ^{13}C NMR (125 MHz, $CDCl_3$) δ 156.2, 141.0, 138.7, 138.2, 134.7, 134.3, 133.0, 129.9, 129.4, 129.3, 129.2, 128.3, 127.8, 126.9, 126.6, 124.4, 124.3, 123.8, 123.6, 123.0, 120.4, 119.7, 112.1, 19.1. HRMS (ESI) calcd. for $C_{26}H_{21}N_2$ (M + H+) 361.1699. Found 361.1690. HPLC (AD-H column, 95:5 *n*-hexane/*i*-PrOH, T= 30 °C, 0.5 mL/min): t_R 35.57 min (minor) and 38.59 min (major).

(S)-N-benzyl-1-(3-methylpyridin-2-yl)naphthalen-2-amine ***6Dk****.*

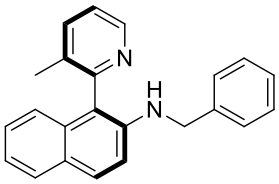

Following the general procedure from (±)-**3D** and **5k** (70 h, 60 °C, (*R*)-**L14a**, 4 equiv. of **5k** and 4 equiv. of NaO*t*Bu), flash chromatography (80:20→75:25 *n*-hexane/EtOAc) afforded (*S*)-**6Dk** (31 mg, 94%) as a light yellow foam. $[\alpha]^{20}_D$ +100.2 (*c* 0.3, $CHCl_3$) for 93 % ee. ^{1}H NMR (400 MHz, $CDCl_3$): δ 8.69 (d, 1H *J* = 4.8 Hz), 7.69-7.78 (m, 3H), 7.34-7.28 (m, 5H), 7.28-7.16 (m, 3H), 7.11 (d, 1H, *J* = 9.0 Hz), 7.00-6.92 (m, 1H), 4.49 (dd, 1H, *J* = 15.5 and 5.9 Hz), 4.43 (dd, 1H, *J* = 15.5 and 5.9 Hz), 4.17 (t, 1H, *J* = 5.6 Hz), 2.12-2.03 (s, 3H). ^{13}C NMR (100 MHz, $CDCl_3$): δ 156.3, 148.3, 142.9, 139.7, 138.5, 134.6, 132.7, 129.5, 128.6, 128.1, 127.4, 126.4, 127.0, 126.9, 126.6, 123.0, 122.8, 121.8, 117.9, 114.3, 48.0, 18.7. HRMS (ESI) calcd. for $C_{23}H_{21}N_2$ (M + H^+) 325.1699. Found 325.1692. HPLC (IA column, 95:5 *n*-hexane/*i*-PrOH, T = 30 °C, 0.5 mL/min): t_R 28.92 min (major) and 35.29 min (minor).

(S)-N-cyclohexyl-1-(3-methylpyridin-2-yl)naphthalen-2-amine ***6Dp****.*

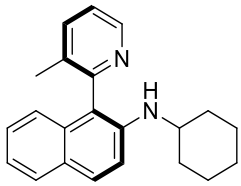

Following the general procedure from (±)-**3D** and **5p** (87 h, 60 °C, (*R*)-**L14a**, 4 equiv. of **5p** and 4 equiv. of NaO*t*Bu), flash chromatography (50:1→10:1 CH_2Cl_2/EtOAc) afforded (*S*)-**6Dp** (19 mg, 60%) as a light yellow foam. $[\alpha]^{20}_D$ +23.1 (*c* 0.5, $CHCl_3$) for 91 % ee. ^{1}H NMR (400 MHz, $CDCl_3$): δ 8.68 (ddd, 1H, *J* = 4.8, 1.7 and 0.6 Hz), 7.77 (d, 1H, *J* = 8.8 Hz), 7.71 (dd, 1H, *J* = 8.2 and 1.7 Hz), 7.70 (ddd, 1H, *J* = 7.7, 1.7 and 0.7 Hz), 7.29 (dd, 1H, *J* = 7.7 and 4.8 Hz), 7.21(ddd, 1H, *J* = 8.3, 6.8 and 1.5 Hz), 7.19 (d, 1H, *J* = 9.1 Hz), 7.16 (ddd, 1H, *J* = 8.0, 6.8 and 1.3 Hz), 6.93-6.85 (m, 1H), 3.51-3.31 (m, 2H), 2.08-1.90 (m, 2H) 2.02 (s, 3H), 1.74-1.53 (m, 3H), 1.42-1.23 (m, 2H), 1.21-0.93 (m, 3H). ^{13}C NMR (100 MHz, $CDCl_3$): δ 156.6, 148.4, 142.5, 138.5, 134.6, 133.1, 129.4, 128.2, 127.3, 126.6, 123.1, 122.7, 121.7, 118.0, 115.2, 52.1, 34.1, 33.7, 25.9, 25.0, 18.7. HRMS (ESI) calcd. for $C_{22}H_{25}N_2$ (M + H^+) 317.2012. Found 317.2006. HPLC (AD-H column, 90:10 *n*-hexane/*i*-PrOH, T = 30 °C, 0.5 mL/min): t_R 21.41 min (major) and 25.22 min (minor). The product was recrystallized by slow evaporation of a solution in *n*-hexane/ CH_2Cl_2 to afford a crystalline sample of ≥99% ee (99.6% ee).

(S)-N-allyl-1-(3-methylpyridin-2-yl)naphthalen-2-amine ***6Dm****.*

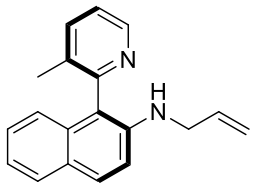

Following the general procedure from (±)-**3D** and **5m** (70 h, 60 °C, (*R*)-**L14a**, 10 equiv. of **5m** and 4 equiv. of NaO*t*Bu), flash chromatography (50:1→10:1 CH_2Cl_2/EtOAc) afforded (*S*)-**6Dm** (16 mg, 59%) as a light yellow viscous oil. $[\alpha]^{20}_D$ +37.4 (*c* 0.2, $CHCl_3$) for 92 % ee. ^{1}H NMR (400 MHz, $CDCl_3$): δ 8.68 (dd, 1H, *J* = 4.7 and 1.1 Hz), 7.79 (d, 1H, *J* = 9.1 Hz), 7.75-7.68 (m, 2H), 7.30 (dd, 1H, *J* = 7.7 and 4.8 Hz), 7.25-7.16 (m, 2H), 7.14 (d, 1H, *J* = 9.0 Hz), 6.93 (d, 1H, *J* = 8.4 Hz), 5.96-5.83 (m, 1H), 5.21 (dd, 1H, *J* = 17.2 and 1.3 Hz), 5.13-5.06 (m, 1H), 3.86 (br s, 2H), 2.04 (s, 3H). ^{13}C NMR (100 MHz, $CDCl_3$): δ 156.4, 148.4, 143.0, 138.6, 135.8, 134.7, 132.8, 129.5, 128.2, 127.4, 126.7, 123.1, 122.8, 121.9, 117.9, 116.0, 114.3, 46.5, 18.8. HRMS (ESI) calcd. for $C_{19}H_{19}N_2$ (M + H^+) 275.1543. Found 275.1544. HPLC (AD-H column, 90:10 *n*-hexane/*i*-PrOH, T = 30 °C, 0.5 mL/min): t_R 19.44 min (major) and 23.11 min (minor).

(R)-2-(isoquinolin-1-yl)-3-methyl-N-phenylaniline ***6Ea****.*

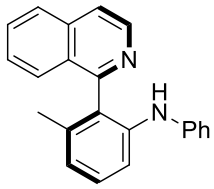

Following the general procedure from (±)-**3E** and **5a** (46 h, 60 °C, (*S*)-**L14a**), flash chromatography (50:1→25:1 CH_2Cl_2/EtOAc) afforded (*R*)-**6Ea** (29 mg, 93%) as a beige foam. $[\alpha]^{20}_D$ –49.8 (*c* 0.5, $CHCl_3$) for 90 % ee. ^{1}H NMR (400 MHz, $CDCl_3$) δ 8.69 (d, 1H, *J* = 5.7 Hz,), 7.88 (d, 1H, *J* = 8.2 Hz), 7.75 (d, 1H, *J* = 8.5 Hz), 7.70-7.66 (m, 2H), 7.49 (ddd, 1H, *J* = 8.1, 7.0 and 1.0 Hz), 7.33 (d, 1H, *J* = 8.0 Hz), 7.28-7.24 (m, 1H), 7.16-7.12 (m, 2H), 6.94-6.91 (m, 3H), 6.83 (t, 1H, *J* = 7.3 Hz), 5.57 (br s, 1H), 1.91 (s, 3H). ^{13}C NMR (100 MHz, $CDCl_3$) δ 159.5, 143.1, 142.8, 141.8, 138.0, 136.8, 130.6, 129.2, 128.9, 128.4, 127.9, 127.8, 127.2, 126.9, 122.8, 121.0, 120.4, 118.7, 114.9, 20.3. HRMS (ESI) calcd. for $C_{22}H_{19}N_2$ (M + H^+) 311.1543. Found 311.1537. HPLC (IA column, 85:15 *n*-hexane/*i*-PrOH, T = 30 °C, 1 mL/min): t_R 5.42 min (major) and 7.68 min (minor).

(R)-2-(isoquinolin-1-yl)-3-methyl-N-(p-tolyl)aniline ***6Eb****.*

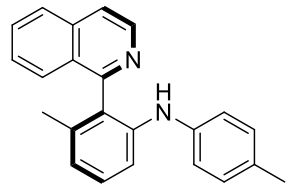

Following the general procedure from (±)-**3E** and **5b** (47 h, 60 °C, (*S*)-**L14a**), flash chromatography (50:1→20:1 CH_2Cl_2/EtOAc) afforded (*R*)-**6Eb** (32 mg, 98%) as a light yellow foam. $[\alpha]^{20}_D$ –44.0 (*c* 0.5, $CHCl_3$) for 90 % ee. ^{1}H NMR (400 MHz, $CDCl_3$) δ 8.68 (d, 1H, *J* = 5.7 Hz), 7.88 (d, 1H, *J* = 8.2 Hz), 7.75 (d, 1H, *J* = 8.4 Hz), 7.72-7.64 (m, 2H), 7.49 (ddd, 1H, *J* = 8.2, 6.9 and 1.0 Hz), 7.24-7.22(m, 2H), 6.97 (d, 2H, *J* = 8.3 Hz), 6.90-6.83 (m, 3H), 5.40 (br s, 1H), 2.23 (s, 3H), 1.89 (s, 3H). ^{13}C NMR (100 MHz, $CDCl_3$) δ 159.5, 142.9, 142.6, 140.3, 137.8, 136.8, 130.9, 130.6, 129.7, 128.9, 127.9, 127.8, 127.6, 127.1, 126.9, 122.1, 120.3, 119.7, 113.9, 20.7, 20.2. HRMS (ESI) calcd. for $C_{23}H_{21}N_2$ (M + H^+) Revisar masas 325.1699. Found 325.1693. HPLC (IA column, 85:15 *n*-hexane/*i*-PrOH, T = 30 °C, 1 mL/min): t_R 5.23 min (major) and 8.77 min (minor).

(R)-2-(isoquinolin-1-yl)-N-(4-methoxyphenyl)-3-methylaniline ***6Ec****.*

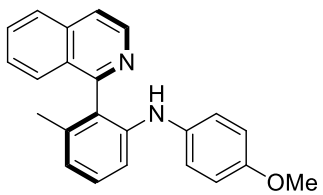

Following the general procedure from (±)-**3E** and **5c** (47 h, 60 °C, (*S*)-**L14a**), purification by preparative TLC (7:3 Et_2O/n-Hexane) afforded (*R*)-**6Ec** (32 mg, 94%) as a yellow foam. $[\alpha]^{20}_D$ –5.8 (*c* 0.5, $CHCl_3$) for 91 % ee. ^{1}H NMR (400 MHz, $CDCl_3$) 8.69 (d, 1H, *J* = 5.7 Hz), 7.89 (d, 1H, *J* = 8.2 Hz), 7.77 (d, 1H, *J* = 8.4 Hz),

7.73-7.67 (m, 2H), 7.51 (ddd, 1H, *J* = 8.1, 6.9 and 1.0 Hz), 7.20 (t, 1H, *J* = 7.9 Hz), 7.03 (d, 1H, *J* = 8.2 Hz), 6.95-6.89 (m, 2H), 6.83 (d, 1H, *J* = 7.5 Hz), 6.78-6.72 (m, 2H), 5.24 (br s, 1H), 3.74 (s, 3H), 1.88 (s, 3H). ^{13}C NMR (100 MHz, $CDCl_3$) δ 159.5, 155.3, 143.8, 143.0, 137.7, 136.8, 135.8, 130.6, 129.0, 128.0, 127.8, 127.2, 126.9, 126.5, 123.0, 121.4, 120.3, 114.5, 112.6, 55.6, 20.2. HRMS (ESI) calcd. for $C_{23}H_{21}N_2O$ (M + H^+) 341.1648. Found 341.1642. HPLC (IA column, 70:30 *n*-hexane/*i*-PrOH, T = 30 °C, 1 mL/min): t_R 4.95 min (major) and 9.09 min (minor).

(R)-N-(4-fluorophenyl)-2-(isoquinolin-1-yl)-3-methylaniline ***6Ed****.*

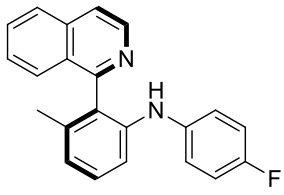

Following the general procedure from (±)-**3E** and **5d** (47 h, 60 °C, (*S*)-**L14a**), flash chromatography (50:1→10:1 CH_2Cl_2/EtOAc) afforded (*R*)-**6Ed** (31 mg, 95%) as a pale yellow foam. $[\alpha]^{20}_D$ −23.3 (*c* 0.5, $CHCl_3$) for 91 % ee. ^{1}H NMR (400 MHz, $CDCl_3$) δ ^{1}H NMR (400 MHz, $CDCl_3$) δ 8.68 (d, 1H, *J* = 5.7 Hz), 7.89 (d, 1H, *J* = 8.2 Hz), 7.76-7.66 (m, 3H), 7.51 (ddd, 1H, *J* = 8.2, 6.9 and 1.1 Hz), 7.23 (d, 1H, *J* = 7.8 Hz), 7.13 (d, 1H, *J* = 8.2 Hz), 6.93-6.81 (m, 5H), 5.38 (br s, 1H), 1.89 (s, 3H). ^{13}C NMR (100 MHz, $CDCl_3$) δ 159.4, 158.1 (d, $^1J_{C\text{-}F}$ = 240 Hz), 142.9, 142.7, 139.0 (d, $^4J_{C\text{-}F}$ = 3 Hz), 138.0, 136.8, 130.7, 129.0, 127.9, 127.8, 127.7, 127.2, 126.8, 122.5, 121.4 (d, 2C, $^3J_{C\text{-}F}$ = 8 Hz), 120.4, 115.8 (d, 2C, $^2J_{C\text{-}F}$ = 22 Hz), 113.9, 20.2. ^{19}F NMR (377 MHz, $CDCl_3$) δ −122.1. HRMS (ESI) calcd. for $C_{22}H_{18}N_2F$ (M + H^+) 329.1449. Found 329.1442. HPLC (IA column, 85:15 *n*-hexane/*i*-PrOH, T = 30 °C, 1 mL/min): t_R 5.42 min (major) and 8.39 min (minor).

(R)-N-(3,5-dimethylphenyl)-2-(isoquinolin-1-yl)-3-methylaniline ***6Eg****.*

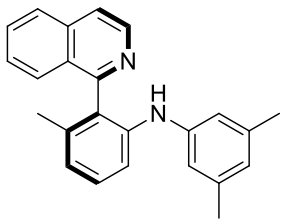

Following the general procedure from (±)-**3E** and **5g** (47 h, 60 °C, (*S*)-**L14a**), flash chromatography (50:1→10:1 CH_2Cl_2/EtOAc) afforded (*R*)-**6Eg** (33 mg, 97%) as a yellow foam. $[\alpha]^{20}_D$ −17.1 (*c* 0.5, $CHCl_3$) for 88 % ee. ^{1}H NMR (400 MHz, $CDCl_3$) δ 8.68 (d, 1H, *J* = 5.7 Hz), 7.88 (d, 1H, *J* = 8.2 Hz), 7.74 (d, 1H, *J* = 8.5 Hz), 7.71-7.65 (m, 2H), 7.49 (ddd, 1H, *J* = 8.2, 7.0 and 1.0 Hz), 7.33 (d, 1H, *J* = 8.0 Hz), 7.29-7.23 (m, 1H), 6.91 (d, 1H, *J* = 7.3 Hz), 6.56 (s, 2H), 6.48 (s, 1H), 5.46 (br s, 1H), 2.18 (s, 6H), 1.89 (s, 3H). ^{13}C NMR (100 MHz, $CDCl_3$) δ 159.5, 143.0, 142.8, 141.9, 138.9, 137.9, 136.7, 130.6, 128.9, 128.2, 127.9, 127.8, 127.1, 126.9, 122.8, 122.5, 120.3, 116.4, 114.9, 21.4, 20.3. HRMS (ESI) calcd.

for $C_{24}H_{23}N_2$ (M + H^+) 339.1856. Found 339.1850. HPLC (AD-H column, 85:15 *n*-hexane/*i*-PrOH, T = 30 °C, 1 mL/min): t_R 5.29 min (minor) and 5.65 min (major).

(R)-N-(2-(isoquinolin-1-yl)-3-methylphenyl)naphthalen-2-amine ***6Ej****.*

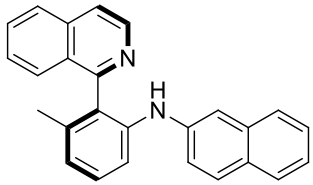

Following the general procedure from (±)-**3D** and **5j** (47 h, 60 °C, (*S*)-**L14a**), two sequential flash chromatographies (50:1→10:1 CH_2Cl_2/EtOAc and 85:15→80:20 *n*-hexane/EtOAc) afforded (*R*)-**6Ej** (26 mg, 72%) as a pale orange foam. $[\alpha]^{20}_D$ −27.1 (*c* 0.5, $CHCl_3$) for 91 % ee. ^{1}H NMR (400 MHz, $CDCl_3$) δ 8.70 (d, 1H, *J* = 5.7 Hz), 7.88 (d, 1H, *J* = 8.2 Hz), 7.81-7.73 (m, 1H), 7.70 (dd, 1H, *J* = 5.8 and 0.6 Hz), 7.68-7.63 (m, 2H), 7.60 (d, 1H, *J* = 8.8 Hz), 7.57 (d, 1H, *J* = 8.3 Hz), 7.49 (ddd, 1H, *J* = 8.2, 6.9 and 1.1 Hz), 7.42 (d, 1H, *J* = 8.1 Hz), 7.34 (ddd, 1H, *J* = 8.1, 6.8 and 1.2 Hz), 7.33-7.28 (m, 2H), 7.24 (ddd, 1H, *J* = 8.1, 6.9 and 1.2 Hz), 7.06 (dd, 1H, *J* = 8.8 and 2.3 Hz), 6.98 (d, 1H, *J* = 7.5 Hz), 5.74 (br s, 1H), 1.93 (s, 3H). ^{13}C NMR (100 MHz, $CDCl_3$) δ 159.4, 142.8, 141.6, 140.9, 138.1, 136.8, 134.6, 130.7, 129.2, 129.0, 128.9, 128.8, 127.9, 127.9, 127.7, 127.2, 126.9, 126.5, 126.4, 123.5, 123.3, 120.6, 120.5, 115.5, 112.6, 20.3. HRMS (ESI) calcd. for $C_{26}H_{21}N_2$ (M + H^+) 361.1699. Found 361.1693. HPLC (IA column, 85:15 *n*-hexane/*i*-PrOH, T = 30 °C, 1 mL/min): t_R 6.59 min (major) and 8.59 min (minor).

Synthesis of IAN Amine (*R*)-7A.

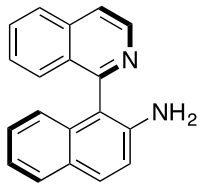

Following a known procedure,[150] a solution of (*R*)-**6Am** (16 mg, 0.05 mmol) in anhydrous CH_2Cl_2 (1.3 mL) was treated with *N,N'*-dimethylbarbituric acid (80 mg, 0.5 mmol) and $Pd(PPh_3)_4$ (2.9 mg, 5 mol %), and the mixture was refluxed for 15 h. 2M NaOH (10 mL) was added and the mixture was extracted with EtOAc (3 × 10 mL), dried ($MgSO_4$), filtered concentrated, and the resulting residue was purified by flash chromatography (1:1 *n*-hexane/EtOAc) to afford (*R*)-**7Aa** (IAN) (9.5 mg, 86%) as an orange oil. $[\alpha]^{20}_D$ −104.9 (*c* 0.2, $CHCl_3$) for 86 % ee. ^{1}H NMR (400 MHz, $CDCl_3$): δ 8.75 (d, 1H, *J* = 5.7 Hz), 7.94 (d, 1H, *J* = 8.2 Hz), 7.81 (d, 1H, *J* = 8.7 Hz), 7.79-7.77 (m, 2H), 7.71 (t, 1H, *J* = 8.0 Hz), 7.58 (d, 1H, *J* = 8.4 Hz), 7.42 (t, 1H, *J* = 8.1 Hz), 7.22 (t, 1H, *J* = 7.9 Hz), 7.16 (t, 1H, *J* = 8.2 Hz), 7.11 (d, 1H, *J* = 8.7 Hz), 6.87 (d, 1H, *J* = 8.3 Hz),

[150] Barluenga, J.; Gómez, A.; Santamaría, J.; Tomás, M. *J. Am. Chem. Soc.* **2009**, *131*, 14628-14629.

3.43 (br s, 2H). ^{13}C NMR (100 MHz, $CDCl_3$): δ 158.6, 142.9, 142.5, 136.9, 133.9, 130.7, 130.1, 128.4, 128.0, 127.7, 127.7, 127.1, 126.7, 124.0, 122.4, 120.5, 118.7, 116.3. HRMS (ESI) calcd. for $C_{19}H_{15}N_2$ (M + H^+) 271.1235. Found 271.1228. HPLC (AD-H column, 90:10*n*-hexane/*i*-PrOH, T = 30 °C, 1.0 mL/min): t_R 16.83 min (minor) and 20.40 min (major).

Isolation of the OA intermediate *OAI⁺(OTf).*

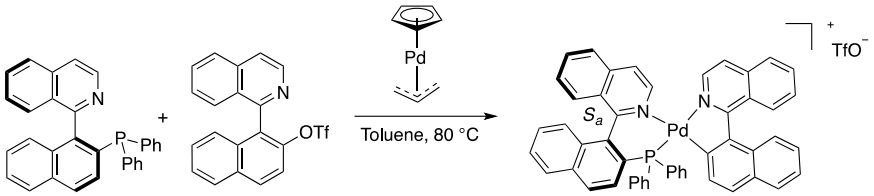

(*S*)-QUINAP 88%

A dried and deoxygenated Schlenk was charged with (*S*)-**L14a** (87 μmol, 38.4 mg) and (±)-**2A** (35.1 mg, 87 μmol). After three cycles of vacuum-N_2, [Pd(Cp)(allyl)] (18.4 mg, 87 μmol) and dry, deoxygenated toluene (2.6 mL) were added. The reaction mixture was stirred overnight at 80 °C and a green precipitated was formed. The mixture was concentrated to dryness and the resulting residue (127.2 mg) was crystallized by slow diffusion of *n*-hexane into a solution of the crude reaction mixture in THF to give **OAI⁺(OTf)** (76 mg, 88%) as pale yellow prisms suitable for X-Ray analysis. M. p. = 170-172 °C (dec.). $[\alpha]^{20}_D$= −71.2° (*c* 0.1, $CHCl_3$). ^{1}H NMR (400 MHz, CD_2Cl_2, 25 °C): A curved baseline was observed. δ 9.15 (d, 1H, *J* = 6.2 Hz), 8.41 (d, 1H, $J_{H,H}$ = 6.2 Hz and $J_{H,P}$ = 2.7 Hz), 8.09 (d, 1H, *J* = 8.7 Hz), 8.07 (d, 1H, *J* = 8.7 Hz), 8.02-7.94 (m, 3H), 7.86-7.82 (m, 2H), 7.78-7.70 (m, 4H), 7.66-7.61 (m, 3H), 7.59-7.53 (m, 3H), 7.44-7.30 (m, 8H), 7.23 (t, 1H, $J_{H,H}$ = $J_{H,P}$ = 8.7 Hz), 7.16 (d, 1H, *J* = 8.7 Hz), 7.05-7.00 (m, 2H), 6.95-6.92 (m, 2H), 6.75 (dd, 1H, $J_{H,H}$ = 8.3 Hz and $J_{H,P}$ = 6.3 Hz). ^{13}C NMR (100 MHz, CD_2Cl_2, 25 °C): δ 167.8 (d, $J_{C,P}$ = 3 Hz), 158.2 (d, $J_{C,P}$ = 8 Hz), 156.7 (d, $J_{C,P}$ = 5 Hz), 143.8 (d, $J_{C,P}$ = 2 Hz), 141.7, 141.3, 140.1 (d, $J_{C,P}$ = 13 Hz), 138.9, 137.2, 136.8 (d, $J_{C,P}$ = 12 Hz), 136.0 (br s), 134.7 (d, $J_{C,P}$ = 2 Hz), 134.3, 134.2, 133.6, 133.6, 133.5, 133.2 133.1 (d, $J_{C,P}$ = 9 Hz), 132.7, 132.4 (d, $J_{C,P}$ = 3 Hz), 131.9, 131.8, 130.5, 130.2 (d, $J_{C,P}$ = 6 Hz), 130.0, 129.9, 129.2, 129.1, 129.1, 129.0, 128.9, 128.8, 128.7, 128.3, 128.2, 127.7, 127.6, 127.3 (d, $J_{C,P}$ = 7 Hz), 126.8 (d, $J_{C,P}$ = 15 Hz), 126.5, 126.4, 126.2, 125.8, 125.8, 125.0 (d, $J_{C,P}$ = 50 Hz), 123.3 (d, $J_{C,P}$ = 54 Hz), 122.0 (d, $J_{C,P}$ = 3 Hz), 121.6 (q, $J_{C,F}$ = 319 Hz). ^{31}P NMR

(161.7 MHz, CD_2Cl_2): δ +42.6. ^{19}F NMR (377 MHz, CD_2Cl_2): δ −78.8. HRMS (ESI) *m/z* calcd for $C_{50}H_{34}N_2PPd$ (M^+) 799.1489, found 799.1468.

DynamiC NMR studies of intermediate OAI$^+$(OTf):

A NMR Young´s tube was charged with a solution of the OA intermediate ***OAI$^+$(OTf).*** (9.9 mg, 0.01 mmol) in 0.5 mL of anhydrous THF-d_8, and then NMR spectra were recorded at different temperatures from 25 °C to −78 °C.

Reactivity studies with intermediate OAI$^+$(OTf).

Tritation of the OAI$^+$(OTf) with aniline.

A Young's NMR tube was charged with a solution of the OA intermediate **OAI$^+$(OTf)** (4.9 mg, 5 μmol) in 0.5 mL of THF-d_8. A series of ^1H and ^{31}P NMR spectra were recorded after subsequent additions of aniline **5a** (0.5 M in THF-d_8).

Stoichiometric C-N coupling reaction starting from OAI+(OTf) intermediate.

A Schlenk tube was charged with **OAI$^+$(OTf)** (9.8 mg, 9.7 μmol) and Cs_2CO_3 (65.2 mg, 0.2 mmol). After three vacuum-N_2 cycles, dry, deoxygenated toluene (2 mL) and aniline **5a** (18 μL, 0.2 mmol) were added. The reaction mixture was stirred at 50 °C and monitored by TLC and NMR, showing full conversion after 7 h. ^{31}P-NMR monitoring of the reaction showed a major peak at 25.8 ppm which was assigned to the Pd^0(**L14a**) species. The mixture was concentrated to dryness and the resulting residue was purified using preparative TLC (CH_2Cl_2) affording 1.9 mg (57%, 74% ee) of **(*R*)-6Aa**.

Isolation of the OA intermediate (*S*)-OAI(Br).

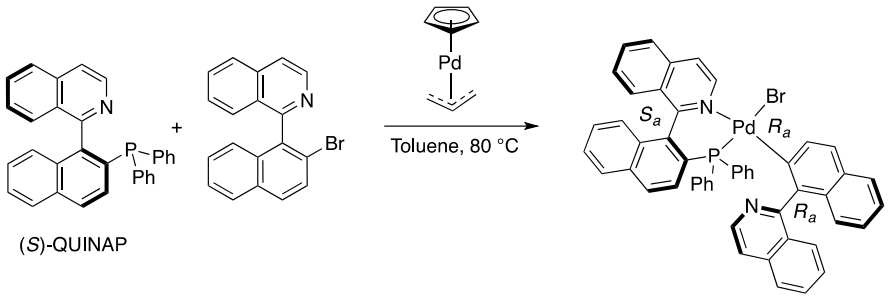

(*S*)-QUINAP

A Schlenk tube was charged with (*S*)-**L14a** (22 mg, 0.05 mmol) and bromide (±)-**3A** (16.7 mg, 0.05 mmol). After three vacuum-N_2 cycles, [Pd(Cp)(allyl)] (10.6 mg, 0.05 mmol) and dry, deoxygenated toluene (1.5 mL) were added. The reaction mixture was stirred overnight at 80 °C and a brown-red

precipitated was formed. The mixture was concentrated to dryness, washed with pentane and the resulting residue (48 mg) was analyzed by ^{1}H and ^{31}P NMR. Crystallization by slow diffusion of pentane into a solution of the crude reaction mixture in CH_2Cl_2, afforded orange-red crystals (prisms) of **(*S*)-OAI(Br)** suitable for X-Ray analysis. M. p. = 152-153 °C (dec.).

Stoichiometric C-N coupling reaction starting from crude OAI(Br)

A dried and deoxygenated Schlenk tube was charged with recently prepared OAI(Br) reaction crude (9.3 mg, 11 μmol) and NaO*t*Bu (0.2 mmol, 19.2 mg). After three cycles of vacuum-nitrogen, anhydrous toluene (2 mL) and then aniline (0.2 mmol, 18 μL) were added. The mixture was stirred at 50 °C for 2 h, concentrated and the resulting residue was purified by preparative TLC (CH_2Cl_2) to afford 3.8 mg (quantitative, 87% ee) of (*R*)-**6Aa**.

3. C-H hydroarylation of vinyl ethers as a desymmetrisation strategy for the synthesis of heterobiaryls with central and axial chirality

Introduction

C-H activation

In recent years, the concern about environmental issues has significantly increased as a response to the forthcoming climate change. Thus, the development of synthetic methodologies that are in line with Green Chemistry postulates[151] is highly desirable and comprises a great challenge for chemists.

Examples of these principles include the reduction of waste and the atom and step economy; and accordingly, an excellent way to reach these postulates is catalysis. In this context, C-H activation[152] has emerged as powerful tool to develop new and improved methodologies in terms of efficiency and environmental concerns. In this regard, catalytic C-H reactions are of major importance as they avoid the functionalization of substrates so that they undergo the desired transformation. Besides, many C-H reactions incorporates all the atoms of the reactants in the products and thereby, achieving full atom economy.

These ideas were already gathered by the visionary words of Jack Halpern in 1968:[153] "the development of successful approaches to the activation of carbon–hydrogen bonds, particularly in saturated hydrocarbons, remains to be achieved and presently constitutes one of the most important and challenging problems in this whole field".

From the industrial and economical point of view, C-H activation has a great interest as it would comprise a route for the functionalization of feedstock into more valuable materials. Thus, the synthesis of acetic acid from CH_4 and CO_2

[151] (1) Anastas, P.; Eghbali, N. Green Chemistry: Principles and Practice. *Chem. Soc. Rev.* **2010**, *39* (1), 301–312. https://doi.org/10.1039/b918763b.

[152] *Handbook of C-H Transformations*, G. Dyker Ed.; Wiley- VCH: Weinheim, **2005.**
(1) Bergman, R. G. C–H Activation. Nature 2007, 446 (7134), 391–393. https://doi.org/10.1038/446391a.

[153] (1) Halpern, J. General Introduction—Homogeneous Catalysis of Hydrogenation, Oxidation and Related Reactions. *Discuss. Faraday Soc.* **1968**, *46*, 7–19. https://doi.org/10.1039/DF9684600007.

or the oxidation of alkanes to achieve more valuable products such as alcohols and carbonyl compounds are example of these goals.

By contrast, alkanes can be converted into oxygenated compounds, though demanding and expensive reagents or harsh conditions are required.[154,155,156] For instance, the most common way to functionalise alkanes needs the previous transformation into alkenes. However, this cracking process is not very efficient due to the use of severe conditions involving high temperatures and pressure.

Hence, C-H functionalization would not only have a big impact on basic but on fine chemical industries too.

C-H activation

When talking about C-H activation, we mean the cleavage of unreactive, neutral C-H bonds by contrast to acidic (pka>25) C-H bonds, which easily partakes in a number of reactions. In this vein, C-H adjacent to electron-withdrawing groups are left out.

Furthermore, despite Friedel-Crafts and related S_EAr reactions deal with the activation of C-H bonds, they are neither considered as they are not based on organometallic C-H activation. In this regard, we will only consider inner-sphere reactions in which there exists a direct interaction between the metal centre and the C-H bond.[157] Therefore, carbene and nitrene C-H insertion[158] or hydrogen transfer-mediated C-H activation (reactions that proceed through radical mechanisms) will not discussed despite they render a route for the functionalization of C-H bonds. Similarly, the functionalization of C-H bonds is not only performed by transition metal catalyst. Thus, it is worth to note that

---

[154] (1) Labinger, J. A.; Bercaw, J. E. Understanding and Exploiting C–H Bond Activation. *Nature* **2002**, *417* (6888), 507–514. https://doi.org/10.1038/417507a.

[155] (1) Shilov, A. E.; Shul'pin, G. B. Activation of C-H Bonds by Metal Complexes. *Chem. Rev.* **1997**, *97* (8), 2879–2932. https://doi.org/10.1021/cr9411886.

[156] . Activation and functionalization of alkanes, Hill, Craig L., Ed.; Wiley: New York, **1989**.

[157] (1) Dick, A. R.; Sanford, M. S. Transition Metal Catalysed Oxidative Functionalization of Carbon-Hydrogen Bonds. *Tetrahedron* **2006**, *62* (11), 2439–2463. https://doi.org/10.1016/j.tet.2005.11.027.

[158] (1) Davies, H. M. L.; Manning, J. R. Catalytic C-H Functionalization by Metal Carbenoid and Nitrenoid Insertion. *Nature* **2008**, *451* (7177), 417–424. https://doi.org/10.1038/nature06485.

there are some strategies based on organocatalysis,[159] main group elements and frustrated Lewis-pairs.[160]

On the one hand, C-H bonds are particularly inert with a dissociation energy of ~105 kcal·mol in H-CH_3 and ~110 kcal·mol in H-Ph,[161] while C-X bonds are much less strong and undergo oxidative addition.[162] On the other hand, the ease with which this C-X bond to undergoes this reaction is a key step in the catalytic applications as the formation of C-M species would ultimately lead to C-C bond forming reaction.

Thus, the difficulty of C-H activation in alkanes relies on the lack of reactivity of these bonds due to the lack of polarization and the absence of non-bonding electron pair and/or π frontier MO of adequate energy to interact with metal centres. Conversely, arylic and vinylic C-H, in spite of their higher C-H bond energy, are more susceptible to undergo such reactions for these reasons.

In addition to the inertness of the C-H bond, this synthetic strategy present other challenging issues regarding the selectivity. Molecules have different C-H that may potentially undergo the activation, so reactions that selectively yield the functionalisation at the desired position are highly desirable.

The C-H activation of not-functionalized hydrocarbons, that is to say, “first functionalization”, is possible despite the above-mentioned difficulties. However, in these cases harsh conditions are required to overcome this lack of reactivity and sometimes the substrate have to be utilized as the solvent.[163]

---

[159] (1) Pan, S. C. Organocatalytic C-H Activation Reactions. *Beilstein J. Org. Chem.* **2012**, *8* (Scheme 1), 1374–1384. https://doi.org/10.3762/bjoc.8.159.

[160] (1) Gandeepan, P.; Müller, T.; Zell, D.; Cera, G.; Warratz, S.; Ackermann, L. 3d Transition Metals for C-H Activation. *Chem. Rev.* **2019**, *119* (4), 2192–2452. https://doi.org/10.1021/acs.chemrev.8b00507.

[161] Kerr J. A. in CRC Handbook of Chemistry and Physics; D. R. Lide D. R., Ed.; CRC: Boston, **1990**.

[162] During a period of time, it was believed C-H bonds could not undergo oxidative addition until the corresponding intermediates could be isolated.

[163] For some examples: (1) Shilov, A. E.; Shteinman, A. A. Activation of Saturated Hydrocarbons by Metal Complexes in Solution. *Coord. Chem. Rev.* **1977**, *24* (2–3), 97–143. https://doi.org/10.1016/S0010-8545(00)80336-7.

(1) Gol'dshleger, N. F.; Es'kova, V. V.; Shilov, A. E.; Shteinman, A. A. "Reactions of alkanes in solutions of platinum chloride complexes" Zh. Fiz. Khim. 1972, 46, 1353-13544.

(1) Chen, H.; Schlecht, S.; Semple, T. C.; Hartwig, J. F. Thermal, Catalytic, Regiospecific Functionalization of Alkanes. *Science (80-.).* **2000**, *287* (5460), 1995–1997. https://doi.org/10.1126/science.287.5460.1995.

Owing to these severe conditions, reaching regioselectivity becomes a problem and activation of several bonds may ensue.

By contrast, in "further functionalization" regioselectivity is a minor problem. In this regard, when the substrate is previously functionalised,[164] the attached group may coordinate the metal and bring it closer to a specific position, affording a selective C-H activation. Nevertheless, functional group tolerance is a big deal as they usually exhibit a higher reactivity toward metal centres than C-H bond do.

Hystorical background

Reactions of hydrocarbons with metallic species are known from the last of XIX century. Indeed, mercuration of benzene and derivatives,[165] which can be seen as the first C-H activation reaction, is known since 1898. However, a turning point was marked in this field in the 1960s with the first cyclometallation: the reaction of azabenzene with $NiCp_2$ reported by Kleiman and Dubeck.[166] In the subsequent years, despite a number of fundamental studies were done, practical synthetic and catalytic applications based on the activation of C-H bond afforded rather poor results. For instance, during this period, Fujiwara-Moritoni reaction (Scheme 0-1.A)[167] was described but the selectivity of this alkenylation was low with substituted arenes.

---

(1) Jia, X.; Huang, Z. Conversion of Alkanes to Linear Alkylsilanes Using an Iridium-Iron-Catalysed Tandem Dehydrogenation-Isomerization-Hydrosilylation. *Nat. Chem.* **2016**, *8* (2), 157–161. https://doi.org/10.1038/nchem.2417.

[164] Engle, K. M.; Yu, J.-Q. Transition Metal-Catalysed C-H Functionalization: Synthetically Enabling Reactions for Building Molecular Complexity; In Organic Chemistry – Breakthroughs and Perspectives; Ding, K.; Dai, L.-X., Eds.; Wiley: Weinheim, **2012**.

[165] (1) Dimroth, O. Ueber Die Mercurirung Aromatischer Verbindungen. *Berichte der Dtsch. Chem. Gesellschaft* **1902**, *35* (2), 2032–2045. https://doi.org/10.1002/cber.190203502154.

(2) Dimroth, O. Ueber Die Einwirkung von Quecksilberoxydsalzen Auf Aromatische Verbindungen. *Berichte der Dtsch. Chem. Gesellschaft* **1899**, *32* (1), 758–765. https://doi.org/10.1002/cber.189903201116.

(3) Dimroth, O. Directe Einführung von Quecksilber in Aromatische Verbindungen. *Berichte der Dtsch. Chem. Gesellschaft* **1898**, *31* (2), 2154–2156. https://doi.org/10.1002/cber.189803102162.

[166] (1) Kleiman, J. P.; Dubeck, M. The Preparation of Cyclopentadienyl [o -(Phenylazo)Phenyl]Nickel. *J. Am. Chem. Soc.* **1963**, *85* (10), 1544–1545. https://doi.org/10.1021/ja008910A040.

[167] (1) Fujiwara, Y.; Moritani, I.; Matsuda, M.; Teranishi, S. Aromatic Substitution of Olefin. IV Reaction with Palladium Metal and Silver Acetate. *Tetrahedron Lett.* **1968**, *9* (35), 3863–3865. https://doi.org/10.1016/S0040-4039(01)99121-X.

Scheme 0-1. Significant catalytic C-H reactions prior to Murai reaction

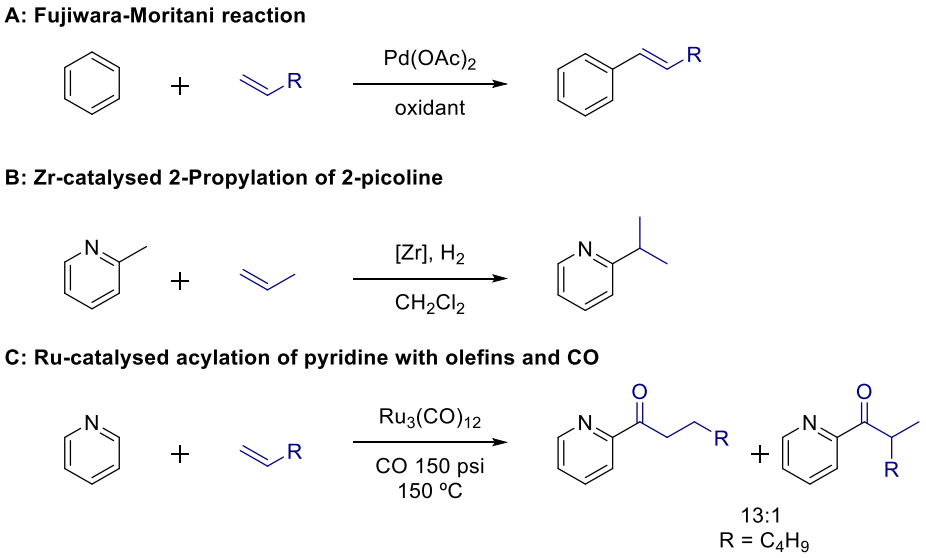

Hence, highly effective C-H functionalization did not appear until the nineties. In this respect, a Zr-catalysed 2-propylation of 2-picoline was reported by Jordan in 1989 (Scheme 0-1.B).[168] Similarly, in 1992 Moore reported a Ru-catalysed acylation of pyridine with CO and alkenes (Scheme 0-1.C). Although these works paved the way for other catalytic reactions based on the activation of C-H bond, however, these methodologies were rather poor as they provided the products in low yields or high catalytic loadings.

In this context, the work of Murai in 1993 on a very efficient and selective alkylation of aromatic ketones[169] represented a major step forward. The key feature to overcome the aforementioned problems relied on the directing effect driven by the ketone which eventually ends up in the formation of a

(1) Fujiwara, Y.; Asano, R.; Moritani, I.; Teranishi, S. Aromatic Substitution of Olefins. 25. Reactivity of Benzene, Naphthalene, Ferrocene, and Furan toward Styrene, and the Substituent Effect on the Reaction of Monosubstituted Benzenes with Styrene. *J. Org. Chem.* **1976**, *41* (10), 1681–1683. https://doi.org/10.1021/jo00879a002.

[168] (1) Jordan, R. F.; Taylor, D. F. Zirconium-Catalysed Coupling of Propene and α-Picoline. *J. Am. Chem. Soc.* **1989**, *111* (2), 778–779. https://doi.org/10.1021/ja00184a081.

[169] (1) Murai, S.; Kakiuchi, F.; Sekine, S.; Tanaka, Y.; Kamatani, A.; Sonoda, M.; Chatani, N. Efficient Catalytic Addition of Aromatic Carbon-Hydrogen Bonds to Olefins. *Nature* **1993**, *366* (6455), 529–531. https://doi.org/10.1038/366529a0.

chelate. This way, the high yields and selectivity[170] can be accounted by the driven force provided by the chelation which additionally impose the activation of *ortho* positions relative to the directing group. Regarding the olefin, the selectivity of mono- and disubstituted terminal alkenes was dictated by steric hindrance. Similarly, 1:1 products were selectively formed for the same reasons.

Scheme 0-2. Murai's alkylation of aromtic ketones via directed C-H activation.

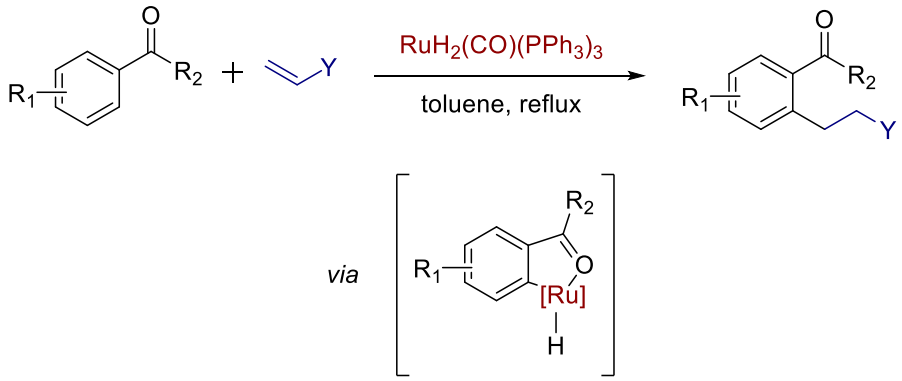

This report represents a milestone in the field of C-H activation, garnering growing attention and providing a source of inspiration for other directed C-H activation methodologies.

This concept was then extended to other directing groups, metals and reactions. Thus, either strong or poor coordinative directing groups,[171] such as

[170] It is worth noting *ortho* activation of benzene also results in the activation of *para* position.

[171](1) Rouquet, G.; Chatani, N. Catalytic Functionalization of C(Sp2)-H and C(Sp3)-H Bonds by Using Bidentate Directing Groups. *Angew. Chemie - Int. Ed.* **2013**, *52* (45), 11726–11743. https://doi.org/10.1002/anie.201301451.

(1) Evano, G.; Theunissen, C. Beyond Friedel and Crafts: Innate Alkylation of C–H Bonds in Arenes. *Angew. Chemie - Int. Ed.* **2019**, *58* (23), 7558–7598. https://doi.org/10.1002/anie.201806631.

(1) Engle, K. M.; Mei, T. S.; Wasa, M.; Yu, J. Q. Weak Coordination as a Powerful Means for Developing Broadly Useful C-H Functionalization Reactions. *Acc. Chem. Res.* **2012**, *45* (6), 788–802. https://doi.org/10.1021/ar200185g

(1) Huang, Z.; Lim, H. N.; Mo, F.; Young, M. C.; Dong, G. Transition Metal-Catalysed Ketone-Directed or Mediated C-H Functionalization. *Chem. Soc. Rev.* **2015**, *44* (21), 7764–7786. https://doi.org/10.1039/c5cs00279a.

(1) Zhang, F.; Spring, D. R. Arene C-H Functionalisation Using a Removable/Modifiable or a Traceless Directing Group Strategy. *Chem. Soc. Rev.* **2014**, *43* (20), 6906–6919. https://doi.org/10.1039/c4cs00137k.

pyridine, ketones, amines, ethers, alcohols, etc (Scheme 0-3).[172] have been employed. Typically, these directing groups approximate the metal to ortho positions, but ingenious designs, the use of traceless directing groups or other pathways afford meta- (Scheme 0-3.B) and para- selectivity.[173] Moreover, non-directed catalytic applications have also been reported.[174]

(1) Snieckus, V. Directed Ortho Metalation. Tertiary Amide and O-Carbamate Directors in Synthetic Strategies for Polysubstituted Aromatics. *Chem. Rev.* **1990**, *90* (6), 879–933. https://doi.org/10.1021/cr00104a001.

[172] (A) Cai, G.; Fu, Y.; Li, Y.; Wan, X.; Shi, Z. Indirect Ortho Functionalization of Substituted Toluenes through Ortho Olefination of N,N-Dimethylbenzylamines Tuned by the Acidity of Reaction Conditions. *J. Am. Chem. Soc.* **2007**, *129* (24), 7666–7673. https://doi.org/10.1021/ja070588a.

(1) Leow, D.; Li, G.; Mei, T. S.; Yu, J. Q. Activation of Remote Meta-C-H Bonds Assisted by an End-on Template. *Nature* **2012**, *486* (7404), 518–522. https://doi.org/10.1038/nature11158.

[173] (1) Dey, A.; Sinha, S. K.; Achar, T. K.; Maiti, D. Accessing Remote Meta- and Para-C(Sp 2)−H Bonds with Covalently Attached Directing Groups. *Angew. Chemie - Int. Ed.* **2019**, 10820–10843. https://doi.org/10.1002/anie.201812116.

(1) Mihai, M. T.; Genov, G. R.; Phipps, R. J. Access to the Meta Position of Arenes through Transition Metal Catalysed C-H Bond Functionalisation: A Focus on Metals Other than Palladium. *Chem. Soc. Rev.* **2018**, *47* (1), 149–171. https://doi.org/10.1039/c7cs00637c.

(1) Wang, X.-G.; Li, Y.; Liu, H.-C.; Zhang, B.-S.; Gou, X.-Y.; Wang, Q.; Ma, J.-W.; Liang, Y.-M. Three-Component Ruthenium-Catalysed Direct Meta- Selective C–H Activation of Arenes: A New Approach to the Alkylarylation of Alkenes. *J. Am. Chem. Soc.* **2019**, *141* (35), 13914–13922. https://doi.org/10.1021/jacs.9b06608.

[174] (1) Dyker, G. Transition Metal Catalysed Coupling Reactions under C−H Activation. *Angew. Chemie Int. Ed.* **1999**, *38* (12), 1698–1712. https://doi.org/10.1002/(SICI)1521-3773(19990614)38:12<1698::AID-ANIE1698>3.3.CO;2-Y.

(1) Kakiuchi, F.; Chatani, N. Catalytic Methods for C-H Bond Functionalization: Application in Organic Synthesis. *Adv. Synth. Catal.* **2003**, *345* (910), 1077–1101. https://doi.org/10.1002/adsc.200303094.

(1) Wencel-Delord, J.; Dröge, T.; Liu, F.; Glorius, F. Towards Mild Metal-Catalysed C-H Bond Activation. *Chem. Soc. Rev.* **2011**, *40* (9), 4740–4761. https://doi.org/10.1039/c1cs150810A.

Scheme 0-3. Selected examples featuring different directing groups.

A: Shi et al. Ref. 22a

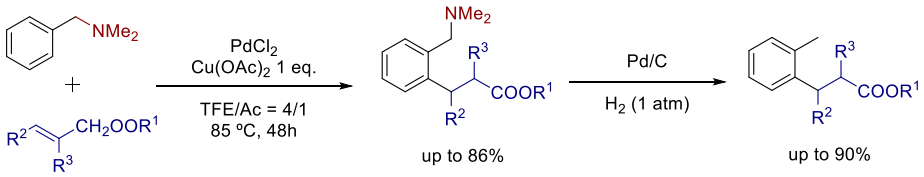

B: Yu et al. Ref. 22b

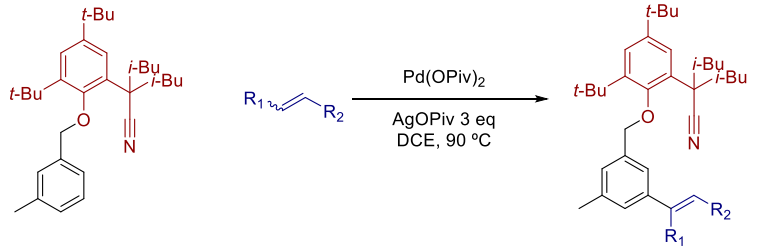

up to 98%, ,
meta selectivity up to 100%

Concerning the metallic centres of these catalysts, 4d and 5d noble metals such as Ru,[175] Rh,[176] Pd[177] Ir[178] are predominant. However, during the last years base 3d transition metals have opened new exciting possibilities.[179,193,180,160]

[175] (1) Arockiam, P. B.; Bruneau, C.; Dixneuf, P. H. Ruthenium(II)-Catalysed C-H Bond Activation and Functionalization. *Chem. Rev.* **2012**, *112* (11), 5879–5918. https://doi.org/10.1021/cr300153j.
(1) Ackermann, L. Carboxylate-Assisted Ruthenium-Catalysed Alkyne Annulations by C-H/Het-H Bond Functionalizations. *Acc. Chem. Res.* **2014**, *47* (2), 281–295. https://doi.org/10.1021/ar3002798.
[176] (1) Colby, D. A.; Tsai, A. S.; Bergman, R. G.; Ellman, J. A. Rhodium Catalysed Chelation-Assisted C-H Bond Functionalization Reactions. *Acc. Chem. Res.* **2012**, *45* (6), 814–825. https://doi.org/10.1021/ar200190g.
(1) Colby, D. A.; Bergman, R. G.; Ellman, J. A. Rhodium-Catalysed C−C Bond Formation via Heteroatom-Directed C−H Bond Activation. *Chem. Rev.* **2010**, *110* (2), 624–655. https://doi.org/10.1021/cr900005n.
[177] (1) Lyons, T. W.; Sanford, M. S. Palladium-Catalysed Ligand-Directed C−H Functionalization Reactions. *Chem. Rev.* **2010**, *110* (2), 1147–1169. https://doi.org/10.1021/cr900184e.
(1) Chen, X.; Engle, K. M.; Wang, D. H.; Jin-Quan, Y. Palladium(II)-Catalyzed C-H Aetivation/C-C Cross-Coupling Reactions: Versatility and Practicality. *Angew. Chemie - Int. Ed.* **2009**, *48* (28), 5094–5115. https://doi.org/10.1002/anie.200806273.
[178] (1) Pan, S.; Shibata, T. Recent Advances in Iridium-Catalysed Alkylation of C-H and N-H Bonds. *ACS Catal.* **2013**, *3* (4), 704–712. https://doi.org/10.1021/cs400066q.
(2) Iglesias, M.; Oro, L. A. A Leap Forward in Iridium-NHC Catalysis: New Horizons and Mechanistic Insights. *Chem. Soc. Rev.* **2018**, *47* (8), 2772–2808. https://doi.org/10.1039/c7cs00743d.
(3) Hartwig, J. F. Regioselectivity of the Borylation of Alkanes and Arenes. *Chem. Soc. Rev.* **2011**, *40* (4), 1992–2002. https://doi.org/10.1039/c0cs00156b.
[179] (1) Yoshikai, N. Cobalt-Catalysed, Chelation-Assisted C-H Bond Functionalization. *Synlett* **2011**, No. 8, 1047–1051. https://doi.org/10.1055/s-0030-1259928.
(1) Moselage, M.; Li, J.; Ackermann, L. Cobalt-Catalysed C–H Activation. *ACS Catal.* **2016**, *6* (2), 498–525. https://doi.org/10.1021/acscatal.5b02344.
[180] (1) Khake, S. M.; Chatani, N. Chelation-Assisted Nickel-Catalysed C−H Functionalizations. *Trends Chem.* **2019**, *1* (5), 524–539. https://doi.org/10.1016/j.trechm.2019.06.002.
(1) Kulkarni, A.; Daugulis, O. Direct Conversion of Carbon-Hydrogen into Carbon-Carbon Bonds by First-Row Transition-Metal Catalysis. *Synthesis (Stuttg).* **2009**, No. 24, 4087–4109. https://doi.org/10.1055/s-0029-1217131.
(1) Su, B.; Cao, Z. C.; Shi, Z. J. Exploration of Earth-Abundant Transition Metals (Fe, Co, and Ni) as Catalysts in Unreactive Chemical Bond Activations. *Acc. Chem. Res.* **2015**, *48* (3), 886–896. https://doi.org/10.1021/ar500345f.
(1) Pototschnig, G.; Maulide, N.; Schnürch, M. Direct Functionalization of C−H Bonds by Iron, Nickel, and Cobalt Catalysis. *Chem. - A Eur. J.* **2017**, *23* (39), 9206–9232. https://doi.org/10.1002/chem.201605657.

With all these advancements, C-H functionalization was not only confined to alkylations and alkenylations, but other C-C[181] and C-X[182] bond forming transformations have took advantage of this strategy.

[181] (1) Ackermann, L.; Vicente, R.; Kapdi, A. R. Transition-Metal-Catalysed Direct Arylation of (Hetero)Arenes by C-H Bond Cleavage. *Angew. Chemie - Int. Ed.* **2009**, *48* (52), 9792–9826. https://doi.org/10.1002/anie.200902996.

(1) Ping, Y.; Ding, Q.; Peng, Y. Advances in C-CN Bond Formation via C-H Bond Activation. *ACS Catal.* **2016**, *6* (9), 5989–6005. https://doi.org/10.1021/acscatal.6b01632.

Alkynylation and others: (1) Messaoudi, S.; Brion, J. D.; Alami, M. Transition-Metal-Catalysed Direct C-H Alkenylation, Alkynylation, Benzylation, and Alkylation of (Hetero)Arenes. *European J. Org. Chem.* **2010**, No. 34, 6495–6516. https://doi.org/10.1002/ejoc.201000928.

[182] (1) Zheng, Q.; Chen, J.; Rao, G. W. Recent Advances in C-O Bond Construction via C-H Activation. *Russ. J. Org. Chem.* **2019**, *55* (4), 569–586. https://doi.org/10.1134/S1070428019040249.

(1) Thirunavukkarasu, V. S.; Kozhushkov, S. I.; Ackermann, L. C-H Nitrogenation and Oxygenation by Ruthenium Catalysis. *Chem. Commun.* **2014**, *50* (1), 29–39. https://doi.org/10.1039/c3cc47028h.

(1) Park, Y.; Kim, Y.; Chang, S. Transition Metal-Catalysed C-H Amination: Scope, Mechanism, and Applications. *Chem. Rev.* **2017**, *117* (13), 9247–9301. https://doi.org/10.1021/acs.chemrev.6b00644.

(1) Kakiuchi, F.; Kochi, T.; Murai, S. Chelation-Assisted Regioselective Catalytic Functionalization of C-H, C-O, C-N and C-F Bonds. *Synlett* **2014**, *25* (17), 2390–2414. https://doi.org/10.1055/s-0034-1379210.

(1) Lin, A.; Huehls, C. B.; Yang, J. Recent Advances in C-H Fluorination. *Org. Chem. Front.* **2014**, *1* (4), 434–438. https://doi.org/10.1039/c4qo00020j.

(1) Ros, A.; Fernández, R.; Lassaletta, J. M. Functional Group Directed C-H Borylation. *Chem. Soc. Rev.* **2014**, *43* (10), 3229–3243. https://doi.org/10.1039/c3cs60418g.

(1) Xu, L.; Wang, G.; Zhang, S.; Wang, H.; Wang, L.; Liu, L.; Jiao, J.; Li, P. Recent Advances in Catalytic C−H Borylation Reactions. *Tetrahedron* **2017**, *73* (51), 7123–7157. https://doi.org/10.1016/j.tet.2017.11.005.

(1) Feng, C. G.; Ye, M.; Xiao, K. J.; Li, S.; Yu, J. Q. Pd(II)-Catalysed Phosphorylation of Aryl C-H Bonds. *J. Am. Chem. Soc.* **2013**, *135* (25), 9322–9325. https://doi.org/10.1021/ja404526x.

(2) Kao, I. H.; Wang, C. Y.; Chang, Y. C.; Wu, C. L.; Chiu, Y. J.; Hong, F. E. Palladium-Catalysed Phosphination and Amination through C–H Bond Functionalization on Biphenyl: Amido-Substituent as Directing Group. *Tetrahedron* **2019**, *75* (3), 387–397. https://doi.org/10.1016/j.tet.2018.12.007.

Reaction mechanisms in C-H activation

With all this plethora of reactions and conditions, including diverse metals at different oxidation states, affording C-H activation; diverse mechanisms are expected.

First, reactions can be classified into direct or directed (directing group assisted) C-H activation. In the latter case, the assistance by a directing group is essential as we have previously described. In contrast, direct C-H activation do not require the action of such groups. In addition to this classification, the activation of C-H bonds by metal complexes have been traditionally considered to occur via mainly 3 different mechanisms: 1) oxidative addition, 2) σ-bond metathesis and 3) electrophilic activation. Nevertheless, advances in this field have revealed that other mechanisms and interactions are also possible,[183,184,185] for instance, 1,2-addition, metalloradical reactions[186] or bases-assisted C-H activation.[187,188]

At any rate, most of the reactions seem to start with an agnostic-type interaction between the metal centre and the C-H bond to form a σ-complex.

Classical mechanism for C-H activation

Oxidative addition

From a classical point of view, the oxidative addition of a C-H is the usual mechanism for electron-rich, low-valent late transition metals such as Fe, Ru, Os, Rh, Ir and Pt. As the active metal centres must be coordinatively

---

[183] (1) Ackermann, L. Carboxylate-Assisted Transition-Metal-Catalysed C-H Bond Functionalizations: Mechanism and Scope. *Chem. Rev.* **2011**, *111* (3), 1315–1345. https://doi.org/10.1021/cr100412j.

[184] (1) Boutadla, Y.; Davies, D. L.; Macgregor, S. A.; Poblador-Bahamonde, A. I. Mechanisms of C–H Bond Activation: Rich Synergy between Computation and Experiment. *Dalt. Trans.* **2009**, No. 30, 5820. https://doi.org/10.1039/b904967c.

[185] (1) Ess, D. H.; Goddard, W. A.; Periana, R. A. Electrophilic, Ambiphilic, and Nucleophilic C-H Bond Activation: Understanding the Electronic Continuum of C-H Bond Activation through Transition-State and Reaction Pathway Interaction Energy Decompositions. *Organometallics* **2010**, *29* (23), 6459–6472. https://doi.org/10.1021/om100879y.

[186] (1) Labinger, J. A.; Bercaw, J. E. Understanding and Exploiting C–H Bond Activation. *Nature* **2002**, *417* (6888), 507–514. https://doi.org/10.1038/417507a.

[187] (1) Balcells, D.; Clot, E.; Eisenstein, O. C-H Bond Activation in Transition Metal Species from a Computational Perspective. *Chem. Rev.* **2010**, *110* (2), 749–823. https://doi.org/10.1021/cr900315k.

[188] (1) Lersch, M.; Tilset, M. Mechanistic Aspects of C-H Activation by Pt Complexes. *Chem. Rev.* **2005**, *105* (6), 2471–2526. https://doi.org/10.1021/cr030710y.

unsaturated, the activation of more stable metallic species is often required(Scheme 0-4).[154]

Scheme 0-4. C-H activation through oxidative addition

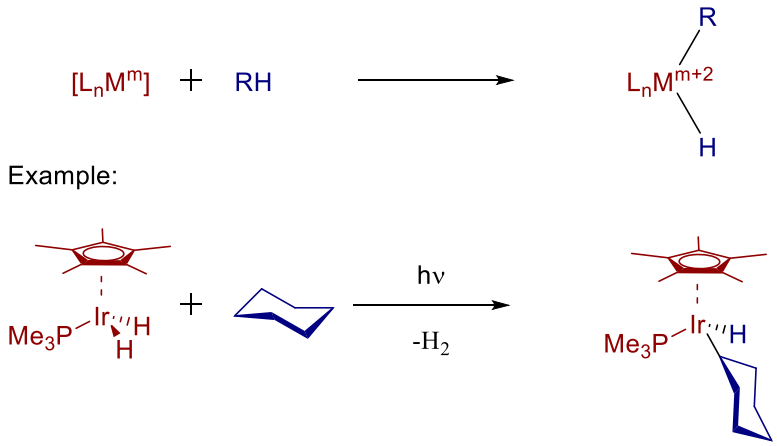

σ-bond metathesis

At the other extreme, σ-bond metathesis is usually the mechanism followed by early, electronically poor d^0 metal complexes. Hence, elements of groups 3 and 4 typically activate C-H bonds through this pathway. Thus, the reaction occurs with alkyl and hydride metal complexes that usually undergo reversible exchange of these ligands with the corresponding alkane. A classic example of alkane exchange can be observed in species of Lu and Y (Scheme 0-5).[189] However, the cross-coupling product through σ-bond metathesis reactions is not commonly observed.[154,190]

[189] (1) Watson, P. L. Methane Exchange Reactions of Lanthanide and Early-Transition-Metal Methyl Complexes. *J. Am. Chem. Soc.* **1983**, *105* (21), 6491–6493. https://doi.org/10.1021/ja00359a023.

[190] (1) Waterman, R. σ-Bond Metathesis: A 30-Year Retrospective. *Organometallics* **2013**, *32* (24), 7249–7263. https://doi.org/10.1021/om400760k.

Scheme 0-5. C-H activation through σ-bond metathesis

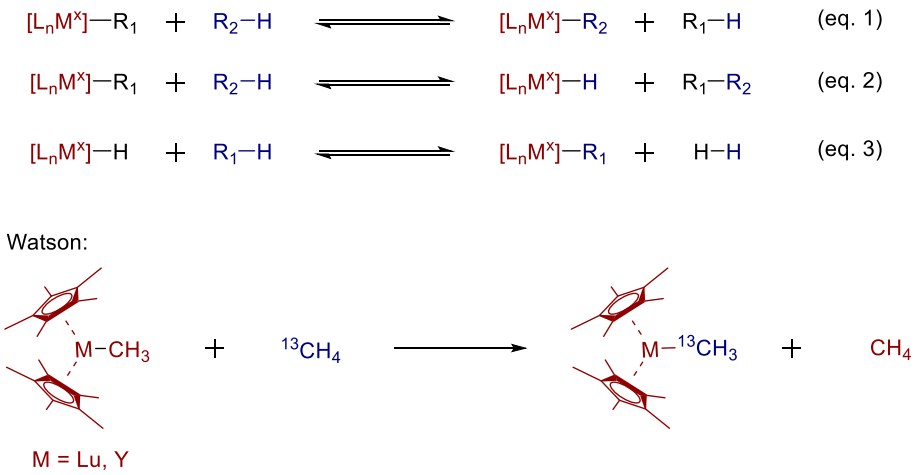

Electrophilic activation

The third main reaction mechanism for C-H activation relies on the electrophilic activation. Although the organometallic species presumably involved in this mechanism have not been isolated, however, experimental data support the existence of this pathway.[154] In this respect, late transition and p-block metals in strongly polar and acidic media are common catalysts for the electrophilic activation of C-H bonds. Examples of reactions following this mechanism are the above-mentioned mercuration[165] of benzene or the Fujiwara-Moritani[167,191] reaction.

[191] Fujiwara-Moritani reaction has traditionally seen to proceed through an electrophilic substitution mechanism; however, the assistance of OAc in the activation process has to be considered as we will see in the next section.

Scheme 0-6. C-H activation through electrophilic substitution.

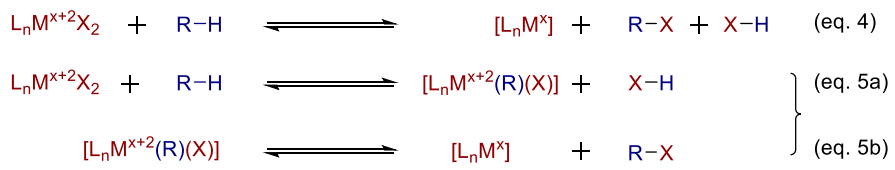

Mercuriation of benzene (ref 15):

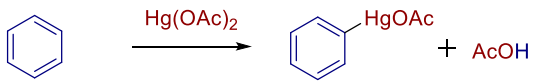

Fujiwara-Moritiani reaction (ref 17, 41):

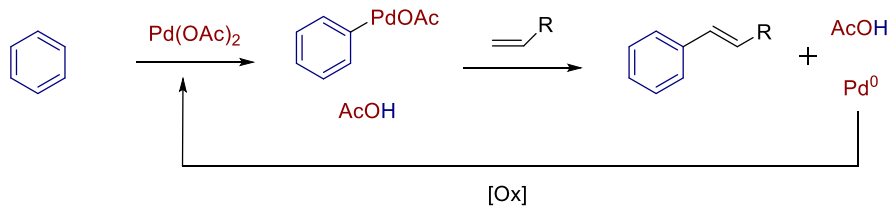

Non-classical mechanism in C-H activation

Although the aim of this section is not to exhaustively describe the whole new advances in the research of the underlying mechanism or the electronic continuum of C-H activations,[185] and some of these pathways have been mentioned before, we would like to shortly describe one of them as it has become a common mechanism in certain synthetic protocols.

Base-assisted deprotonation mechanism

In most instances, ligands tune the activity and/or selectivity of the metal centres. However, in some cases of C-H activation, the ligand might be directly involved in the metalation process. This way, a Lewis-basic atom in the ligand may interact with H atom in different ways during the transition state (Scheme 0-7). Thus, these kind of interactions can be seen at least formally as 1,2-additions or as electrophilic activation.[183,160,184,187]

Scheme 0-7. Base-assisted C-H activation.

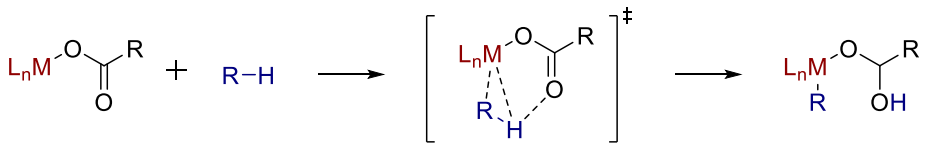

Stereoselectivity in C-H functionalisations.

By virtue of the continued expansion of C-H strategies, asymmetric methodologies[192,193] in this field have also evolved. This way, in order to achieve stereocontrol of the reactions, approaches including diastereo-,[194] enantio- and even atroposelective[195] transformations have been explored; particularly with the advent of C(sp3)-H functionalization.

As a consequence, the successful development of this subject and the number of reactions based on C-H strategies have garnered the attention for the synthesis of complex molecules such as natural products and pharmaceuticals. In this context, the advantage of C-H functionalization does not only rely on the fact that simple C-H bonds are transformed into other groups, but on a revision of the (retro)synthetic strategies and analysis which opens up new perspectives.[196]

---

[192] (1) Saint-Denis, T. G.; Zhu, R.-Y.; Chen, G.; Wu, Q.-F.; Yu, J.-Q. Enantioselective C(Sp 3)–H Bond Activation by Chiral Transition Metal Catalysts. *Science (80-.).* **2018**, *359* (6377), eaao4798. https://doi.org/10.1126/science.aao4798.

(1) Newton, C. G.; Wang, S. G.; Oliveira, C. C.; Cramer, N. Catalytic Enantioselective Transformations Involving C-H Bond Cleavage by Transition-Metal Complexes. *Chem. Rev.* **2017**, *117* (13), 8908–8976. https://doi.org/10.1021/acs.chemrev.6b00692.

(2) Woźniak, Ł.; Cramer, N. Enantioselective C H Bond Functionalizations by 3d Transition-Metal Catalysts. *Trends Chem.* **2019**, *1* (5), 471–484. https://doi.org/10.1016/j.trechm.2019.03.013.

(3) Loup, J.; Dhawa, U.; Pesciaioli, F.; Wencel-Delord, J.; Ackermann, L. Enantioselective C−H Activation with Earth-Abundant 3d Transition Metals. *Angew. Chemie Int. Ed.* **2019**, *58* (37), 12803–12818. https://doi.org/10.1002/anie.201904214.

[193] (1) Woźniak, Ł.; Cramer, N. Enantioselective C H Bond Functionalizations by 3d Transition-Metal Catalysts. *Trends Chem.* **2019**, *1* (5), 471–484. https://doi.org/10.1016/j.trechm.2019.03.013.

[194] (1) Herrmann, P.; Bach, T. Diastereotopos-Differentiating C-H Activation Reactions at Methylene Groups. *Chem. Soc. Rev.* **2011**, *40* (4), 2022–2038. https://doi.org/10.1039/c0cs00027b.

[195] (1) Murai, S.; Ohtaki, H.; Yamada, A.; Le Gendre, P.; Kakiuchi, F. Atropselective Alkylation of Biaryl Compounds by Means of Transition Metal-Catalysed C–H/Olefin Coupling. *Tetrahedron: Asymmetry* **2000**, *11* (13), 2647–2651. https://doi.org/10.1016/s0957-4166(00)00244-5.

[196] (1) Yamaguchi, J.; Yamaguchi, A. D.; Itami, K. C-H Bond Functionalization: Emerging Synthetic Tools for Natural Products and Pharmaceuticals. *Angew. Chemie - Int. Ed.* **2012**, *51* (36), 8960–9009. https://doi.org/10.1002/anie.201201666.

(1) Gutekunst, W. R.; Baran, P. S. C–H Functionalization Logic in Total Synthesis. *Chem. Soc. Rev.* **2011**, *40* (4), 1976–1991. https://doi.org/10.1039/c0cs00189a.

In addition, the use of mild conditions,[197] functional group tolerance and their use as directing groups comprise very appealing benefits to introduce different functionalities into complex molecules (late stage functionalization[198]), accessing new libraries of compounds (Scheme 0-8. Late stage functionalisation for the synthesis of celecoxib analogues.Scheme 0-8).[198a]

(1) McMurray, L.; O'Hara, F.; Gaunt, M. J. Recent Developments in Natural Product Synthesis Using Metal-Catalysed C-H Bond Functionalisation. *Chem. Soc. Rev.* **2011**, *40* (4), 1885–1898. https://doi.org/10.1039/c1cs15013h.

[197] (1) Wencel-Delord, J.; Dröge, T.; Liu, F.; Glorius, F. Towards Mild Metal-Catalysed C-H Bond Activation. *Chem. Soc. Rev.* **2011**, *40* (9), 4740–4761. https://doi.org/10.1039/c1cs150810A.

[198] (A) Dai, H. X.; Stepan, A. F.; Plummer, M. S.; Zhang, Y. H.; Yu, J. Q. Divergent C-H Functionalizations Directed by Sulfonamide Pharmacophores: Late-Stage Diversification as a Tool for Drug Discovery. *J. Am. Chem. Soc.* **2011**, *133* (18), 7222–7228. https://doi.org/10.1021/ja201708f.

(1) Cernak, T.; Dykstra, K. D.; Tyagarajan, S.; Vachal, P.; Krska, S. W. The Medicinal Chemist's Toolbox for Late Stage Functionalization of Drug-like Molecules. *Chem. Soc. Rev.* **2016**, *45* (3), 546–576. https://doi.org/10.1039/c5cs00628g.

(2) Abrams, D. J.; Provencher, P. A.; Sorensen, E. J. Recent Applications of C-H Functionalization in Complex Natural Product Synthesis. *Chem. Soc. Rev.* **2018**, *47* (23), 8925–8967. https://doi.org/10.1039/c8cs00716k.

Scheme 0-8. Late stage functionalisation for the synthesis of celecoxib analogues.

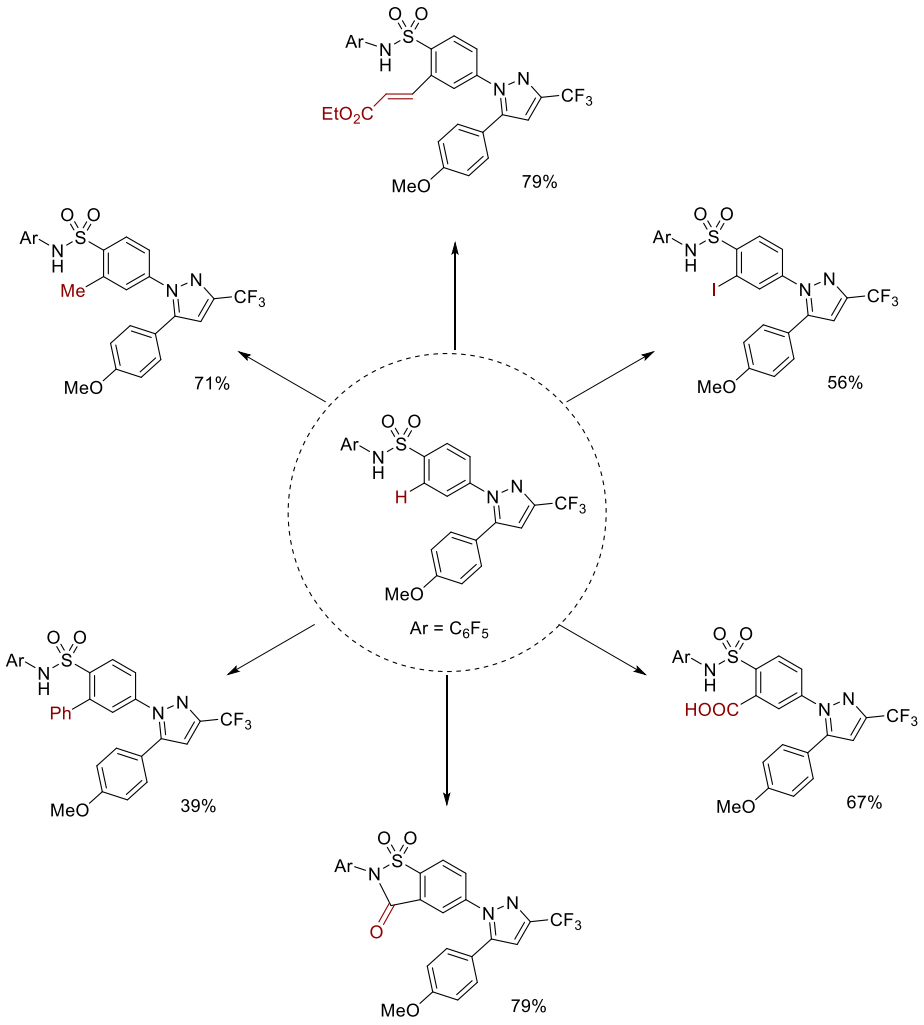

Thus, all these attractive features related to C-H activation together with the rather small number of reports in which this approach has been applied to the asymmetric synthesis of heterobiaryls, drew our attention.

Background: Asymmetric synthesis of (hetero)biaryls through C-H activation strategies.

The application of C-H functionalisations to asymmetric protocols is not only confined to point chirality as we have previously mentioned. Along the evolution of this synthetic tool, enantioselective and deracemisation-desymmetrisation-based methods for the synthesis of axially[199] and planar chiral[200] compounds have also arisen.

In this connection, the enantioselective synthesis of biaryls is known for a quite a long time. For instance, chiral BINOL and BINOL derivatives have been prepared *via* phenolic oxidative coupling using Cu(II) and a chiral auxiliary since 1978 by Feringa and Wynberg[201] while the first catalytic version was later uncovered by Kočovský.[202]

---

[199] Methods for the synthesis of axially chiral (hetero)biaryls will be next discussed.

[200] Selected examples and reviews:

(1) Cai, Z. J.; Liu, C. X.; Wang, Q.; Gu, Q.; You, S. L. Thioketone-Directed Rhodium(I) Catalysed Enantioselective C-H Bond Arylation of Ferrocenes. *Nat. Commun.* **2019**, *10* (1), 4168. https://doi.org/10.1038/s41467-019-12181-x.

(1) Pi, C.; Li, Y.; Cui, X.; Zhang, H.; Han, Y.; Wu, Y. Redox of Ferrocene Controlled Asymmetric Dehydrogenative Heck Reaction via Palladium-Catalysed Dual C-H Bond Activation. *Chem. Sci.* **2013**, *4* (6), 2675–2679. https://doi.org/10.1039/c3sc50577d.

(1) Pi, C.; Cui, X.; Liu, X.; Guo, M.; Zhang, H.; Wu, Y. Synthesis of Ferrocene Derivatives with Planar Chirality via Palladium-Catalysed Enantioselective C-H Bond Activation. *Org. Lett.* **2014**, *16* (19), 5164–5167. https://doi.org/10.1021/ol502509f.

(2) Zhu, D. Y.; Chen, P.; Xia, J. B. Synthesis of Planar Chiral Ferrocenes by Transition-Metal-Catalysed Enantioselective C-H Activation. *ChemCatChem* **2016**, *8* (1), 68–73. https://doi.org/10.1002/cctc.201500895.

(1) Pi, C.; Cui, X.; Liu, X.; Guo, M.; Zhang, H.; Wu, Y. Synthesis of Ferrocene Derivatives with Planar Chirality via Palladium-Catalysed Enantioselective C-H Bond Activation. *Org. Lett.* **2014**, *16* (19), 5164–5167. https://doi.org/10.1021/ol502509f.

(2) D.-W. Gao, Y. Gu, S.-B. Wang, Q. Gu, S.-L. You, Pd-catalysed highly enantioselective synthesis of planar chiral ferrocenylpyridine derivatives. Organometallics 35, 3227–3233 (2016). doi: 10.1021/acs.organomet.6b00569

[201] (1) Feringa, B.; Wynberg, H. Biomimetic Asymmetric Oxidative Coupling of Phenols. *Bioorg. Chem.* **1978**, *7* (4), 397–408. https://doi.org/10.1016/0045-2068(78)90031-7.

(2) Brunel, J. M. BINOL: A Versatile Chiral Reagent. *Chem. Rev.* **2005**, *105* (3), 857–898. https://doi.org/10.1021/cr040079g.

[202] (1) Smrčina, M.; Poláková, J.; Vyskočil, Š.; Kočovský, P. Synthesis of Enantiomerically Pure Binaphthyl Derivatives. Mechanism of the Enantioselective, Oxidative Coupling of Naphthols and Designing a Catalytic Cycle. *J. Org. Chem.* **1993**, *58* (17), 4534–4538. https://doi.org/10.1021/jo00069a010.

These reactions can be formally viewed as C-H activations, however, the underlying mechanism proceeds through the generation of radicals and abstraction of H. Thereby, they cannot be considered true C-H functionalisations.

Indeed, the application of C-H activation tools for the synthesis of heterobiaryls took longer time to be uncovered. Once the spurt in C-H functionalization had started, it was Murai and his group who first reported this class of atroposelective synthesis (Scheme 0-9).[203] Smartly, the basis of this seminal reaction is the 2-(naphthalen-1-yl)-3-picoline system in which the heterocycle behaved an *ortho* directing group, i.e. toward 2' position. The subsequent hydroarylation of the olefin blocks such position, preventing the rotation around the axis. In this vein, the use of a chiral catalyst delivers the axial chirality.

Despite this hydroarylation of ethylene gave a poor yield and moderate enantioselectivity (37%, 49% ee), the significance of this desymmetrisation on the conceptual level has had a huge impact on subsequent investigations.

Scheme 0-9. C-H Desymmetrisation strategy for the atroposelective synthesis of naphthylpicoline.

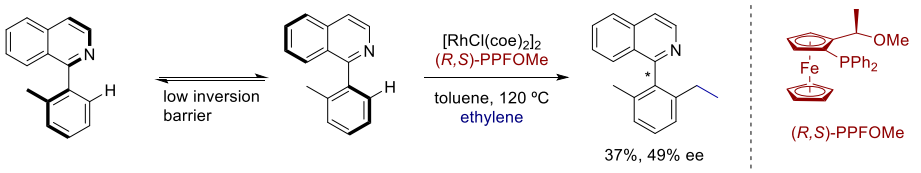

Synthesis of axially chiral biaryls via C-H activation.

Murai's application of C-H hydroarylation as a strategy for the desymmetrisation of 2-(naphthalen-1-yl)-3-picoline marked the beginning of the popularisation of this approach in the realm of asymmetric synthesis of (hetero)biaryls. In this regard, methodologies leading to the synthesis of axially chiral biaryls is by far more profuse than those leading to heterobiaryls. Despite this is not the aim of this chapter, however, we consider highlighting some remarkable cases may serve as a connection to heterobiaryls and as a contextualization of these approaches.

[203] (1) Murai, S.; Ohtaki, H.; Yamada, A.; Le Gendre, P.; Kakiuchi, F. Atropselective Alkylation of Biaryl Compounds by Means of Transition Metal-Catalysed C–H/Olefin Coupling. *Tetrahedron: Asymmetry* **2000**, *11* (13), 2647–2651. https://doi.org/10.1016/s0957-4166(00)00244-5.

As we have previously described in the introductory chapter, two groups of tactics aim to the synthesis of axially chiral (hetero)biaryls:

- Scenario I: Construction of the (hetero)biaryl scaffold
- Scenario II: Further functionalisation of previously assembled (hetero)biaryls.

Owing to the aforementioned direct-bond formation issues and the plethora of reactions accomplishing *ortho*-directed functionalisation C-H, Scenario II is more widely employed.

Synthesis of axially chiral biaryls via desymmetrisation and deracemisation techniques

The group of Colobert, with a longstanding interest in the synthesis of axially chiral biaryls,[204] was one of the first groups pioneering the application of *ortho*-directed C-H functionalization in such a purpose.

Drawn by the works of Murai[203] and Yamaguchi,[219,220] they embarked on the development of a diastereoselective C-H methodology for the synthesis of axially chiral biaryls. Prompted by her previous finding on the sulfinyl group as a chiral auxiliary in a Suzuki-Miyaura diastereoselective methodology,[204] they envisioned these directing groups could also act as an *ortho* directing group in a C-H functionalization but as a diastereoselective inductor.[205]

By means of this directing group, 2-*p*-tolylsulfinylbiphenyls could be alkenylated with methyl acrylate under the action of $Pd(OAc)_2$ and AgOAc as the catalyst and the oxidant respectively. This Fujiwara-Moritani reaction afforded the corresponding products with good to moderate diastereoselectivities up to 1:50 (Scheme 0-10).

[204] (1) Colobert, F.; Valdivia, V.; Choppin, S.; Leroux, F. R.; Fernández, I.; Álvarez, E.; Khiar, N. Axial Chirality Control during Suzuki-Miyaura Cross-Coupling Reactions: The Tert-Butylsulfinyl Group as an Efficient Chiral Auxiliary. *Org. Lett.* **2009**, *11* (22), 5130–5133. https://doi.org/10.1021/ol9020755.

[205] (1) Wesch, T.; Leroux, F. R.; Colobert, F. Atropodiastereoselective C-H Olefination of Biphenyl p-Tolyl Sulfoxides with Acrylates. *Adv. Synth. Catal.* **2013**, *355* (11–12), 2139–2144. https://doi.org/10.1002/adsc.201300446.

Subsequently, they decided to extend this protocol to the Pd(II)-catalysed acetoxylation and iodination of biaryls by using the same chiral sulfinyl group as directing group(Scheme 0-10).[206,207]

[206] (1) Hazra, C. K.; Dherbassy, Q.; Wencel-Delord, J.; Colobert, F. Synthesis of Axially Chiral Biaryls through Sulfoxide-Directed Asymmetric Mild C-H Activation and Dynamic Kinetic Resolution. *Angew. Chemie - Int. Ed.* **2014**, *53* (50), 13871–13875. https://doi.org/10.1002/anie.2 01407865.

[207] Reviews: (1) Wencel-Delord, J.; Panossian, A.; Leroux, F. R.; Colobert, F. Recent Advances and New Concepts for the Synthesis of Axially Stereoenriched Biaryls. *Chem. Soc. Rev.* **2015**, *44* (11), 3418–3430. https://doi.org/10.1039/c5cs00012b.

(1) Wencel-Delord, J.; Colobert, F. Stereoselective Metal-Catalysed C-C Bond Coupling Reactions by Stereoconvergence, Dynamic Kinetic Asymmetric Transformation, or Dynamic Kinetic Resolution. *Synthesis* **2016**, *48* (18), 2981–2996. https://doi.org/10.1055/s-0035-1562512.

Scheme 0-10. Colobert's atroposelecive synthesis of biphenyl p-tolyl sulfoxides

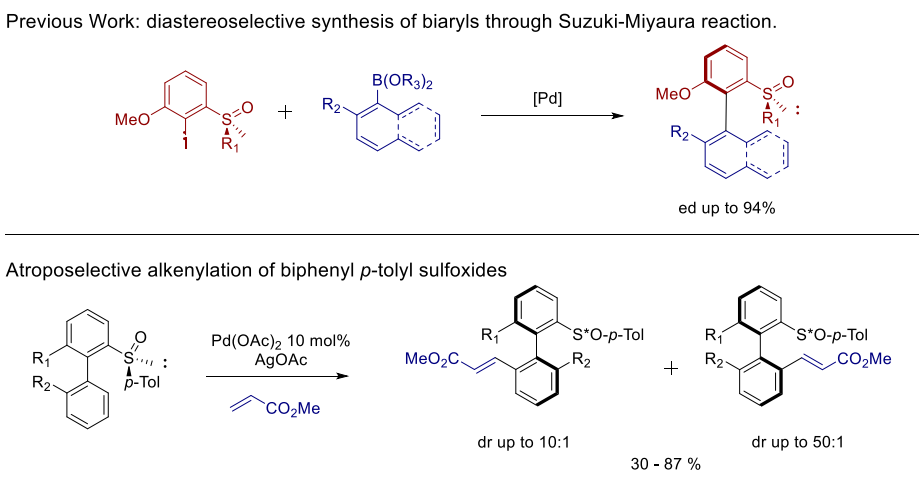

Relying on a similar idea, Yang used (*S*)-menthyl phosphinates[208] as directing groups in the diastereoselective alkenylation, acetoxylation and other transformations of biaryls, obtaining the corresponding axially chiral

[208] (1) Ma, Y. N.; Zhang, H. Y.; Yang, S. D. Pd(II)-Catalysed P(O)R^1R^2-Directed Asymmetric C-H Activation and Dynamic Kinetic Resolution for the Synthesis of Chiral Biaryl Phosphates. *Org. Lett.* **2015**, *17* (8), 2034–2037. https://doi.org/10.1021/acs.orglett.5b00844.

compounds in moderate to good yields and excellent diastereoselectivities (Scheme 0-11). Subsequently, the replacement of phosphinate moiety for a phosphine oxide as the directing group, and the use of mono protected amino acids (MPAA)[209] as ligands, led to an effective method for the asymmetric catalytic alkenylation of biaryls (Scheme 0-11). [210]

Scheme 0-11. Asymmetric synthesis of phosphinates and phosphine oxide biaryls.

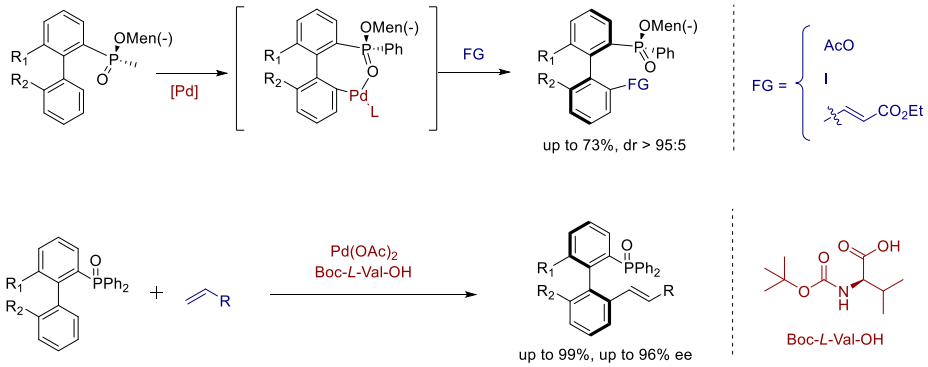

On the other hand, the group Bing-Feng Shi gave a twist to the concept of *ortho*-directed functionalisation of atropisomers employing transient chiral auxiliaries. Chiral amino acids are suitable auxiliaries for such a purpose, and indeed, Shi and co-workers used them to develop a Fujiwara-Moritani-type reaction affording chiral biaryls (Scheme 0-12).[211] Relying on the same

[209] (1) Engle, K. M.; Wang, D. H.; Yu, J. Q. Ligand-Accelerated C-H Activation Reactions: Evidence for a Switch of Mechanism. *J. Am. Chem. Soc.* **2010**, *132* (40), 14137–14151. https://doi.org/10.1021/ja105044s.

[210] (1) Li, S. X.; Ma, Y. N.; Yang, S. D. P(O)R2-Directed Enantioselective C-H Olefination toward Chiral Atropoisomeric Phosphine-Olefin Compounds. *Org. Lett.* **2017**, *19* (7), 1842–1845. https://doi.org/10.1021/acs.orglett.7b00608.

[211] (1) Yao, Q. J.; Zhang, S.; Zhan, B. B.; Shi, B. F. Atroposelective Synthesis of Axially Chiral Biaryls by Palladium-Catalysed Asymmetric C–H Olefination Enabled by a Transient Chiral Auxiliary. *Angew. Chemie - Int. Ed.* **2017**, *56* (23), 6617–6621. https://doi.org/10.1002/anie.201701849.

concept, the corresponding alkynylation (Scheme 0-12) and allylation reaction (Scheme 0-12)[212] were subsequently reported by the same group.[213]

[212] (1) Liao, G.; Li, B.; Chen, H. M.; Yao, Q. J.; Xia, Y. N.; Luo, J.; Shi, B. F. Pd-Catalysed Atroposelective C−H Allylation through β-O Elimination: Diverse Synthesis of Axially Chiral Biaryls. *Angew. Chemie - Int. Ed.* **2018**, *57* (52), 17151–17155. https://doi.org/10.1002/anie.201811256.

[213] (1) Liao, G.; Yao, Q. J.; Zhang, Z. Z.; Wu, Y. J.; Huang, D. Y.; Shi, B. F. Scalable, Stereocontrolled Formal Syntheses of (+)-Isoschizandrin and (+)-Steganone: Development and Applications of Palladium(II)-Catalysed Atroposelective C−H Alkynylation. *Angew. Chemie - Int. Ed.* **2018**, *57* (14), 3661–3665. https://doi.org/10.1002/anie.201713106.

Scheme 0-12. Ortho functionalisation of biaryl ketones through transcient chiral auxiliaries.

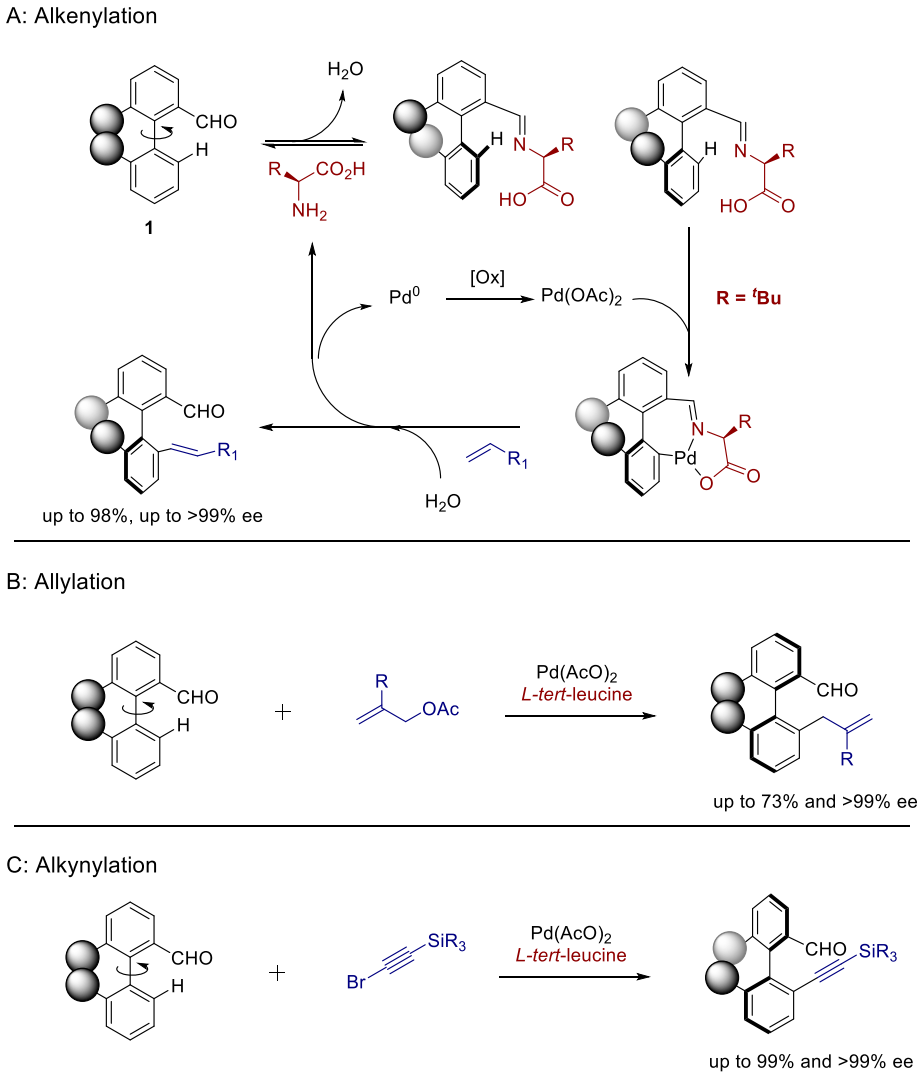

Synthesis of axially chiral biaryls through direct formation of the axis.

Despite the fact of being a less popular approach for the synthesis of biaryls, approaches involving the direct formation of axis have appeared in the literature providing interesting routes to this type of compounds. For these reasons, we would like to remark some of these works.

For instance, Cramer et al.[214] reported a desymmetrisation of phosphine oxides as an enantio- and diastereoselective method for the synthesis of biaryls using an Ir/chiral cyclpentadienyl[215] catalyst. Thus, after the *ortho* C-H activation in a phenyl group, the subsequent trapping of the diazo compound and insertion into the Ir-C ends up in the formation of the chiral axis (Scheme 0-13).

Scheme 0-13. Biaryls with axial and P-chirality through Cp^{x}Ir(III)-catalysed arylations.

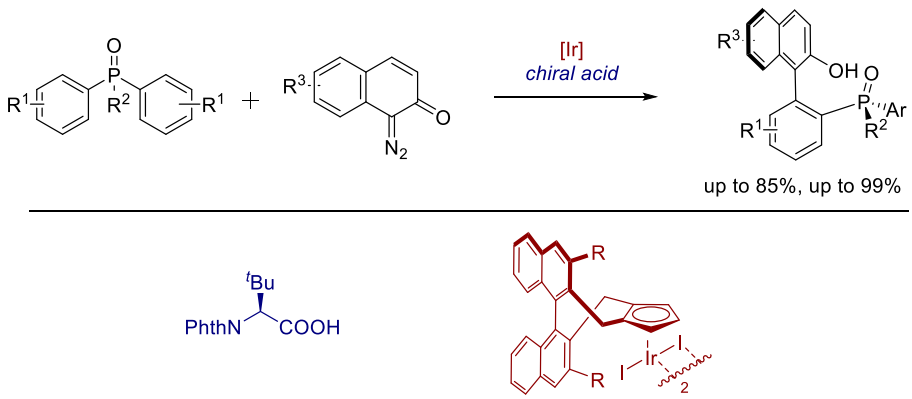

Other similar approaches were carried out by Antonchick and Waldmann,[216] who also develop an asymmetric C-H method by generating one of the rings in the biaryl moiety.[217]

[214] (1) Jang, Y. S.; Woźniak, Ł.; Pedroni, J.; Cramer, N. Access to P- and Axially Chiral Biaryl Phosphine Oxides by Enantioselective CpxIrIII-Catalysed C−H Arylations. *Angew. Chemie - Int. Ed.* **2018**, *57* (39), 12901–12905. https://doi.org/10.1002/anie.201807749.

[215] (1) Ye, B.; Cramer, N. Chiral Cyclopentadienyl Ligands as Stereocontrolling Element in Asymmetric C-H Functionalization. *Science (80-.).* **2012**, *338* (6106), 504–506. https://doi.org/10.1126/science.1226938.

(1) Ye, B.; Cramer, N. Chiral Cyclopentadienyls: Enabling Ligands for Asymmetric Rh(III)-Catalysed C-H Functionalizations. *Acc. Chem. Res.* **2015**, *48* (5), 1308–1318. https://doi.org/10.1021/acs.accounts.5b00092.

[216] (1) Jia, Z. J.; Merten, C.; Gontla, R.; Daniliuc, C. G.; Antonchick, A. P.; Waldmann, H. General Enantioselective C−H Activation with Efficiently Tunable Cyclopentadienyl Ligands. *Angew. Chemie - Int. Ed.* **2017**, *56* (9), 2429–2434. https://doi.org/10.1002/anie.201611981.

[217] (1) Shan, G.; Flegel, J.; Li, H.; Merten, C.; Ziegler, S.; Antonchick, A. P.; Waldmann, H. C−H Bond Activation for the Synthesis of Heterocyclic Atropisomers Yields Hedgehog Pathway Inhibitors. *Angew. Chemie - Int. Ed.* **2018**, *57* (43), 14250–14254. https://doi.org/10.1002/anie.201809680.

Finally, and as a point of interest, Cramer also developed a non-directed C-H cyclisation for the synthesis of axially chiral dibenzazepinones through the direct formation of the axis.[218]

Scheme 0-14. Atroposelective synthesis of dibenzazepinones by a Pd(0)-catalysed C-H arylation.

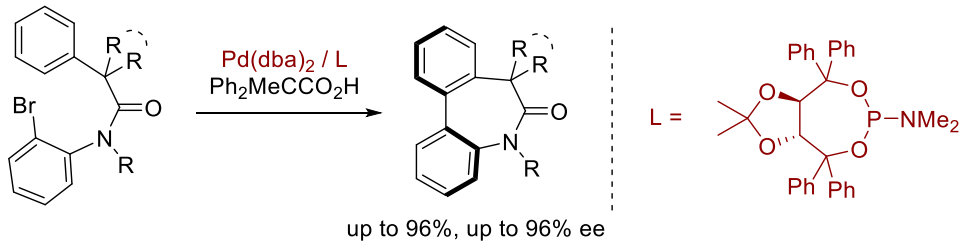

Synthesis of axially chiral heterobiaryls via C-H activation.

As we have seen in the previous section, Murai's seminal work on the C-H desymmetrisation of the naphthylpicoline (isoquinoline)[203] system represented a milestone in the synthesis of axially chiral heterobiaryls from the conceptual point of view. Since then, many reports on the development of asymmetric methodologies for the preparation of chiral all-carbon biaryls have come to fruition.

By contrast, the application of C-H activation strategies to the synthesis of axially chiral heterobiaryls has remained rather scarce, presumably owing to the lower configurational stability of these scaffolds if compared to their biaryl counterparts.

In this respect, we would like to outline the progress and different approaches that have been made over the subsequent years.

Synthesis of axially chiral heterobiaryls through direct formation of the axis.

After 12 years with no advancements in this field, Yamaguchi, Itami and co-workers reported the synthesis of tiophene-based heterobiaryls through a palladium-catalysed coupling (Scheme 0-15).[219] This methodology achieved

[218] (1) Newton, C. G.; Braconi, E.; Kuziola, J.; Wodrich, M. D.; Cramer, N. Axially Chiral Dibenzazepinones by a Palladium(0)-Catalysed Atropo-Enantioselective C–H Arylation. *Angew. Chemie* **2018**, *130* (34), 11206–11210. https://doi.org/10.1002/ange.201806527.

[219] (1) Yamaguchi, K.; Yamaguchi, J.; Studer, A.; Itami, K. Hindered Biaryls by C-H Coupling: Bisoxazoline-Pd Catalysis Leading to Enantioselective C-H Coupling. *Chem. Sci.* **2012**, *3* (6), 2165–2169. https://doi.org/10.1039/c2sc20277h.

the corresponding heterobiaryls with complete β-selectivity and it could be also applied to the synthesis of tetra-*ortho*-substituted heterobiaryls. Nevertheless, the most interesting fact from this procedure relies on the demonstration that asymmetric heterobiaryl coupling based on a C-H activation is possible, comprising the first and only example so far. Despite the significance of this achievement as a proof of concept, however, the best ee value was merely 72% at the expense of a low yield (27%).

This group also developed a similar methodology combining two catalytic systems based on Pd(II)/sulfoxide-oxazoline (sox) and Fe/phthalocyanine (FePc); and taking advantage of aerobic oxidation (Scheme 0-15).[220] Regarding the chiral version of the methodology, however, the selectivity remained moderate and the naphthyl thiophene was obtained with a lower optical purity although the yield was improved.

At all events, these results open the door to improve C-H protocols in the challenging field of asymmetric heterobiaryl synthesis through cross-coupling reactions, which still comprises a major methodology gap.

[220] (1) Yamaguchi, K.; Kondo, H.; Yamaguchi, J.; Itami, K. Aromatic C-H Coupling with Hindered Arylboronic Acids by Pd/Fe Dual Catalysts. *Chem. Sci.* **2013**, *4* (9), 3753–3757. https://doi.org/10.1039/c3sc51206a.

Scheme 0-15. Assymmetric C-H cross-coupling for the synthesis of tiophene-based heterobiaryls

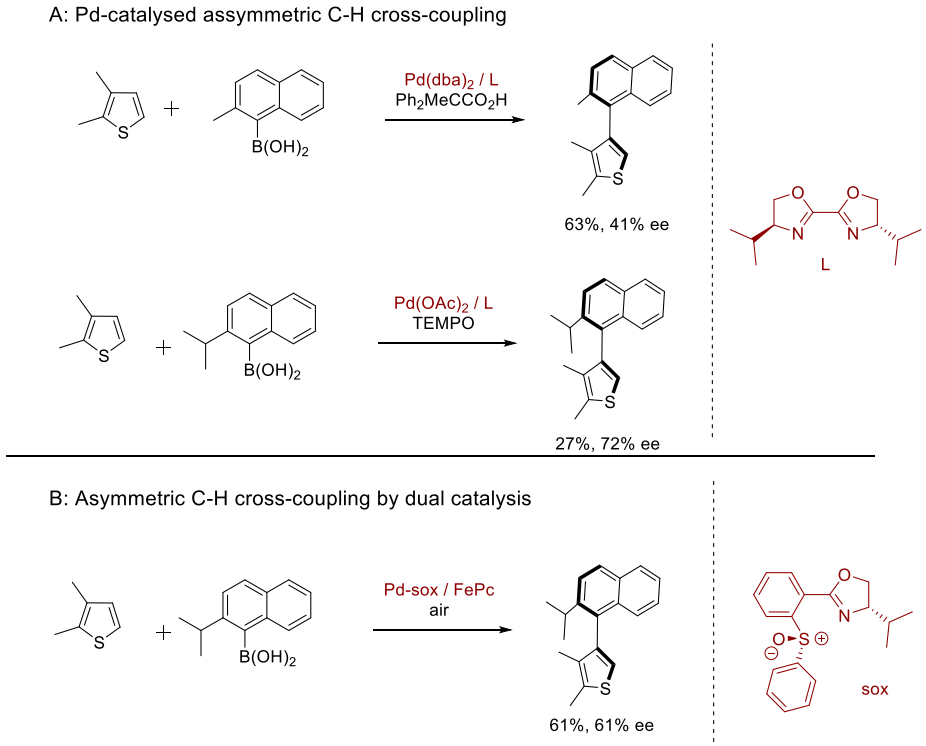

Synthesis of axially chiral heterobiaryls via desymmetrisation techniques

In the same way as all-carbon biaryls, the combination of deracemisation and desymmetrisation approaches with C-H functionalisation are more widely used since the difficulties which may arise from heterobiaryls cross-coupling reactions are avoided. Notwithstanding, the application of these techniques and, therefore, the synthesis of this class of scaffolds is not as prolific as for biaryls.

In this context, the group of You was pioneering in this field. Inspired by the works of Yu[221] and Wang[222] on the use of mono protected amino acids as chiral ligands for C-O and C-I bond forming reactions; they introduced a kinetic

[221] (1) Chu, L.; Wang, X. C.; Moore, C. E.; Rheingold, A. L.; Yu, J. Q. Pd-Catalysed Enantioselective C-H Iodination: Asymmetric Synthesis of Chiral Diarylmethylamines. *J. Am. Chem. Soc.* **2013**, *135* (44), 16344–16347. https://doi.org/10.1021/ja408864c.

[222] (1) Cheng, X. F.; Li, Y.; Su, Y. M.; Yin, F.; Wang, J. Y.; Sheng, J.; Vora, H. U.; Wang, X. S.; Yu, J. Q. Pd(II)-Catalysed Enantioselective C-H Activation/C-O Bond Formation: Synthesis of Chiral Benzofuranones. *J. Am. Chem. Soc.* **2013**, *135* (4), 1236–1239. https://doi.org/10.1021/ja311259x.

resolution of 2-napthyl-1-isoquinoline *N*-oxides *via* C-H iodination (Scheme 0-16).[223]

This palladium-catalysed reaction is thought to proceed through a Pd(II)/Pd(IV) cycle, while the C-H activation seems to take place through a concerted-metalation-deprotonation process (CMD), i.e., a base-assisted deprotonation mechanism.[183,184]

To demonstrate the potential application of these products, naphthylisoquinoline iodide naphthyl isoquinoline *N*-oxide was subjected to a Suzuki-Miyaura reaction with phenylboronic acid and the corresponding *N*-oxide was subsequently utilized as an organocatalyst for the asymmetric allylation of benzaldehyde. (Scheme 0-16).

Scheme 0-16. KR of Naphthylisoquinoline N-oxides

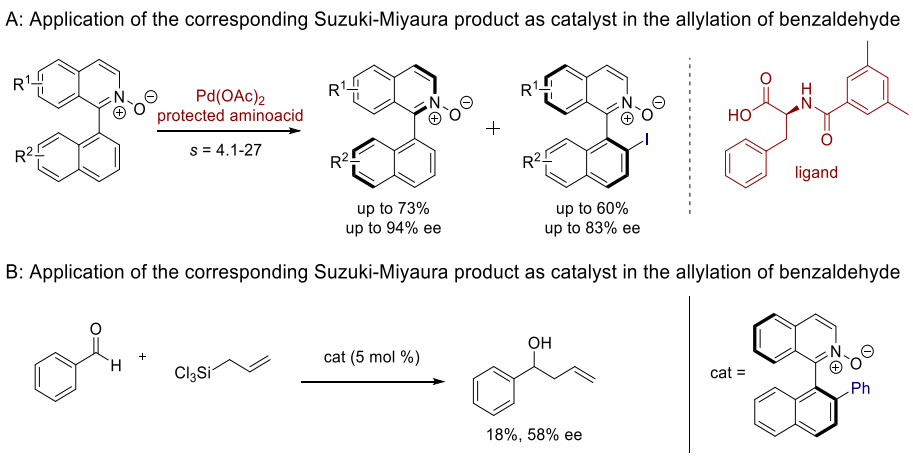

Despite the value of these products as coupling partners, the main limitation of this procedure is ascribed to those of a kinetic resolution. In other words, the yield of the reaction is limited to 50% yield although the remaining starting material is parallelly enantioenriched and can be recovered.

The reason why a KR process takes place could be explained by the formation of a 6-membered ring palladacycle where the widening of the angles do not destabilize the axis enough so that the sterically encumbered heterobiaryls undergo a racemisation process prior to iodination.

[223] (1) Gao, D. W.; Gu, Q.; You, S. L. Pd(II)-Catalysed Intermolecular Direct C-H Bond Iodination: An Efficient Approach toward the Synthesis of Axially Chiral Compounds via Kinetic Resolution. *ACS Catal.* **2014**, *4* (8), 2741–2745. https://doi.org/10.1021/cs500813z.

Scheme 0-17. Putative intermediate of C-H iodination of naphthyl isoquinoline N-oxides and oxidative addition intermediate in DYKAT processes.

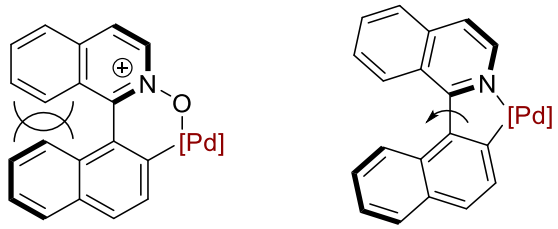

Nevertheless, the limitations of kinetic resolution of naphthylisoquinoline-like substrates was subsequently overcome by the same group through the development of other strategies which will be discussed hereunder.

Based on Cramer catalysts,[224] a family of chiral cyclopentadienyl-based catalysts which have emerged as a powerful tool in the context of asymmetric C-H functionalisation, an atroposelective alkenylation of these systems was developed.[225] Thus, this Rh(I)-catalysed transformation is based on an oxidative coupling between the heterobiaryls and the alkene (Scheme 0-18). That is to say, the transformation can be seen as a Fujiwara-Moritani or a dehydrogenative Heck reaction. As an application of this methodology, some of the new products were tested as N/olefin ligands in a Rh-catalysed conjugate addition of phenylboronic acid to cyclohexanone.

In line with this work, You and co-workers developed a Cramer-type cyclopentadienyl ligand in which the chiral naphthalene unit was substituted by a 1,1'-spirobiindane skeleton (SCp).[226] The use of this ligand in the Rh(I)-catalysed alkenylation resulted in a better chiral environment and therefore, better enantioselectivities were obtained. Thus, while Cramer catalyst afforded ee values around 80%, this new catalytic system gave rise to

[224] (1) Ye, B.; Cramer, N. Chiral Cyclopentadienyl Ligands as Stereocontrolling Element in Asymmetric C-H Functionalization. *Science (80-.).* **2012**, *338* (6106), 504–506. https://doi.org/10.1126/science.1226938.

[225] (1) Zheng, J.; You, S. L. Construction of Axial Chirality by Rhodium-Catalysed Asymmetric Dehydrogenative Heck Coupling of Biaryl Compounds with Alkenes. *Angew. Chemie - Int. Ed.* **2014**, *53* (48), 13244–13247. https://doi.org/10.1002/anie.201408805.

[226] (1) Zheng, J.; Cui, W. J.; Zheng, C.; You, S. L. Synthesis and Application of Chiral Spiro Cp Ligands in Rhodium-Catalysed Asymmetric Oxidative Coupling of Biaryl Compounds with Alkenes. *J. Am. Chem. Soc.* **2016**, *138* (16), 5242–5245. https://doi.org/10.1021/jacs.6b02302.

enantiomeric excesses around 90%. Furthermore, the activity of the catalyst was also enhanced in such a way that the reaction could be optimised at room temperature (Scheme 0-18).

Scheme 0-18. Rh-catalysed Atroposelective alkenylation of naphthyl benzo[h]isoquinolines

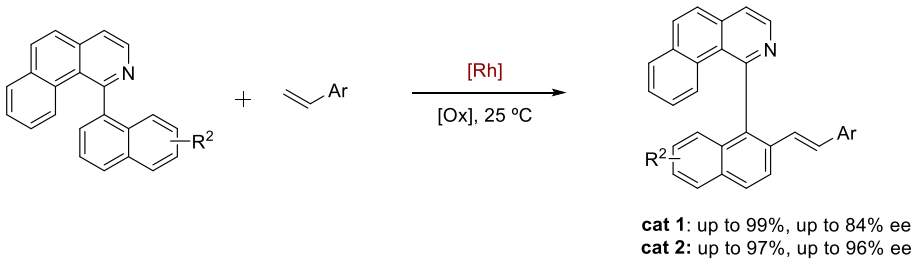

Drawing inspiration from the pioneering Dynamic Kinetic Asymmetric Suzuki-Miyaura previously reported by our group,[227] and the use of a Rh(I)/TADDOL-phosphonite system for the directed arylation of tetrahydroquinolines described by Glorius et al.; [228] You and co-workers designed a new methodology affording axially chiral heterobiaryls (Scheme 0-19).[229] Thus, as in the case of our procedure based on the Suzuki-Miyaura reaction, this new system provided aryl pyridines and isoquinolines in excellent yield and enantioselectivities (up to 99% and 97% ee). Remarkably, the reaction was suitable for a broad range of heterobiaryls as substrates and, especially, aromatic coupling partners. In this regard, this system proved to be superior

[227] (1) Ros, A.; Estepa, B.; Ramírez-López, P.; Álvarez, E.; Fernández, R.; Lassaletta, J. M. Dynamic Kinetic Cross-Coupling Strategy for the Asymmetric Synthesis of Axially Chiral Heterobiaryls. *J. Am. Chem. Soc.* **2013**, *135* (42), 15730–15733. https://doi.org/10.1021/ja4087819.

[228] (1) Greßies, S.; Klauck, F. J. R.; Kim, J. H.; Daniliuc, C. G.; Glorius, F. Ligand-Enabled Enantioselective Csp3 –H Activation of Tetrahydroquinolines and Saturated Aza-Heterocycles by RhI. *Angew. Chemie - Int. Ed.* **2018**, *57* (31), 9950–9954. https://doi.org/10.1002/anie.201805680.

[229] (1) Wang, Q.; Cai, Z.-J.; Liu, C.-X.; Gu, Q.; You, S.-L. Rhodium-Catalysed Atroposelective C–H Arylation: Efficient Synthesis of Axially Chiral Heterobiaryls. *J. Am. Chem. Soc.* **2019**, *141* (24), 9504–9510. https://doi.org/10.1021/jacs.9b03862.

to our methodology, which was rather limited to the coupling with boroxines containing electron-rich aryl groups. Additionally, among other applications, one of these products were transformed into the corresponding *N*-oxide and tested in the allylation of benzaldehyde in a similar vein to his previous work.[223]

Scheme 0-19. Rh(I)-catalysed C-H arylation of aryl pyridines and isoquinolines

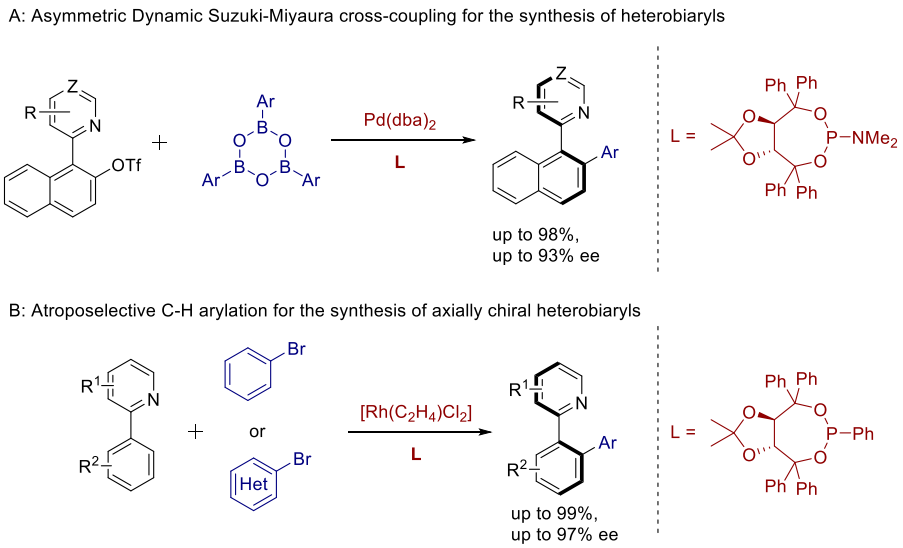

Another prolific group in the field of biaryls synthesis is that of Bing-Feng Shi. Thus, their work not only comprises the synthesis of all-carbon biaryls as we have seen in the previous section; but most recently, they have also contributed to the asymmetric preparation of heterobiaryls.

In this connection, they have newly reported an enantioselective method for the alkenylation of quinoline-derived atropisomers (Scheme 0-20).[230] In this context, chiral phosphoric acids appeared as an alternative family of ligands to monoprotected amino acids (MPAA). Moreover, a new spiro phosphoric acid, (*R*)-STRIP, showcased the best enantioselectivity and its subsequent application afforded a number of arylquinolines derivatives with good yield and excellent enantioselectivities (up to 98% ee).

[230] (1) Luo, J.; Zhang, T.; Wang, L.; Liao, G.; Yao, Q. J.; Wu, Y. J.; Zhan, B. B.; Lan, Y.; Lin, X. F.; Shi, B. F. Enantioselective Synthesis of Biaryl Atropisomers by Pd-Catalysed C–H Olefination Using Chiral Spiro Phosphoric Acid Ligands. *Angew. Chemie - Int. Ed.* **2019**, *58* (20), 6708–6712. https://doi.org/10.1002/anie.201902126.

Scheme 0-20. Atroposelective C-H alkenylation of quinoline heterobiaryls

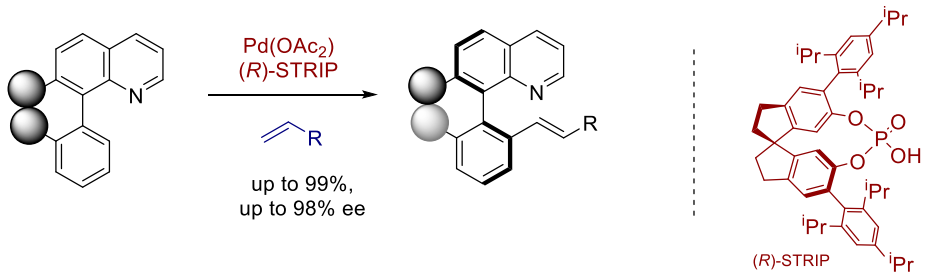

In addition to the synthesis of chiral heterobiaryls containing 6-member heterocycles, Shi, Chen and co-workers also worked on the synthesis of atropisomers bearing 5-member rings. That is to say, pyrroles, thiophenes, etc.

Probably due to the more labile character of the axis connecting 5-member rings, methods for the synthesis of these class of axially chiral heterobiaryls through C-H activation are scarce and only reported by Gu and Yamaguchi.[219,220]

Prompted by this lack of methodologies, they developed a procedure based on a C-H Pd(II)-catalysed alkynylation using *L-tert*-leucine as transient chiral auxiliary rather than as a ligand. This way, axially chiral systems connecting one or two 5-member rings, could be prepared with yields and enantioselectivities up to 98% and >99% respectively (Scheme 0-21).[231]

Scheme 0-21. Asymmetric C-H alkynylation of biaryls featuring 5-member heteroaromatic rings.

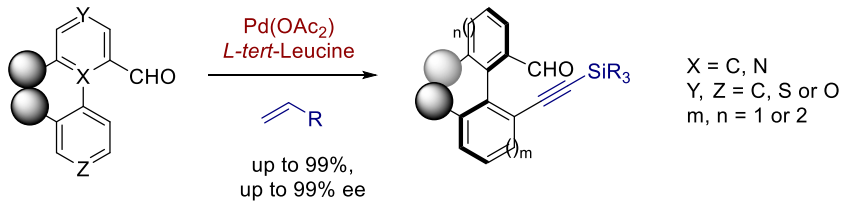

As we can see, all these methods rely on a directing group to successfully achieve the asymmetric C-H functionalisation of the heterobiaryls. However, it is worth to point out a method designed by Gu and co-workers, in which a

[231] (1) Zhang, S.; Yao, Q.-J.; Liao, G.; Li, X.; Li, H.; Chen, H.-M.; Hong, X.; Shi, B. F. Enantioselective Synthesis of Atropisomers Featuring Pentatomic Heteroaromatics by Pd-Catalysed C-H Alkynylation. *ACS Catal.* **2019**, *9* (3), 1956–1961. https://doi.org/10.1021/acscatal.8b04870.

functional group does not direct the C-H activation.[232] Hence, the combination of a catalytic system comprised by Pd(II), a TADDOL-derived phosphoramidite and pivalic acid afforded the corresponding heterobiaryls with excellent results and enantioselectivities up to 92% ee (Scheme 0-22). Importantly, the reaction was regioselective at H_a, and very selective despite the intermediates did not involve the axis.

Scheme 0-22. Intramolecular asymmetric C-H cyclisation for the synthesis of indole-based heterobiaryls.

[232] (1) He, C.; Hou, M.; Zhu, Z.; Gu, Z. Enantioselective Synthesis of Indole-Based Biaryl Atropisomers via Palladium-Catalysed Dynamic Kinetic Intramolecular C-H Cyclization. *ACS Catal.* **2017**, *7* (8), 5316–5320. https://doi.org/10.1021/acscatal.7b01855.

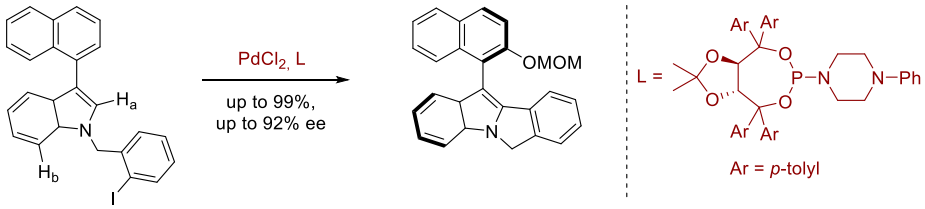

C-H borylation of naphthylisoquinoline and related systems

Despite the Ir-catalysed borylation of arenes was a very well-known transformation in the realm of C-H activation since the pioneering works by the groups of Smith,[233] Hartwig and Miyaura,[234] the regioselectivity of these reactions remained as a difficult task for a while. In this regard, the selectivity of this reaction relied on steric factors and therefore, the *ortho*-directed versions of this transformation appeared much later.[235,182] Thus, the emergence of these regioselective methods prompted our group to adapt this strategy to our classical naphthyl isoquinoline systems.[236]

In this connection, the lack of selectivity afforded when typical the [Ir(m-X)(cod)]2/di-tert-butylbipyridine (dtbpy; X=Cl, OMe; cod=1,5-cyclooctadiene) catalyst is employed, can be ascribed to the saturation of the complex upon coordination of the directing group. Under these conditions, the cyclometallation is completely prevented and the reaction needs to follow an unselective pathway ruled by steric factors (Scheme 0-23).

---

[233] (1) Cho, J. Y.; Tse, M. K.; Holmes, D.; Maleczka, R. E.; Smith, M. R. Remarkably Selective Iridium Catalysts for the Elaboration of Aromatic C-H Bonds. *Science (80-.).* **2002**, *295* (5553), 305–308. https://doi.org/10.1126/science.1067074.

[234] (1) Ishiyama, T.; Takagi, J.; Hartwig, J. F.; Miyaura, N. A Stoichiometric Aromatic C-H Borylation Catalysed by Iridium(I)/2,2′-Bipyridine Complexes at Room Temperature. *Angew. Chemie Int. Ed.* **2002**, *41* (16), 3056–3058. https://doi.org/10.1002/1521-3773(20020816)41:16<3056::AID-ANIE3056>3.0.CO;2-#.

[235] (1) Boebel, T. A.; Hartwig, J. F. Silyl-Directed, Iridium-Catalysed Ortho-Borylation of Arenes. A One-Pot Ortho-Borylation of Phenols, Arylamines, and Alkylarenes. *J. Am. Chem. Soc.* **2008**, *130* (24), 7534–7535. https://doi.org/10.1021/ja8015878.

(1) Miyaura, N. Metal-Catalysed Reactions of Organoboronic Acids and Esters. *Bull. Chem. Soc. Jpn.* **2008**, *81* (12), 1535–1553. https://doi.org/10.1246/bcsj.81.1535.

[236] (1) Ros, A.; Estepa, B.; López-Rodríguez, R.; Álvarez, E.; Fernández, R.; Lassaletta, J. M. Use of Hemilabile N,N Ligands in Nitrogen-Directed Iridium-Catalysed Borylations of Arenes. *Angew. Chemie - Int. Ed.* **2011**, *50* (49), 11724–11728. https://doi.org/10.1002/anie.201104544.

Scheme 0-23. Possible mechanism for the non-selective borylation of arenes.

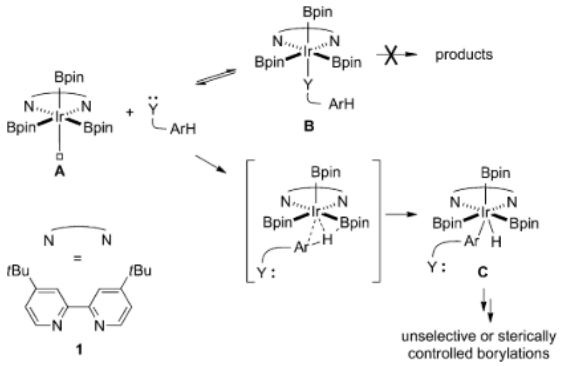

If this premise is right, a hemilabile bidentate ligand would overcome this limitation. Thus, the *ortho* borylation of 2-arylpyridine could be successfully achieved by our research group utilizing a pyridine-hydrazone ligand.

Scheme 0-24. Directed Ir-catalysed C-H borylation of N-heterobiaryls

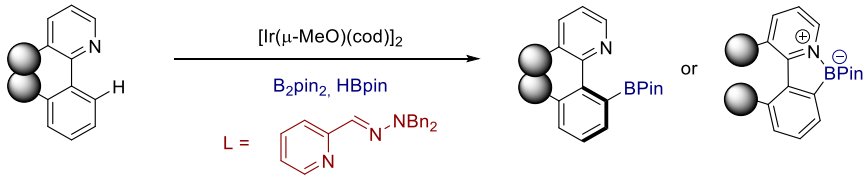

Interestingly, when the scope of the reaction was studied, two classes of products were found in accordance to their solution and solid structures. On the one hand, sterically hindered heterobiaryls exhibited axially chiral structures in which both rings were arranged in a perpendicular manner. On the other, the simplest heterobiaryls with lower steric hindrance featured a B-N interaction resulting in a distortion and the subsequent planarization of the scaffold.

Figure 35. Examples of two types of borylated arylpyridines (isoquinolines).

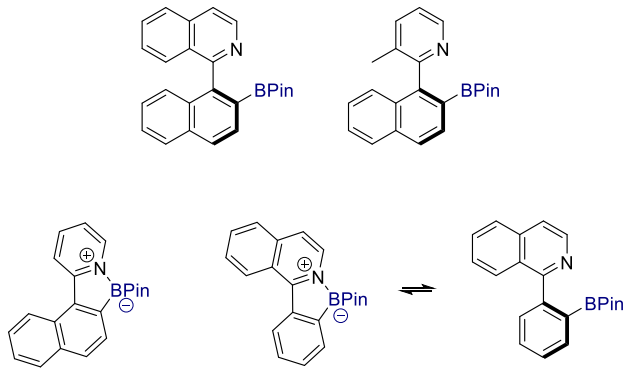

Triggered by these results, our research group decided to explore an asymmetric version of this reaction. At the outset of our investigations, we tried to resolve the racemic naphthylisoquinoline boronic ester (Figure 35) by chiral HPLC techniques but despite our struggle, all the attempts were in vain. This lack of resolution led us to assess the possibility of a dynamic behaviour which might derive in a racemisation process (Scheme 0-25). In this regard, both enantiomers seemed to be in a rapid interconversion through the assistance of the interaction between B and N atoms.[237]

Scheme 0-25. Atropoisomerisation of N-heterobiaryl boronic esters.

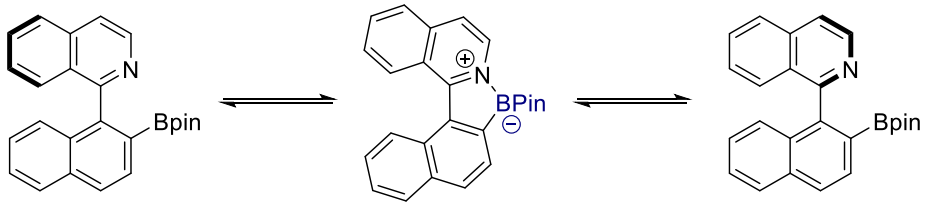

Hence, any methodology aiming at the asymmetric borylation of these systems would need to disrupt this interaction. With this idea in mind, the substitution of 8 position in naphthalene ring was envisaged as potential solution. Unfortunately, after a screening of reaction conditions and chiral ligands, the products were obtained in a racemic form.

[237] Lopez-Rodriguez, R (2016): *Borilación C(sp2)-H de arenos: Desarrollo y aplicaciones (Doctoral thesis).* Instituto de investigaciones Científicas – Universidad de Sevilla, Sevilla.

Scheme 0-26. 8'-substituted napthylisoquinolines boronic esters.

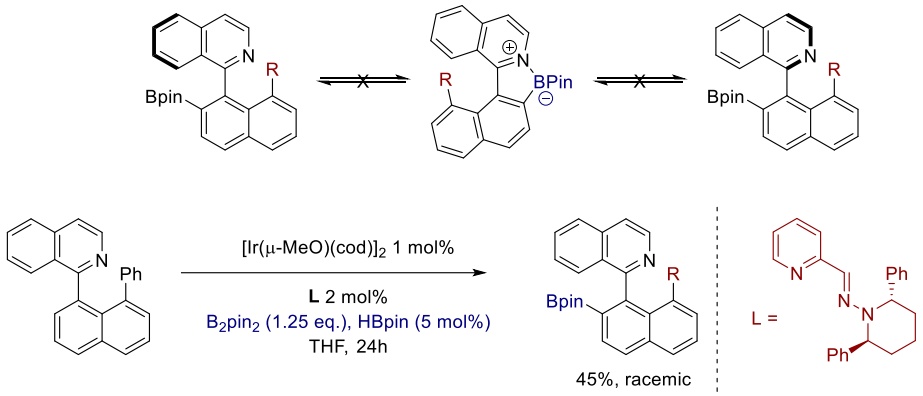

Regardless, this methodology provided the evidence that our naphthylisoquinoline-type heterobiaryls could undergo ortho-directed C-H activation, paving the way to other reactions.

Hence, this finding encouraged as to find alternative transformations which could lead to the desymmetrisation of the axis of these systems.

Directed Enantioselective C-H hydroarylation of alkenes.

Hydroarylation of double bonds has played a crucial role in the development of C-H activation strategies. In fact, Murai's work on the Ru-catalysed hydroarylation of aromatic ketones in 1993[169] represented a milestone in this field. Since that moment, C-H activation drew the attention of chemical community and emerged as a reliable, atom economical and powerful tool in synthesis.

As one would expect, the evolution of this reaction is parallel to that of the C-H activation itself. In this regard, both intra- and intermolecular reactions, and the use of different metal as catalytic centres have been reported.[238]

[238] Selected reports and reviews dealing with C-N interaction:
(1) Nishiyabu, R.; Kubo, Y.; James, T. D.; Fossey, J. S. Boronic Acid Building Blocks: Tools for Sensing and Separation. *Chem. Commun.* **2011**, *47* (4), 1106–1123. https://doi.org/10.1039/c0cc02920c.
(2) Nishiyabu, R.; Kubo, Y.; James, T. D.; Fossey, J. S. Boronic Acid Building Blocks: Tools for Self Assembly. *Chem. Commun.* **2011**, *47* (4), 1124–1150. https://doi.org/10.1039/c0cc02921a.
(3) Collins, B. E.; Sorey, S.; Hargrove, A. E.; Shabbir, S. H.; Lynch, V. M.; Anslyn, E. V. Probing Intramolecular B-N Interactions in Ortho-Aminomethyl Arylboronic Acids. *J. Org. Chem.* **2009**, *74* (11), 4055–4060. https://doi.org/10.1021/jo900187a.

Since our central goal is the synthesis of chiral heterobiaryls through coupling reactions with naphthylisoquinoline-like units, we will focus on the asymmetric intermolecular versions.

In this regard, we have already underscored the impact of the hydroarylation reaction with naphthypicoline reported by Murai[203] on the application of C-H strategies in the synthesis of axially chiral (hetero)biaryls. Moreover, this seminal work is a great source of inspiration for this work.

In addition to the application in the desymmetrisation of these axially chiral compounds, the Murai-type reaction, that is to say, hydroarylation of terminal olefins, has also been applied to enantioselective synthesis of compounds with planar chirality. Thus, Shibata and Shizuno[239] developed a protocol in which ferrocenes bearing 1-isoquinolines as directing groups could undergo a desymmetrisation process by means of this reaction. In this Ir(I)-catatalysed hydroarylation using chiral dienes as ligands, besides searching high enantioselectivities, regioselectivity was also important; as dihydroarylation products are symmetrical and lack interest. In this respect, the isoquinoline moiety played an essential role as a directing and steric group. Thus, this protocol delivered the hydroarylation of a number of alkenes, mainly electron-poor, with (isoquinolin-1-yl)ferrocene in different yields and enantioselectivities up to 93% ee (Scheme 0-27).

(4) Zhu, L.; Shabbir, S. H.; Gray, M.; Lynch, V. M.; Sorey, S.; Anslyn, E. V. A Structural Investigation of the N-B Interaction in an o-(N,N-Dialkylaminomethyl)Arylboronate System. *J. Am. Chem. Soc.* **2006**, *128* (4), 1222–1232. https://doi.org/10.1021/ja055817c.

(5) Wiskur, S. L.; Lavigne, J. J.; Ait-Haddou, H.; Lynch, V.; Chiu, Y. H.; Canary, J. W.; Anslyn, E. V. PKa Values and Geometries of Secondary and Tertiary Amines Complexed to Boronic Acids - Implications for Sensor Design. *Org. Lett.* **2001**, *3* (9), 1311–1314. https://doi.org/10.1021/ol0156805.

(6) Höpfl, H. The Tetrahedral Character of the Boron Atom Newly Defined - A Useful Tool to Evaluate the N → B Bond. *J. Organomet. Chem.* **1999**, *581* (1–2), 129–149. https://doi.org/10.1016/S0022-328X(99)00053-4.

[239] (1) Shibata, T.; Shizuno, T. Iridium-Catalysed Enantioselective C-H Alkylation of Ferrocenes with Alkenes Using Chiral Diene Ligands. *Angew. Chemie - Int. Ed.* **2014**, *53* (21), 5410–5413. https://doi.org/10.1002/anie.201402518.

Scheme 0-27. Directed Ir-catalysed C-H hydroalkylation of ferrocenes

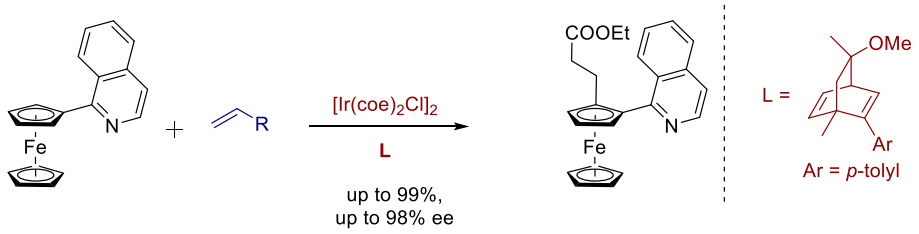

On the subject of point chirality, the hydroarylation of acyclic exhibited a big limitation: mostly, the Muray-type reaction with alkenes was characterised to be linear selective.[240] Therefore, reaching branch selectivity is a prerequisite for the development of chiral versions of the reaction.

With this regard, some reactions have proved to achieve branch selectivity by means of Co, Ni[241] and Ru catalysts but still, they did not exhibit a general character and they were confined to the use of styrenes.[242]

---

[240] (a) Kakiuchi, F.; Sekine, S.; Tanaka, Y.; Kamatani, A.; Sonoda, M.; Chatani, N.; Murai, S. Bull. Chem. Soc. Jpn. **1995**, 68, 62. (b) Lim, Y.-G.; Kang, J.-B.; Kim, Y. H. J. Chem. Soc., Perkin Trans. 1 **1996**, 2201. (c) Matsumoto, T.; Periana, R. A.; Taube, D. J.; Yoshida, H. J. Mol. Catal. A **2002**, 180, 1. (d) Jun, C.-H.; Moon, C. W.; Hong, J.-B.; Lim, S.-G.; Chung, K.-Y.; Kim, Y.-H. Chem. Eur. J. **2002**, 8, 485. (e) Tan, K. L.; Bergman, R. G.; Ellman, J. A. J. Am. Chem. Soc. **2002**, 124, 13964. (f) Tsuchikama, K.; Kasagawa, M.; Hashimoto, Y.; Endo, K.; Shibata, T. J. Organomet. Chem. 2008, 693, 3939. (g) Martinez, R.; Genet, J.-P.; Darses, S. Chem. Commun. **2008**, 3855. (h) Zhang, Y. J.; Skucas, E.; Krische, M. J. Org. Lett. **2009**, 11, 4248. (i) Martinez, R.; Simon, M.-O.; Chevalier, R.; Pautigny, C.; Genet, J.-P.; Darses, S. J. Am. Chem. Soc. **2009**, 131, 7887. (j) Ilies, L.; Chen, Q.; Zeng, X.; Nakamura, E. J. Am. Chem. Soc. **2011**, 133, 5221. (k) Takebayashi, S.; Shibata, T. Organometallics **2012**, 31, 4114. (l) Schinkel, M.; Marek, I.; Ackermann, L. Angew. Chem., Int. Ed. **2013**, 52, 3977. (m) Shibata, T.; Shizuno, T. Angew. Chem., Int. Ed. **2014**, 53, 5410.

[241] (a) Mukai, T.; Hirano,K.; Satoh, T.; Miura, M. J. Org. Chem. **2009**, 74, 6410. (b) Nakao, Y.; Kashihara, N.; Kanyiva, K. S.; Hiyama, T. Angew. Chem., Int. Ed. **2010**, 49, 4451. (c) Jiang, Y.-Y.; Li, Z.; Shi, J. Organometallics **2012**, 31, 4356.

[242] (a) Gao, K.; Yoshikai, N. J. Am. Chem. Soc. **2011**, 133, 400.
(b) Lee, P.-S.; Yoshikai, N. Angew. Chem., Int. Ed. **2013**, 52, 1240. In this latter report, formal carbonyl-directed, branch-selective hydroarylation can be achieved but requires the formation and subsequent hydrolysis of the imine directing group. Bis-alkylation was problematic in cases where two ortho sites were available.
(6) Ruthenium: Uchimaru, Y. Chem. Commun. **1999**, 1133. (7) Branch-selective, nondirected alkene hydroheteroarylation reactions enable the coupling of specific heterocycles and styrenes: (a) Mukai, T.; Hirano, K.; Satoh, T.; Miura, M. J. Org. Chem. **2009**, 74, 6410. (b) Nakao, Y.; Kashikara, N.; Kanyiva, K. S.; Hiyama, T. Angew. Chem., Int. Ed. 2010, 49, 4451. (8) Specific combinations of N-based directing group and

In this line, Shibata and co-workers[243] had previously developed a directed C-H method for the regioselective C2 alkylation of indoles in which the branch or linear selectivity could be achieved by switching the protecting group (Scheme 0-28). Thus, when acetyl group was employed as the protecting/directing group, the linear alkylation was obtained. By contrast, when benzoyl group was the directing group, the product showed branch selectivity. After an optimisation of the reaction conditions, bisphosphines such as *rac*-BINAP, (*S*)-DM-SEGPHOS and (*R*)-SDP were found to be suitable ligands for this cationic Ir(I)-catalysed reaction. Importantly, the use of the latter non-racemic ligand in the branch selective version of the reaction, afforded a modest 42% ee, but opened the door to an asymmetric version.

Scheme 0-28. Selective linear or Branched 2-alkylindoles through Ir(I)-catalysed hydroalkylation.

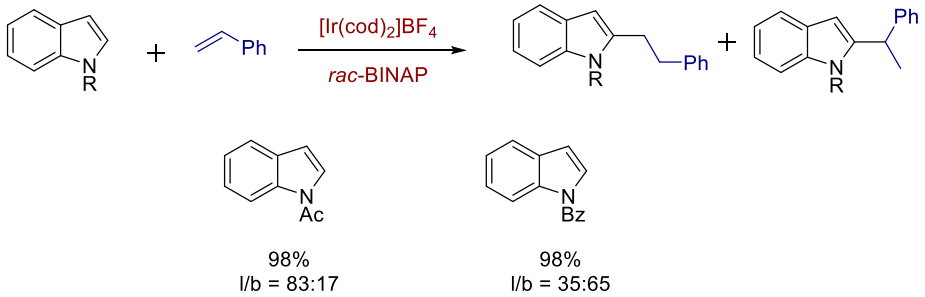

Aiming to develop a branch-selective methodology for the alkylation of aryl rings through C-H direct activation, Bower et al. drew inspiration from a previous Shibata's report.[244] In this report, an Ir(I)/BINAP complex promoted the branch-alkylation of aromatic ketones with styrene, although low

---

phosphine ligand promote linear- or branch-selective hydroheteroarylation at the 2-position ofindoles: Shibata, T.; Ryu, N.; Pan, S. J. Am. Chem. Soc. **2012**, 134, 17474. (9) Styrenes represent "special cases" and often lead to significant levels of branched products: (a) Tanaka, M.; Watanabe, Y.; Mitsudo, T.-a.; Takegami, Y. Bull. Chem. Soc. Jpn. **1974**, 47, 1698. (b) Casey, C. P.; Petrovich, L. M. J. Am. Chem. Soc. **1995**, 117, 6007. (c) Jiang, Y.-Y.; Li, Z.; Shi, J. Organometallics **2012**, 31, 4356. (4g) Ilies, L.; Chen, Q.; Zeng, X.; Nakamura, E. J. Am. Chem. Soc. **2011**, 133, 5221.

[243] (1) Pan, S.; Ryu, N.; Shibata, T. Ir(I)-Catalysed C-H Bond Alkylation of C2-Position of Indole with Alkenes: Selective Synthesis of Linear or Branched 2-Alkylindoles. *J. Am. Chem. Soc.* **2012**, *134* (42), 17474–17477. https://doi.org/10.1021/ja308742x.

[244] (1) Tsuchikama, K.; Kasagawa, M.; Hashimoto, Y. K.; Endo, K.; Shibata, T. Cationic Iridium-BINAP Complex-Catalysed Addition of Aryl Ketones to Alkynes and Alkenes via Directed C-H Bond Cleavage. *J. Organomet. Chem.* **2008**, *693* (26), 3939–3942. https://doi.org/10.1016/j.jorganchem.2008.09.065.

selectivity values were obtained (7:1 to 3:1 branch/linear). They then wondered which features could lead to this preferential selectivity and which modifications of the catalytic system could enhance it.[245] Related studies had revealed that metalation and alkene coordination were reversible and therefore, the regioselectivity was not governed by these steps. Conversely, the preference for the linear or branch product could arise from the species in equilibrium depicted below (Scheme 0-29).

Scheme 0-29. Factors favouring Branch selectivity: "cooperative destabilisation"

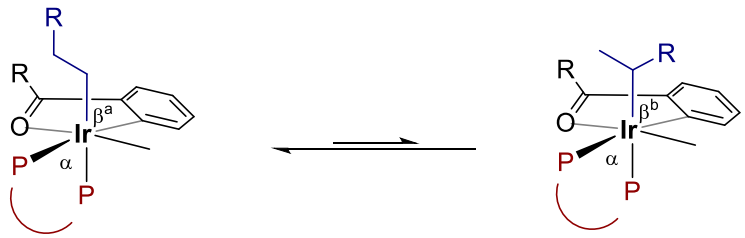

– wide bite angles increases α and compreses β
– 2° alkyl groups increases steric destabilisation

In this equilibrium, the predominant complex should be the species on the left owing to the lower steric crowding exerted by the linear alkyl ligand. In contrast, the complex on the right is disfavoured for the same reason. Bower and his group then proposed that a perturbation of the system leading to the enhancement of the reductive elimination of the latter could increase the branch selectivity of the reaction. As a solution, they hypothesised that: 1) wider angle bite bisphosphine ligands would compress the angle x and 2) bulky branch alkyl ligands would also enhance the rate of reductive elimination by destabilising the corresponding intermediate.

To probe this idea, the effect of a battery of ligands with different bite angles was examined (Table 15). Pleasingly, the increasing bite angle translated to increasing branch:linear selectivities. Unfortunately, this selectivity was obtained at expense of the yield. Nevertheless, this problem could be circumvented by the use of the equivalent fluorinated bisphosphines as electronically poor ligands. In these cases, the reaction delivered the desired product in better yields.

[245] (1) Crisenza, G. E. M.; McCreanor, N. G.; Bower, J. F. Branch-Selective, Iridium-Catalysed Hydroarylation of Monosubstituted Alkenes via a Cooperative Destabilization Strategy. *J. Am. Chem. Soc.* **2014**, *136* (29), 10258–10261. https://doi.org/10.1021/ja505776m.

Table 15. Ligand effect on the yield and regioselectivity of the reaction.

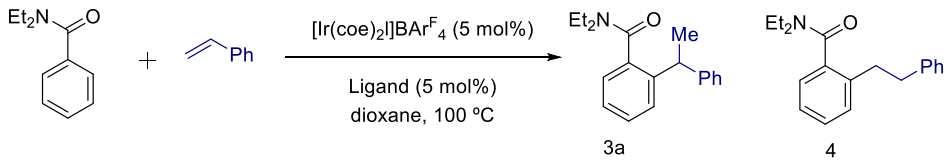

Entry	ligand	Yield (%)	Branch/linear
1	*rac*-BINAP	100	29:71
2	dppm	73	8:92
3	dppe	82	23:77
4	dppp	52	60:40
5	dppb	28	100:0
6	d^Fppe	100	36:64
7	d^Fppb	100	100:0

Thus, the cationic Ir(I)/dFppb system emerged as an efficient catalyst to achieve branch selectivity[246] in the hydroarylation of different terminal alkenes with different aromatic ketones, benzamides[245] and acetanilides.[247]

Most importantly, this protocol opened the door to the development of asymmetric versions of the hydroarylation reaction, which was rather confined to strained olefins.[248]

In order to verify the reversibility of oxidative addition and hydrometallation of alkene, deuterium labelling experiments were accomplished. Besides, these

[246] (1) Crisenza, G. E. M.; Bower, J. F. Branch Selective Murai-Type Alkene Hydroarylation Reactions. *Chem. Lett.* **2016**, *45* (1), 2–9. https://doi.org/10.1246/cl.150913.

[247] (1) Crisenza, G. E. M.; Sokolova, O. O.; Bower, J. F. Branch-Selective Alkene Hydroarylation by Cooperative Destabilization: Iridium-Catalysed Ortho-Alkylation of Acetanilides. *Angew. Chemie - Int. Ed.* **2015**, *54* (49), 14866–14870. https://doi.org/10.1002/anie.201506581.

[248] (A) Aufdenblatten, R.; Diezi, S.; Togni, A. Iridium(I)-Catalysed Asymmetric Intermolecular Hydroarylation of Norbornene with Benzamide. *Monatshefte fur Chemie* **2000**, *131* (12), 1345–1350. https://doi.org/10.1007/s007060070014.

(B) Sevov, C. S.; Hartwig, J. F. Iridium-Catalysed Intermolecular Asymmetric Hydroheteroarylation of Bicycloalkenes. *J. Am. Chem. Soc.* **2013**, *135* (6), 2116–2119. https://doi.org/10.1021/ja312360c.

(1) Nagamoto, M.; Fukuda, J.; Hatano, M.; Yorimitsu, H.; Nishimura, T. Hydroxoiridium-Catalysed Hydroarylation of Alkynes and Bicycloalkenes with N -Sulfonylbenzamides. *Org. Lett.* **2017**, *19* (21), 5952–5955. https://doi.org/10.1021/acs.orglett.7b02950.

experiments also underpinned reductive elimination was the rate-determining step.

On the other hand, Nishimura and Nagamoto found that 1,5-cyclooctadiene (cod) ligand accelerated the Ir(I)-catalysed [3+2] annulation of ketimines with alkynes *via* C-H activation.[249] Encouraged by this work, Nishimura and Ebe[250] applied the same catalytic system to the hydroarylation of vinyl ethers with phenylpyridine. This procedure gave the desired products with total branch selectivity and little amount of dialkylated product with several directing groups and a variety of vinyl ethers, including cyclic ones (Scheme 0-30).

As a proof of concept, they also utilized a chiral diene in the branch-alkylation of phenylpyridine, obtaining the desired products with very good yield and encouraging enantioselectivities (Scheme 0-30).

Scheme 0-30. Ir(I)-catalysed C-H branch-selective hydroarylation of vinyl ethers.

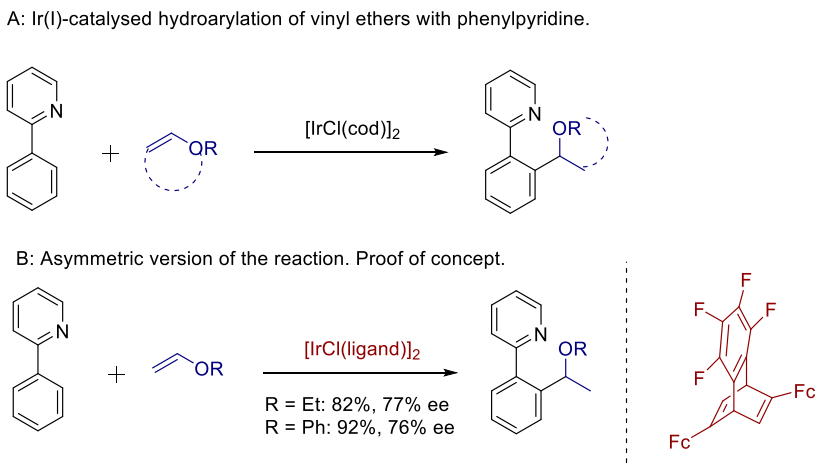

Subsequently, Nishimura and co-workers improved their protocol to access the corresponding asymmetric benzylic ethers with better enantioselectivities.[251] Interestingly, this Ir-catalysed C-H reaction utilized

[249] (1) Nagamoto, M.; Nishimura, T. Catalytic [3 + 2] Annulation of Ketimines with Alkynes via C-H Activation by a Cationic Iridium(Cod) Complex. *Chem. Commun.* **2014**, *50* (47), 6274–6277. https://doi.org/10.1039/c4cc01874e.

[250] (1) Ebe, Y.; Nishimura, T. Iridium-Catalysed Branch-Selective Hydroarylation of Vinyl Ethers via C-H Bond Activation. *J. Am. Chem. Soc.* **2015**, *137* (18), 5899–5902. https://doi.org/10.1021/jacs.5b03099.

[251] (1) Ebe, Y.; Onoda, M.; Nishimura, T.; Yorimitsu, H. Iridium-Catalysed Regio- and Enantioselective Hydroarylation of Alkenyl Ethers by Olefin Isomerisation. *Angew. Chemie - Int. Ed.* **2017**, *56* (20), 5607–5611. https://doi.org/10.1002/anie.201702286.

internal alkenyl ethers, which were more challenging substrates from a regioselectivity point of view. In fact, previous attempts by the group to achieve the hydroarylation of acyclic internal vinyl ethers were rather sluggish. this regard, the reaction proceeded comprising an isomerisation step previous to the hydroarylation reaction, gaving the α-alkoxy hydroarylated products exclusively (Scheme 0-31).

Scheme 0-31. Regio- and enantioselective hydroarylation of alkenyl ethers

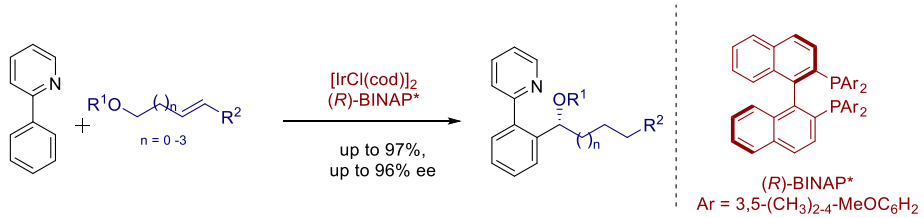

Considering the resemblance between our naphthylisoquinoline system and phenylpyridine, these works by Nishimura triggered us to explore the branch-selective hydroarylation reaction as a new strategy to access chiral heterobiaryls. Furthermore, if this hypothesis were proved to be true, two chiral elements will be simultaneously generated. In other words, the products will not only be axially chiral, but point chirality will also arise. To successfully achieve this goal, not only a good enantio- and regiocontrol is mandatory, but the products have to be synthesised in high diastereoselectivity (Scheme 0-32).

Scheme 0-32. Working hypothesis for the hydroarylation of naphtylisoquinoline and related systems.

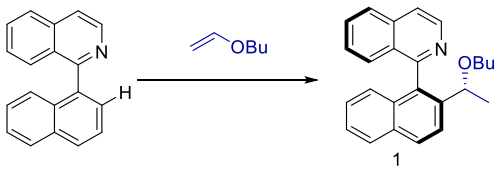

Objective

Considering the shortage and limitations of the previously described methodologies delivering axially chiral heterobiaryls, and the longstanding interest in our research group in the synthesis these compounds, we envisioned the C-H activation of naphthyl isoquinolines and substituted aryl pyridines to achieve this goal.

In this regard, these scaffolds are potentially excellent substrates to develop this type of methodologies for the following reasons:

1. Disubstituted phenylpyridines lacking functionalisation at the 2'-position, are characterised by the free rotation around the axis and hence are configurationally unstable.
2. Pyridine and isoquinoline rings are groups which direct the C-H reaction at the ortho position.
3. The subsequent functionalisation at such position encumbers the rotation around the axis, and therefore, the products are configurationally stable due to the steric hindrance.

Scheme 0-33. Configurationally labile heterobiaryls

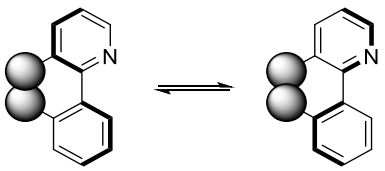

configurationally labile
achiral, conformers

As these substrates are achiral, the most suitable strategy to develop an asymmetric methodology is the desymmetrisation.

This idea was initially demonstrated by Murai,[203] who first desymmetrised this type of compounds by C-H hydroaryilation but poor results were obtained. In the same line, Dr. Rocío López Rodríguez also tested this approach in her doctoral thesis in our group by using an *ortho*-directed C-H borylation.[236,237]

However, the desymmetrisation of these heterobiaryls were unsuccessful either because lower selectivities were obtained (C-H hydroarylation, Scheme 0-34) or because the products were configurationally labile by intramolecular interactions (C-H borylation, Scheme 0-34).

Scheme 0-34. Desymmetrisation of substituted aryl pyridines and isoquinolines

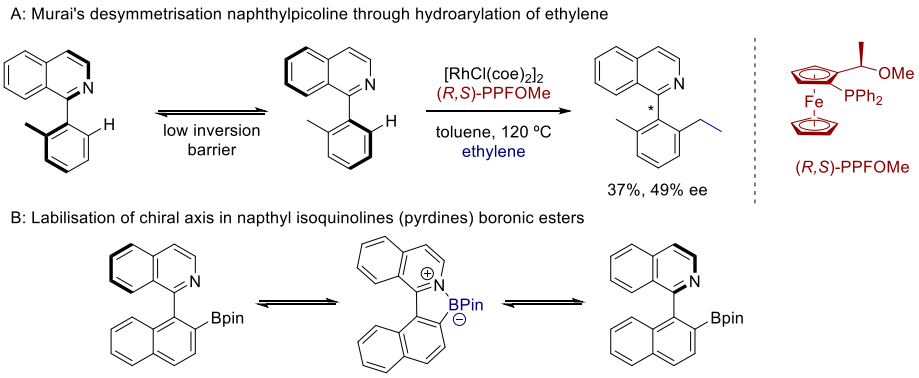

Thus, we hypothesised that any other C-H transformation in which the new function did not interact with the pyridinic N would lead to configurationally stable products.

More recently, several works on the branch-selective hydroarylation with phenyl pyridines have been reported;[250,251] and more interestingly, the products could be synthesised in an enantioselective manner.

Scheme 0-35. Branch-selective C-H hydroarylation of vinyl ethers with phenylpyridines.

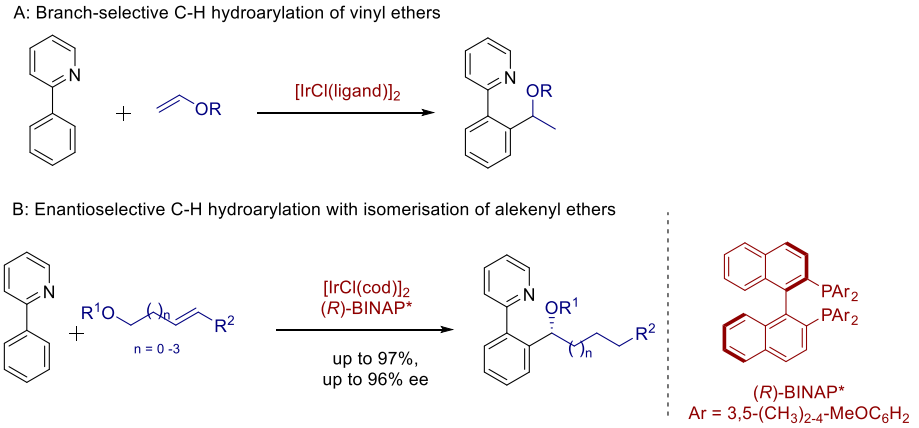

Considering naphthylisoquinoline systems can be functionalised by C-H activation reactions and its desymetrisation through hydroarylation has been proved, we envisaged the application of a branch-selective hydroarylation as a promising strategy for the synthesis of chiral heterobiaryls. Thus, this methodology would lead to the simultaneous generation of the axial and central chirality. It is worth to notice that this is a challenging task, as a total control of the regio-, diastreo- and enantioselectivity is then required.

Scheme 0-36. Working hypothesis on the C-H hydroaryltion for the syntheis of heterobiaryls with axial and central chirality.

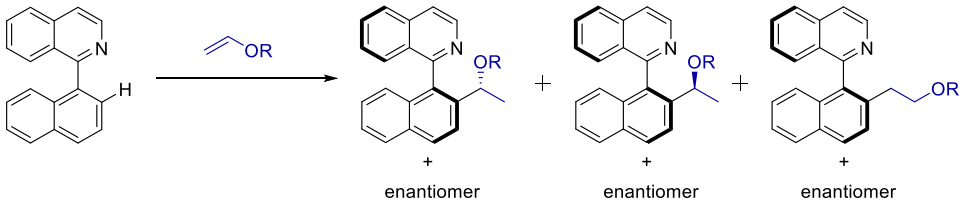

Results and discussion

Optimisation of the reaction conditions for the hydroarylation of naphthylisoquinoline.

Model reaction and solvent screening

As we mentioned before, encouraged by the C-H borylation developed in our group and the works by Murai and Nishimura, we began our investigations by setting the reaction between naphthylisoquinoline and butyl vinyl ether as the model reaction.

Since bisphosphines are widely used ligands in this kind of transformation and in view of the similarities of our system to that of Nishimura,[251] we started our investigations exploring a similar catalytic system. Hence, as the starting point conditions for the hydroarylation we used $[IrCl(cod)]_2$/$NaBAr^F_4$ and (*R*)-BINAP in toluene at 80 °C (Scheme 0-37).

Scheme 0-37. Model reaction.

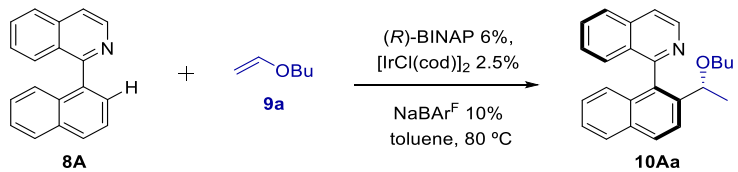

Despite the yield was rather disappointing, affording a conversion of ~25% by NMR, the reaction gave a very good enantioselectivity (83% ee) and excellent diastereoselectivity (dr>20:1) for the branched regioisomer was obtained as the single product. In order to improve the yield, we also carried out the reaction with 5 equivalent of butyl vinyl ether. Thus, the yield was increased to ~50%, keeping the enantioselectivity unaltered (84% ee).

On the other hand, careful examination of ^1H NMR spectra of the crudes revealed the presence of other products that seemed to be the result of a polymerization reaction of vinyl ether. Ir(I) forms complexes of different nature which may include some unsaturated species, leaving vacant positions for its coordination. Due to the acid and cationic character of the metal, the double bond might be activated toward other reactions such as polymerization. We then thought that the use of a coordinating solvent may help to prevent this polymerization. Thus, we performed a solvent screening including several ethers among others (Table 16).

In this respect, the reaction showed a superior performance when ethers were used as solvents, especially 1,4-dioxane (~95%, 83% ee). DCE also gave good

results (~80%, 83%) while $CHCl_3$ gave low conversions and the highly polar DMSO inhibited the reaction. Interestingly, the selectivity of the reactions remained stable/homogenous (83% - 88% ee) irrespective of the solvent; possibly indicating the stereodetermining step of the reaction is not affected by the polarity of the media.

On the other hand, the reactions were performed using 2 or 5 equivalents of butyl vinyl ether but, as expected, lowering the amount of the olefin, just decreased the reaction yield.

Table 16. Solvent Screening

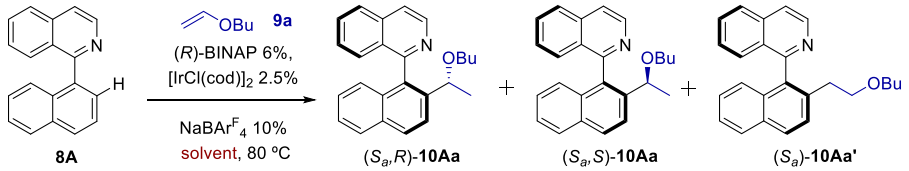

Entry	Equiv. butyl vinyl ether	Solvent	Conv (%)[b]	ee (%)[c]
1	2	Toluene	25	85
2	5	Toluene	50	84
3	2	Dioxane	60	85
4	5	Dioxane	>95	83
5	2	THF	25	88
6	5	THF	80	84
7	2	DME	30	86
8	5	DME	50	83
9	2	DCE	25	84
10	5	DCE	80[d]	83

[a] Reactions performed on a 0.1 mmol scale using anhydrous solvent (1 mL/0.1 mmol **8A**) for a 24 h period at 80 °C. [b] Determined by ^{1}H NMR spectroscopy of the crude reaction mixture. The *branched/linear* ratio (**10Aa/10Aa´**) and the diastereoselectivity ((*Sa,R*)-**10Aa**/(*Sa,S*)-**10Aa**) were also determined by ^{1}H NMR on the reaction crude, being >50:1 and >20:1, respectively, in all cases. [c] Determined by chiral HPLC analysis. [d] Formation of unknown products were observed.

Given that 1,4-dioxane was the best solvent, we next studied the effect of the concentration by performing two reactions with 2 and 5 equivalents of ether doubling the concentration of all the reagents (Table 17). Thus, when doubling the concentration of all the reagents, the observed effect is the opposite to the expected: lower yields were obtained. Nevertheless, this is not surprising as we have previously mentioned, polymerisation reactions may also take place. In this regard, by doubling the concentration side reactions are enhanced at the expense of the productive one.

Table 17. Concentration effect and optimisation of the stoichiometry of vinyl ether

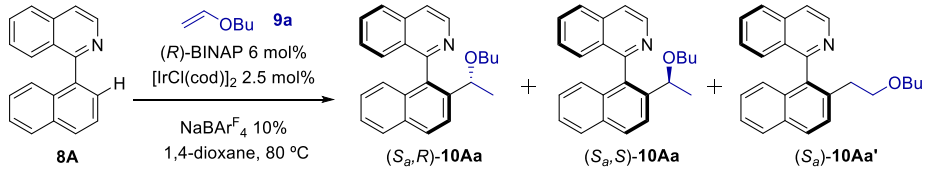

Entry	Equiv. butyl vinyl ether	[C]/M[a]	Conv (%)[b]	ee (%)[c]
1	2	0,1	60	88
2	5	0,1	95	83
3	2	0,2	40	87
4	5	0,2	80	84

[a]The concentration is referred to the substrate. Reactions performed on a 0.1 mmol scale using anhydrous solvent (1 mL/0.1 mmol **8A**) for a 24 h period at 80 °C. [b] Determined by ^{1}H NMR spectroscopy of the crude reaction mixture. The *branched/linear* ratio (**10Aa/10Aa´**) and the diastereoselectivity ((*Sa,R*)-**10Aa**/(*Sa,S*)-**10Aa**) were also determined by ^{1}H NMR on the reaction crude, being >50:1 and >20:1, respectively, in all cases. [c] Determined by chiral HPLC analysis.

In view of these promising results, we continued to further refine the rest of conditions to improve the selectivity and decrease the polymerisation.

Ligand screening

As we previously mentioned, chiral C_2-symmetric bis(phosphines) are commonly used ligands in directed Ir(I)-catalysed C-H hydroarylations. Representative ligands in this transformations are Segphos,[243,248b] MeO-BIPHEP[248b] or SDP,[243] in addition to BINAP. Thus, these families of ligands were of first choice in our screening (Table 18).

Table 18. Ligand screening.

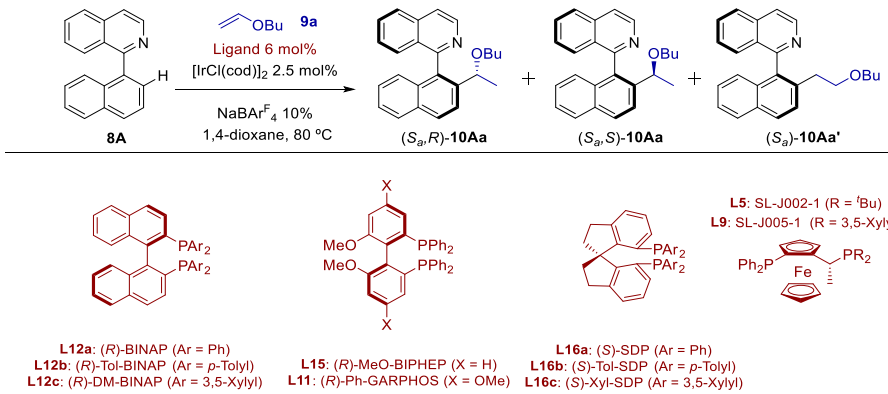

Entry	Ligand	Solvent	Conv (%)[b]	ee (%)[c]
1	**L12a**	Dioxane	>95	83
2	**L12b**	Dioxane	>95	90
3	**L12c**	Dioxane	90	84
4	**L15**	Dioxane	85	33
5	**L11**	Dioxane	30	34
6	**L16a**	Dioxane	65	87
7	**L16b**	Dioxane	**>95**	**93**
8	**L16c**	Dioxane	60	95
9	**L5**	Dioxane	10	45
10	**L9**	Dioxane	10	12

[a] Reactions performed on a 0.1 mmol scale using anhydrous solvent (1 mL/0.1 mmol **8A**) and 5 equiv. of vinyl ether **9a**, for a 24 h period at 80 °C. [b]Determined by ^{1}H NMR spectroscopy of the crude reaction mixture. The *branched/linear* ratio (**10Aa/10Aa´**) and the diastereoselectivity ((*S*$_a$,*R*)-**10Aa**/(*S*$_a$,*S*)-**10Aa**) were also determined by ^{1}H NMR on the reaction crude, being >50:1 and >20:1, respectively, in all cases. [c] Determined by chiral HPLC analysis.

To begin with, as (*R*)-BINAP proved to be a very good ligand in the reaction, we wanted to verify if other bulkier ligands of this family would have an impact on the selectivity (Table 18). Thus, **L12b** and **L12c** also showed very good activity, affording the desired products in very good yields (>90%). On the other, **L12c** showed a similar selectivity to the parent BINAP (84% ee), although (*R*)-Tol-BINAP **L12b** increased the optical purity of the product to 90% ee. By contrast, biphenyl-like ligands **L15** and **L11** gave the product with poorer results (Table 18).

Regarding the spiro diphosphino (SDP) ligands, this family showed the best selectivities as a whole, affording the products in a range of 87% to 95% ee. However, the tolyl-substituted ligand **L16b** gave the product in full yield whereas the parent (*S*)-SDP and its bulkier xylyl-substituted **L16c** afforded moderate yields (Table 18). Interestingly, this family showed a parallel behaviour to BINAP-type ligands concerning both activity and selectivity.

On the other hand, we also tested other chiral C_1-symmetric Josiphos-type bisphosphines we had in our laboratory which had excellent results in other reactions and previous projects in our group.[252] Unfortunately, none of the two Josiphos ligands afforded the product in good yield, while the selectivity was moderate at best. It should be noted that C_1-symmetric ligands may

[252] (1) Ramírez-López, P.; Ros, A.; Estepa, B.; Fernández, R.; Fiser, B.; Gómez-Bengoa, E.; Lassaletta, J. M. A Dynamic Kinetic C–P Cross–Coupling for the Asymmetric Synthesis of Axially Chiral P,N Ligands. *ACS Catal.* **2016**, *6* (6), 3955–3964. https://doi.org/10.1021/acscatal.6b00784.

increase the number of diastereomeric species during the reaction, especially in an Ir(III)-octahedral environment, competing with the productive pathway. Hence, C_2-symmetric ligands proved to be superior in this regard.

Temperature

As we have seen in the previous section, ligands of the family of BINAP and SDP are very convenient for the hydroarylation of butyl vinyl ether. Thus, (*R*)-Tol-BINAP **L12b** and (*S*)-SDP **L16b** delivered excellent yields and very good selectivities of 90% and 93% ee respectively. However, the best ligand regarding this feature is **L16c**, affording the product in 95% ee although the yield was rather modest. In view of this situation, we selected these three ligands in order to study the effect of the temperature on the enantioselectivity and yields (Table 19).

Table 19. Temperature optimisation for selected ligands.

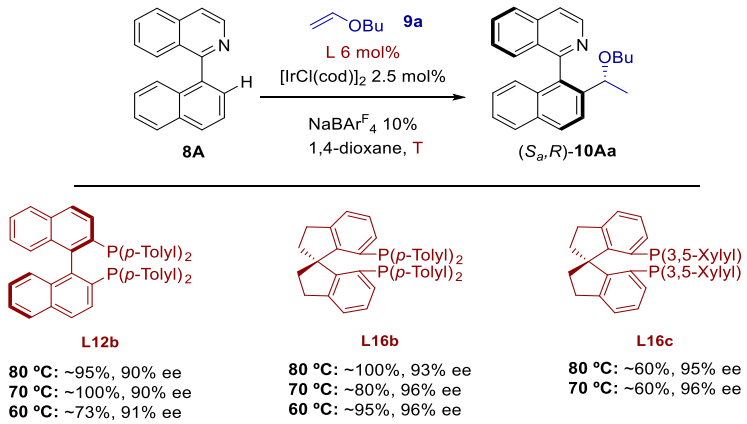

[a] Reactions performed on a 0.1 mmol scale using anhydrous 1,4-dioxane (1 mL/0.1 mmol **8A**) and 5 equiv. of vinyl ether **9a**, for a 24 h period at the given temperature. Yields were determined by ^{1}H NMR spectroscopy of the crude reaction mixture. The *branched/linear* ratio (**10Aa/10Aa´**) and the diastereoselectivity ((*S*$_a$,*R*)-**10Aa**/(*S*$_a$,*S*)-**10Aa**) were also determined by ^{1}H NMR on the reaction crude, being >50:1 and >20:1, respectively, in all cases. [c] The ee values were determined by chiral HPLC analysis. [d] The reaction time was 48 h.

In general terms, decreasing the temperature translated to lower yields and negligible improvement of the selectivity, except for **L16b,** which reached 96% ee (Table 19). In the case of **L16c**, we attributed the low conversion to side-reactions. However, lowering the temperature did not result in any improvement in this regard.

Hence, the optimal conditions were achieved when using **L16b** at 80 ^{o}C; however, extending the reaction time to 48 h at 60 ^{o}C, still provided excellent results in the event of side-reactions.

Chloride scavenger

We have investigated the effect of the ligand in the activity and selectivity of the catalysts. However, we have carried out this screening using the same chloride scavenger, NaBAr$^F_4$. Since the abstraction of chloride from the iridium precursor to activate the catalyst is essential, we decided to screen more available halide-abstracting agents than NaBAr$^F_4$.

From Table 18, we can conclude the best scavenger was by far NaBAr$^F_4$ and hence, it will be utilized in the development of the methodology.

Table 20. Chloride scavenger screening.

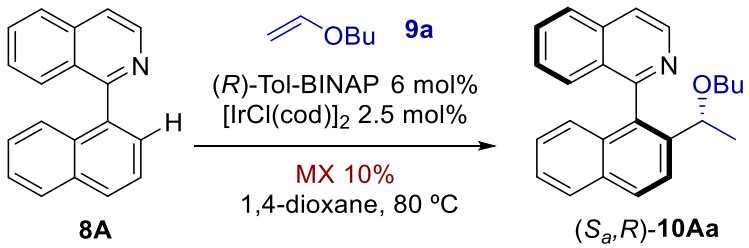

Entry	Halide scavenger	Conv (%)[b]	ee (%)[c]
1	$NaBAr_F$	>95	90
2	$NaBF_4$	n.r.	-
3	KPF_6	n.r	-
4	AgTfO	~8	n.d.
5	$AgSbF_6$	~12	90
6	$AgPF_6$	n.r.	-

[a] Reactions performed on a 0.1 mmol scale using anhydrous solvent (1 mL/0.1 mmol **8A**) and 5 equiv. of vinyl ether **9a**, for a 24 h period at 80 °C. [b]Determined by ^{1}H NMR spectroscopy of the crude reaction mixture. The *branched/linear* ratio (**10Aa/10Aa´**) and the diastereoselectivity ((*Sa,R*)-**10Aa**/(*Sa,S*)-**10Aa**) were also determined by ^{1}H NMR on the reaction crude, being >50:1 and >20:1, respectively, in all cases. [c] Determined by chiral HPLC analysis.

Precatalyst

There exists a number of Ir(I) precatalyst such as $[IrCl(cod)]_2$, $[Ir(OMe)(cod)]_2$, $[IrCl(coe)]_2$, etc. that are used in C-H activation and other reactions. However, the excellent results obtained with the previous optimization of the reaction conditions, make the exploration of other precatalyst redundant. Hence, $[IrCl(cod)]_2$ was maintained as the precatalyst.

Scope

Hydroarylation of vinyl ethers

With these conditions that allows the hydroarylation of butyl vinyl ether with **8A** affording the desired product with excellent results regarding yield, enantio-, diastereo- and regioselectivity; we decided to explore the applicability of this methodology to other heterobiaryls **8B**-**8E** and vinyl ethers **9a-9c**.

As can be seen in Table 21, the reactions gave very good results with alkyl vinyl ethers such as butyl **9a**, cyclohexyl **9b** and ethyl **9c**. However, in the latter case, the reaction had to be carried out at 60 ºC to prevent side-reactions, and using larger amounts of vinyl ethers due to its high volatility (b.p: 33 ºC). It is worth to note these are the only cases in which the diastereoselectivity dropped

slightly from >20:1 to 10:1-15:1 (**10Ac-10Ec**). Additionally, **9c** is also the vinyl ether that afforded the lower enantioselectivity in each series. Thus, it seems that the smaller size of this vinyl ether may account for these poorer selectivites.

On the other hand, the hydroarylation product of **8C** with cyclohexyl vinyl ether, **10Cb**, could be crystallised, obtaining enantioenriched single crystals (from 91 to 99% ee) suitable for X-ray analysis (Figure 36), providing a way to determine the absolute configuration as (S_a,*R*). Assuming chemical analogy is applicable, the rest of the products were subsequently assigned with this configuration.

*Figure 36. X-ray analysis of (Sa,R)-**10Cb***

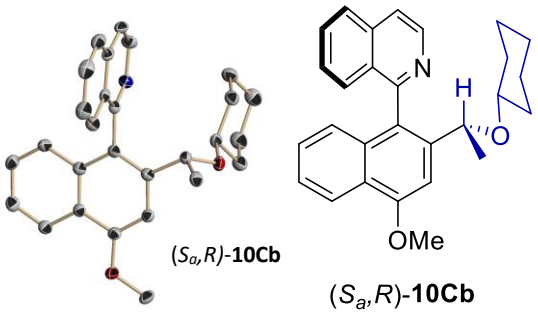

(S_a,*R*)-**10Cb**

Table 21. Reaction Scope: alkyl vinyl ethers.

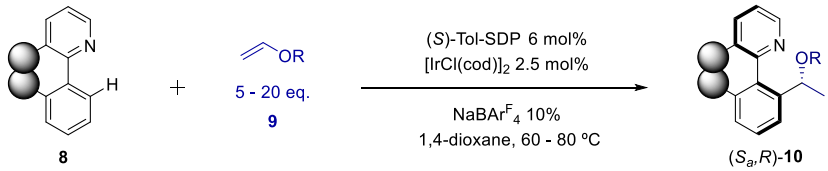

8 (*S*_a,*R*)-**10**

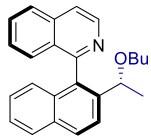

10Aa: 95%, 94% ee

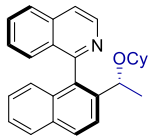

10Ab: 87%, 96%

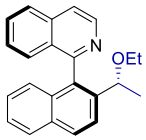

10Ac: 89%[b], 93% ee

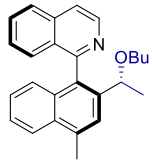

10Ba: 92%, 95% ee

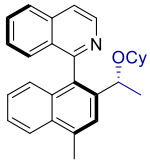

10Bb: 89%,98% ee

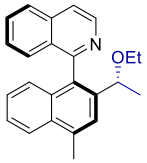

10Bc: 94%[b], 86% ee

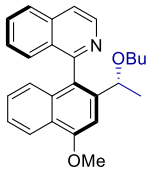

10Ca: 91%, 80% ee

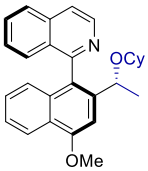

10Cb: 92%,91% ee[d]

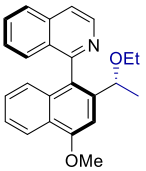

10Cc: 92%[b], 53% ee

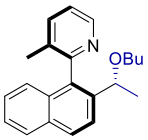

10Da: 94%, 98% ee

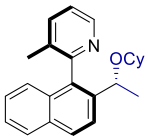

10Db: 87%, 98% ee

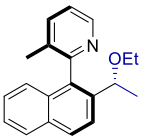

10Dc: 96%[b], 96% ee

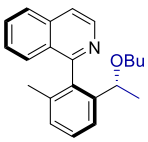

3Ea: 88%[b], 98% ee

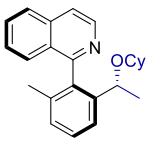

3Eb: 78%[b], 98% ee

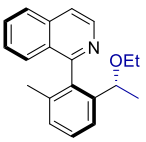

3Ec: 65%[b], 95% ee

[a]Reactions performed on a 0.1 mmol scale using anhydrous 1,4-dioxane (1 mL/0.1 mmol **8A-1E**) and 5 equiv. of vinylether **9a–b**, for a 24 h period at 80 °C. Isolated yields refer to major isomer after chromatography. *Branched/linear (b/l)* ratio and *diastereoisomers ratio (dr)* were determined by ^{1}H NMR in the crude reaction mixtures. The *b/l* ratio and *dr* was >50:1 and >20:1 respectively. Ee's determined by chiral HPLC analysis. [b]20 equiv. of vinyl ether **1c** were used and the reaction was carried at 60 °C for 48 h. The *dr* was 10:1-15:1 in these cases. [c] >99% ee was obtained after single crystallization.

On the other hand, another goal of this methodology is the deprotection of the ethers to achieve the corresponding alcohols and perform other transformations. Thus, we first envisioned the use of trimethylsilyl vinyl ether as an easily removable protecting group upon the hydroarylation (Scheme 0-38). Nevertheless, the reaction with this reactant shut off even under forcing conditions. The reason of this lack of reactivity can be attributed to the bulkier character of the trimethylsilyl moiety.

Scheme 0-38. Hydrosilylation of trimethylsilyl vinyl ether.

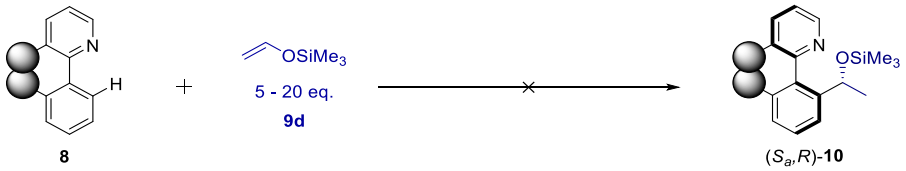

8 (*S*$_a$,*R*)-**10**

Facing this reality, we decided to overcome this problem by using other removable protecting groups. Hence, we carried out the reaction with different vinyl ethers **9e-g** to achieve this goal. In these cases, the reactions proceeded with lower yields, still being good in most cases (Table 22). Among these reagents, PMB vinyl ether **9f** achieved the poorest yields, presumably due to steric reasons. By contrast, benzyl vinyl ether **9e**, despite its similar size afforded slightly better results possibly owing to the flexibility provided by the allylic methylene group. Nevertheless, both enantio- and diastereoselectivity were very good and, in some cases, excellent. The deprotection of these groups will be discuss later though.

Table 22. Reaction scope: vinyl ethers as protected alcohols.

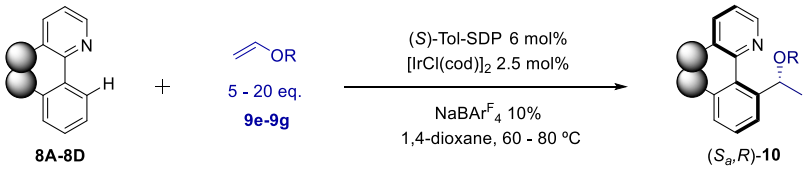

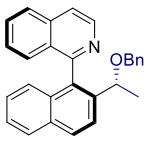

(*S*$_a$,*R*)-**10Ae:** 70%, 97% ee

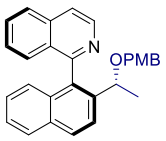

(*S*$_a$,*R*)-**10Af:** 66%, 91% ee

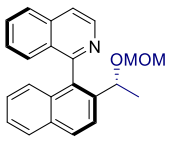

(*S*$_a$,*R*)-**10Ag:**70%, 97% ee

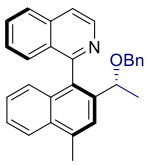

(*S*$_a$,*R*)-**10Be:** 72%, 96% ee

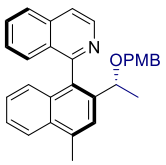

(*S*$_a$,*R*)-**10Bf:** 44%, 98% ee

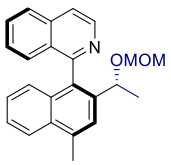

(*S*$_a$,*R*)-**10Bg:** 76%, 98% ee

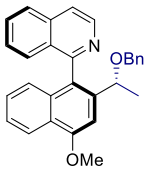

(*S*$_a$,*R*)-**10Ce:** 91%, 91% ee

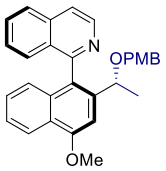

(*S*$_a$,*R*)-**10Cf:** 51%, 89% ee

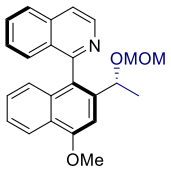

(*S*$_a$,*R*)-**10Cg:** 90%, 89% ee

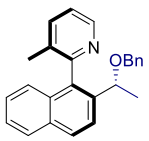

(*S*$_a$,*R*)-**10De:** 45%, 99% ee

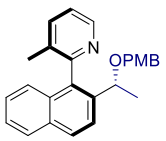

(*S*$_a$,*R*)-**10Df:** 33%, 99% ee

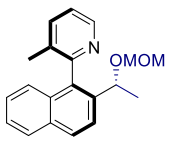

(*S*$_a$,*R*)-**10Dg:** 79%, 99% ee

[a] Reactions performed on a 0.1 mmol scale using anhydrous 1,4-dioxane (1 mL/0.1 mmol **8A-8D**) and 5 equiv. of vinylether **9e-9g**, for a 24 h period at 80 °C. Isolated yields refer to major isomer after chromatography. *Branched/linear (b/l)* ratio and *diastereoisomers ratio (dr)* were determined by ^{1}H NMR in the crude reaction mixtures. The *b/l* ratio and *dr* was in all cases >50:1 and >20:1 respectively. Ee's determined by chiral HPLC analysis. 20 equiv. of vinyl ether **9g-9g** were used and the reaction was carried at 80 °C for 24 h.

Regarding the heterobiaryls, all the three naphthylisoquinoline-based electrophiles (**8A-1C**) underwent the reaction with the different vinyl ethers with very good yield, above 87% in all cases and up to 96%. Interestingly, in the series **3C** corresponding to the 1-(4-methoxynaphthalen-1-yl)isoquinoline, the products could be obtained without loss of enantiopurity, in stark contrast

to the IAN-amine counterparts that underwent racemisation. The reason for this difference might be attributed to the less electronically rich naphthalene ring obtained in the hydroarylation. That is to say, in IAN-type amines, we introduce an amine in the *ortho* substitution, which enhances the electron-rich character of the naphthalene along with the -OMe in *para* position. This way, the strong polarization of isoquinoline and naphthalene ring in the IAN-amines may account for the partial double bond of the axis and consequently, the racemisation of the product. By contrast, the hydroarylation affords a net alkylation at the C2'-position. As alkyl groups are not as donating as amines, the naphthalene is not that electronically rich. Hence, the electronic difference between the rings connected by the axis is not as large as in the previous case and the racemisation is not appreciable.

Regarding the series **D** and **E**, corresponding to 2-(naphthalen-1-yl)-3-picoline and 1-(*o*-tolyl)isoquinoline respectively, we observed a similar behaviour to that of the Buchwald-Hartwig amination. Thus, 2-(naphthalen-1-yl)-3-picoline **D** underwent the hydroarylation reaction with all the selected vinyl ethers in a similar fashion to naphthylisoquinolines. Conversely, when 1-(*o*-tolyl)isoquinoline **E** was used as the substrate, the yields were significantly lower despite the selectivities were maintained. Due to this lack of reactivity, we did not apply the hydroarylation of protected ethers with this substrate.

Likewise, the electronic nature rather than steric factors of the rings seems to be the reason of the different reactivity. Additionally, as the enantioselectivities are not affected in any of the cases, the nature of the heterobiaryls is irrespective to the stereodetermining step of the reaction. Thus, both the stereo- and the turnover determining steps must/could be different.

Other heterobiaryls (Figure 37) that were tested in this reaction were 4-(naphthalen-1-yl)quinazoline **8F** and 1-(naphthalen-1-yl)phthalazine **8G** although these substrates remained unreacted. It is worth to remind that these substrates were troublesome in the dynamic kinetic asymmetric amination, but in this case, a complete lack of reactivity was found.

Figure 37. Studied heterobiaryls for the scope of the hydroarylation of vinyl ethers

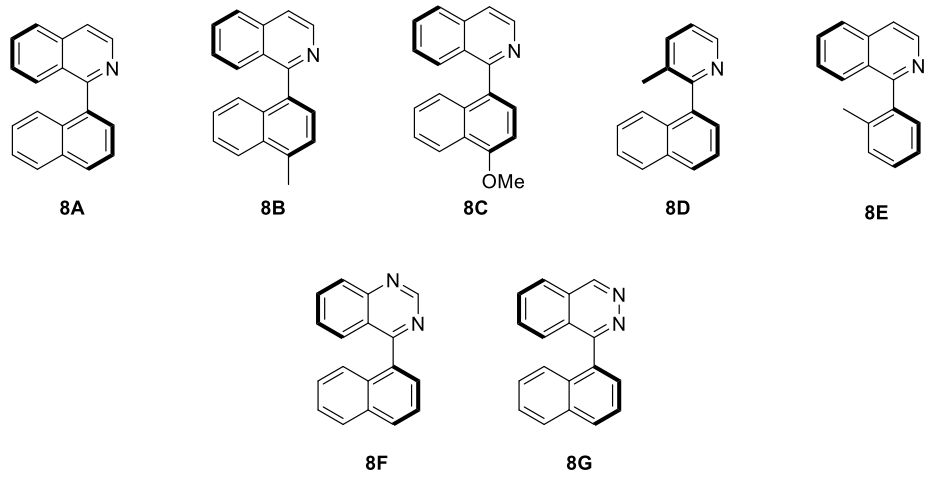

Acyclic internal ethers

Once we have explored the hydroarylation of vinyl ethers, we also wondered if the elongation of alkenyl chain would lead to the product of the hydroarylation and if the stereochemistry of the reaction would be maintained.

In this regard, we performed the reaction with the simplest alkenyl vinyl ether fulfilling this feature; ethyl-1-propenyl ether (Scheme 0-39). However, despite the subtle difference with the corresponding ethyl vinyl ether, the reaction only afforded polymerization products at the best.

Scheme 0-39. Ir(I)-catalysed C-H hydroarylation of ethyl propenyl ether

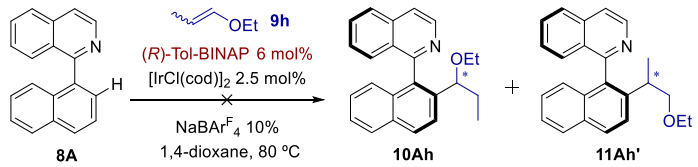

[a] The reaction was performed on a 0.1 mmol scale using anhydrous 1,4-dioxane (1 mL/0.1 mmol **8A**) and 5 equiv. of ethyl-1-propenyl ether (mixture of *cis* and *trans*), for a 24 h period at 80 °C. The axial configuration is arbitrary of the products is arbitrary.

Cyclic vinyl ethers

As the reaction did not work with acyclic internal ethers, we wondered whether the cyclic counterparts would behave in a different way. For this purpose, we chose 2,3-dihydrofuran **9i** as the model vinyl ether and, in this case, the reaction did proceed (Table 23).

Nevertheless, some interesting facts were revealed. First, the diastereoselectivity dropped significantly (~3:1) and therefore, the individual yields were modest at the best. On the other hand, the enantioselectivity for the major diastereoisomers were in accordance to those obtained so far and above 92% ee. By contrast, the minor isomer was obtained in much lower enantiopurity (from 12% ee to 32% ee). The only exception was the case of the rather unreactive (*o*-tolyl)isoquinoline **8E**; in which the minor isomer were obtained with moderate enantioselectivity (76% ee). In this regard, the small size of the 2,3-dihydrofuran **9i** and its relative rigidity may result in a bad enantio- and diastereo-differentiation during the reaction.

Table 23. Scope of the Hydroarylation of 2,3-dihydrofuran.

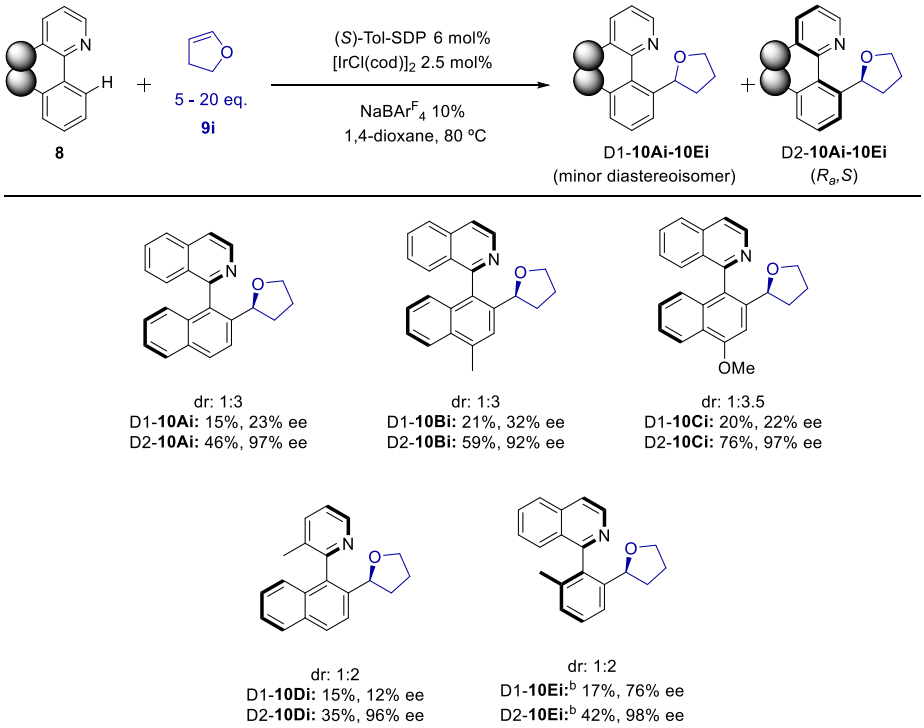

[a] Reactions performed on a 0.1 mmol scale using anhydrous 1,4-dioxane (1 mL/0.1 mmol **8A-1E**) and 10 equiv. of vinyl ether **2i**, for a 24 h period at 80 °C. Isolated yields refer to major isomer after chromatography. *Diastereoisomers ratio (dr)* were determined by ^{1}H NMR in the crude reaction mixtures. Ee's determined by chiral HPLC analysis. [b] 20 equiv. of vinyl ether **2i** were used and the reaction was carried at 80 °C for 24 h.

As we have previously mentioned, the absolute configuration of the products were assigned by analogy (*S*$_a$,*R*)-**10Cb**. However, as the hydroarylation products of 1,2-dihydrofuran were obtained with low diastereoselectivity (**10Ai**-**10Di**) and chemical correlation is no longer applicable, the confirmation

of the absolute configuration was mandatory. Indeed, after crystallisation of D2-**10Ai**, X-ray analysis of the crystals revealed the absolute configuration of the major diastereoisomer was the opposite to that of the products obtained so far (Figure 38).

*Figure 38. X-ray structures of (S_a,R)-**10Cb** and(R_a,S)-D2-**10Ai***

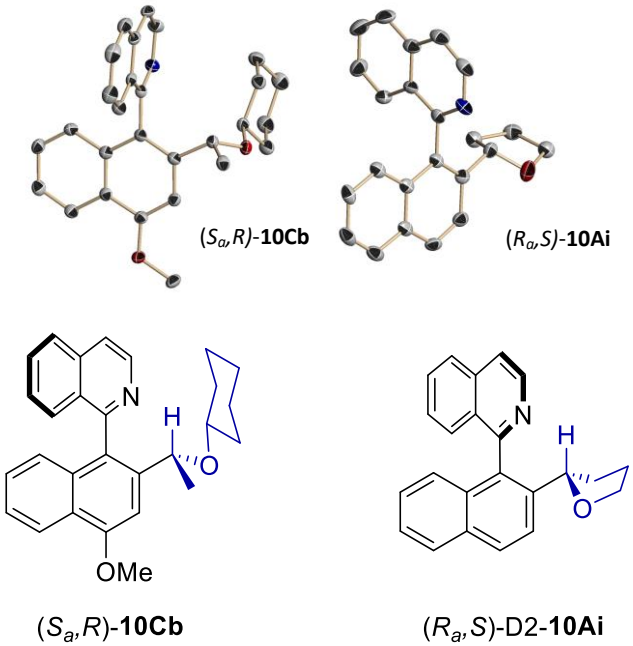

(S_a,R)-**10Cb** (R_a,S)-D2-**10Ai**

The reaction was also carried out with 2,5-dihydrofuran **9j** and 3,4-dihydro-2*H*-pyran **9k** (Figure 39.A); however, even under forcing conditions the hydroarylated product was not obtained. On the one hand, the absence of polarisation and the internal character of the double bond in **9j** may account for its lack of reactivity (Figure 39.C). On the other, **9k** seems to function as an acyclic internal alkenyl ether. This difference in reactivity between these two internal cyclic vinyl ethers **9i** and **9k** may be explained in terms of steric hindrance and strain energy in the case of dihydrofuran **9i**.

Figure 39. Cyclic alkenyl ethers for the scope for the hydroarylation reaction

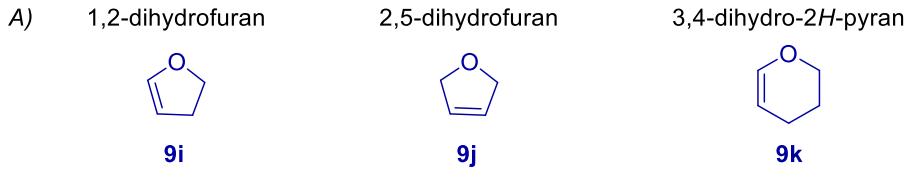

Hydroarylation of other alkenes

As we have seen with the case of 2,5-dihydrofuran **9j**, the reaction showed a completely lack of reactivity, presumably due to both to the lack of polarisation of the double bond and mainly, its internal character. With this hypothesis in mind, we then wondered whether acyclic alkenes would be more reactive to undergo the hydroarylation reaction (Scheme 0-1Scheme 0-40).

Scheme 0-40. Hydroarylation of other terminal alkenes

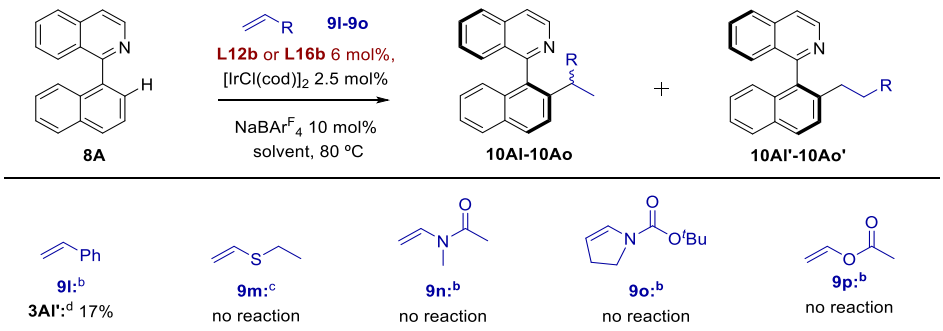

[a] The reaction was performed on a 0.1 mmol scale using anhydrous 1,4-dioxane (1 mL/0.1 mmol **8A**) and 5 equiv. of vinyl ether **9l**, for a 24 h period at 80 °C. [b] **L12b** was used as the ligand. [c] **L16b** was used as the ligand. [d] Enantiomeric excess was not determined and the absolute configuration is arbitrary.

Hence, we tested styrene **9l** as model substrate for this reaction. Unfortunately, the reaction was incomplete although two products were formed. Thus, the major product of the reaction was the linear regioisomer

which was obtained in a 17% yield. The minor pointed to be the branched product but it could not be characterized due to the low yield. This result made us thought that an important feature was the electronically rich character of the vinyl ethers in contrast to styrene.

This being the case, we decided to study the behaviour of other alkenes bearing heteroatom-based functionalities different to ethers. Thus, the electron donation from these functionalities to the vinyl group would lead to its activation in relation to the hydroarylation reaction. First, we attempted the reaction with ethyl vinyl sulphide **9m**, which is a very challenging substrate owing to the poisoning nature of sulphur compounds. Unfortunately, the vinyl sulphide did not undergo the hydroarylation reaction, possibly due to the aforementioned reason.

Regarding the nitrogen analogues, we selected methyl vinyl acetamide **9n** and *N*-Boc 2,3-dihydropyrrole **9o**, which proved to be reactive in the Heck-based DYKAT,[253] to explore their reactivity. It is worth to notice that the secondary substitution at the heteroatom position is necessary to avoid the imine-enamine tautomerism, although the steric hindrance of these substrates is subsequently higher. Thus, it is not surprising that these vinyl derivatives did not underwent the reaction. Nevertheless, not only steric factors can be attributed for this lack of reactivity; the electronic nature may play an important role, though. Hence, in these cases, the electron-withdrawing character of the *t*-butoxycarbonyl and acetyl groups make the alkenes less electronically rich than expected. In addition, the contribution of the electron-rich alkene at the β position to the structure of these compounds is the least important; and the substrate is furtherly stabilized by resonance. In a similar vein, we can explain the lack of reactivity of vinyl acetyl ether **9p** (Scheme 0-41).

Scheme 0-41. Resonance structures of alkenes bearing electron-withdrawing groups in α-position.

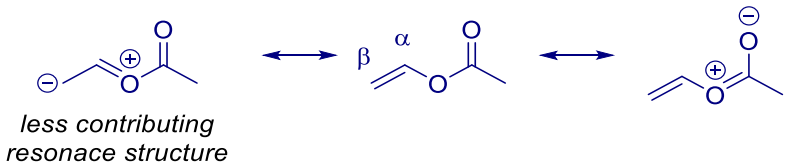

[253] (1) Carmona, J. A.; Hornillos, V.; Ramírez-López, P.; Ros, A.; Iglesias-Siguënza, J.; Gómez-Bengoa, E.; Fernández, R.; Lassaletta, J. M. Dynamic Kinetic Asymmetric Heck Reaction for the Simultaneous Generation of Central and Axial Chirality. *J. Am. Chem. Soc.* **2018**, *140* (35), 11067–11075. https://doi.org/10.1021/jacs.8b05819.

Hydroarylation of strained cycloalkenes

In view of this different reactivity relying presumably on the strain of the cyclic vinyl ethers, we decided to explore the reactivity of strained alkenes and check whether the strain energy could balance the lack of an electron-donor group attaching the α position. As the model reaction, we selected the hydroarylation of norbornene[248] **9q** using (*R*)-BINAP **L12a** as the ligand, which also showed good results in the reaction with vinyl ethers and its lower cost in contrast to SDP ligands makes this bisphosphine be an excellent ligand in preliminary experiments (Table 18). Thus, norbornene **9q** underwent the hydroarylation with full conversion affording the *exo* product, which is the normal isomer for these reactions, [248a,254] with excellent enantioselectivities (~94% ee, Scheme 0-42).

By contrast, the reaction with norbornadiene **9r** did not take place. This is not surprising, since cyclic dienes are common ligands for transition metal complexes. Indeed, the iridium precursor is a cyclooctadiene complex, and some hydroarylations have been reported to be catalysed with this and other chiral dienes as ligand.[239,249,250] Hence, the large molar amount related to the metal and the possible formation of stable chelated complexes may prevent the reaction (Scheme 0-42).

[254] (1) Shibata, K.; Natsui, S.; Tobisu, M.; Fukumoto, Y.; Chatani, N. An Unusual Endo-Selective C-H Hydroarylationof Norbornene by the Rh(I)-Catalysed Reactionof Benzamides. *Nat. Commun.* **2017**, *8* (1), 1–8. https://doi.org/10.1038/s41467-017-01531-2.

Scheme 0-42. Preliminary experiments for the hydroarylation of norbornene and norbornadiene

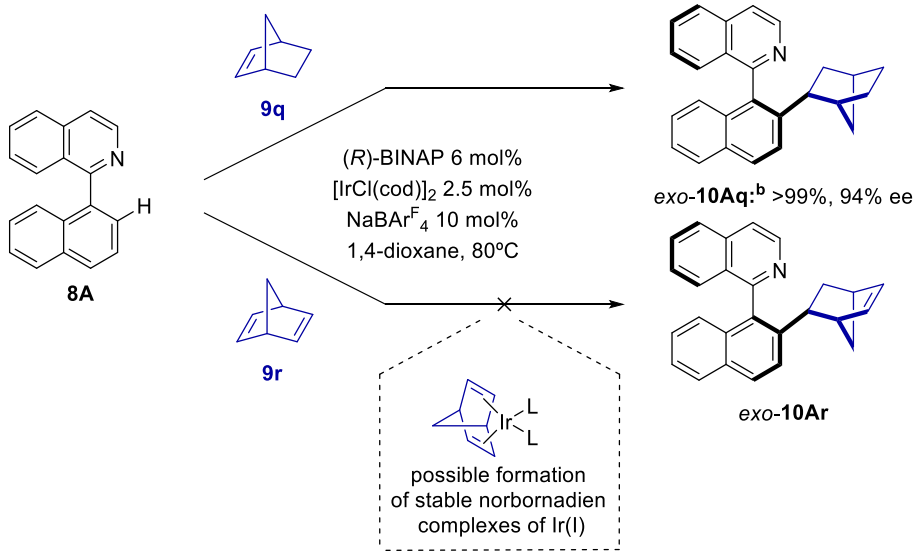

[a] Reactions weree performed on a 0.1 mmol scale using anhydrous 1,4-dioxane (1 mL/0.1 mmol **8A**) and 5 equiv. of vinyl ether **9q**-**9r**, for a 24 h period at 80 °C. [b] ee value was determined by chiral HPLC analysis.

Screening of the reaction conditions

Optimization of the stoichiometry and temperature of the reaction

Taking into consideration the very good results achieved with the use of norbornene as the substrate for the hydroarylation reaction, we first optimised the stoichiometry of the norbornene and the catalyst for 2 reasons. First, we might achieve complete yield and enantioselectivity owing to the excellent starting point of this optimisation. Second, once these parameters have been optimised, the ligand screening would be more straightforward. In the table below, the results of this optimisation are summarised.

Table 24. Optimisation of the reaction temperature and stoichiometry.

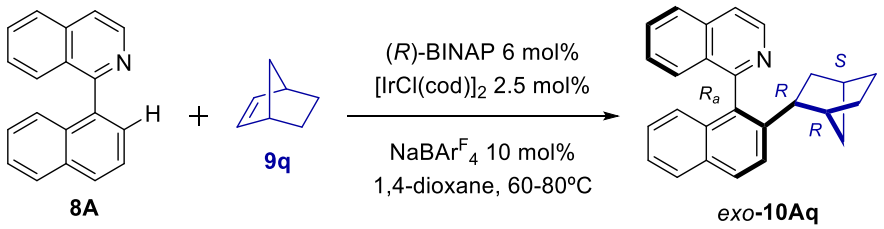

Entry	[Ir]	Norb / eq	T / ºC	Yield (%)[b]	ee (%)[c]
1[a]	5%	5	80	>99%	~94%
2[a]	**5%**	**5**	**60**	**95%**	**98%**
3[a]	5%	2	80	90%	92%
4[a]	5%	2	60	~50%[d]	96%
5[e]	2.5%	5	60	~85%[d]	96%
6[f]	2.5%	5	60	>99%	77%

[a] 0.1 mmol scale, 1 mL dioxane/0.1 mmol substrate, 24 h reaction time. **L12A** was used as ligand. [b] Isolated yield. [c] Determined by HPLC. [d] ^{1}H-NMR yield. [e] 0.2 mmol scale, 1 mL dioxane/0.1 mmol substrate. [f] 0.2 mmol scale, 0.5 mL dioxane/0.1 mmol substrate. [g] 0.1 mmol scale, 0.5 mL dioxane/0.1 mmol substrate.

As expected, a drop in the temperature from 80 ºC to 60 ºC gave the product in lower yields but the enantioselectivity rose slightly. This phenomenon can be observed in both reactions using 5 and 2 equivalents of the alkene (Table 24, entries 1-2 and 3-4). In this regard, the reaction took place providing better results with 5 equivalents of norbornene. As the coordination of the alkene might play a key role in the reaction, this step would be influenced by its concentration. By contrast, when the catalyst loading is lowered from 5 mol% to 2.5 mol%, a drop in the yield was observed (Table 24, entry 2 vs 5). In addition, when doubling the concentration of all of the reagents (Table 24, entry 5 vs 6) the product was obtained in full conversion. Actually, the yield of entry 6 was even better than that of entry 2. However, the selectivity was lower and could be ascribed to the modification of the catalytic system under such a big change in the reaction conditions.

In short, the enantioselectivity could be improved by lowering the temperature to 60 ºC and utilizing 5 equivalents of norbornene. Thus, the product *exo*-**10Aq** was obtained in 95% and 98% ee.

Ligand screening

Encouraged by the results provided by the optimisation of stoichiometry and temperature, we decided to further improve the selectivity and yield of the hydroarylation of this kind of substrate by screening other ligands. For this

purpose, we made a selection of the ligands previously screened for the hydroarylation of vinyl ethers (Table 25).

First, the family of BINAP was significantly most active and afforded better enantioselectivities in general terms. Parallel to the hydroarylation of vinyl ethers, (*R*)-DM-BINAP **L12c** showed the lowest activity within this family. Similarly, (*R*)-Tol-BINAP **L12b** afforded the best results. Disappointingly, (*S*)-Tol-SDP **L16b**, which previously gave excellent results with vinyl ethers, is now a less active catalyst despite its excellent enantioselectivity (Table 25, entry 5). On the other hand, biphenyl-based bisphosphines **L15** and **L17** afforded the product in much lower yields and selectivities. Interestingly, **L17** gave the product with the opposite absolute configuration albeit almost racemic. Therefore, the best ligand performing this reaction was (*R*)-Tol-BINAP **L12b.**

Table 25. Screening of the reaction conditions and ligands for the hydroarylation of norbornene.

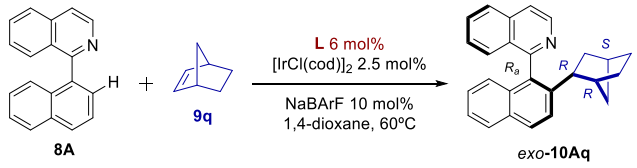

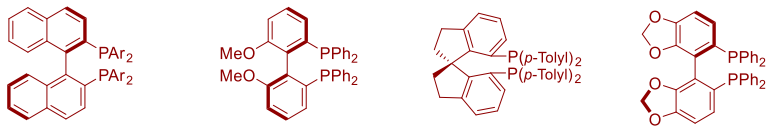

L12a: (*R*)-BINAP (Ar = Ph)
L12b: (*R*)-Tol-BINAP (Ar = *p*-Tolyl)
L12c: (*R*)-DM-BINAP (Ar = 3,5-Xylyl)

L15:: (*R*)-MeO-BIPHEP

L16b: (*S*)-Tol-SDP (Ar = *p*-Tolyl)

L17: (*R*)-SEGPHOS

Entry	[Ir]	Ligand	Yield (%)[b]	ee (%)c
1	2.5%	**L12a**	~85[d]	96
2	2.5%	**L12b**	>96	97
3	2.5%	**L12c**	81	75
4	2.5%	**L15**	60	51
5	2.5%	**L16b**	27	98
6	2.5%	**L17**	7.5	-5

[a] 0.1 mmol scale, 1 mL dioxane/0.1 mmol substrate, 24 h reaction time. [b] Isolated yield. [c] Determined by HPLC. [d] ^{1}H-NMR yield.

Scope of the hydroarylation reaction with norbornenes

With the best conditions in hand, we next decided to study the scope of the reaction. Thus, we made a selection of different N-containing heterobiaryls with norbornene and some derivatives (Table 26).

Regarding the parent norbornene **9q**, most of the reactions afforded the product in excellent yield and enantioselectivity (>88%, >90% ee). The only exception was the reaction carried out with 1-(4-methoxy-1-naphthyl)-isoquinoline **8C**, which gave the product in modest yield (43%) despite the optical purity was excellent (97%). Significantly, 2-(4-methoxy-1-naphthyl)-3-picoline **8H** gave a much better yield than the corresponding isoquinoline counterpart (**10Hq** vs. **10Cq**). This structure could be crystallised and analysed by X-ray diffraction, revealing the *exo* and the absolute configuration (R_a,*R*,*R*,*S*) of the product (Figure 40).[255] On the other hand, the reaction with the less reactive 1-(*o*-tolyl)isoquinoline **8E** and 4-(naphthalen-1-yl)quinazoline **8F**, which did not underwent the hydroarylation of vinyl ethers, were accomplished at 80 °C to enhance the reactivity. Thus, the products were obtained with excellent yield but with the lowest enantioselectivity of the series, specially **10Fq**.

Table 26. Scope for the hydroarylation of norbornene.

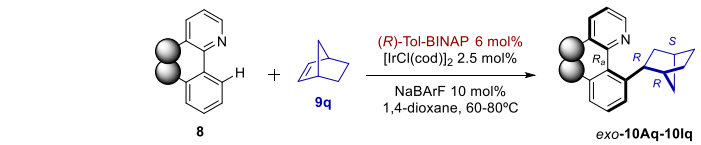

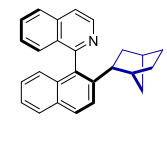

(R_a,*R*,*R*,*S*)-**10Aq:** >99%, 98% ee

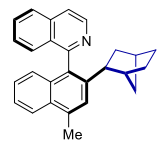

(R_a,*R*,*R*,*S*)-**10Bq:** 99%, 95% ee

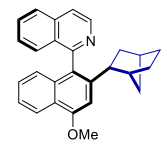

(R_a,*R*,*R*,*S*)-**10Cq:** 43%, 97% ee

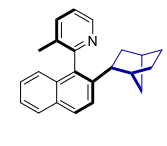

(R_a,*R*,*R*,*S*)-**10Dq:** 96%, 99% ee

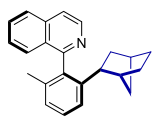

(R_a,*R*,*R*,*S*)-**10Eq:** 88%, 94% ee[b]

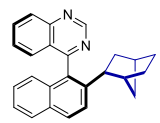

(R_a,*R*,*R*,*S*)-**10Fq:** 95%, 90% ee[b]

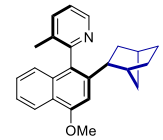

(R_a,*R*,*R*,*S*)-**10Hq:** >99%, >99% ee

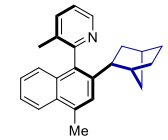

(R_a,*R*,*R*,*S*)-**10Iq:** 89%, 97% ee

[a] Reactions performed on a 0.1 mmol scale using anhydrous 1,4-dioxane (1 mL/0.1 mmol **8A-8F, 8H** or **8I**) and 5 equiv. of norbornene **9q**, for a 24h period at 60 °C. Isolated yields after chromatography purification. Only *exo* diastereoisomer was observed by ^{1}H NMR analysis of the reaction crudes. Ee's determined by chiral HPLC analysis. [b] Reaction carried out at 80 °C for 24h.

[255] The rest of the series were assigned by chemical analogy.

Figure 40. X-ray structure of 3-Hq

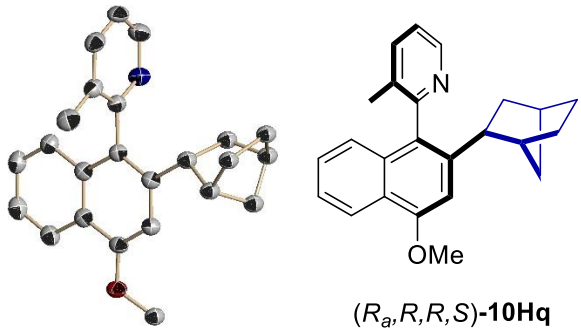

(R_a,*R*,*R*,*S*)-**10Hq**

On the other hand, diol **9r** did undergo the reaction affording the hydroarylation product with excellent results, and hence, it was selected to extend the scope to the rest of the heterobiaryls (Table 27). In general terms, the reaction proceeded with moderate to very good results; although they were not as good as those provided by the parent norbornene **9q**. However, **10Cr** was obtained in a higher yield than the corresponding **10Cq**. Nevertheless, the optical purity of the products was still excellent and above 89% ee.

Norbornene **9r** was also set up to react with 4-(naphthalen-1-yl)quinazoline **8F** and 1-(*o*-tolyl)isoquinoline **8E**; but not surprisingly, no product was obtained due to the poor reactivity of these heterobiaryl systems.

*Table 27. Scope for the hydroarylation of norbornene-derived diol **2r***

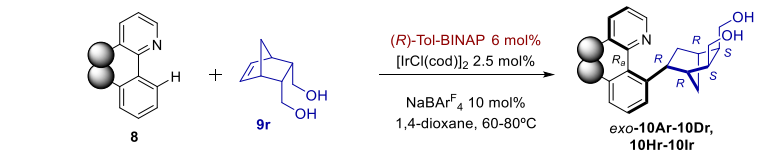

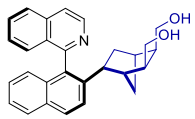

(R_a,*R*,*R*,*R*,*S*,*S*)-**10Ar:**
>99%, 98% ee

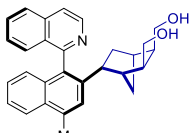

(R_a,*R*,*R*,*R*,*S*,*S*)-**10Br:**
77%, 89% ee

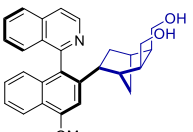

(R_a,*R*,*R*,*R*,*S*,*S*)-**10Cr:**
72%, 92% ee

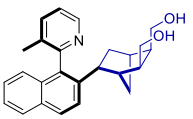

(R_a,*R*,*R*,*R*,*S*,*S*)-**10Dr:**
80%, 93% ee

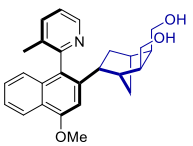

(R_a,*R*,*R*,*R*,*S*,*S*)-**10Hr:**
83%, 98% ee

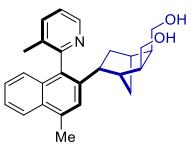

(R_a,*R*,*R*,*R*,*S*,*S*)-**10Ir:**
86%, 92% ee

[a] Reactions performed on a 0.1 mmol scale using anhydrous 1,4-dioxane (1 mL/0.1 mmol **8A-8D**, **8H-8I**) and 5 equiv. of norbornene **9r**, for a 24h period at 60 °C. Isolated yields after chromatography purification. Only *Exo* diastereoisomer was observed by ^{1}H NMR analysis of the reaction crude. Ee's determined by chiral HPLC analysis. [b] Reaction carried out at 80 °C for 24h.

As we also wanted to extend the scope to other norbornene derivatives we carried out the hydroarylation reaction of different compounds of this nature with naphthylisoquinoline **8A** as preliminary experiments (Table 28). Unfortunately, the reactions with **9s** and **9t** did not took place. By contrast, **9u** underwent the hydroarylation with naphthylisoquinoline **8A** affording the product in a 33% yield.[256] However, since the yield was rather low, we ruled out this norbornene as a substrate for the scope of the reaction.

Given the good reactivity provided by some norbornenes, we also wanted to study the reactivity of other strained cyclic alkenes in the hydroarylation reaction. Thus, we selected indene **9w**, cyclopentene **9y**, and we also applied these new conditions to the previously studied 2,5-dihydrofuran **9j** (Table 28). First, the reaction of cyclopentene **9y** with naphthylisoquinoline **8A** using (*R*)-Tol-BINAP as the catalyst, afforded the product in 19% and 97% ee (**10Ay**) and other side-products were detected by TLC. Despite the excellent enantiopurity of the product, the yield was quite poor. In a similar manner, indene **9w** did not undergo the hydroarylation.

Table 28. Selected norbornene-like structures and other strained alkenes to study the scope of the reaction.

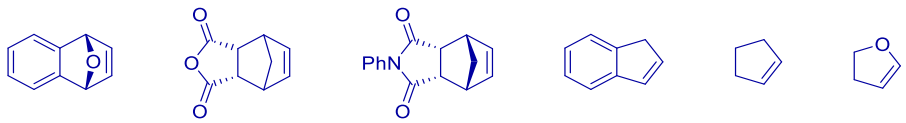

9s **9t** **9u** **9w** **9y** **9j**

By contrast, when the reaction of 2,5-dihydrofuran **9j** was examined, an increase of the yield was observed and the major diastereoisomer was obtained in 58% although the enantioselectivity dropped to 86% ee. Interestingly, the hydroarylation seem to occurs at C2, that is to say, the product obtained corresponds to D1-**10Ai** according to the HPLC and ^{1}H NMR traces. The other diastereoisomer was not isolated but the analysis of the crude seems to indicate that there is a correlation to D2-**10Ai**. In a similar vein to 1,2-dihydrofuran, the diastereoselectivity was also lower in this case (dr ~1:3). However, this process is not surprising as Nishimura have already

[256] The ee value was not determined.

coupled the isomerisation of alkenyl ethers to the hydroarylation reaction (Scheme 0-43).[251]

Scheme 0-43. Plausible mechanism for the hydroarylation of 2-hydrofuran at C2-position.

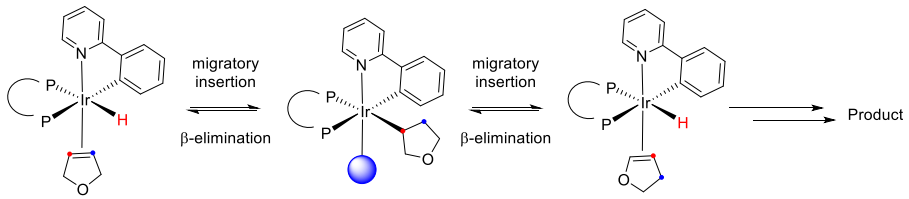

[a] Sterechemistry of octahedral complexes is arbitrary and naphthylisoquinoline is represented by phenylpyridine.

Ether deprotection and subsequent derivatization of the corresponding alcohols

Considering the synthetic utility of the heterobiaryls controlling both axial and central chirality and the possibility of being transformed in other functional group, we envisaged the deprotection of the corresponding ethers **3** as a starting point to achieve this goal (Scheme 0-44).

Scheme 0-44. Ether deprotection and further transformation.

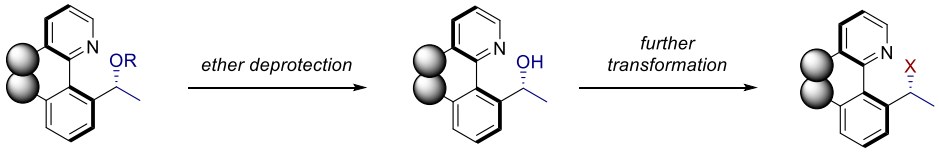

On the other hand, we have seen that heterobiaryls benzylic ethers **10** can be obtained from a broad number of vinyl ethers **9**; however, the deprotection to afford the corresponding alcohols is limited to the lability of the "protecting group". In this regard, most of alkyl ethers are quite stable, while allylic and benzylic groups are easier to remove.

Hence, we thoroughly performed the hydroarylation reaction with several vinyl ethers that could be potentially easy to deprotect. These were the cases of benzyl **9e**, *p*-methoxybenzyl **9f** and methoxymethyl **9g** vinyl ethers, whose results have already been described (Table 22). By contrast, the attempts to remove these groups in order to achieve the free alcohols will be described below.

Deprotection of heterobiaryl benzylic ethers

Benzyl group cleavage

We first endeavoured to deprotect benzyl ether (S_a,*R*)-**10Ad**, as there exists a greater number of methods for the cleavage of this group. In this regard, a classic removal of benzyl groups is achieved by hydrogenation under catalytical conditions using Pd/C. It is worth to notice that our ether is comprised by two benzylic groups and therefore, selectivity issues may ensue from the use of this method. Hopefully, relying on the steric differentiation of the two benzylic groups we performed the reaction to obtain the alcohol selectively. Unfortunately, the reaction did not take place and the substrate remain unreactive (Scheme 0-45).

Scheme 0-45. Hydrogenolysis of benzyl group

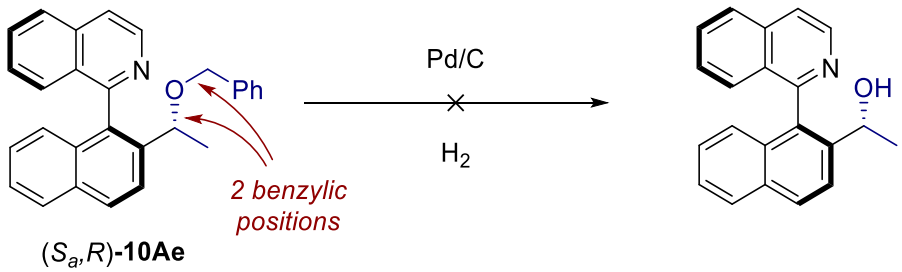

(S_a,*R*)-**10Ae**

In view of this lack of reactivity under these mild conditions we decided to apply a slightly more severe procedure. Thus, we attempted the cleavage of the benzyl group using BBr_3 in DCM, assuming a selective reaction by steric reasons. This time, the reaction took place at room temperature and a product could be obtained in high yield. However, the isolated product did not correspond to the free alcohol **11A** but the bromide **12A** (Scheme 0-46).

*Scheme 0-46. Reaction of (S_a,R)-**10Ae** with BBr_3.*

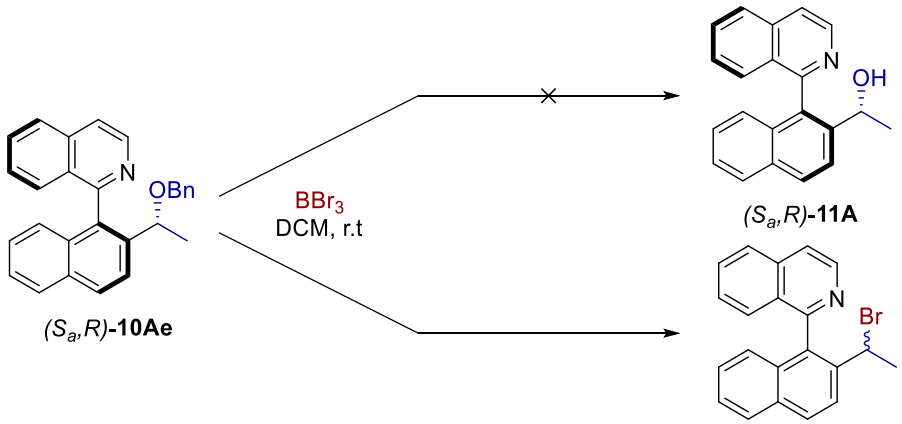

(S_a,*R*)-**10Ae**

(S_a,*R*)-**11A**

12A: 90%, 85:15 dr

Moreover, not only the substitution product was obtained with a significant drop of the diastereomeric ratio (from >20:1 to ~6:1), but with partial racemisation as well. These two processes, the epimerisation and racemisation, can be explained by the activation of the ether by BBr_3 and the subsequent attack of the naphthylisoquinoline nitrogen atom (Scheme 0-47). The resulting cyclic intermediate, results in a labilisation of the axis, in a similar vein to the 5-membered cycle intermediates of the hydrosilylation of ketones;[257] and the subsequent attack of the bromide anion also translates to the racemisation of the stereocenter.

Scheme 0-47. Substitution reaction with subsequent epimerization and racemisation processes

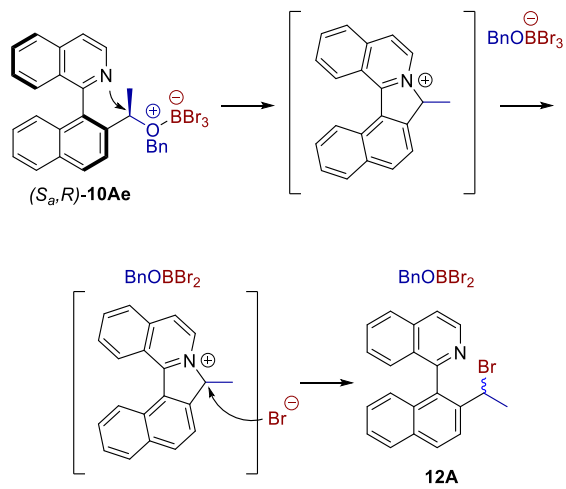

On the other hand, *p*-methoxybenzyl groups are reported to undergo ether cleavage by the action of DDQ as oxidant and subsequent hydrolysis. Applying this procedure (Scheme 0-48), the substrate underwent the deprotection and the alcohol could be obtained in low yields though. It is noteworthy that the reaction proceeded through a complex slurry mixture and the substrate is prone to oxidation at the nitrogen. Then, it is not surprising the lack of a smooth and efficient deprotection using this method.

Scheme 0-48. Deprotection of PMB group and mechanism of deprotection.

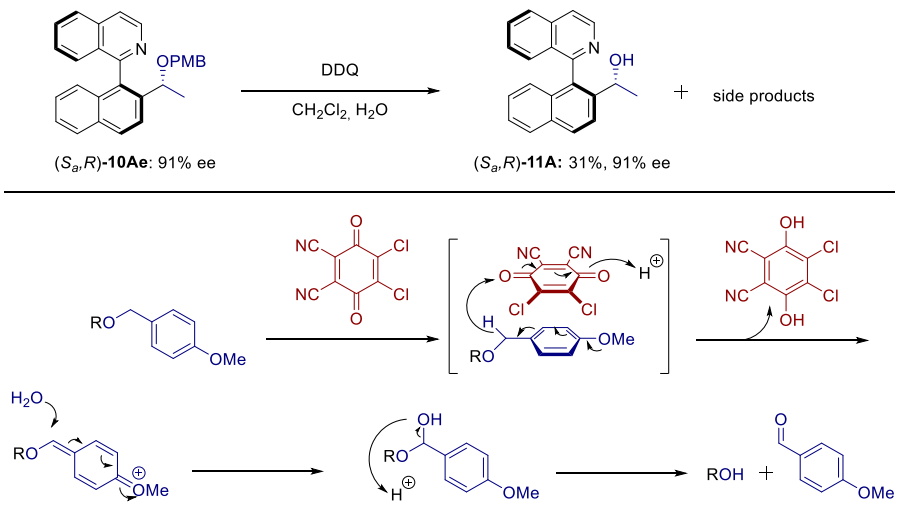

Methoxymethyl group cleavage

Since the previous ethers could not be easily deprotected, we needed another one that was much more labile. In relation to this, we envisioned the use of methoxymethyl vinyl ether, which could be easily removed in acidic media.

Once the corresponding hydroarylation products of this ether were synthesised, we accomplished several experiments with (S_a,*R*)-**10Ag** to find the optimal conditions for the deprotection. After several sets of acidic conditions, we observed that the alcohol could be obtained in good yields and excellent enantiorretention employing TfOH in DCM. The procedure was then apply to the rest of MOM-derivatives obtaining the corresponding alcohols in moderate to very good yield and without loss of chiral information (Scheme 0-49).

Scheme 0-49. Deprotection of MOM group

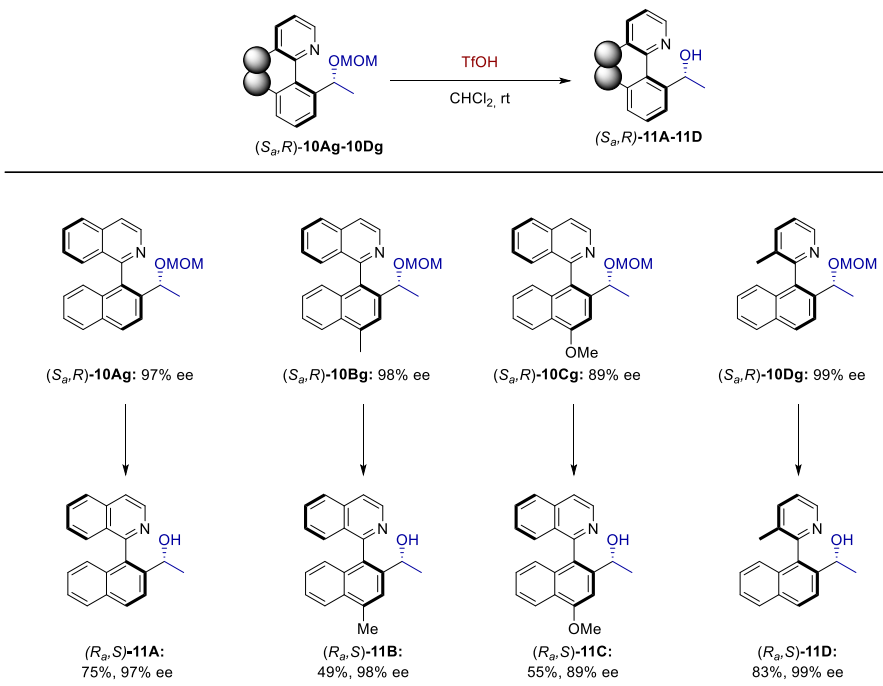

Derivatization of the heterobiaryl benzylic alcohols

With the desired amino-alcohols (R_a,*S*)-**4** in hand, and considering hydroxyl groups are very versatile functionalities, we considered the further transformation of these compounds. In fact, the corresponding amines can be seen as *N,N*-diamines, closely related to IAN-type ones. Moreover, these *N,N*-amines have a great potential as catalysts by themselves or by transformation into more complex organocatalysts.

In this regard, our group have recently proved the versatility of (R_a,*R*)-alcohols derived from the hydrosilylation of ketones[257] as they also were transformed into the corresponding azide, amine, etc. Thus, we applied the same procedures to the alcohols (S_a,*R*)-**11A** and (S_a,*R*)-**11D**. First, the treatment with DPPA (diphenyl phosphorazidate) with DBU afforded the corresponding azides (S_a,*S*)-**13A** and (S_a,*S*)-**13D** which were then reduced applying Staudinger reaction. The amines (S_a,*S*)-**14A** and (S_a,*S*)-**14D** were then obtained in good yields and excellent enantioselectivities (Scheme 0-50).

Scheme 0-50. Synthesis of N,N-diamines from the corresponding alcohols.

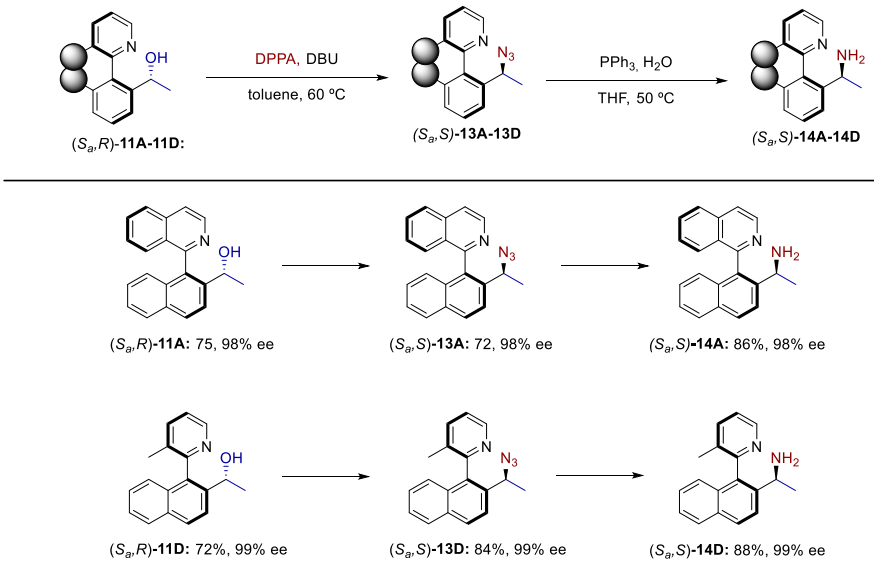

In addition, if we analyse the absolute configuration of these alcohols **11A**-**11D** with those obtained by the previously reported method, i.e. the hidrosilylation of ketones,257 we can notice that both series are diastereoisomeric. Hence, combining both methodologies we can access to all the possible diastereo- and enantiomers (Scheme 0-51).

[257] (1) Hornillos, V.; Carmona, J. A.; Ros, A.; Iglesias-Sigüenza, J.; López-Serrano, J.; Fernández, R.; Lassaletta, J. M. Dynamic Kinetic Resolution of Heterobiaryl Ketones by Zinc-Catalysed Asymmetric Hydrosilylation. *Angew. Chemie - Int. Ed.* **2018**, *57* (14), 3777–3781. https://doi.org/10.1002/anie.201713200.

Scheme 0-51. Complementary methods for the synthesis of heterobiaryl amino-alcohols.

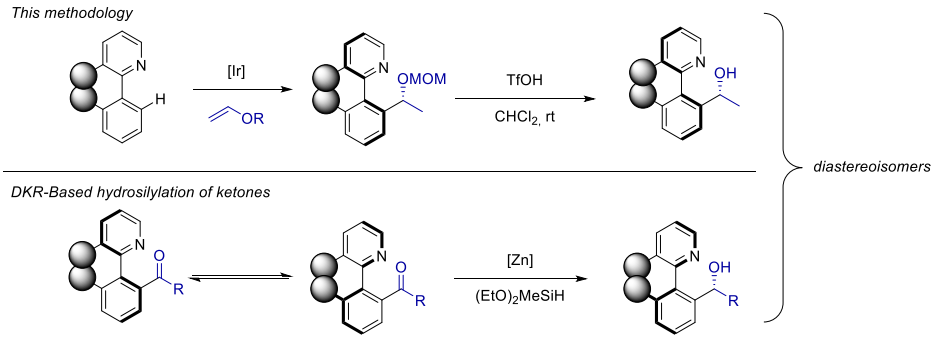

Reaction mechanism

Taking into account that this methodology can promote the formation of heterobiaryls exhibiting both axial and central chirality with complete regio-, diastereo- and enantioselectivities; we decided to obtain further insight into the reaction mechanism by means of experimental and theoretical techniques.

Isotopical labelling and KIE determination

In this regard, we first accomplished an experiment using the deuterated version of our model substrate, naphthylisoquinoline **8A**. The aim of this experiment is to determine if there exists a Kinetic Isotopic Effect (KIE) and to monitor the fate of the deuterium atom. Therefore, this information could disclose some fundamental aspects of the reaction.

First, the determination of the KIE would allow us to know if the rate-determining step is governed by the cleavage/formation of the C-H bond. And second, the resulting isotopically labelled product and recovered starting material would inform us about the regiochemistry of the reaction.

In order to determine the KIE we performed two parallel reactions using respectively the heavy and the light naphthylisoquinoline **8A-d$_1$** and **8A**. Then, the KIE value was determined by the conversion/yield after 4 h, i.e., before complete conversion could be achieved (Scheme 0-52). These data were measured by NMR, isolated products and mass spectrometry depending on each case.

Performing this experiment, important information could be obtained and all these results are summarized in the following figure and table.

Scheme 0-52. KIE determination by parallel reactions.

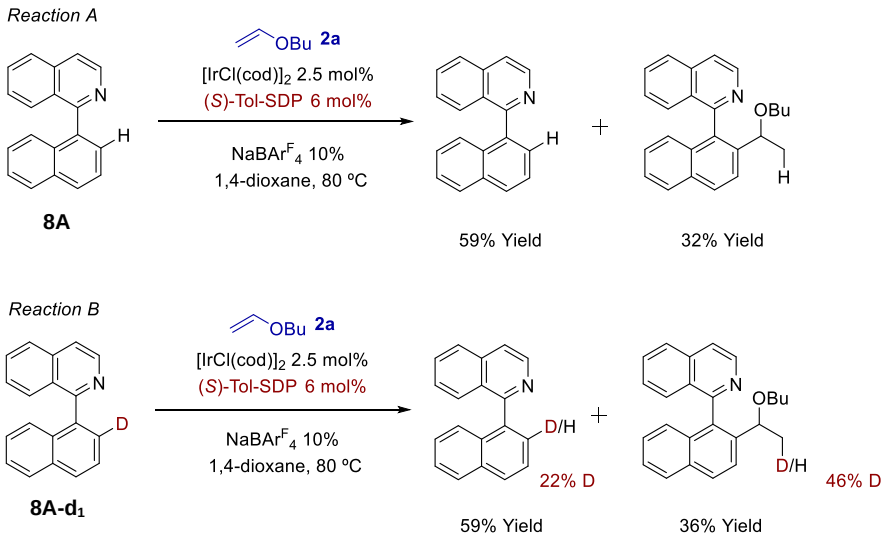

Experiment	Reaction A	Reaction B
Isolated Yield	32%	46%
1H NMR Yield	38%	40%
KIE	**~0.9**	**~0.9**
deuterated product	-	38% (NMR) / 46% (MS)
Deuterated recovered starting material	-	20% (NMR) / 22.4% (MS)

First, the value KIE was determined to be ~0.9 and therefore no primary kinetic isotopic effect was observed. It is worth to notice that the accuracy of this value is not very reliable and owing to this uncertainty, we cannot assure the existence of an inverse secondary KIE. However, we can rule out an inverse KIE since we do not expect a change in the hybridization on the α-C (2'-position).

On the other hand, the deuterated starting material **2-d$_1$**, was recovered with a severe loss of deuterium (Figure 41). In other words, the oxidative addition and the migratory insertion of the olefin must be reversible to make this exchange possible (Scheme 0-53).

Figure 41. Reaction B: recovered material NMR spectra

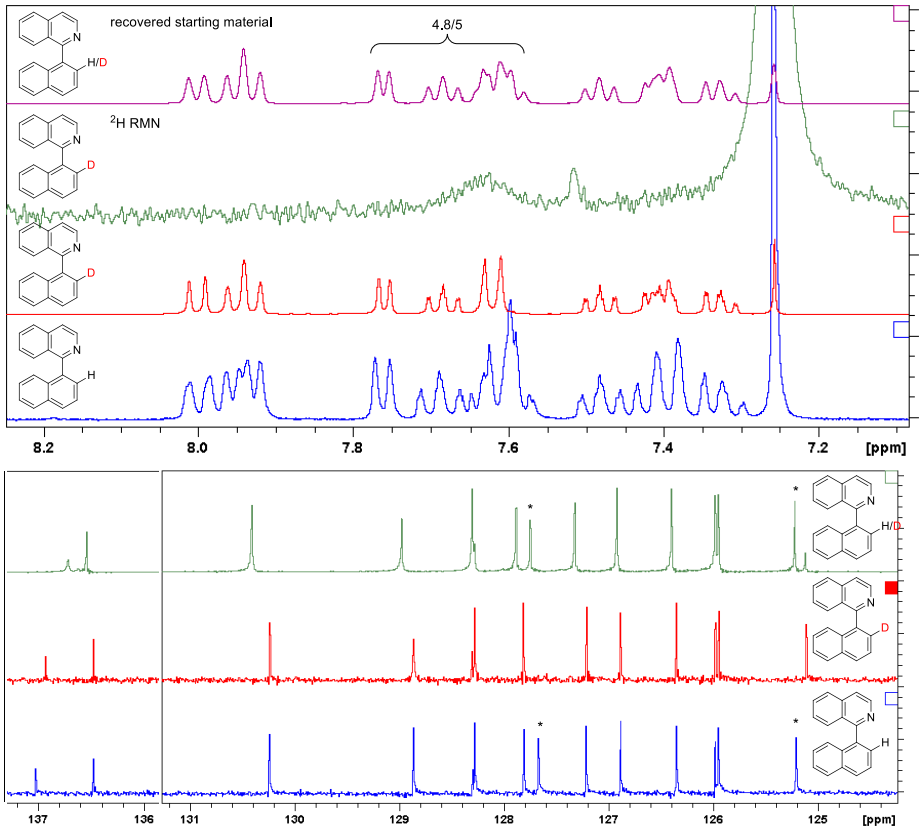

Scheme 0-53. Plausible mechanism for the deuterium/hydrogen scrambling

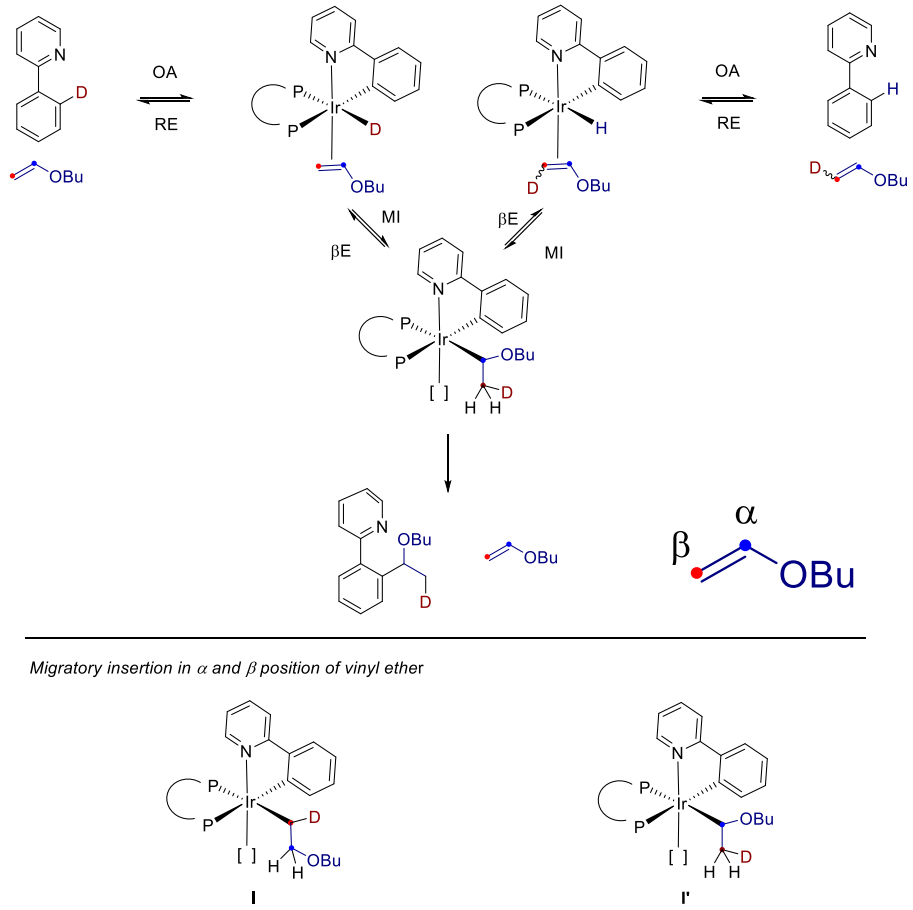

[a] For simplification, naphthylisoquinoline-like systems have been simplified to the corresponding phenylpyridine. Isomery and relative orientations are arbitrary and only the Chalk-Harrod mechanism has been considered. OA = oxidative addition. RE = reductive elimination. MI = migratory insertion. βE = β-elimination.

On the other hand, the isotopically labeled product was obtained with selective incorporation of the deuterium atom at corresponding β position of the parent vinyl ether **9a**. However, the deuteration was not complete and, indeed, the product was only deuterated in a 46% as a result of a deuterium/hydrogen exchange (Scheme 0-52, Figure 42). In fact, assuming reductive elimination is irreversible, among the possible migratory insertions intermediates, the only which can lead to the scrambling of H/D at both substrate and product is the one resulting from an insertion into the Ir-H bond forming an Ir-C bond at the α position of the parent vinyl ether (Scheme 0-53).

Figure 42. Reaction B: isolated product NMR spectra.

1H NMR

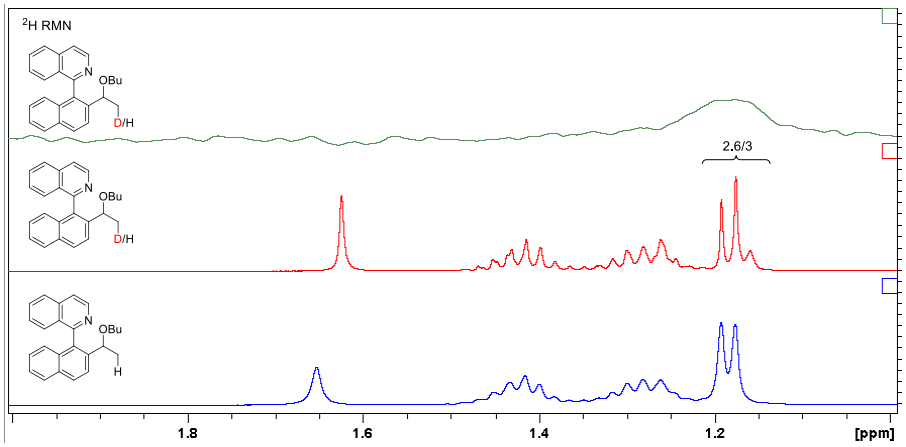

^{13}C RMN

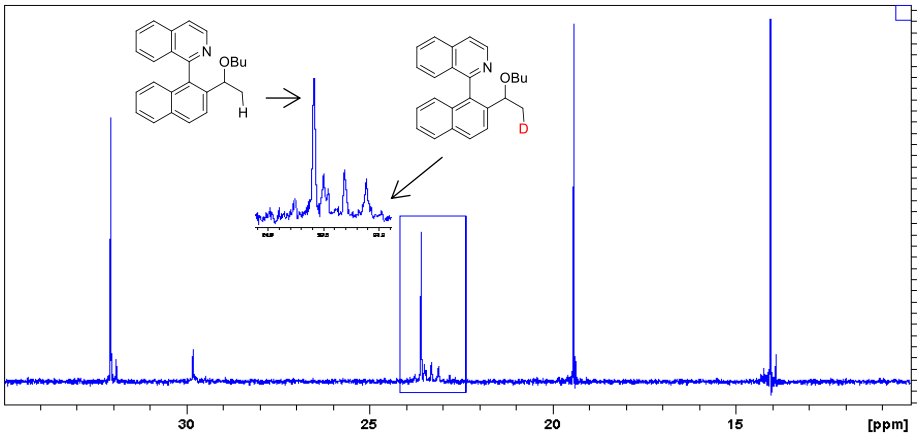

In order to gather more information about the underlying mechanism of our methodology we decided to monitor the reaction by NMR experiments.

Study on the oxidative addition by NMR monitoring

In order to shed light on the oxidative addition intermediate, we tried to monitor this step by NMR. Thus, the mixture of the Ir precursor, the ligand and naphthylisoquinoline in the presence of $NaBAr^F_4$ resulted in a complex ^{31}P spectrum with a number of both symmetrical ([Ir(COD)((*R*)-tol-BINAP))]BAr^F_4]) and non-symmetrical species. Regarding the ^{1}H NMR (Figure 43 - Figure 45), the examination of the hydride region revealed the coexistence of several

hydride-complexes with all-cis geometry regarding the phosphines.[258] On the other hand, this complexity was also observed by examination of the C3-H shift of the isoquinoline ring as multiple signals appeared in the spectrum. In addition, it is worth to notice the system was rather inert as the system evolved very slowly (the spectra were recorded in the course of several days) (Figure 46).

[258] $^{2}J_{PH(\textit{trans})}$ ~90-160 Hz, $^{2}J_{PH(cis)}$ ~ 10 – 30 Hz.

Figure 43. ^{1}H NMR spectrum during reaction monitoring with enlargement of C3-H area

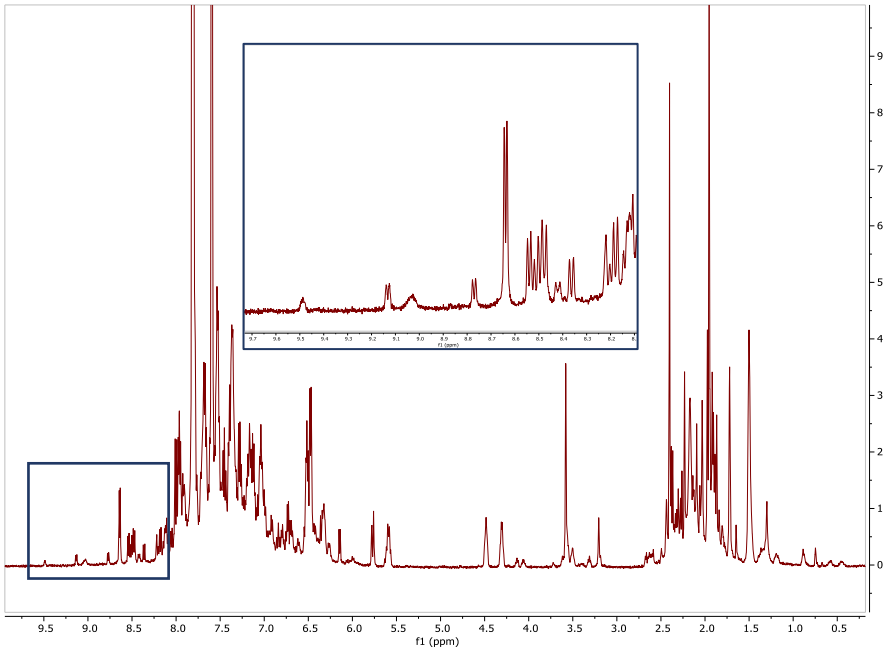

Figure 44. $^{1}H\{^{31}P\}$ and ^{1}H NMR spectra during reaction monitoring.

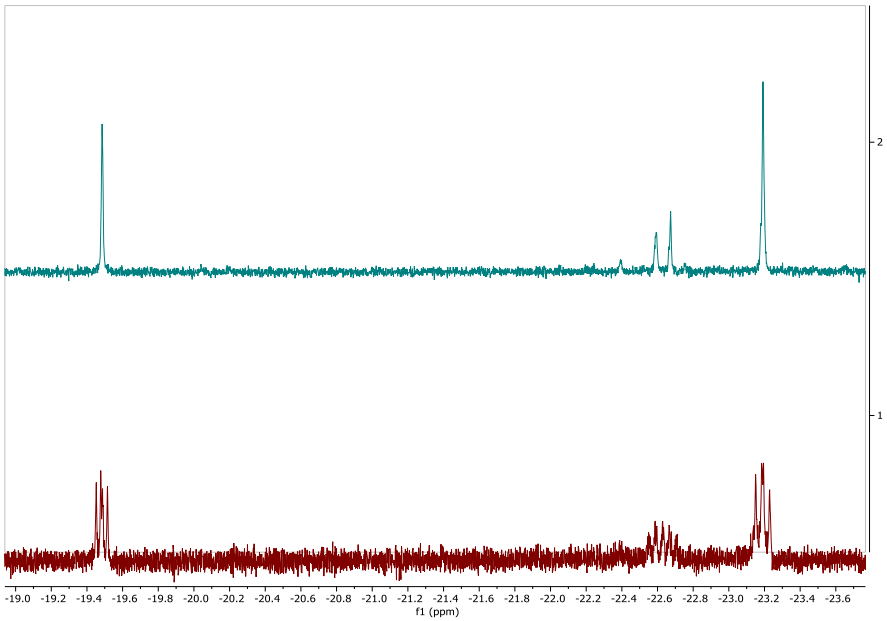

Figure 45. ^{31}PNMR spectra during reaction monitoring.

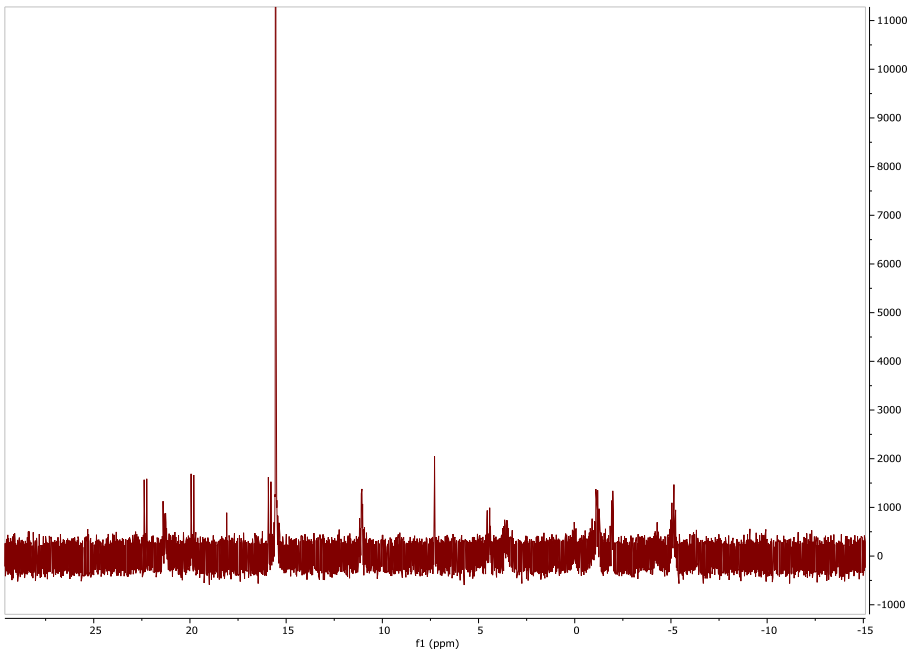

Figure 46. Reaction monitoring by 1H{31P} for over one week

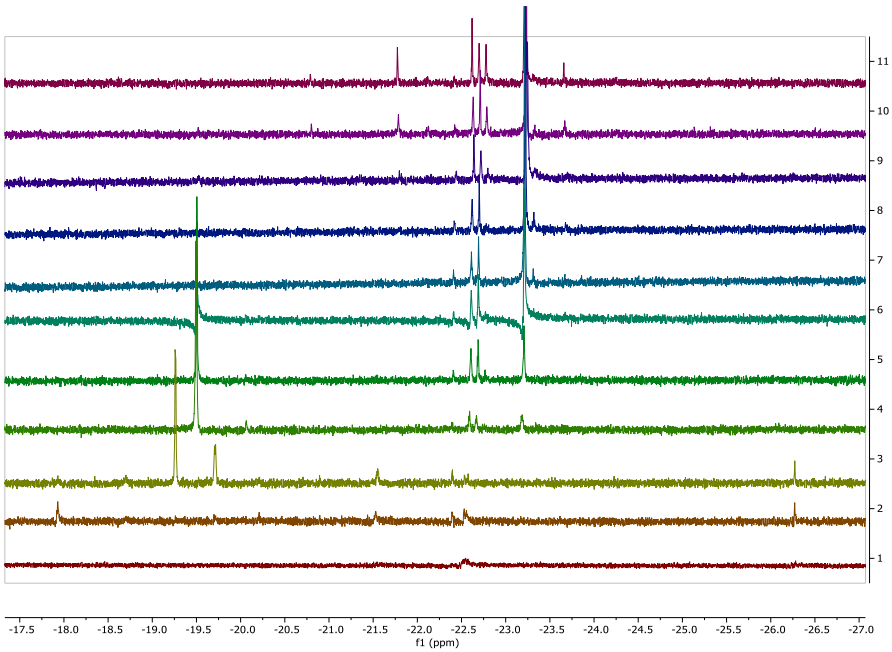

Despite these spectra were difficult to analyse due to the complexity, one conclusion can be extracted from these experiments. On the one hand, the oxidative addition seems to be slow on the basis of the slow consumption of the starting material. On the other, the hydride complexes are subjected to an isomerisation process. Despite these data did not offer a vision of the whole picture of the reaction mechanism, however, they did provide useful information of some aspects of the cycle.

With this information in hand, and intrigued by the mechanism that rule the stereochemistry of the transformation, we decided to shed light on this aspect of the reaction invoking theoretical calculations.

Computational studies

Based on previous reports on hydroarylation reactions catalysed by (cationic) Ir(I) species[245,251] as well as related DFT studies[259] we propose the next catalytic cycles as a working hypothesis.

It is worth to notice that the activation of the catalyst by means of chloride abstraction and ligand exchange will not be depicted as in accordance to these works, these steps are not troublesome or determining steps.

[259] (1) Zhang, M.; Hu, L.; Lang, Y.; Cao, Y.; Huang, G. Mechanism and Origins of Regio- and Enantioselectivities of Iridium-Catalysed Hydroarylation of Alkenyl Ethers. *J. Org. Chem.* **2018**, *83* (5), 2937–2947. https://doi.org/10.1021/acs.joc.8b00377.
(2) Huang, G.; Liu, P. Mechanism and Origins of Ligand-Controlled Linear Versus Branched Selectivity of Iridium-Catalysed Hydroarylation of Alkenes. *ACS Catal.* **2016**, *6* (2), 809–820. https://doi.org/10.1021/acscatal.5b02201.
(3) Zhang, M.; Huang, G. Mechanism of Iridium-Catalysed Branched-Selective Hydroarylation of Vinyl Ethers: A Computational Study. *Dalt. Trans.* **2016**, *45* (8), 3552–3557. https://doi.org/10.1039/c5dt04973c.

Scheme 0-54. Simplified catalytic cycles

A) Simplified catalytic cycles leading to the formation of branch-selective hydroarylation of heterobiaryls.

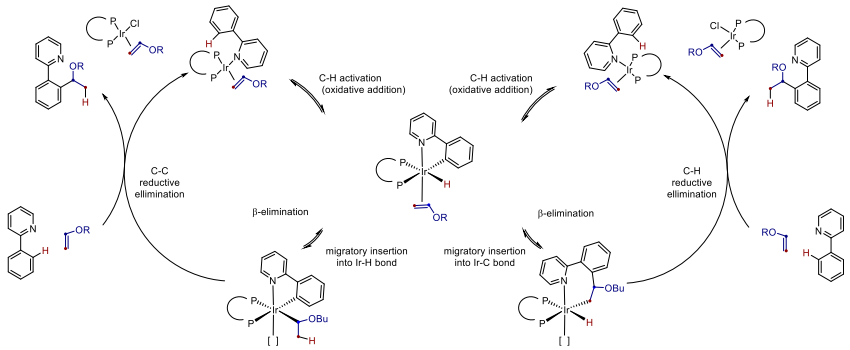

B) Simplified catalytic cycles leading to the formation of linear-selective hydroarylation of heterobiaryls.

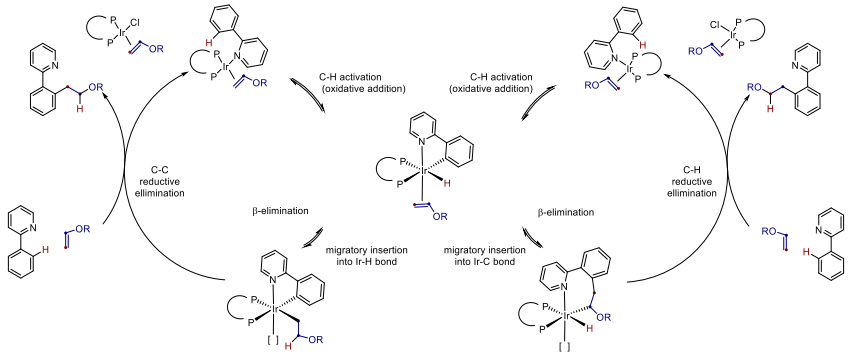

[a] For simplification, naphthylisoquinoline-like systems have been simplified to the corresponding phenylpyridine. Additionally, the relative orientation does not have to account for the actual geometry of the species and are arbitrarious and isomerisations process may happen.

As shown in these schemes, there are two sets of mechanisms leading respectively to the branch (Scheme 0-54.A) or the linear (Scheme 0-54.B) hydroarylation products. In this line, the hydroarylation reaction should follow a pathway in which the alkene is inserted into the Ir-R bond (R = H, C). Thus, depending on which of them the alkene is inserted, two scenarios are possible: a Chalk-Harrod mechanism or a modified Chalk-Harrod one.

This way, the regioselectivity of the reaction depends on two factors at the same time: According to the working hypothesis, the regioselectivity should be accounted for which type of mechanism is preferred (insertion into the Ir-C or into Ir-H bond), and for the direction in which the insertion occurs (“1,2-insertion” vs. “2,1-insertion”).

On the other hand, our methodology exhibits an excellent branch/linear selectivity and therefore, pathways leading to linear products can be ruled out. In this instance, the reaction can only proceed through the corresponding original or modified Chalk-Harrod mechanism.

As we have already indicated, there exist several computational studies[259] on the Ir-catalysed hydroarylation of alkenes, and even the asymmetric version of the reaction has also been studied. However, the simultaneous generation of axial and central chirality have not been described so far and therefore, the stereochemical course of the reaction have not been studied either.

Hence, we decided to use computational techniques to reveal this feature. In this regard, all the previous experimental data were very useful for the computational predictions to be contrasted with. On the other hand, these computational studies were carried out by Dr. Joaquín López-Serrano as a collaboration with our group.

Since many aspects of this reaction have been revealed by these reports, our collaboration has been focused on the explanation of the phenomena related to the complexity of our system. That is to say, the enantio-, the diastereo- and regioselectivity of the reaction. In this vein, the determination of the stereo- and rate-determining steps of the reaction were other two aims of these studies. Additionally, these calculations should discriminate the two model catalytic cycles and point out which is the most likely for our reaction.

To keep the calculations affordable but still with high degree of correlation, naphthylpicoline **8D**, (*R*)-BINAP and methyl vinyl ether were first chosen as the model system.

C-H Activation step

If we ignore the steps previous to the oxidative addition, i.e. the ligand substitution from the catalyst and coordination of the naphthylisoquinoline that are described elsewhere[259], the first catalytic step would be the oxidative addition of naphthylpicoline **8D** (Scheme 0-55).

Scheme 0-55. Activation of the catalyst and oxidative addition step

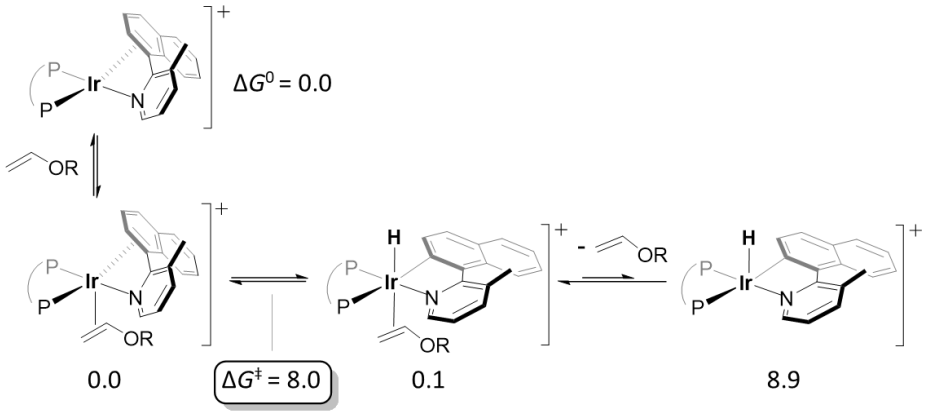

After the coordination of the heterocycle, the oxidative addition is activated when vinyl ether is placed in *trans* position relative to hydride. Thus, this step results in the formation of 8 diastereomeric octahedral species if we take into account the configuration of the axis and the 4 different relative orientations of the olefin (Figure 47).

Figure 47. 8 affordable diastereoisomeric complexes resulting from the oxidative addition step

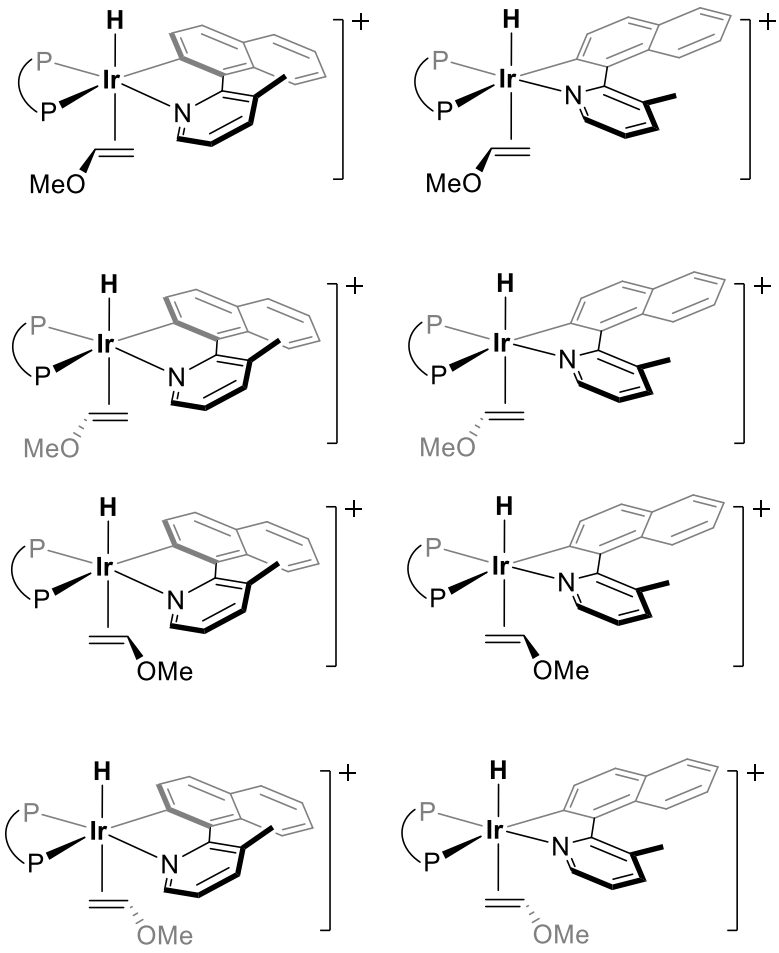

A$_{H\text{-}t\text{-}vinyl}$

Isomerisation of octahedral complexes and labilization of the axis

Although the oxidative addition is favoured by the coordination of the vinyl ether, however, these species do not necessarily undergo the following step and other isomers resulting from the rearrangement of the ligands have to be considered. In this regard, after olefin unbinding, these isomerisation processes have lower energy barriers (below 20 kcal·mol^{-1}) than the migratory insertion of $A_{H\text{-}t\text{-}vinyl}$ into the Ir-C bond, which were over 30 kcal·mol^{-1} overall (above 40 kcal·mol^{-1} in most of cases). Moreover, these energies were higher than any barrier for all the steps in the hydroarylation reaction of some octahedral isomers (Figure 48).

Figure 48. Possible subsequent steps of $A_{H\text{-}t\text{-}vinyl}$

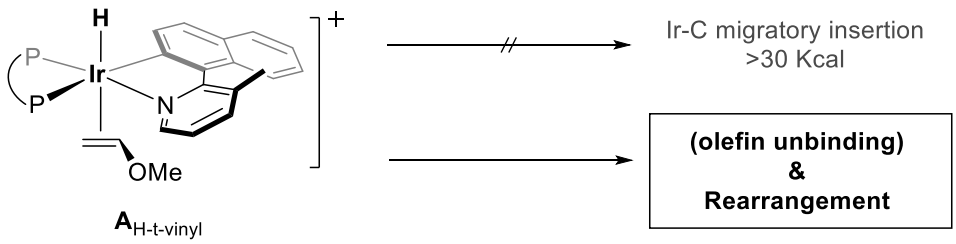

$\mathbf{A}_{H\text{-}t\text{-}vinyl}$

only one diastereoisomer depicted for clarity

All these calculations are in accordance to our previous experiments in which we observed a slow oxidative addition of the substrate in the absence of vinyl ether as well as the formation of different stereoisomeric hydride complexes (Figure 44-Figure 46).

Figure 49. Isomers resulting from the rearrangement of $A_{H\text{-}t\text{-}vinyl}$. Only one diastereoismer of each set is depicted for simplicity.

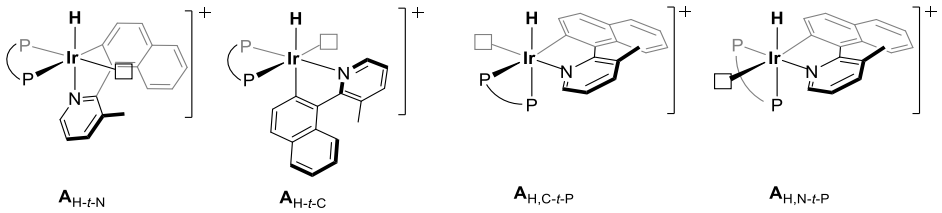

$\mathbf{A}_{H\text{-}t\text{-}N}$ $\mathbf{A}_{H\text{-}t\text{-}C}$ $\mathbf{A}_{H,C\text{-}t\text{-}P}$ $\mathbf{A}_{H,N\text{-}t\text{-}P}$

On the other hand, the barrier for the epimerization of the substrate axis upon oxidative addition is ca. 15 kcal mol^{-1}. That is to say, the isomerisation of the axis, which is necessary for the desymmetrisation process, not only happens outside the catalytic cycle but also takes place during the reaction itself (Figure 50).

Figure 50. Isomerisation of the chiral axis of the substrate.

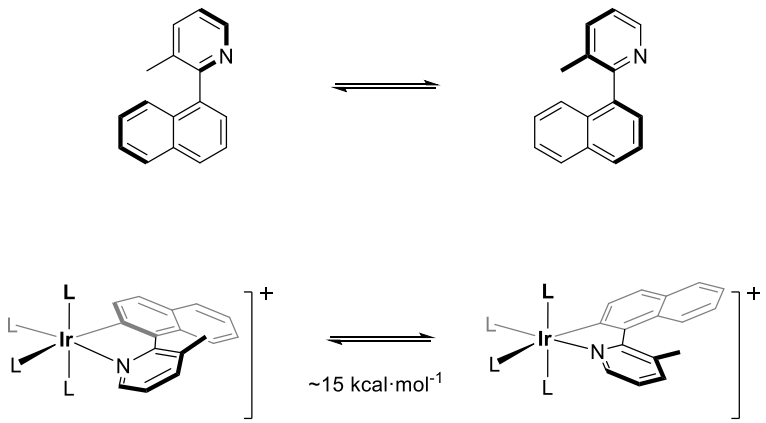

Migratory insertion into Ir-C or Ir-H bond

As we have just described, the rearrangement of the oxidative addition products is necessary so as the migratory insertion takes place. Since there is a big number of complexes, only those following the lower energy pathways will be discussed. At this point, one important question arises: does the migratory insertion of the vinyl ether takes place into the Ir-H (Chalk-Harrod type mechanism) or into the Ir-C bond (modified Chalk-Harrod type mechanism)[260]

Insertion into the Ir-H bond. Chalk-Harrod mechanism.

Due to the large number of possible routes, we will just focus on the lowest energy pathways involving olefin insertion into the Ir-H bond that could lead to the formation of the products as described by our methodology. Thus, olefin coordination to S_a-$\mathbf{A}_{\text{H-t-C}}$ yields the formation of S_a-$\mathbf{B}_{\text{H-t-C,1}}$ that has a low energy barrier to undergo insertion of the vinyl ether into the Ir-H bond through an overall energy barrier of 16.1 kcal·mol^{-1}. However, the barrier of the C-C bond forming reductive elimination from the resulting alkyl S_a-$\mathbf{C}_{\text{H-t-C,1}}$ is rather high (overall energy barrier of 28.5 kcal·mol^{-1}) to afford the final (S_a,*R*)-product. Hence, this route is unlikely, and other pathways having a more affordable energy profile will be now discussed (Figure 51).

[260] Homogeneous Catalysis. I. Double Bond Migration in n-Olefins, Catalyzed by Group VIII Metal Complexes. Chalk, A. J.; Harrod, J. F. J. Am. Chem. Soc. **1965**, 87, 16−21 b) Why Does the Rhodium-Catalyzed Hydrosilylation of Alkenes Take Place through a Modified Chalk−Harrod Mechanism? A Theoretical Study. Sakaki, S.; Sumimoto, M.; Fukuhara, M.; Sugimoto, M.; Fujimoto, H.; Matsuzaki, S. Organometallics **2002**, 21, 3788−3802 c) Iridium-Catalyzed, Intermolecular Hydroamination of Unactivated Alkenes with Indoles. Christo S. Sevov, Jianrong (Steve) Zhou, John F. Hartwig. *J. Am. Chem. Soc.***2014**, 136, 3200-3207 d) Asymmetric Cycloisomerization of o-Alkenyl-N-Methylanilines to Indolines by Iridium-Catalyzed C(sp3)−H Addition to Carbon–Carbon Double Bonds. Dr. Takeru Torigoe, Prof. Dr. Toshimichi Ohmura, Prof. Dr. Michinori Suginome. Angew.Chem. Int. Ed. **2017**, 56,14272 –14276.

Figure 51. Free energy profile for the migratory insertion of methyl vinyl ether into Ir-H bond and subsequent reductive elimination.

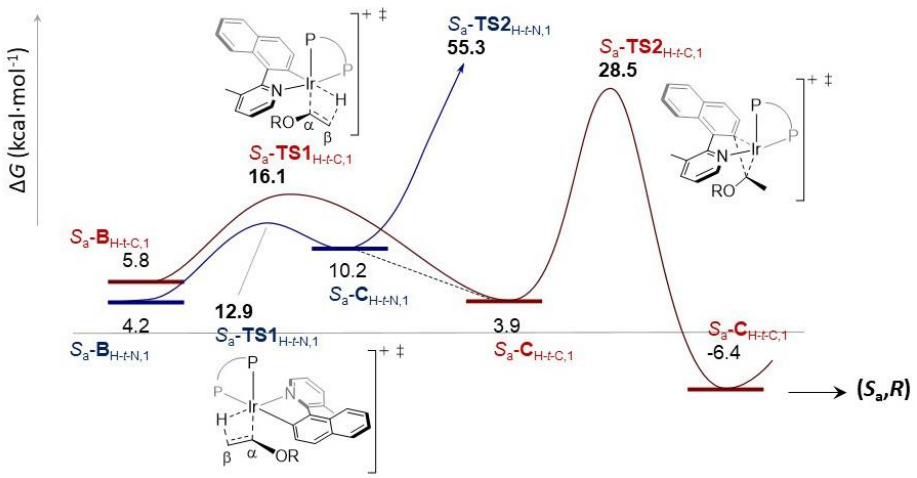

Considering $\mathbf{A}_{H\text{-}t\text{-}N}$ isomers (Figure 52), the coordination and subsequent insertion of the olefin into the Ir-C bond is also affordable and therefore, it may result in the formation of S_a-$\mathbf{C}_{H\text{-}t\text{-}N,1}$. In fact, the overall barrier for this process (12.9 kcal·mol^{-1}) is lower than in the previous case (Figure 51). By contrast, the reductive elimination from this S_a-$\mathbf{C}_{H\text{-}t\text{-}N,1}$ is completely inaccessible (>50 kcal·mol^{-1}). Nevertheless, both routes are connected through the isomerisation of S_a-$\mathbf{C}_{H\text{-}t\text{-}N,1}$ into S_a-$\mathbf{C}_{H\text{-}t\text{-}C,1}$, and therefore, the subsequent barrier for the reductive elimination would be lower. At any rate, as we have previously said, this step is still energetically difficult.

Figure 52. $A_{H\text{-}t\text{-}N}$ isomers

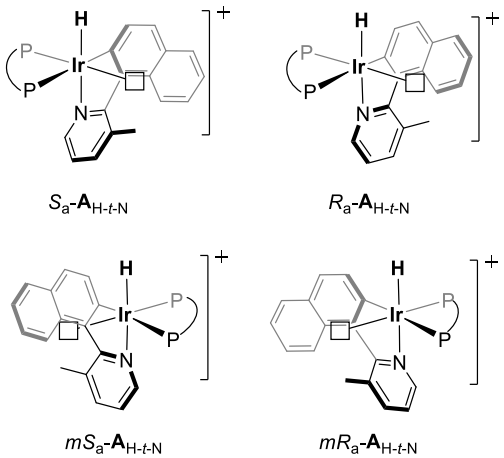

Notwithstanding these pathways do not account for the formation of the hydroarylation product, they prove the reversibility of the migratory insertion and they comprise a route for hydrogen/deuterium exchange in accordance to our previous isotopical labelling experiments.

Insertion into the Ir-C bond. Modified Chalk-Harrod mechanism.

Now we will describe the lowest energy profiles leading to the formation of the products involving a catalytic cycle in which migratory of the alkene into the Ir-C bond is involved.

In contrast to the previous pathways in which the insertion into the Ir-H bond is reversible, in the following cases the olefin insertion into the Ir-C counterpart is irreversible and exorgenic (Figure 53). Moreover, the corresponding reductive elimination steps are much more affordable too. However, the overall energy of the insertions is generally slightly higher in these cases. Thus, S_a-$\mathbf{B}_{\text{H-t-N,1}}$ undergoes this step through an overall barrier of 16.5 kcal·mol^{-1} affording the corresponding S_a-$\mathbf{E}_{\text{H-t-C,1}}$ and similarly, the isomer S_a-$\mathbf{B}_{\text{H-t-N,2}}$ can also move toward the formation of the analogous migratory insertion complex S_a-$\mathbf{E}_{\text{H-t-N,2}}$ (energy barrier of 15.9 kcal·mol^{-1}). Subsequently this species isomerizes into S_a-$\mathbf{E'}_{\text{H-t-N,2}}$. Next, the corresponding S_a-$\mathbf{E}_{\text{H-t-C,1}}$ and S_a-$\mathbf{E'}_{\text{H-t-N,2}}$ yield the expected (S_a,*R*)-product by overcoming the reductive elimination barriers (18.5 and 17.7 kcal·mol^{-1} respectively).

Figure 53. Free energy profile for the migratory insertion of methyl vinyl ether into Ir-C bond and subsequent reductive elimination.

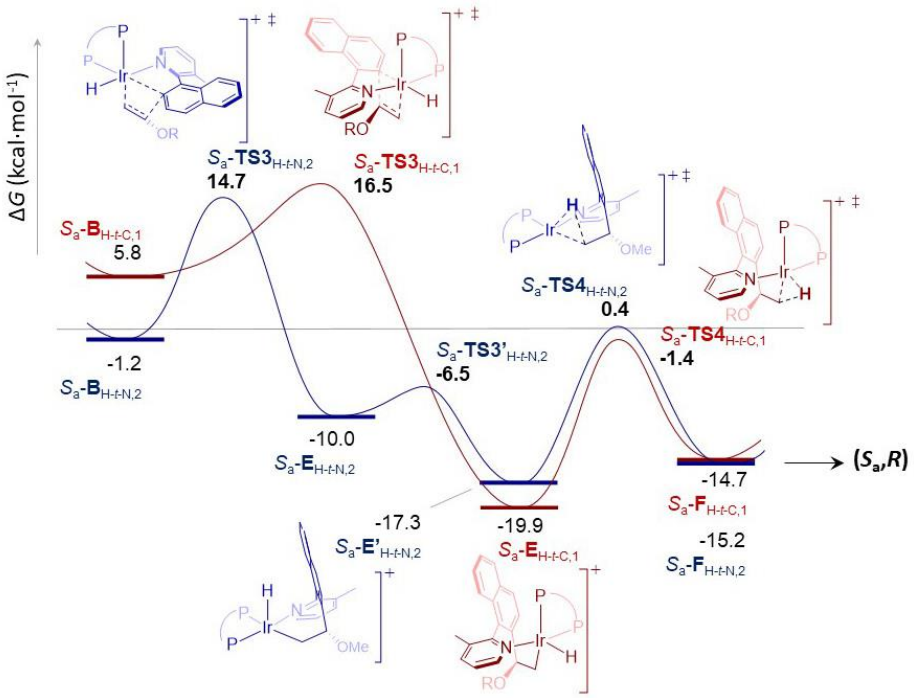

Hence, the reaction proceeds *via* the modified Chalk-Harrod mechanism, i.e. the productive pathway involves the migratory insertion of the vinyl ether into the Ir-C bond. However, since there are different steps in the cycle for which the energy barriers are similar, the rate-determining step cannot be clearly and precisely identified. Instead, the rate of the reaction must be defined by all these points of the catalytic cycle.

Regioselectivity

Once we have determined which type of pathways describes the best the course of the reaction, there are still pending questions to resolve. One of them is the regioselectivity. The regioselectivity of the reaction is determined by the preferential C-C bond formation at the α position of the vinyl ether. Therefore, we need to compare the lowest energy profiles yielding the (S_a,*R*)-branched and the linear product respectively (Figure 54).

This way, the two lowest energetic barriers for the migratory α-insertion are of 16.5 and 15.9 Kcal·mol^{-1}, as we have just seen. By contrast, if the migratory insertion results in a C-C$_\beta$ bond formation, which would lead to the linear product, the corresponding barriers are energetically higher, and indeed, the above 20 kcal·mol^{-1}. Regarding the subsequent reductive elimination steps, all

the barriers are similar and around 18 kcal·mol^{-1} and hence, the regioselectivity is determined by the insertion.

Figure 54. Comparation between the routes yielding the branched and linear products.

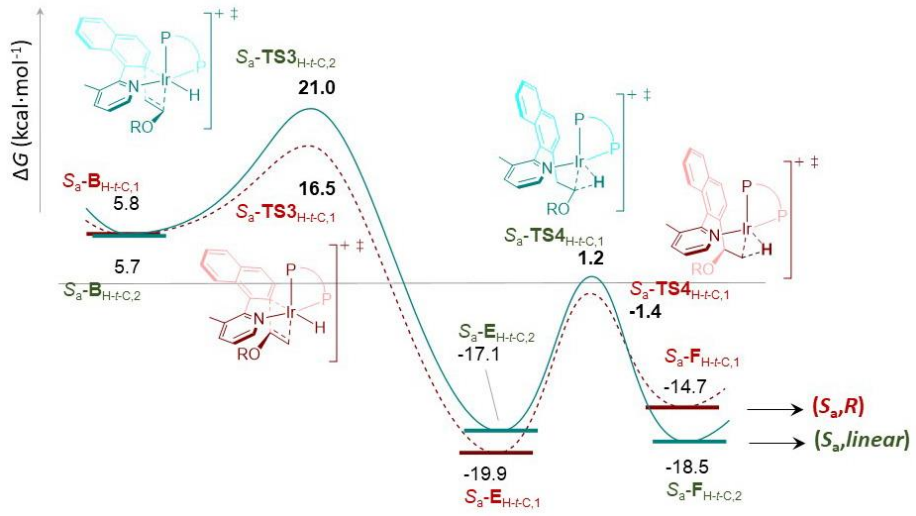

On the other hand, the origin of this selectivity can be explained in terms of the electronic nature of the vinyl ether. In this regard, the alkoxy group makes the β-carbon electronically rich, and then, it will react with electrophilic Ir(III). Similarly, the α position is rather electrophilic and hence, it is preferentially attacked by the aryl group (Scheme 0-56).

Scheme 0-56. Resonance structures in vinyl ethers contributing to their regioselectivity

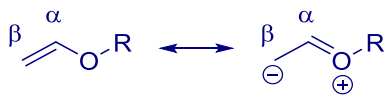

Enantioselectivity and diastereoselectivity

Last but not least, the origin and the level of stereoselectivity are questions that must be accounted for by these DFT calculations:

Although there is not a simple explanation about the origin of the enantio- and diastereoselectivity of this reaction, three main contributions support formation of the branched (*S*$_a$,*R*) product.

First, the main contribution is determined by the relative orientation of the axis relative to the vinyl ether in octahedral complexes **B**. Thus, while in complex *S*$_a$-**B**$_{H\text{-}t\text{-}N,2}$ C$_{aryl}$ points toward the α position of the methyl vinyl ether; in the corresponding *R*$_a$-**B**$_{H\text{-}t\text{-}N,2}$ isomer, the aryl group points away (Figure 55).

Therefore, the efficiency to form a C-C bond in the latter case is lost due to this distortion and, consequently, the corresponding transition state (R_a-**TS3$_{H\text{-}t\text{-}N,2}$**) is much higher (overall energy barrier of 31.7 kcal·mol^{-1}). By contrast, the transition state leading to the formation of the product with the same absolute configuration experimentally observed (S_a-**TS3$_{H\text{-}t\text{-}N,2}$**) is just 15.8 kcal·mol^{-1} above the origin of energy (Figure 55).

Second, the other two contributions are related to attractive dispersive interactions between the chiral ligand and the substrate, and the relative orientation (*endo* or *exo*) of the vinyl ether. In the figure, we can observe the different contributions of both the axial configuration of the substrate and the *endo*/*exo* orientation of the vinyl ether on the transition state for the α-insertion in **H-t-N** complexes.

Figure 55. Transition states for the α-insertion from H-t-N complexes.

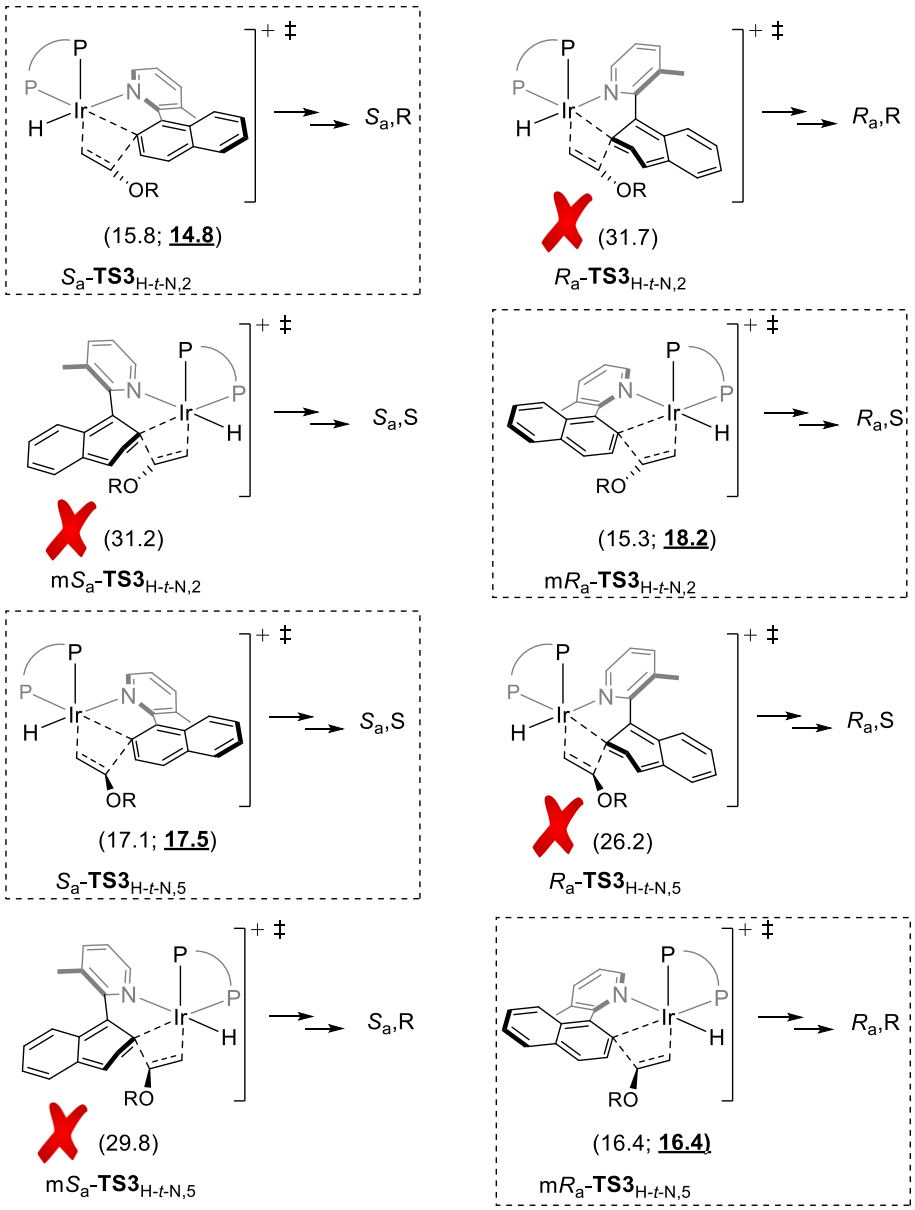

[a] Values in parentheses correspond to Gibbs energies in Kcal·mol^{-1} for R = Me and, highlighted, for R = Cy.

In the calculations, methoxy vinyl ether was utilized as the model olefin. In this context, we can observe that there are 4 transition states with similar energy (their difference in energy is less than 2 kcal·mol^{-1}) that would lead to the formation of different stereoisomers. Moreover, a difference of more than 2

kcal·mol^{-1} is required to afford high values of enantioselectivity (>90% ee). Hence, these differences in energy do not account for the enantioselectivity.

However, methyl vinyl ether is not an olefin that has been used experimentally. Hence, these transition states were recalculated for more realistic vinyl ethers since longer alkoxy substituents were used in the methodology. The substitution of methyl for the bulkier cyclohexyl vinyl ether in these calculations reached more energetically differentiated transition states (Figure 55). In addition, for the two most stable ones, it could be observed some positive dispersive interactions between the *endo*-orientated cyclohexyl group and the substrate. In the case of the most stable transition state, a larger π-π interaction between this substrate and the ligand could be observed too (Figure 56).

*Figure 56. pi-pi interaction between the ligand and the substrate in S_a-**TS3**$_{H\text{-}t\text{-}N,2,Cy}$ and mR_a-**TS3**$_{H\text{-}t\text{-}N,2,Cy}$.*

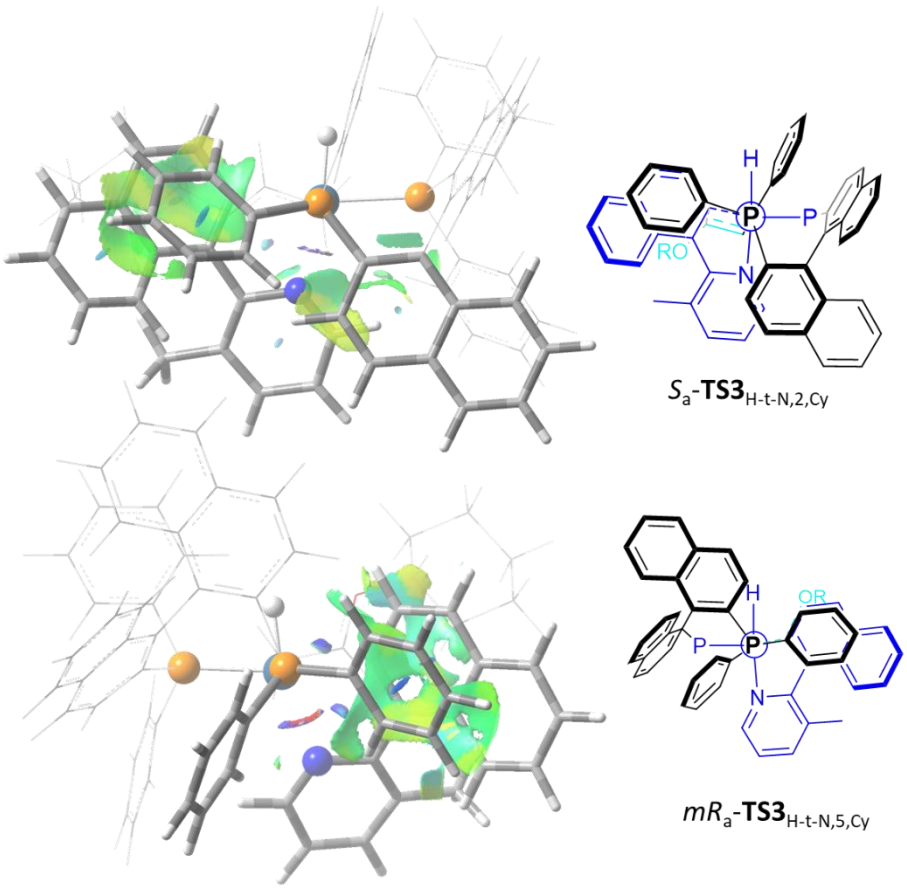

In this line, we now observe that the TS leading to the (S_a,*R*) product has the lowest energetic barrier. Moreover, the largest energetic difference is found between this and its enantiomeric TS by 3.4 kcal·mol^{-1}, which is in accordance to the high enantioslectivity.

Conclusions

To summarise, in this chapter, a new methodology for the synthesis of heterobiaryls with both axial and central chirality has been developed. These heterobiaryls has been synthesised applying an Ir(I)-catalysed C-H hydroarylation with vinyl ethers and norbornenes resulting in a desymmetrisation of the parent scaffolds.

Thus, the products have been obtained efficiently with excellent results of regio-, diastereo- and enantio- selectivity. In order to shed light of the mechanism of the reaction and the high selectivities, we accomplished isotopical labelling and computational studies.

As application, these benzylic ethers could be deprotected to obtain the corresponding alcohols which could be later transformed into azides and amines.

In order to shed light of the mechanism of the reaction and the high selectivities, we accomplished isotopical labelling and computational studies.

Experimental section

General considerations

^{1}H NMR and ^{13}C NMR spectra were recorded at 400 MHz and 100 MHz respectively, using a Bruker DRX-400 spectrometer and CDCl3 as the solvent. Spectra were referenced using the residual protio solvent peaks as internal standard (7.26 ppm for 1H NMR and 77.0 ppm for 13C NMR experiments). Column chromatography was performed on silica gel (Merck Kieselgel 60). Analytical TLC was performed on aluminum backed plates (1.5 × 5 cm) pre-coated (0.25 mm) with silica gel (Merck, Silica Gel 60 F_{254}). Compounds were visualized by exposure to UV light or by dipping the plates in a solution of 5% $(NH_4)_2Mo_7O_{24}{\cdot}4\ H_2O$ in 95% EtOH (w/v) or followed by heating. Enantiomeric excesses were determined by HPLC using chiral columns (Chiralpak® IA and Chiralcel® OD-H) and *n*-Hexane/isopropanol mixtures as eluent.

All chemical reactions were carried out in oven-dried Schlenk tubes under argon atmosphere employing standard techniques. Anhydrous Toluene and THF were obtained using Grubbs-type solvent drying columns, whereas anhydrous 1,4-dioxane and DME were obtained by distilling from sodium/benzophenone under N_2 atmosphere. Ligands **L5, L9, L11, L15-L16a**, **L16c** and $[Ir(\mu\text{-}Cl)(cod)]_2$ were purchased from Aldrich, and ligand **L16b** was supplied by Hebei Ligandchiral Co. Ltd. Vinyl ethers **9a-9c** and **9i** were purchased from TCI Chemicals, norbornene **9q** from Sigma-Aldrich and used without further purification. Vinyl ethers **9e-g**,[261a-b] norbornene **9r**[1c] and the starting substrates **8A-8G**[262] were synthesized following procedures described in the literature.

---

[261] (a) Matake, R.; Adachi, Y.; Matsubara, H. *Green Chem.,* **2016**, *18*, 2614. (b) Tamao, K.; Nakagawa, Y.; Ito, Y. *Organic Syntheses*, **1996**, *73*, 94. (c) Polo, E.; Forlini, F.; Bertolasi, V.; Boccia, A.C.; Sacchi, M.C. *Adv. Synth. Catal.* **2008**, 350, 1544–1556.

[262] (a) Ros, A.; Estepa, B.; López-Rodríguez, R.; Álvarez, E.; Fernández, R.; Lassaletta, J. M. *Angew. Chem. Int. Ed.* **2011**, *50*, 11724. (b) Pais, V. F.; El-Sheshtawy, H. S.; Fernández, R.; Lassaletta, J. M.; Ros, A.; Pischel, U. *Chem. Eur. J.* **2013**, *19*, 6650.

General procedure for the hydroarylation reaction of vinyl etheres

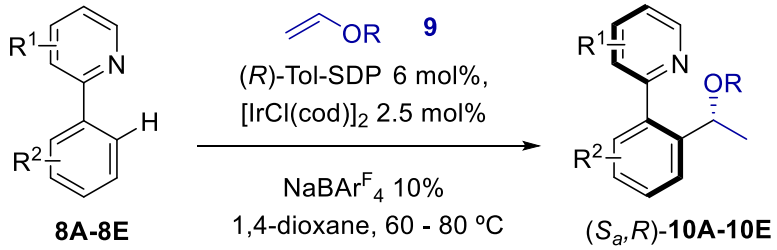

*From heterobiaryls (±)-8**A-8D** and vinyl ethers **9a-9g***: A dried Schlenk tube was charged with [Ir(μ-Cl)(cod)]$_2$ (0.0025 mmol, 1.7 mg) and (*S*)-Tol-SDP **L16b** (0.006 mmol, 3.9 mg). After three cycles of vacuum-N_2, anhydrous 1,4-dioxane (1 mL) was added and the resulting mixture was stired at room temperature for 10 minutes. Then, vinyl ether **9a-9g** (5-20 equiv.; see Table 2), the corresponding substrate (±)-**8A-8D** (0.1 mmol) and $NaBAr^F$ (0.01 mmol, 8.9 mg) were added in this order. The mixture was stirred at 60-80 °C for 48-24 hours (see Table 2), concentrated to dryness and purified by flash chromatography on silica gel.

*From heterobiaryl (±)-**E** and vinyl ethers **9a-9c***: A dried Schlenk tube was charged with [Ir(μ-Cl)(cod)]$_2$ (0.0025 mmol, 1.7 mg) and (*S*)-Tol-SDP **L16** (0.006 mmol, 3.9 mg). After three cycles of vacuum-N_2, anhydrous 1,4-dioxane (1 mL) was added and the resulting mixture was stired at room temperature for 10 minutes. Then, vinyl ether **9a-9c** (20 equiv.) was added and the resulting solution was transfered *via* cannula to a Schlenk tube containing the substrate (±)-**E** (0.1 mmol, 21.9 mg) and $NaBAr^F$ (0.01 mmol, 8.9 mg). The mixture was stirred at 60°C for 48 hours, concentrated to dryness and purified by flash chromatography on silica gel.

*From heterobiaryls (±)-**A-E** and vinyl ether **9i***: A dried Schlenk tube was charged with [Ir(μ-Cl)(cod)]$_2$ (0.0025 mmol, 1.7 mg) and (*S*)-Tol-SDP **L16** (0.006 mmol, 3.9 mg). After three cycles of vacuum-N_2, anhydrous 1,4-dioxane (1 mL) was added and the resulting mixture was stired at room temperature for 10 minutes. Then, vinyl ether **9i** (10-20 equiv., 76-152 μL; see Table 3), the corresponding substrate (±)-**A-D** (0.1 mmol) and NaBAr^F (0.01 mmol, 8.9 mg) were added in this order. The mixture was stirred at 80°C for 24 hours, concentrated to dryness and purified by flash chromatography on silica gel.

Note: For the preparation of the racemic products (HPLC references), the reactions were carried out at 80 °C in 0.025 mmol scale, and using (±)-BINAP (6 mol%)/[Ir(μ-Cl)(cod)]$_2$ *(2.5 mol%) as the catalyst and 10 equiv. of vinyl ethers **2a-1i**.*

Yields, solvent used for chromatography purification, and characterization data for products **10** are as follows:

*(S)-1-(2-((R)-1-butoxyethyl)naphthalen-1-yl)isoquinoline (S$_a$,R)-**10Aa**.*

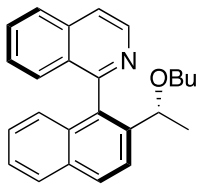

Following the general procedure using **8A** (0.1 mmol, 25.5 mg) and butyl vinyl ether **9a** (0.5 mmol, 65 μL), purification by flash chromatography (*n*-Hexane/EtOAc 7:1) afforded *(Sa,R)*-**10Aa** (34 mg, 95%) as a light brown viscous oil. $[\alpha]^{20}_D$ −2.35 (*c* 0.5, $CHCl_3$) for 95 % ee. ^{1}H NMR (400 MHz, $CDCl_3$) δ 8.74 (d, *J* = 5.7 Hz, 1H), 8.04 (d, *J* = 8.6 Hz, 1H), 7.95 (d, *J* = 8.3 Hz, 1H), 7.91 (d, *J* = 8.1 Hz, 1H), 7.81 (d, *J* = 8.7 Hz, 1H), 7.79 (d, *J* = 5.6 Hz, 1H), 7.69 (t, *J* = 6.6 Hz, 1H), 7.43 (t, *J* = 7.5 Hz, 1H), 7.36 (m, 2H), 7.24 (t, *J* = 7.2 Hz, 1H), 6.95 (d, *J* = 8.5 Hz, 1H), 4.08 (q, *J* = 6.4 Hz, 1H), 3.35 (dt, *J* = 9.6, 6.7 Hz, 1H), 3.20 (dt, *J* = 9.6, 6.3 Hz, 1H), 1.42 (m, 2H), 1.26 (m, 2H), 1.19 (d, *J* = 6.5 Hz, 3H), 0.83 (t, *J* = 7.3 Hz, 3H). ^{13}C NMR (100 MHz, $CDCl_3$) δ 159.6, 142.5, 140.5, 136.0, 134.3, 132.8, 132.3, 130.4,

129.3, 129.1, 127.9, 127.5, 127.4, 127.0, 126.4, 126.0, 125.7, 123.5, 120.2, 73.7, 68.3, 31.9, 23.4, 19.3, 13.9. HRMS (ESI) calcd. for $C_{25}H_{26}NO$ (M + H^+) 356.2009. Found 356.2005. HPLC (IA column, 97:3 *n*-Hex/*i*-PrOH, 30 °C, 1 mL/min): t_R 5.42 min (minor) and 6.44 min (major).

*(S)-1-(2-((R)-1-(cyclohexyloxy)ethyl)naphthalen-1-yl)isoquinoline (S_a,R)-**10Ab**.*

Following the general procedure using **8A** (0.1 mmol, 25.5 mg) and cyclohexyl vinyl ether **9b** (0.5 mmol, 71 μL), purification by flash chromatography (*n*-Hexane/EtOAc 7:1) afforded (S_a,*R*)-**7Ab** (33 mg, 87%) as a white amorphous solid. $[\alpha]^{20}_D$ +6.7 (*c* 0.5, $CHCl_3$) for 96 % ee. ^{1}H NMR (400 MHz, $CDCl_3$) δ 8.73 (d, *J* = 5.7 Hz, 1H), 8.03 (d, *J* = 8.6 Hz, 1H), 7.95 (d, *J* = 8.3 Hz, 1H), 7.91 (d, *J* = 8.2 Hz, 1H), 7.86 (d, *J* = 8.7 Hz, 1H), 7.79 (d, *J* = 5.6 Hz, 1H), 7.69 (m, 1H), 7.49–7.40 (m, 1H), 7.38 (m, 2H), 7.23 (d, *J* = 7.3 Hz, 1H), 6.96 (d, *J* = 8.4 Hz, 1H), 4.22 (q, *J* = 6.4 Hz, 1H), 3.29 (m, 1H), 1.80-1.52 (m, 4H), 1.45 (m, 1H), 1.35-0.80 (m, 8H). ^{13}C NMR (100 MHz, $CDCl_3$) δ 159.8, 142.5, 141.1, 136.0, 134.2, 132.78, 132.2, 130.4, 129.2, 129.1, 127.9, 127.5, 127.4, 127.0, 126.3, 126.1, 125.6, 123.9, 120.3, 73.9, 69.8, 33.5, 31.3, 25.8, 24.3, 23.9, 23.8. HRMS (ESI) calcd. for $C_{27}H_{28}NO$ (M + H^+) 382.2165. Found 382.2159. HPLC (IA column, 99:1 *n*-Hex/*i*-PrOH, 30 °C, 1 mL/min): t_R 5.97 min (major) and 6.78 min (minor).

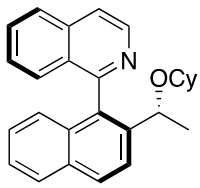

*(S)-1-(2-((R)-1-ethoxyethyl)naphthalen-1-yl)isoquinoline (S_a,R)-**10Ac**.*

Following the general procedure using **8A** (0.1 mmol, 25.5 mg) and ethyl vinyl ether **9c** (2 mmol, 192 μL), purification by flash chromatography (CH_2Cl_2/EtOAc 10:1→5:1) afforded (S_a,*R*)-**10Ac** (29 mg, 89%) as a colorless viscous oil. $[\alpha]^{20}_D$

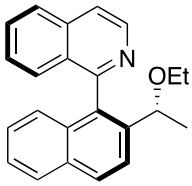

+9.2 (*c* 0.5, $CHCl_3$) for 93 % ee. ^{1}H NMR (400 MHz, Chloroform-*d*) δ 8.77 (d, *J* = 5.7 Hz, 1H), 8.07 (d, *J* = 8.7 Hz, 1H), 7.98 (d, *J* = 8.3 Hz, 1H), 7.94 (d, *J* = 8.1 Hz, 1H), 7.85 (d, *J* = 8.7 Hz, 1H), 7.82 (d, *J* = 5.7 Hz, 1H), 7.46 (t, *J* = 7.4 Hz, 2H), 7.39 (m, 2H), 7.26 (d, *J* = 7.3 Hz, 1H), 6.98 (d, *J* = 8.4 Hz, 1H), 4.13 (q, *J* = 6.4 Hz, 1H), 3.44 (dq, *J* = 9.6, 7.0 Hz, 1H), 3.28 (dq, *J* = 9.7, 7.0 Hz, 1H), 1.23 (d, *J* = 6.4 Hz, 3H), 1.10 (t, *J* = 7.0 Hz, 3H). ^{13}C NMR (100 MHz, $CDCl_3$) δ 159.6, 142.5, 140.3, 136.0, 134.3, 132.8, 132.3, 130.4, 129.4, 129.1, 127.9, 127.4, 127.4, 127.0, 126.35, 126.0, 125.7, 123.4, 120.2, 73.5, 63.8, 23.4, 15.2. HRMS (ESI) calcd. for $C_{23}H_{22}NO$ ($M + H^+$) 328.1696. Found 328.1693. HPLC (IA column, 97:3 *n*-Hex/*i*-PrOH, 30 °C, 1 mL/min): t_R 5.71 min (minor) and 8.84 min (major).

*(S)-1-(2-((R)-1-(benzyloxy)ethyl)naphthalen-1-yl)isoquinoline (S_a,R)-**10Ae**.*

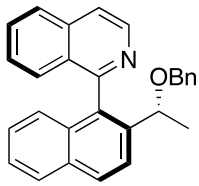

Following the general procedure using **A** (0.1 mmol, 25.5 mg) and benzyl vinyl ether **9e** (0.5 mmol, 70 μL), purification by flash chromatography (*n*-Hexane/EtOAc 8:1) afforded (S_a,*R*)-**10Ae** (27 mg, 70%) as a colorless viscous oil. $[\alpha]^{20}_D$ −76.3 (*c* 0.4, $CHCl_3$) for 97 % ee. ^{1}H NMR (400 MHz, $CDCl_3$) δ 8.72 (d, *J* = 5.7 Hz, 1H), 8.08 (d, *J* = 8.7 Hz, 1H), 7.95-7.91 (m, 3H), 7.76 (d, *J* = 5.7 Hz, 1H), 7.68 (ddd, *J* = 8.2, 6.1 and 2.0 Hz, 1H), 7.46 (ddd, *J* = 8.1, 6.8 and 1.2 Hz, 1H), 7.39-7.34 (m, 2H), 7.28-7.24 (m, 6H), 6.97 (dd, *J* = 8.5 and 1.1 Hz, 1H), 4.47 (d, *J* = 11.9 Hz, 1H), 4.26 (d, *J* = 11.9 Hz, 1H), 4.21 (q, *J* = 6.5 Hz, 1H), 1.25 (d, *J* = 6.5 Hz, 3H). ^{13}C NMR (100 MHz, $CDCl_3$) δ 159.6, 142.7, 140.0, 138.9, 136.1, 134.8, 133.0, 132.4, 130.4, 129.6, 129.1, 128.1 (2C), 128.0, 127.8 (2C), 127.4 (2C), 127.2, 127.1, 126.5, 126.2, 125.9, 123.6, 120.3, 73.7, 70.5, 23.6. HRMS (ESI) calcd. for $C_{28}H_{24}NO$ ($M + H^+$) 390.1852. Found 390.1856. HPLC (OD column, 99:1 *n*-Hex/*i*-PrOH, 30 °C, 1 mL/min): t_R 14.14 min (minor) and 19.45 min (major).

(S)-1-(2-((R)-1-((4-methoxybenzyl)oxy)ethyl)naphthalen-1-yl)isoquinoline *(S_α,R)-**10Ae**.*

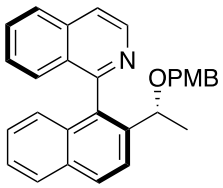

Following the general procedure using **8A** (0.1 mmol, 25.5 mg) and 4-methoxybenzyl vinyl ether **9f** (0.5 mmol, 80 μL), purification by flash chromatography (toluene/ EtOAc 10:1) afforded (S_α,*R*)-**10Af** (27.7 mg, 66%) as a beige amorphous solid. $[\alpha]^{20}_D$ –67.9 (*c* 0.5, $CHCl_3$) for 91 % ee. ^{1}H NMR (400 MHz, $CDCl_3$) δ 8.78 (d, *J* = 5.7 Hz, 1H), 8.11 (d, *J* = 8.7 Hz, 1H), 7.96 (m, 3H), 7.81 (d, *J* = 5.7 Hz, 1H), 7.71 (ddd, *J* = 8.2, 5.9, 2.2 Hz, 1H), 7.49 (ddd, *J* = 8.1, 6.8, 1.1 Hz, 1H), 7.40 (m, 2H), 7.29 (s, 1H), 7.24 (m, 2H), 7.00 (d, *J* = 8.4 Hz, 1H), 6.84 (m, 2H), 4.43 (d, *J* = 11.4 Hz, 1H), 4.23 (t, *J* = 6.5 Hz, 1H) 4.21 (d, *J* = 11.4 Hz, 1H), 3.80 (s, 3H), 1.26 (d, *J* = 6.5 Hz, 3H). ^{13}C NMR (100 MHz, $CDCl_3$) δ 159.6, 158.9, 142.6, 140.2, 136.1, 134.7, 132.9, 132.4, 131.1, 130.46, 129.5, 129.4 (2C), 129.1, 128.0, 127.4, 127.4, 127.1, 126.5, 126.1, 125.9, 123.7, 120.3, 113.6 (2C), 73.5, 70.1, 55.3, 23.6. HRMS (ESI) calcd. for $C_{29}H_{26}NO_2$ (M + H^+) 420.1958. Found 420.1957. HPLC (OD column, 95:5 *n*-Hex/*i*-PrOH, 30 °C, 1 mL/min): t_R 8.70 min (major) and 17.44 min (minor).

(S)-1-(2-((R)-1-(methoxymethoxy)ethyl)naphthalen-1-yl)isoquinoline *(S_α,R)-**10Ag**.*

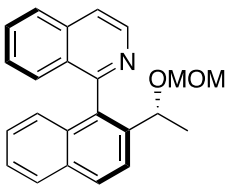

Following the general procedure using **A8** (0.1 mmol, 25.5 mg) and methoxymethyl vinyl ether **9g** (2.0 mmol, 200 μL), purification by flash chromatography (8:2 *n*-Hexane /EtOAc) afforded (S_α,*R*)-**10Ag**. (26.3 mg, 77%) as a beige syrup. $[\alpha]^{20}_D$ +79.6 (*c* 0.5, $CHCl_3$) for 98 % ee. ^{1}H NMR (400 MHz, $CDCl_3$) δ 8.75 (d, *J* = 5.8 Hz, 1H), 8.04 (d, *J* = 8.1 Hz, 1H), 7.95 (d, *J* = 8.3 Hz, 1H), 7.91 (d, *J* = 8.5 Hz, 1H), 7.83 (d, *J* = 8.7 Hz, 1H), 7.78 (d, *J* = 5.8 Hz, 1H), 7.68 (m, 1H), 7.44 (m, 1H), 7.38-7.34 (m, 2H), 7.24 (m, 1H), 6.95 (d, *J* = 8.5 Hz, 1H), 4.61 (d, *J* = 5.6 Hz, 1H), 4.45 (d, *J* = 5.6 Hz, 1H), 4.39 (q, *J* = 6.5 Hz, 1H), 3.24 (s, 3H), 1.29 (d, *J* = 6.5 Hz, 3H). ^{13}C NMR (101 MHz, $CDCl_3$) δ 159.4, 142.7, 139.7, 136.1, 134.3, 132.8, 132.3, 130.4, 129.3, 129.1, 127.9, 127.4, 127.3, 127.1, 126.5,

126.3, 125.9, 123.9, 120.3, 94.6, 70.8, 55.4, 23.0. HRMS (ESI) calcd. for $C_{23}H_{22}NO_2$ (M + H^+) 344.1645. Found 344.1646. HPLC (IA column, 95:5 *n*-Hex/*i*-PrOH, 30 °C, 1 mL/min): t_R 7.60 min (minor) and 12.84 min (major).

1-(2-(-tetrahydrofuran-2-yl)naphthalen-1-yl)isoquinoline ***10Ai.***

Following the general procedure using **8A** (0.1 mmol, 25.5 mg) and 2,3-dihydrofuran **9i** (1 mmol, 76 μL), purification by flash chromatography (*n*-Hexane/EtOAc 3:1→1:1) afforded **D1-10Ai** (5 mg, 15%) and **D2-10Ai** (15 mg, 46%) as a colorless viscous oils.

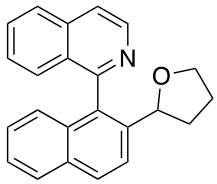

^{1}H NMR (400 MHz, $CDCl_3$) δ 8.74 (d, *J* = 5.7 Hz, 1H), 8.05 (d, *J* = 8.7 Hz, 1H), 7.96 (d, *J* = 8.3 Hz, 1H), 7.93 (d, *J* = 8.3 Hz, 1H), 7.84 (s, 1H), 7.83–7.78 (m, 1H), 7.71 (t, *J* = 7.5 Hz, 1H), 7.51 (d, *J* = 8.4 Hz, 1H), 7.43 (m, 2H), 7.26 (t, *J* = 7.6 Hz, 1H), 6.98 (d, *J* = 8.5 Hz, 1H), 4.38 (m, 1H), 4.12 (q, *J* = 7.0 Hz, 1H), 3.78 (m, 1H), 2.12 (m, 1H), 2.03 (m, 1H), 1.89 (m, 1H), 1.81 (m, 1H). ^{13}C NMR (100 MHz, $CDCl_3$) δ 159.5, 142.2, 140.0, 136.2, 133.1, 132.8, 132.4, 130.6, 129.2, 128.3, 127.9, 127.7, 127.3, 126.7, 126.3, 125.8, 125.5, 123.1, 120.3, 78.7, 69.1, 35.2, 26.5. HRMS (ESI) calcd. for $C_{23}H_{20}NO$ (M + H^+) 326.1539. Found 326.1536. For 23 % ee HPLC (IB column, 95:5 *n*-Hex/*i*-PrOH, 30 °C, 1 mL/min): t_R 8.50 min (minor) and 10.97 min (major).

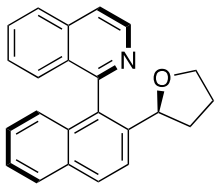

$[\alpha]^{20}_D$ −72.3 (*c* 0.5, $CHCl_3$) for 97 % ee. ^{1}H NMR (400 MHz, $CDCl_3$) δ 8.74 (d, *J* = 5.8 Hz, 1H), 8.01 (d, *J* = 8.6 Hz, 1H), 7.95 (d, *J* = 8.3 Hz, 1H), 7.90 (d, *J* = 8.2 Hz, 1H), 7.79 (m, 2H), 7.69 (m, 1H), 7.41 (t, *J* = 7.3 Hz, 1H), 7.36 (m, 2H), 7.22 (t, *J* = 7.6 Hz, 1H), 6.91 (d, *J* = 8.5 Hz, 1H), 4.66 (t, *J* = 7.4 Hz, 1H), 3.94 (q, *J* = 7.1 Hz, 1H), 3.72 (q, *J* = 7.5 Hz, 1H), 1.88 (m, 1H), 1.65 (m, 2H), 1.56 (m, 1H). ^{13}C NMR (100 MHz, $CDCl_3$) δ 159.7, 142.4 (2C), 140.1, 136.0, 132.7, 132.5, 130.4 (2C), 129.1, 127.9, 127.7, 127.3, 127.0, 126.3, 125.9, 125.5, 123.5, 120.2, 78.4, 68.7, 34.5, 26.4. HRMS (ESI) calcd. for $C_{23}H_{20}NO$ (M + H^+) 326.1539. Found

326.1534. HPLC (IA column, 90:10 *n*-Hex/*i*-PrOH, 30 °C, 1 mL/min): t_R 9.62 min (major) and 11.68 min (minor).

*(S)-1-(2-((R)-1-butoxyethyl)-4-methylnaphthalen-1-yl)isoquinoline (S_a,R)-**10Ba.***

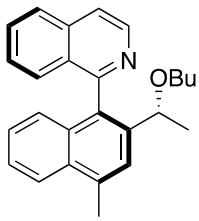

Following the general procedure using **8B** (0.1 mmol, 26.9 mg) and butyl vinyl ether **9a** (0.5 mmol, 65 μL), purification by flash chromatography (*n*-Hexane/EtOAc 10:1) afforded (S_a,*R*)-**10Ba** (34 mg, 92%) as a colorless viscous oil. $[\alpha]^{20}_D$ +5.7 (*c* 0.5, $CHCl_3$) for 95% ee. ^{1}H NMR (400 MHz, $CDCl_3$) δ 8.73 (d, *J* = 5.7 Hz, 1H), 8.06 (d, *J* = 8.4 Hz, 1H), 7.94 (d, *J* = 8.3 Hz, 1H), 7.77 (d, *J* = 5.7 Hz, 1H), 7.71–7.66 (m, 1H), 7.64 (s, 1H), 7.47 (t, *J* = 7.6 Hz, 1H), 7.36 (d, *J* = 3.8 Hz, 2H), 7.22 (d, *J* = 7.3 Hz, 1H), 6.97 (d, *J* = 8.4 Hz, 1H), 4.04 (q, *J* = 6.4 Hz, 1H), 3.40–3.31 (dt, *J* = 9.6, 6.3 Hz, 1H), 3.19 (dt, *J* = 9.6, 6.3 Hz, 1H), 2.82 (s, 3H), 1.51–1.24 (m, 4H), 1.19 (d, *J* = 6.5 Hz, 3H), 0.83 (t, *J* = 7.3 Hz, 3H). ^{13}C NMR (100 MHz, $CDCl_3$) δ 159.9, 142.5, 139.8, 136.0, 135.6, 132.7, 132.5, 132.1, 130.3, 129.3, 127.6, 127.2, 126.9, 126.7, 126.0, 125.5, 124.0, 124.0, 120.1, 73.6, 68.2, 31.9, 23.3, 19.8, 19.24, 13.9. HRMS (ESI) calcd. for $C_{26}H_{28}NO$ ($M + H^+$) 370.2165. Found 370.2159. HPLC (IA column, 99:1 *n*-Hex/*i*-PrOH, 30 °C, 1 mL/min): t_R 8.06 min (minor) and 8.7 min (major).

*(S)-1-(2-((R)-1-(cyclohexyloxy)ethyl)-4-methylnaphthalen-1-yl)isoquinoline (S_a,R)-**10Bb.***

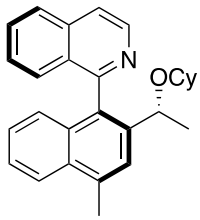

Following the general procedure using **8B** (0.1 mmol, 26.9 mg) and cyclohexyl vinyl ether **9b** (0.5 mmol, 71 μL), purification by flash chromatography (*n*-Hexane/EtOAc 10:1) afforded (S_a,*R*)-**10Bb** (35 mg, 89%) as a white amorphous solid. $[\alpha]^{20}_D$ +18.6 (*c* 0.5, $CHCl_3$) for 98 % ee. ^{1}H NMR (400 MHz, $CDCl_3$) δ 8.72 (d, *J* = 5.7 Hz, 1H), 8.07 (d, *J* = 8.4 Hz, 1H), 7.94 (d, *J* = 8.2 Hz, 1H), 7.77 (d, *J* = 5.6 Hz, 1H), 7.69 (m, 2H), 7.47 (t, *J* = 7.6 Hz, 1H),

7.39 (m, 2H), 7.23 (d, *J* = 7.2 Hz, 1H), 6.98 (d, *J* = 8.4 Hz, 1H), 4.18 (q, *J* = 6.4 Hz, 1H), 3.30 (m, 1H), 2.82 (s, 3H), 1.95-1.51 (m, 4H), 1.51-1.41 (m, 1H), 1.32-1.02 (m, 8H). ^{13}C NMR (100 MHz, $CDCl_3$) δ 160.1, 142.5, 140.5, 135.9, 135.4, 132.6, 132.34, 132.1, 130.3, 129.3, 127.6, 127.3, 127.0, 126.7, 126.0, 125.5, 124.4, 124.1, 120.1, 73.8, 69.7, 33.5, 31.3, 25.8, 24.3, 23.9, 23.7, 19.8. HRMS (ESI) calcd. for $C_{28}H_{30}NO$ (M + H^+) 396.2322. Found 396.2315. HPLC (IA column, 99:1 *n*-Hex/*i*-PrOH, 30 °C, 1 mL/min): t_R 5.52 min (major) and 6.85 min (minor).

*(S)-1-(2-((R)-1-ethoxyethyl)-4-methylnaphthalen-1-yl)isoquinoline (S_a,R)-**10Bc.***

Following the general procedure using **8B** (0.1 mmol, 26.9 mg) and ethyl vinyl ether **9c** (2 mmol, 192 μL), purification by flash chromatography (CH_2Cl_2/EtOAc 10:1) afforded (S_a,*R*)-**10Bc** (32 mg, 94%) as a colorless viscous oil. $[\alpha]^{20}_D$ +10.3 (*c* 0.5, $CHCl_3$) for 86 % ee. ^{1}H NMR (400 MHz, $CDCl_3$) δ 8.74 (d, *J* = 5.7 Hz, 1H), 8.07 (d, *J* = 8.5 Hz, 1H), 7.94 (d, *J* = 8.4 Hz, 1H), 7.78 (d, *J* = 5.7 Hz, 1H), 7.67 (m, 1H), 7.65 (s, 1H), 7.47 (t, *J* = 7.6 Hz, 1H), 7.36 (d, *J* = 3.7 Hz, 2H), 7.23 (d, *J* = 7.1 Hz, 1H), 6.96 (d, *J* = 8.4 Hz, 1H), 4.06 (q, *J* = 6.4 Hz, 1H), 3.42 (dq, *J* = 9.4, 7.1 Hz, 1H), 3.25 (dq, *J* = 9.2, 6.9 Hz, 1H), 2.83 (s, 3H), 1.20 (d, *J* = 6.5 Hz, 3H), 1.07 (t, *J* = 7.0 Hz, 3H). ^{13}C NMR (100 MHz, $CDCl_3$) δ 159.9, 142.4, 139.7, 136.0, 135.7, 132.6, 132.5, 132.1, 130.4, 129.3, 127.6, 127.3, 127.0, 126.7, 126.0, 125.5, 124.0, 123.9, 120.2, 73.5, 63.8, 23.3, 19.8, 15.2. HRMS (ESI) calcd. for $C_{24}H_{24}NO$ (M + H^+) 342.1852. Found 342.1853. HPLC (IA column, 97:3 *n*-Hex/*i*-PrOH, 30 °C, 1 mL/min): t_R 5.90 min (minor) and 8.20 min (major).

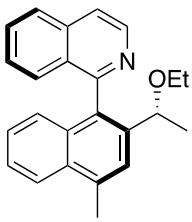

*(S)-1-(2-((R)-1-(benzyloxy)ethyl)-4-methylnaphthalen-1-yl)isoquinoline (S_a,R)-**10Be.***

Following the general procedure using **8B** (0.1 mmol, 26.9 mg) and benzyl vinyl ether **9d** (0.5 mmol, 70 μL), purification by flash chromatography (*n*-Hexane/EtOAc 8:1) afforded (S_a,*R*)-**10Be** (29 mg, 72%) as a colorless viscous oil. $[\alpha]^{20}_D$ –50.4 (*c* 0.5, $CHCl_3$) for 96 % ee. ^{1}H NMR (400 MHz, $CDCl_3$) δ 8.71 (d, *J* = 5.7 Hz, 1H), 8.09 (d, *J* = 8.4 Hz, 1H), 7.93 (d, *J* = 8.3 Hz, 1H), 7.74 (m, 2H), 7.67 (m, 1H), 7.50 (t, *J* = 7.4 Hz, 1H), 7.38 (m, 2H), 7.26 (m, 5H), 7.22 (m, 1H), 6.98 (d, *J* = 8.4 Hz, 1H), 4.48 (d, *J* = 12.0 Hz, 1H), 4.27 (d, *J* = 12.0 Hz, 1H), 4.17 (q, *J* = 6.4 Hz, 1H), 2.84 (s, 3H), 1.25 (d, *J* = 6.5 Hz, 3H). ^{13}C NMR (100 MHz, $CDCl_3$) δ 159.7, 142.5, 139.4, 138.9, 136.0, 135.9, 132.4, 132.2, 130.8, 130. (2C), 129.2, 128.8, 128.0, 127.7, 127.5, 127.3, 127.1, 127.0, 126.7, 126.1, 125.7, 124.1, 124.1, 120.2, 73.7, 70.4, 23.4, 19.8. HRMS (ESI) calcd. for $C_{29}H_{26}NO$ (M + H^+) 404.2009. Found 404.2002. HPLC (OD column, 90:10 *n*-Hex/*i*-PrOH, 30 °C, 1 mL/min): t_R 5.14 min (major) and 6.18 min (minor).

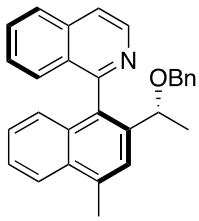

*(S)-1-(2-((R)-1-((4-methoxybenzyl)oxy)ethyl)-4-methylnaphthalen-1-yl)isoquinoline (S_a,R)-**10Bf.***

Following the general procedure using **8B** (0.1 mmol, 26.9 mg) and 4-methoxybenzyl vinyl ether **9f** (0.5 mmol, 80 μL), purification by preparative TLC (toluene/Et_2O 7:1) afforded (S_a,*R*)-**10Bf** (19.2 mg, 44%) as a white amorphous solid. $[\alpha]^{20}_D$ –68.8 (*c* 0.3, $CHCl_3$) for 98 % ee. ^{1}H NMR (400 MHz, $CDCl_3$) δ 8.72 (d, *J* = 5.7 Hz, 1H), 8.09 (d, *J* = 8.4 Hz, 1H), 7.93 (d, *J* = 8.3 Hz, 1H), 7.75 (d, *J* = 5.7 Hz, 1H), 7.73 (s, 1H), 7.67 (m, 1H), 7.49 (m, 1H), 7.36 (d, *J* = 3.6 Hz, 2H), 7.26 (m, 1H), 7.20 (d, *J* = 8.6 Hz, 2H), 6.98 (d, *J* = 8.4 Hz, 1H), 6.80 (d, *J* = 8.6 Hz, 2H), 4.40 (d, *J* = 11.6 Hz, 1H), 4.17 (d, *J* = 11.6 Hz, 1H), 4.14 (q, *J* = 6.5 Hz, 1H), 3.77 (s, 3H), 2.84 (s, 3H), 1.21 (d, *J* = 6.5 Hz, 3H). ^{13}C NMR (100 MHz, $CDCl_3$) δ 159.8, 158.9, 142.6, 139.5, 136.0, 135.8, 133.1, 132.5, 132.2, 131.1, 130.3, 129.4 (2C), 129.2, 127.5, 127.3, 127.0, 126.7,

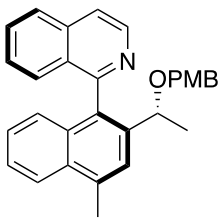

126.1, 125.6, 124.1 (2C), 120.1, 113.5 (2C), 73.4, 70.1, 55.2, 23.4, 19.8. HRMS (ESI) calcd. for $C_{30}H_{28}NO_2$ (M + H^+) 434.2115 Found 434.2112. HPLC (OD column, 90:10 *n*-Hex/*i*-PrOH, 30 °C, 1 mL/min): t_R 6.05 min (major) and 12.68 min (minor).

(*S*)-1-(2-((*R*)-1-(methoxymethoxy)ethyl)-4-methylnaphthalen-1-yl)isoquinoline (S_α,*R*)-**10Bg.**

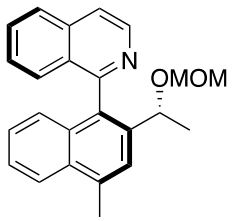

Following the general procedure using **8B** (0.1 mmol, 26.9 mg) and methoxymethyl vinyl ether **9g** (2.0 mmol, 200 μL), purification by flash chromatography (*n*-Hexane/EtOAc 7:3) afforded (S_α,*R*)-**10Bg** (27.0 mg, 76%) as a beige syrup. $[\alpha]^{20}_D$ +108.2 (*c* 0.4, $CHCl_3$) for 98 % ee. ^{1}H NMR (400 MHz, $CDCl_3$) δ 8.78 (d, *J* = 5.7 Hz, 1H), 8.09 (d, *J* = 8.4 Hz, 1H), 7.97 (d, *J* = 8.3 Hz, 1H), 7.80 (d, *J* = 5.7 Hz, 1H), 7.69 (m, 2H), 7.50 (ddd, *J* = 8.3, 6.8, 1.2 Hz, 1H), 7.38 (m, 2H), 7.27 (m, 1H), 7.00 (d, *J* = 8.4 Hz, 1H), 4.65 (d, *J* = 6.3 Hz, 1H), 4.50 (d, *J* = 6.3 Hz, 1H), 4.39 (q, *J* = 6.5 Hz, 1H), 3.28 (s, 3H), 2.85 (s, 3H), 1.29 (d, *J* = 6.5 Hz, 3H). ^{13}C NMR (100 MHz, $CDCl_3$) δ 159.7, 142.8, 139.1, 136.0, 135.7, 132.8, 132.5, 132.2, 130.3, 129.2, 127.4, 127., 127.1, 126.9, 126.1, 125.7, 124.4, 124.1, 120.2, 94.5, 70.9, 55.4, 22.9, 19.8. HRMS (ESI) calcd. for $C_{24}H_{24}NO_2$ (M + H^+) 358.1802. Found 358.1802. HPLC (IA column, 95:5 *n*-Hex/*i*-PrOH, 30 °C, 1 mL/min): t_R 7.26 min (minor) and 10.25 min (major).

1-(4-methyl-2-(tetrahydrofuran-2-yl)naphthalen-1-yl)isoquinoline ***10Bi.***

Following the general procedure using **8B** (0.1 mmol, 26.9 mg) and 2,3-dihydrofuran **9g** (1 mmol, 76 μL), purification by flash chromatography (*n*-Hexane/EtOAc 3:1→1:1) afforded **D1-10Bi** (7 mg, 21%) and **D2-10Bi** (20 mg, 59%) as light brown amorphous solids.

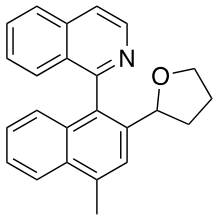

^{1}H NMR (400 MHz, $CDCl_3$) δ 8.70 (d, *J* = 5.7 Hz, 1H), 8.06 (d, *J* = 8.4 Hz, 1H), 7.92 (d, *J* = 8.3 Hz, 1H), 7.75 (d, *J* = 5.7 Hz, 1H), 7.67 (t, *J* = 7.6 Hz, 1H), 7.64 (s, 1H), 7.50-7.43 (m, 2H), 7.37 (t, *J* = 7.6 Hz, 1H), 7.23 (t, *J* = 8.0 Hz, 1H), 6.96 (d, *J* = 8.4 Hz, 1H), 4.31 (t, *J* = 7.1 Hz, 1H), 4.08 (q, *J* = 7.2 Hz, 1H), 3.74 (q, *J* = 7.2 Hz, 1H), 2.81 (s, 3H), 2.09 (m, 1H), 2.00 (m, 1H), 1.89-1.73 (m, 2H). ^{13}C NMR (100 MHz, $CDCl_3$) δ 159.9, 142.4, 139.3, 136.1, 135.5, 132.6, 132.1, 131.7, 130.4, 128.5, 127.6, 127.4, 126.7, 126.5, 125.9, 125.3, 124.1, 123.7, 120.1, 78.8, 69.1, 35.2, 26.5, 19.8. HRMS (ESI) calcd. for $C_{24}H_{22}NO$ ($M + H^+$) 340.1696. Found 340.1692. For 32 % ee HPLC (OD-H column, 90:10 *n*-Hex/*i*-PrOH, 30 °C, 1 mL/min): t_R 7.45 min (minor) and 10.79 min (major).

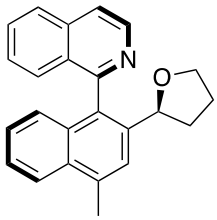

$[\alpha]^{20}_D$ −48.7 (*c* 0.5, $CHCl_3$) for 92 % ee. ^{1}H NMR (400 MHz, $CDCl_3$) δ 8.73 (d, *J* = 5.8 Hz, 1H), 8.06 (d, *J* = 8.4 Hz, 1H), 7.93 (d, *J* = 8.3 Hz, 1H), 7.77 (d, *J* = 5.8 Hz, 1H), 7.68 (dt, *J* = 8.2, 4.0 Hz, 1H), 7.63 (s, 1H), 7.45 (t, *J* = 7.3 Hz, 1H), 7.37 (d, *J* = 3.8 Hz, 2H), 7.22 (t, *J* = 7.4 Hz, 1H), 6.93 (d, *J* = 8.4 Hz, 1H), 4.61 (t, *J* = 7.6 Hz, 1H), 3.96 (q, *J* = 7.3 Hz, 1H), 3.71 (q, *J* = 7.7 Hz, 1H), 2.81 (s, 3H), 1.89 (m, 1H), 1.65 (m, 2H), 1.55 (m, 1H). ^{13}C NMR (100 MHz, $CDCl_3$) δ 160.0, 142.4 (2C), 139.4, 136.0, 135.4, 132.6, 131.9, 131.4, 130.3, 129.2, 127.7, 127.1, 126.9, 126.5, 125.9, 125.3, 124.0, 120.1, 78.4, 68.7, 34.4, 26.4, 19.7. HRMS (ESI) calcd. for $C_{24}H_{22}NO$ ($M + H^+$) 340.1696. Found 340.1691. HPLC (IA column, 90:10 *n*-Hex/*i*-PrOH, 30 °C, 1 mL/min): t_R 9.31 min (major) and 10.41 min (minor).

(*S*)-1-(2-((*R*)-1-butoxyethyl)-4-methoxynaphthalen-1-yl)isoquinoline (S_a,*R*)-**10Ca**.

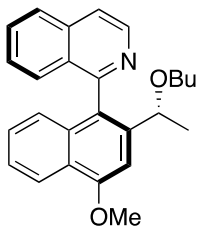

Following the general procedure using **8C** (0.1 mmol, 28.5 mg) and butyl vinyl ether **9a** (0.5 mmol, 65 μL), purification by flash chromatography (*n*-Hexane/EtOAc 5:1) afforded (S_a,*R*)-**10Ca** (35 mg, 91%) as a colorless viscous oil. $[\alpha]^{20}_D$ −14.2 (*c* 0.5, $CHCl_3$) for 80% ee. ^{1}H NMR (400 MHz, $CDCl_3$) δ 8.73 (d, *J* = 5.7 Hz, 1H), 8.33 (d, *J* = 8.4 Hz, 1H), 7.93 (d, *J* = 8.3 Hz, 1H), 7.76 (d, *J* = 5.7 Hz, 1H), 7.67 (m, 1H), 7.45–7.34 (m, 3H), 7.23 (d, *J* = 7.2 Hz, 1H), 7.15 (s, 1H), 6.89 (d, *J* = 8.4 Hz, 1H), 4.11 (s, 3H), 4.09 (q, *J* = 6.4 Hz, 1H), 3.40 (dt, *J* = 9.5, 6.7 Hz, 1H), 3.24 (dt, *J* = 9.7, 6.1 Hz, 1H), 1.44 (m, 2H), 1.32 (m, 2H), 1.18 (d, *J* = 6.5 Hz, 3H), 0.85 (t, *J* = 7.3 Hz, 3H). ^{13}C NMR (100 MHz, $CDCl_3$) δ 159.8, 156.3, 142.6 (2C), 140.9, 136.1, 133.5, 130.3 (2C), 129.5, 127.6, 127.3, 126.9, 126.8, 125.8, 125.1, 121.9, 120.1, 100.8, 73.8, 68.3, 55.7, 32.0, 23.4, 19.4, 13.9. HRMS (ESI) calcd. for $C_{26}H_{28}NO_2$ ($M + H^+$) 386.2115. Found 386.2109. HPLC (IA column, 99:1 *n*-Hex/*i*-PrOH, 30 °C, 1 mL/min): t_R 9.44 min (major) and 10.43 min (minor).

*(S)-1-(2-((R)-1-(cyclohexyloxy)ethyl)-4-methoxynaphthalen-1-yl)isoquinoline (S_a,R)-**10Cb**.*

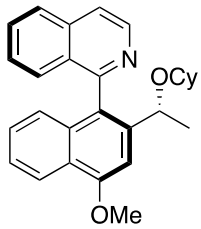

Following the general procedure using **8C** (0.1 mmol, 28.5 mg) and cyclohexyl vinyl ether **9b** (0.5 mmol, 71 μL), purification by flash chromatography (*n*-Hexane/EtOAc 5:1) afforded (S_a,*R*)-**10Cb** (34 mg, 92%) as a pale solid. Single crystals suitable for X-ray analysis were obtained by slow diffusion of *n*-hexane into a solution of (S_a,*R*)-**10Cb** in Et_2O. $[\alpha]^{20}_D$ +5.7 (*c* 0.5, $CHCl_3$) for 91% ee.. ^{1}H NMR (400 MHz, $CDCl_3$) δ 8.72 (d, *J* = 5.7 Hz, 1H), 8.33 (d, *J* = 8.4 Hz, 1H), 7.94 (d, *J* = 8.2 Hz, 1H), 7.77 (d, *J* = 5.4 Hz, 1H), 7.68 (t, *J* = 7.3 Hz, 1H), 7.46-7.34 (m, 3H), 7.23 (d, *J* = 7.2 Hz, 1H), 7.20 (s, 1H), 6.90 (d, *J* = 8.4 Hz, 1H), 4.23 (q, *J* = 6.4 Hz, 1H), 4.11 (s, 3H), 3.33 (s, 1H), 1.93-1.55 (m,

4H), 1.51-1.41 (m, 1H), 1.37-0.80 (m, 8H). ^{13}C NMR (100 MHz, $CDCl_3$) δ 160.0, 156.2, 142.7 (2C), 141.7, 136.1, 133.4, 130.4 (2C), 129.5, 127.8, 127.4, 127.0, 126.9, 125.8, 125.1, 121.9, 120.2, 101.3, 74.0, 70.1, 55.8, 33.8, 31.4, 25.9, 24.4, 24.0, 23.8. HRMS (ESI) calcd. for $C_{28}H_{30}NO_2$ (M + H^+) 412.2271. Found 412.2265. HPLC (IA column, 99:1 *n*-Hex/*i*-PrOH, 30 °C, 1 mL/min): t_R 5.59 min (major) and 7.83 min (minor).

*(S)-1-(2-((R)-1-ethoxyethyl)-4-methoxynaphthalen-1-yl)isoquinoline (S$_a$,R)-**10Cc**.*

Following the general procedure using **8C** (0.1 mmol, 28.5 mg) and ethyl vinyl ether **9c** (2 mmol, 192 μL), purification by flash chromatography (CH_2Cl_2/EtOAc 10:1→5:1) afforded (*S$_a$,R*)-**10Cc** (33 mg, 92%) as a white amorphous solid. $[\alpha]^{20}_D$ −2.6 (*c* 0.5, $CHCl_3$) for 53 % ee. ^{1}H NMR (400 MHz, $CDCl_3$) δ 8.74 (d, *J* = 5.7 Hz, 1H), 8.33 (d, *J* = 8.4 Hz, 1H), 7.93 (d, *J* = 8.2 Hz, 1H), 7.77 (d, *J* = 5.7 Hz, 1H), 7.67 (m, 1H), 7.45-7.35 (m, 3H), 7.23 (d, *J* = 7.1 Hz, 1H), 7.15 (s, 1H), 6.89 (d, *J* = 8.4 Hz, 1H), 4.12 (m, 4H), 3.47 (dq, *J* = 9.5, 7.1 Hz, 1H), 3.29 (dq, *J* = 9.4, 7.0 Hz, 1H), 1.20 (d, *J* = 6.4 Hz, 3H), 1.10 (t, *J* = 7.0 Hz, 3H). ^{13}C NMR (100 MHz, $CDCl_3$) δ 159.8, 156.3, 142.5 (2C), 140.8, 136.1, 133.43, 130.4 (2C), 129.5, 127.6, 127.3, 126.9, 126.9, 125.8, 125.1, 121.9, 120.2, 100.7, 73.7, 63.9, 55.7, 23.4, 15.3. HRMS (ESI) calcd. for $C_{24}H_{24}NO_2$ (M + H^+) 358.1802. Found 358.1802. HPLC (IA column, 97:3 *n*-Hex/*i*-PrOH, 30 °C, 1 mL/min): t_R 6.49 min (minor) and 8.15 min (major).

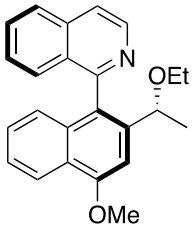

*(S)-1-(2-((R)-1-(benzyloxy)ethyl)-4-methoxynaphthalen-1-yl)isoquinoline (S$_a$,R)-**10Ce**.*

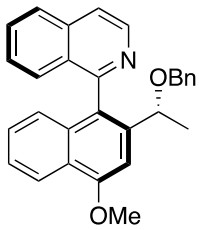

Following the general procedure using **8C** (0.1 mmol, 28.5 mg) and benzyl vinyl ether **1e** (0.5 mmol, 70 μL), purification by flash chromatography (*n*-Hexane/EtOAc 8:1) afforded (*S$_a$,R*)-**10Ce** (38 mg, 91%) as a colorless viscous oil. $[\alpha]^{20}_D$ −59.3 (*c* 0.5, $CHCl_3$) for 91 % ee. ^{1}H NMR

(400 MHz, $CDCl_3$) δ 8.72 (d, *J* = 5.7 Hz, 1H), 8.36 (d, *J* = 8.3 Hz, 1H), 7.92 (d, *J* = 8.3 Hz, 1H), 7.75 (d, *J* = 5.8 Hz, 1H), 7.67 (t, *J* = 7.2 Hz, 1H), 7.45 (t, *J* = 7.3 Hz, 1H), 7.40 (m, 2H), 7.28 (m, 7H), 6.92 (d, *J* = 8.4 Hz, 1H), 4.51 (d, *J* = 11.9 Hz, 1H), 4.31 (d, *J* = 11.9 Hz, 1H), 4.23 (q, *J* = 6.4 Hz, 1H), 4.12 (s, 3H), 1.25 (d, *J* = 6.4 Hz, 3H). ^{13}C NMR (100 MHz, $CDCl_3$) δ 159.7, 156.5, 142.6 (2C), 140.5, 138.9, 136.1, 133.5, 130.4 (2C), 129.4, 128.1 (2C), 127.8 (2C), 127.6, 127.3, 127.2, 127.0 (2C), 125.8, 125.2, 121.9, 120.2, 100.8, 73.93, 70.5, 55.7, 23.4. HRMS (ESI) calcd. for $C_{29}H_{26}NO_2$ (M + H^+) 420.1958. Found 420.1961. HPLC (OD column, 99:1 *n*-Hex/*i*-PrOH, 30 °C, 1 mL/min): t_R 15.61 min (major) and 20.13 min (minor).

*(S)-1-(4-methoxy-2-((R)-1-((4-methoxybenzyl)oxy)ethyl)naphthalen-1-yl)isoquinoline (S_α,R)-**10Cf**.*

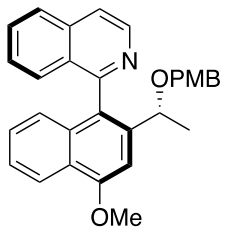

Following the general procedure using **8C** (0.1 mmol, 28.5 mg) and 4-methoxybenzyl vinyl ether **9f** (0.5 mmol, 80 μL), purification by flash chromatography (*n*-Hexane/EtOAc 9:1→7:3) afforded (S_α,*R*)-**10Cf** (23.1 mg, 51%) as a beige amorphous solid. $[\alpha]^{20}_D$ −83.4 (*c* 0.4, $CHCl_3$) for 89 % ee. ^{1}H NMR (400 MHz, $CDCl_3$) δ 8.76 (d, *J* = 5.7 Hz, 1H), 8.39 (d, *J* = 8.4 Hz, 1H), 7.95 (d, *J* = 8.3 Hz, 1H), 7.78 (d, *J* = 5.7 Hz, 1H), 7.70 (ddd, *J* = 8.1, 6.3, 1.7 Hz, 2H), 7.47 (t, *J* = 7.6 Hz, 1H), 7.42 (m, 2H), 7.26 (m, 3H), 6.95 (d, *J* = 8.4 Hz, 1H), 6.85 (m, 2H), 4.46 (d, *J* = 11.4 Hz, 1H), 4.24 (m, 2H), 4.15 (s, 3H), 3.81 (s, 3H), 1.25 (d, *J* = 6.5 Hz, 3H). ^{13}C NMR (100 MHz, $CDCl_3$) δ 159.8, 159.0, 156.5, 142.7, 140.6, 136.1, 133.5, 131.1, 130.3, 129.5 (2C), 129.5, 127.6, 127.4, 127.3, 127.0 (2C), 125.9, 125.2, 122.0, 120.2, 113.6 (2C), 100.9, 73.7, 70.2, 55.8, 55.3, 23.5. HRMS (ESI) calcd. for $C_{30}H_{28}NO_3$ (M + H^+) 450.2064. Found 450.2067. HPLC (OD column, 95:5 *n*-Hex/*i*-PrOH, 30 °C, 1 mL/min): t_R 8.72 min (major) and 13.27 min (minor).

*(S)-1-(4-methoxy-2-((R)-1-(methoxymethoxy)ethyl)naphthalen-1-yl)isoquinoline (S_a,R)-**10Cg**.*

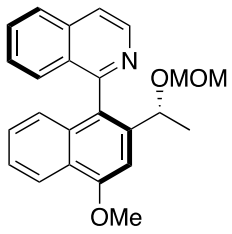

Following the general procedure using **8C** (0.1 mmol, 28.5 mg) and methoxymethyl vinyl ether **9g** (2.0 mmol, 200 μL), purification by flash chromatography (*n*-Hexane/EtOAc 8:2→6:4) afforded (S_a,*R*)- **10Cg** (33.5 mg, 90%) as a beige amorphous solid. $[\alpha]^{20}_D$ +44.8 (*c* 0.5, $CHCl_3$) for 89 % ee. ^{1}H NMR (400 MHz, $CDCl_3$) δ 8.77 (d, *J* = 5.7 Hz, 1H), 8.36 (d, *J* = 8.4 Hz, 1H), 7.96 (d, *J* = 8.3 Hz, 1H), 7.79 (d, *J* = 5.7 Hz, 1H), 7.70 (m, 1H), 7.45 (t, *J* = 7.6 Hz, 1H), 7.41 (m, 2H), 7.26 (d, *J* = 7.0 Hz, 1H), 7.18 (s, 1H), 6.93 (d, *J* = 8.4 Hz, 1H), 4.68 (d, *J* = 6.3 Hz, 1H), 4.52 (d, *J* = 6.3 Hz, 1H), 4.43 (q, *J* = 6.5 Hz, 1H), 4.16 (s, 3H), 3.29 (s, 3H), 1.28 (d, *J* = 6.5 Hz, 3H). ^{13}C NMR (101 MHz, $CDCl_3$) δ 159.6, 156.2, 142.8, 140.1, 136.1, 133.4, 130.3, 129.4, 127.5, 127.3, 127.1, 127.0 (2C), 126.0, 125.3, 125.2, 121.9, 120.2, 101.2, 94.6, 71.1, 55.7, 55.5, 23.0. HRMS (ESI) calcd. for $C_{24}H_{24}NO_3$ ($M + H^+$) 374.1751. Found 374.1743. HPLC (IA column, 95:5 *n*-Hex/*i*-PrOH, 30 °C, 1 mL/min): t_R 7.65 min (minor) and 10.60 min (major).

*1-(4-methoxy-2-(tetrahydrofuran-2-yl)naphthalen-1-yl)isoquinoline **10i**.*

Following the general procedure using **8C** (0.1 mmol, 28.5 mg) and 2,3-dihydrofuran **9i** (1 mmol, 76 μL), purification by flash chromatography (*n*-Hexane/EtOAc 2:1→1:1) afforded **D1-10Ci** (7 mg, 20%) and **D2-10Ci** (27 mg, 76%) as pale amorphous solids.

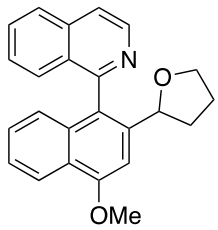

^{1}H NMR (400 MHz, $CDCl_3$) δ 8.70 (d, *J* = 5.8 Hz, 1H), 8.31 (d, *J* = 8.4 Hz, 1H), 7.93 (d, *J* = 8.2 Hz, 1H), 7.76 (d, *J* = 5.8 Hz, 1H), 7.68 (t, *J* = 7.5 Hz, 1H), 7.53 (d, *J* = 8.4 Hz, 1H), 7.42-7.37 (m, 2H), 7.25 (t, *J* = 8.9 Hz, 1H), 7.14 (s, 1H), 6.88 (d, *J* = 8.4 Hz, 1H), 4.33 (t, *J* = 7.0 Hz, 1H), 4.12 (s, 3H), 4.09 (q, *J* = 7.8 Hz, 1H), 3.74 (q, *J* = 7.8 Hz, 1H), 2.09 (m, 1H), 1.97 (m, 1H), 1.90-1.73 (m, 2H). ^{13}C NMR (100 MHz, $CDCl_3$) δ 159.7, 156.3, 141.9, 140.4, 136.3, 133.5,

130.7, 128.7, 127.8, 127.6, 126.8, 126.7, 125.5, 125.1, 124.9, 122.0, 120.3, 100.6, 100.0, 79.0, 69.0, 55.6, 35.1, 26.4. HRMS (ESI) calcd. for $C_{24}H_{22}NO_2$ (M + H^+) 356.1645. Found 356.1640. For 22 % ee HPLC (IA column, 97:3 *n*-Hex/*i*-PrOH, 30 °C, 1 mL/min): t_R 16.55 min (major) and 20.13 min (minor).

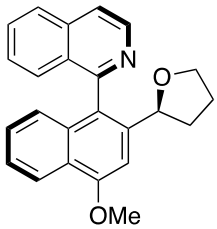

$[\alpha]^{20}_D$ −21.7 (*c* 0.5, $CHCl_3$) for 97 % ee. ^{1}H NMR (400 MHz, $CDCl_3$) δ 8.73 (d, *J* = 5.7 Hz, 1H), 8.32 (d, *J* = 8.4 Hz, 1H), 7.92 (d, *J* = 8.3 Hz, 1H), 7.75 (d, *J* = 5.7 Hz, 1H), 7.66 (m, 1H), 7.39 (m, 3H), 7.21 (t, *J* = 7.3 Hz, 1H), 7.17 (s, 1H), 6.86 (d, *J* = 8.4 Hz, 1H), 4.68 (m, 1H), 4.12 (s, 3H), 3.99 (q, *J* = 7.0 Hz, 1H), 3.73 (q, *J* = 7.8 Hz, 1H), 1.86 (m, 1H), 1.61 (m, 2H), 1.47 (m, 1H). ^{13}C NMR (100 MHz, $CDCl_3$) δ 160.0, 156.1, 142.7 (2C), 140.6, 136.1, 133.7, 130.3 (2C), 129.5, 127.9, 127.2, 127.0, 126.8, 125.7, 124.9, 121.9, 120.1, 101.1, 78.5, 68.6, 55.7, 34.3, 26.3. HRMS (ESI) calcd. for $C_{24}H_{22}NO_2$ (M + H^+) 356.1645. Found 356.1641. HPLC (IA column, 90:10 *n*-Hex/*i*-PrOH, 30 °C, 1 mL/min): t_R 9.95 min (minor) and 13.95 min (major).

*(S)-2-(2-((R)-1-butoxyethyl)naphthalen-1-yl)-3-methylpyridine (S_a,R)-**10Da**.*

Following the general procedure using **8D** (0.1 mmol, 21.9 mg) and butyl vinyl

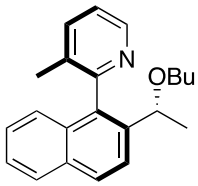

ether **9a** (0.5 mmol, 65 μL), purification by flash chromatography (*n*-Hexane/EtOAc 10:1) afforded (S_a,*R*)-**10Da** (30 mg, 94%) as a colorless viscous oil. $[\alpha]^{20}_D$ +46.1 (*c* 0.5, $CHCl_3$) for 98 % ee. ^{1}H NMR (400 MHz, $CDCl_3$): δ 8.64 (d, *J* = 4.6 Hz, 1H), 7.95 (d, *J* = 8.7 Hz, 1H), 7.87 (d, *J* = 8.4 Hz, 1H), 7.75 (d, *J* = 8.6 Hz, 1H), 7.66 (d, *J* = 7.8 Hz, 1H), 7.44 (t, *J* = 7.4 Hz, 1H), 7.33 (m, 2H), 7.08 (d, *J* = 8.4 Hz, 1H), 4.22 (q, *J* = 6.5 Hz, 1H), 3.33 (dt, *J* = 9.7, 6.5 Hz, 1H), 3.22 (dt, *J* = 9.7, 6.5 Hz, 1H), 1.97 (s, 3H), 1.56–1.38 (m, 2H), 1.38–1.17 (m, 2H), 1.32 (d, *J* = 6.5 Hz, 3H), 0.84 (t, *J* = 7.3 Hz, 3H). ^{13}C NMR (100 MHz, $CDCl_3$): δ ^{13}C NMR (100 MHz, $CDCl_3$) δ 157.2, 147.2, 139.4, 137.6, 135.5, 133.6, 132.9, 131.3, 128.9, 128.1, 126.4, 125.7, 125.3, 123.6, 122.6, 73.4, 68.3, 32.1, 23.3, 19.4,

18.8, 14.0. HRMS (ESI) calcd. for $C_{22}H_{26}NO$ (M + H^+) 320.2009. Found 320.2006. HPLC (IA column, 97:3 *n*-Hex/*i*-PrOH, 30 °C, 1 mL/min): t_R 4.69 min (minor) and 5.22 min (major).

*(S)-2-(2-((R)-1-(cyclohexyloxy)ethyl)naphthalen-1-yl)-3-methylpyridine (S$_a$,R)-**10Db**.*

Following the general procedure using **8D** (0.1 mmol, 21.9 mg) and cyclohexyl vinyl ether **9b** (0.5 mmol, 71 μL), purification by flash chromatography (*n*-Hexane/EtOAc 10:1) afforded (*S$_a$,R*)-**10Db** (30 mg, 87%) as a white amorphous solid. $[\alpha]^{20}_D$ +52.2 (*c* 0.6, $CHCl_3$) for 98 % ee. ^{1}H NMR (400 MHz, $CDCl_3$) δ 8.62 (d, *J* = 4.2 Hz, 1H), 7.93 (d, *J* = 8.6 Hz, 1H), 7.87 (d, *J* = 8.1 Hz, 1H), 7.80 (d, *J* = 8.6 Hz, 1H), 7.67 (d, *J* = 7.5 Hz, 1H), 7.44 (t, *J* = 7.4 Hz, 1H), 7.33 (m, 2H), 7.08 (d, *J* = 8.4 Hz, 1H), 4.37 (q, *J* = 6.4 Hz, 1H), 3.28 (m, 1H), 1.99 (s, 3H), 1.64 (m, 4H), 1.45 (m, 1H), 1.35-0.93 (m, 8H). ^{13}C NMR (101 MHz, $CDCl_3$) δ 157.3, 147.2, 140.0, 137.5, 135.4, 133.5, 132.9, 131.2, 128.7, 128.1, 126.4, 125.6, 125.3, 124.0, 122.6, 73.7, 69.5, 33.6, 31.4, 25.9, 24.3, 24.0, 23.6, 18.8. HRMS (ESI) calcd. for $C_{24}H_{28}NO$ (M + H^+) 346.2165. Found 346.2158. HPLC (AS-H column, 99:1 *n*-Hex/*i*-PrOH, 30 °C, 0.5 mL/min): t_R 8.27 min (minor) and 9.34 min (major).

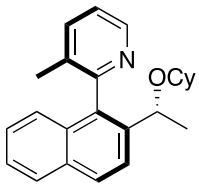

*(S)-2-(2-((R)-1-ethoxyethyl)naphthalen-1-yl)-3-methylpyridine (S$_a$,R)-**10Cc**.*

Following the general procedure using **8D** (0.1 mmol, 21.9 mg) and ethyl vinyl ether **9c** (2 mmol, 192 μL), purification by flash chromatography (CH_2Cl_2/EtOAc 10:1→5:1) afforded (*S$_a$,R*)-**10Cc** (28 mg, 96%) as a colorless viscous oil. $[\alpha]^{20}_D$ +60.1 (*c* 0.5, $CHCl_3$) for 96 % ee. ^{1}H NMR (400 MHz, $CDCl_3$) δ 8.64 (d, *J* = 4.4 Hz, 1H), 7.95 (d, *J* = 8.6 Hz, 1H), 7.87 (d, *J* = 8.1 Hz, 1H), 7.75 (d, *J* = 8.6 Hz, 1H), 7.68 (d, *J* = 7.6 Hz, 1H), 7.44 (t, *J* = 7.4 Hz, 1H), 7.33 (m, 2H), 7.07 (d, *J* = 8.4 Hz, 1H), 4.24 (q, *J* = 6.5 Hz, 1H), 3.39 (dq, *J* = 9.4, 7.0 Hz, 1H), 3.28 (dq, *J* = 9.5, 7.0 Hz, 1H), 1.97 (s, 3H), 1.33 (d, *J* = 6.5 Hz, 3H), 1.09 (t, *J* = 7.0 Hz, 3H).

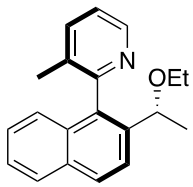

^{13}C NMR (100 MHz, $CDCl_3$) δ 157.0, 147.1, 139.2, 137.7, 135.4, 133.7, 132.9, 131.3, 129.0, 128.1, 126.4, 125.7, 125.3, 123.5, 122.6, 73.2, 63.8, 23.2, 18.8, 15.3. HRMS (ESI) calcd. for $C_{20}H_{22}NO$ (M + H^+) 292.1696. Found 292.1699. HPLC (IA column, 97:3 *n*-Hex/*i*-PrOH, 30 °C, 1 mL/min): t_R 5.12 min (minor) and 6.35 min (major).

*(S)-2-(2-((R)-1-(benzyloxy)ethyl)naphthalen-1-yl)-3-methylpyridine (S$_a$,R)-**10De.***

Following the general procedure using **8D** (0.1 mmol, 21.9 mg) and benzyl vinyl ether **9e** (0.5 mmol, 70 μL), purification by flash chromatography (*n*-Hexane/EtOAc 8:1) afforded (*S$_a$,R*)-**10De** (16 mg, 45%) as a colorless viscous oil. $[\alpha]^{20}_D$ −27.0 (*c* 0.5, $CHCl_3$) for 99 % ee. ^{1}H NMR (400 MHz, $CDCl_3$) δ 8.62 (d, *J* = 4.2 Hz, 1H), 7.99 (d, *J* = 8.6 Hz, 1H), 7.90 (d, *J* = 8.1 Hz, 1H), 7.85 (d, *J* = 8.6 Hz, 1H), 7.66 (d, *J* = 7.6 Hz, 1H), 7.47 (t, *J* = 7.3 Hz, 1H), 7.36 (t, *J* = 7.4 Hz, 1H), 7.30 (m, 5H), 7.23 (m, 1H), 7.10 (d, *J* = 8.4 Hz, 1H), 4.45 (d, *J* = 11.9 Hz, 1H), 4.36 (q, *J* = 6.4 Hz, 1H), 4.29 (d, *J* = 11.9 Hz, 1H), 1.98 (s, 3H), 1.39 (d, *J* = 6.5 Hz, 3H). ^{13}C NMR (100 MHz, $CDCl_3$) δ 157.0, 147.2 (2C), 139.0, 138.9, 137.7 (2C), 135.7, 133.6, 133.0, 131.3, 129.1, 128.1, 128.1, 127.7, 127.1, 126.5, 125.8, 125.3, 123.6, 122.6, 73.5, 70.4, 23.3, 18.7. HRMS (ESI) calcd. for $C_{25}H_{24}NO$ (M + H^+) 354.1852. Found 354.1846. HPLC (OJ-H column, 95:5 *n*-Hex/*i*-PrOH, 30 °C, 1 mL/min): t_R 13.14 min (minor) and 15.81 min (major).

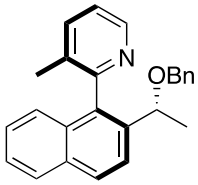

*(S)-2-(2-((R)-1-((4-methoxybenzyl)oxy)ethyl)naphthalen-1-yl)-3-methylpyridine (S$_a$,R)-**10Df.***

Following the general procedure using **8D** (0.1 mmol, 21.9 mg) and methoxybenzyl vinyl ether **9f** (0.5 mmol, 80 μL), purification by flash chromatography (*n*-Hexane/EtOAc 9:1→7:3) afforded (*S$_a$,R*)-**10Df** (12.7 mg,

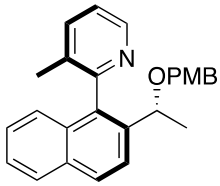

33%) as a beige amorphous solid. $[\alpha]^{20}_{D}$ −49.0 (*c* 0.5, $CHCl_3$) for 99 % ee. ^{1}H NMR (400 MHz, $CDCl_3$) δ 8.66 (d, *J* = 4.8 Hz, 1H), 8.02 (d, *J* = 8.7 Hz, 1H), 7.93 (d, *J* = 8.1 Hz, 1H), 7.87 (d, *J* = 8.6 Hz, 1H), 7.69 (d, *J* = 7.7 Hz, 1H), 7.49 (ddd, *J* = 8.1, 6.9, 1.1 Hz, 2H), 7.38 (ddd, *J* = 8.2, 6.9, 1.3 Hz, 2H), 7.33 (dd, *J* = 7.7, 4.8 Hz, 1H), 7.24 (d, *J* = 8.7 Hz, 2H), 7.13 (d, *J* = 8.6 Hz, 1H), 6.85 (m, 2H), 4.39 (m, 2H), 4.23 (d, *J* = 11.4 Hz, 1H), 3.81 (s, 3H), 2.01 (s, 3H), 1.39 (d, *J* = 6.5 Hz, 3H). ^{13}C NMR (100 MHz, $CDCl_3$) δ 158.9, 157.1, 147.4, 139.0, 137.6, 135.9, 133.5, 133.0, 131.4, 131.2, 129.4 (2C), 129.0, 128.1, 126.5, 125.8, 125.4, 123.7, 122.7, 113.6 (2C), 73.3, 70.1, 55.3, 23.3, 18.8. HRMS (ESI) calcd. for $C_{26}H_{26}NO_2$ (M + H^+) 384.1958. Found 384.1950. HPLC (OD column, 90:10 *n*-Hex/*i*-PrOH, 30 °C, 1 mL/min): t_R 6.13 min (major) and 8.23 min (minor).

(S)-2-(2-((R)-1-(methoxymethoxy)ethyl)naphthalen-1-yl)-3-methylpyridine *(S_a,R)-**10Dg.***

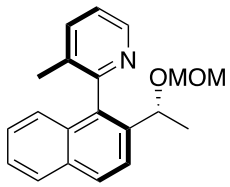

Following the general procedure using **8D** (0.1 mmol, 21.9 mg) and methoxymethyl vinyl ether **9g** (2.0 mmol, 200 μL), purification by flash chromatography (*n*-Hexane/EtOAc 7:3) afforded (S_a,*R*)-**10Dg** (24.1 mg, 79%) as a beige oil. $[\alpha]^{20}_{D}$ +139.7 (*c* 0.5, $CHCl_3$) for >99 % ee. ^{1}H NMR (400 MHz, $CDCl_3$) δ 8.67 (d, *J* = 4.8 Hz, 1H), 7.98 (d, *J* = 8.7 Hz, 1H), 7.90 (d, *J* = 8.1 Hz, 1H), 7.80 (d, *J* = 8.7 Hz, 1H), 7.69 (d, *J* = 7.7 Hz, 1H), 7.48 (ddd, *J* = 8.1, 6.9, 1.2 Hz, 1H), 7.36 (m, 2H), 7.11 (d, *J* = 8.3 Hz, 1H), 4.66 (d, *J* = 6.2 Hz, 1H), 4.56 (q, *J* = 6.5 Hz, 1H), 4.52 (d, *J* = 6.4 Hz, 1H), 3.32 (s, 3H), 2.00 (s, 3H), 1.42 (d, *J* = 6.5 Hz, 3H). ^{13}C NMR (101 MHz, $CDCl_3$) δ 157.0, 147.5, 138.6, 137.5, 135.5, 133.4, 132.9, 131.3, 128.9, 129.0, 126.5, 125.8, 125.5, 123.9, 122.7, 94.6, 70.7, 55.4, 22.9, 18.8. HRMS (ESI) calcd. for $C_{20}H_{22}NO_2$ (M + H^+) 308.1645. Found 308.1644. HPLC (IA column, 95:5 *n*-Hex/*i*-PrOH, 30 °C, 1 mL/min): t_R 9.34 min (minor) and 10.2 min (major).

3-methyl-2-(2-(tetrahydrofuran-2-yl)naphthalen-1-yl)pyridine ***10Di.***

Following the general procedure using **8D** (0.1 mmol, 21.9 mg) and 2,3-dihydrofuran **9i** (1 mmol, 76 μL), purification by flash chromatography (*n*-Hexane/EtOAc 3:1→1:1) afforded **D1-10Di** (4 mg, 15%) and **D2-10Di** (10 mg, 35%) as pale viscous oils.

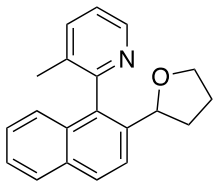

^{1}H NMR (400 MHz, $CDCl_3$) δ 8.61 (d, *J* = 4.8 Hz, 1H), 7.93 (d, *J* = 8.7 Hz, 1H), 7.86 (d, *J* = 8.2 Hz, 1H), 7.71 (d, *J* = 8.6 Hz, 1H), 7.67 (d, *J* = 7.7 Hz, 1H), 7.43 (t, *J* = 7.2 Hz, 1H), 7.34-7.28 (m, 2H), 7.07 (d, *J* = 8.4 Hz, 1H), 4.44 (t, *J* = 7.4 Hz, 1H), 4.14 (q, *J* = 7.3 Hz, 1H), 3.86 (q, *J* = 7.3 Hz, 1H), 2.17-2.01 (m, 2H), 2.00 (s, 3H), 1.88-1.81 (m, 2H). ^{13}C NMR (100 MHz, $CDCl_3$) δ 157.4, 147.1, 138.5, 137.7, 134.7, 133.0, 133.0, 131.4, 128.7, 128.1, 126.3, 125.5, 125.2, 123.3, 122.6, 78.8, 69.2, 35.1, 26.6, 18.8. HRMS (ESI) calcd. for $C_{20}H_{20}NO$ ($M + H^+$) 290.1539. Found 290.1542. For 12 % ee HPLC (IB column, 99:1 *n*-Hex/*i*-PrOH, 30 °C, 1 mL/min): t_R 16.98 min (major) and 21.65 min (minor).

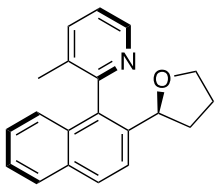

$[\alpha]^{20}_D$ −111.0 (*c* 0.5, $CHCl_3$) for 96 % ee. ^{1}H NMR (400 MHz, $CDCl_3$) δ 8.65 (d, *J* = 4.0 Hz, 1H), 7.92 (d, *J* = 8.6 Hz, 1H), 7.87 (d, *J* = 8.1 Hz, 1H), 7.72 (d, *J* = 8.9 Hz, 1H), 7.69 (d, *J* = 8.1 Hz, 1H), 7.43 (t, *J* = 7.4 Hz, 1H), 7.32 (t, *J* = 7.6 Hz, 2H), 7.05 (d, *J* = 8.4 Hz, 1H), 4.77 (t, *J* = 7.4 Hz, 1H), 3.94 (t, *J* = 7.2 Hz, 1H), 3.80 (q, *J* = 7.8, 7.4 Hz, 1H), 1.97 (s, 3H), 1.96-1.69 (m, 4H). ^{13}C NMR (100 MHz, $CDCl_3$) δ 157.3, 146.8, 139.0, 137.9, 133.9, 132.7, 131.4, 128.7, 128.1, 126.4, 125.5, 124.9, 123.7, 122.6, 78.5, 68.7, 33.9, 29.7, 26.4, 18.9. HRMS (ESI) calcd. for $C_{20}H_{20}NO$ ($M + H^+$) 290.1539. Found 290.1541. HPLC (IA column, 90:10 *n*-Hex/*i*-PrOH, 30 °C, 1 mL/min): t_R 7.85 min (major) and 10.03 min (minor).

*(S)-1-(2-((R)-1-butoxyethyl)-6-methylphenyl)isoquinoline (S_a,R)-**10Ea.***

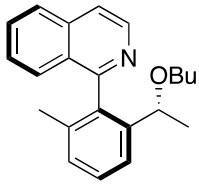

Following the general procedure using **8E** (0.1 mmol, 21.9 mg) and butyl vinyl ether **9a** (2 mmol, 260 μL), purification by flash chromatography (*n*-Hexane/EtOAc 10:1) afforded (S_a,*R*)-**10Ea** (28 mg, 88%) as a colorless viscous oil. $[\alpha]^{20}_D$ −35.9 (*c* 0.5, $CHCl_3$) for 98 % ee. ^{1}H NMR (400 MHz, $CDCl_3$) δ 8.65 (d, *J* = 5.7 Hz, 1H), 7.90 (d, *J* = 8.2 Hz, 1H), 7.68 (m, 2H), 7.51 (d, *J* = 7.8 Hz, 1H), 7.47 (d, *J* = 3.8 Hz, 2H), 7.43 (t, *J* = 7.7 Hz, 1H), 7.23 (d, *J* = 7.4 Hz, 1H), 3.90 (q, *J* = 6.4 Hz, 1H), 3.34 (dt, *J* = 9.2, 6.7 Hz, 1H), 3.15 (dt, *J* = 9.4, 6.3 Hz, 1H), 1.87 (s, 3H), 1.39 (m, 2H), 1.25 (m, 2H), 1.05 (d, *J* = 6.4 Hz, 3H), 0.83 (t, *J* = 7.3 Hz, 3H). ^{13}C NMR (100 MHz, $CDCl_3$) δ 160.5, 143.2, 142.3, 137.3, 136.1, 136.0, 130.3, 128.8, 128.68, 128.2, 127.3, 127.0, 127.0, 123.3, 119.9, 73.7, 68.2, 32.0, 24.1, 19.8, 19.3, 13.9. HRMS (ESI) calcd. for $C_{22}H_{26}NO$ ($M + H^+$) 320.2009. Found 320.2005. HPLC (OD-H column, 99:1 *n*-Hex/*i*-PrOH, 30 °C, 1 mL/min): t_R 5.80 min (minor) and 6.91 min (major).

*((S)-1-(2-((R)-1-(cyclohexyloxy)ethyl)-6-methylphenyl)isoquinoline (S_a,R)-**10Eb.***

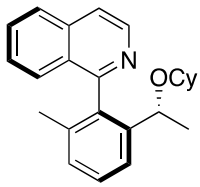

Following the general procedure using **8E** (0.1 mmol, 21.9 mg) and cyclohexyl vinyl ether **9b** (2 mmol, 284 μL), purification by flash chromatography (*n*-Hexane/EtOAc 5:1) afforded (S_a,*R*)-**10Eb** (27 mg, 78%) as a colorless viscous oil. $[\alpha]^{20}_D$ −16.7 (*c* 0.5, $CHCl_3$) for 98 % ee. ^{1}H NMR (400 MHz, $CDCl_3$) δ 8.64 (d, J = 5.8 Hz, 1H), 7.91 (d, J = 8.2 Hz, 1H), 7.79–7.68 (m, 2H), 7.57 (d, J = 7.8 Hz, 1H), 7.49 (m, 2H), 7.43 (t, J = 7.7 Hz, 1H), 7.23 (d, J = 7.5 Hz, 1H), 4.06 (q, J = 6.4 Hz, 1H), 3.25 (m 1H), 1.88 (s, 3H), 1.78-1.53 (m, 4H), 1.50-1.39 (m, 1H), 1.32-0.83 (m, 5H), 1.02 (d, J = 6.4 Hz, 3H). ^{13}C NMR (100 MHz, $CDCl_3$) δ 160.6, 144.0, 142.3, 137.16, 136.0, 135.7, 130.3, 128.7, 128.5, 128.2, 127.4, 127.0, 123.6, 119.9, 73.8, 69.7, 33.5, 31.3, 25.8, 24.5, 24.3, 23.9, 19.8. HRMS (ESI) calcd. for $C_{24}H_{28}NO$ ($M + H^+$) 346.2165. Found 346.2161. HPLC (IA column,

99:1 *n*-Hex/*i*-PrOH, 30 °C, 0.5 mL/min): t_R 9.20 min (major) and 9.68 min (minor).

*((S)-1-(2-((R)-1-ethoxyethyl)-6-methylphenyl)isoquinoline (S_a,R)-**10Ec**.*

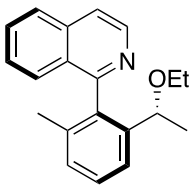

Following the general procedure using **8E** (0.1 mmol, 21.9 mg) and ethyl vinyl ether **9c** (2 mmol, 192 μL), purification by flash chromatography (CH_2Cl_2/EtOAc 10:1→5:1) afforded (S_a,*R*)-**10Ec** (19 mg, 65%) as a colorless viscous oil. $[\alpha]^{20}_D$ −21.9 (*c* 0.5, $CHCl_3$) for 95 % ee. ^{1}H NMR (400 MHz, $CDCl_3$) δ 8.62 (d, *J* = 5.8 Hz, 1H), 7.91 (d, *J* = 8.3 Hz, 1H), 7.70 (m, 2H), 7.47 (m, 4H), 7.24 (d, *J* = 7.3 Hz, 1H), 3.92 (q, *J* = 6.4 Hz, 1H), 3.37 (dq, *J* = 9.4, 7.1 Hz, 1H), 3.20 (dq, *J* = 9.5, 7.0 Hz, 1H), 1.87 (s, 3H), 1.07 (d, *J* = 6.4 Hz, 3H), 1.03 (t, *J* = 7.0 Hz, 3H). ^{13}C NMR (100 MHz, $CDCl_3$) δ 160.4, 143.1, 141.9, 136.2, 136.1, 130.6, 129.0, 128.8, 128.2, 127.5, 127.1, 127.0, 123.4, 120.1, 77.3, 73.6, 63.8, 24.0, 19.8, 15.2. HRMS (ESI) calcd. for $C_{20}H_{22}NO$ ($M + H^+$) 292.1696. Found 292.1698. HPLC (OD-H column, 99:1 *n*-Hex/*i*-PrOH, 30 °C, 1 mL/min): t_R 6.97 min (minor) and 7.65 min (major).

*1-(2-methyl-6-(tetrahydrofuran-2-yl)phenyl)isoquinoline **10Ei**.*

Following the general procedure using **8E** (0.1 mmol, 21.9 mg) and 2,3-dihydrofuran **9i** (2 mmol, 152 μL), purification by flash chromatography (*n*-Hexane/EtOAc 3:1→1:1) afforded **D1-10Ei** (6 mg, 17%) and **D2-10Ei** (12 mg, 42%) as pale viscous oils.

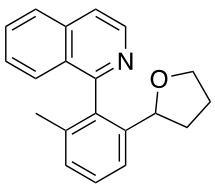

^{1}H NMR (400 MHz, $CDCl_3$) δ 8.63 (d, *J* = 5.8 Hz, 1H), 7.90 (d, *J* = 8.2 Hz, 1H), 7.71 (m, 2H), 7.58 (d, *J* = 8.3 Hz, 1H), 7.50 (m, 2H), 7.41 (t, *J* = 7.7 Hz, 1H), 7.23 (d, *J* = 7.5 Hz, 1H), 4.16 (t, *J* = 6.9 Hz, 1H), 3.99 (q, *J* = 6.5 Hz, 1H), 3.66 (m, 1H), 1.91 (m, 2H), 1.87 (s, 3H), 1.71 (s, 2H). ^{13}C NMR (101 MHz, $CDCl_3$) δ 160.3, 142.7, 141.7, 141.5, 136.3, 136.1, 130.8, 128.9, 128.8, 127.9, 127.5,

126.9, 126.9, 122.6, 120.2, 78.6, 68.8, 35.2, 26.2, 19.7. HRMS (ESI) calcd. for $C_{20}H_{20}NO$ (M + H^+) 290.1539. Found 290.1537. For 76 % ee HPLC (OD column, 90:10 *n*-Hex/*i*-PrOH, 30 °C, 1 mL/min): t_R 5.37 min (major) and 8.84 min (minor).

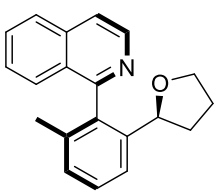

$[\alpha]^{20}_D$ –22.9 (*c* 0.5, $CHCl_3$) for 98 % ee. ^{1}H NMR (400 MHz, $CDCl_3$) δ 8.64 (d, *J* = 5.7 Hz, 1H), 7.89 (d, *J* = 8.2 Hz, 1H), 7.69 (s, 2H), 7.49 (m, 3H), 7.39 (t, *J* = 7.7 Hz, 1H), 7.22 (d, *J* = 7.5 Hz, 1H), 4.57 (t, *J* = 7.5 Hz, 1H), 3.81 (q, *J* = 7.2 Hz, 1H), 3.64 (q, *J* = 7.8 Hz, 1H), 1.85 (s, 3H), 1.75 (m, 1H), 1.58 (m, 1H), 1.44 (m, 1H), 1.31 (m, 1H). ^{13}C NMR (100 MHz, $CDCl_3$) δ 160.58, 142.59, 142.12, 136.24, 136.04, 130.32, 128.60, 128.27, 127.30, 127.14, 126.97, 122.98, 119.91, 78.32, 68.34, 34.39, 26.17, 19.75. ^{13}C NMR (100 MHz, $CDCl_3$) δ 160.6, 142.6 (2C), 142.1, 136.2, 136.0, 135.9, 130.3, 128.6, 128.3, 127.3, 127.1, 127.0, 123.0, 119.9, 78.3, 68.3, 34.4, 26.2, 19.8. HRMS (ESI) calcd. for $C_{20}H_{20}NO$ (M + H^+) 290.1539. Found 290.1541. HPLC (IA column, 90:10 *n*-Hex/*i*-PrOH, 30 °C, 1 mL/min): t_R 6.34 min (major) and 8.39 min (minor).

General procedure for MOM-derivatives (*S*$_a$,*R*)-10Ag-10Dg deprotection. Synthesis of alcohols (*S*$_a$,*R*)-11A-11D.

A freshly prepared solution of triflic acid (0.04 M, DCM) was dropwise added to cooled (0 °C) solution of the corresponding MOM-protected alcohols (*S*$_a$,*R*)-**7f-10f** in DCM (final concentration 0.04 M for every reactant). The resulting bright yellow solution was allowed to warm up from 0 °C to room temperature for 3 h and then it was diluted with DCM (5 mL), washed with saturated $NaHCO_3$ (3 x 5 mL) and brine (5 mL). The organic phase is concentrated to dryness and the crude is then purified by flash chromatography on silica gel.

*(R)-1-(1-((S)-isoquinolin-1-yl)naphthalen-2-yl)ethanol (S_a,R)-**11A.***

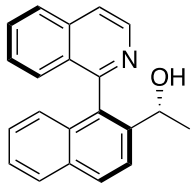

Following the general procedure using (S_a,*R*)-**10Ag**(0.13 mmol, 45.0 mg), purification by flash chromatography (*n*-Hexane/EtOAc 3:7) afforded (S_a,*R*)-**11A** (77%, 30.1 mg) as a beige amorphous solid. $[\alpha]^{20}_D$ +139.3 (*c* 0.5, $CHCl_3$) for 98 % ee. ^{1}H NMR (400 MHz, $CDCl_3$) δ 8.64 (d, *J* = 5.8 Hz, 1H), 7.97 (d, *J* = 9.2 Hz, 1H), 7.95 (d, *J* = 9.4 Hz, 1H), 7.91 (d, *J* = 8.2 Hz, 1H), 7.83 (d, *J* = 8.7 Hz, 1H), 7.78 (d, *J* = 5.7 Hz, 1H), 7.74 – 7.65 (m, 1H), 7.44 (t, *J* = 7.5 Hz, 1H), 7.42 – 7.31 (m, 2H), 7.23 (t, *J* = 7.6 Hz, 1H), 6.92 (d, *J* = 8.5 Hz, 1H), 4.48 (q, *J* = 6.4 Hz, 1H), 3.97 (br s, 1H), 1.35 (d, *J* = 6.5 Hz, 3H). ^{13}C NMR (100 MHz, $CDCl_3$) δ 159.6, 142.1, 141.9, 136.2, 133.7, 132.7, 132.3, 130.6, 129.4, 128.8, 128.0, 127.7, 127.6, 127.0, 126.3, 126.2, 125.7, 123.2, 120.7, 66.3, 21.9. HRMS (ESI) calcd. for $C_{21}H_{18}NO$ (M + H^+) 300.1383. Found 300.1385. HPLC (AS-H column, 85:15 *n*-Hex/*i*-PrOH, 30 °C, 1 mL/min): t_R 4.45 min (minor) and 4.98 min (major).

*(R)-1-(1-((S)-isoquinolin-1-yl)-4-methylnaphthalen-2-yl)ethanol (S_a,R)-**11B.***

Following the general procedure using (S_a,*R*)-**10Bg** (0.082 mmol, 29.3 mg),

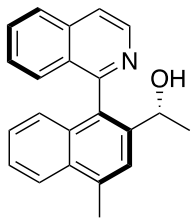

purification by flash chromatography (*n*-Hexane/EtOAc 1:1 → 3:7) afforded (S_a,*R*)-**11B** (14.7 mg, 57%) as a yellow amorphous solid. $[\alpha]^{20}_D$ +109.3 (*c* 0.4, $CHCl_3$) for 98 % ee. ^{1}H NMR (400 MHz, $CDCl_3$) δ 8.66 (d, *J* = 5.8 Hz, 1H), 8.08 (d, *J* = 8.5 Hz, 1H), 7.98 (d, *J* = 8.3 Hz, 1H), 7.85 (d, *J* = 5.9 Hz, 1H), 7.79 – 7.69 (m, 2H), 7.53 – 7.44 (m, 2H), 7.42 (d, *J* = 4.1 Hz, 2H), 7.28 – 7.19 (m, 1H), 6.92 (d, *J* = 8.4 Hz, 1H), 4.44 (q, *J* = 6.4 Hz, 1H), 2.82 (s, 3H), 1.37 (d, *J* = 6.5 Hz, 3H). ^{13}C NMR (100 MHz, $CDCl_3$) δ 159.8, 141.7, 141.4, 136.2, 136.0, 132.4, 132.0, 131.7, 130.8, 129.0, 127.9, 127.7, 127.0, 126.8, 126.1, 125.6, 124.2, 123.9, 120.7, 77.3, 77.2, 77.0, 76.7, 66.3, 21.8, 19.8. HRMS (ESI) calcd. for $C_{22}H_{20}NO$ (M + H^+) 314.1539. Found 314.1540. HPLC (IA column, 90:10 *n*-Hex/*i*-PrOH, 30 °C, 1 mL/min): t_R 7.96 min (minor) and 8.95 min (major).

*(R)-1-(1-((S)-isoquinolin-1-yl)-4-methoxynaphthalen-2-yl)ethanol (S_a,R)-**11C**.*

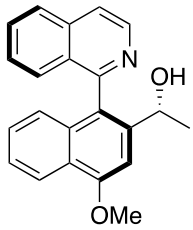

Following the general procedure using (S_a,*R*)-**10Cg** (0.08 mmol, 29.9 mg), purification by flash chromatography (*n*-Hexane/EtOAc 1:1 → 3:7) afforded (S_a,*R*)-**11C** (17.7 mg, 67%) as a brown amorphous solid. $[\alpha]^{20}_D$ +64.3 (*c* 0.5, $CHCl_3$) for 92 % ee. ^{1}H NMR (400 MHz, $CDCl_3$) δ 8.65 (d, *J* = 5.9 Hz, 1H), 8.34 (d, *J* = 8.4 Hz, 1H), 7.98 (d, *J* = 8.3 Hz, 1H), 7.84 (d, *J* = 5.8 Hz, 1H), 7.78 – 7.70 (m, 1H), 7.47 – 7.37 (m, 3H), 7.28 – 7.19 (m, 1H), 7.20 (s, 1H), 6.85 (d, *J* = 8.5 Hz, 1H), 4.50 (q, *J* = 6.4 Hz, 1H), 4.10 (s, 3H), 2.73 (br s, 1H), 1.35 (d, *J* = 6.5 Hz, 3H). ^{13}C NMR (100 MHz, $CDCl_3$) δ 159.8, 156.3, 142.8, 141.8, 136.3, 133.4, 130.7, 129.2, 128.0, 127.5, 127.0, 126.8, 125.8, 125.6, 125.0, 124.9, 122.1, 120.6, 100.8, 66.4, 55.53, 22.2. HRMS (ESI) calcd. for $C_{22}H_{20}NO_2$ (M + H^+) 330.1489. Found330.1489. HPLC (IA column, 90:10 *n*-Hex/*i*-PrOH, 30 °C, 1 mL/min): t_R 6.43 min (minor) and 10.54 min (major).

*(R)-1-(1-((S)-3-methylpyridin-2-yl)naphthalen-2-yl)ethanol (S_a,R)-**11D**.*

Following the general procedure using (S_a,*R*)-**10Dg** (0.21 mmol, 64.5 mg), purification by flash chromatography (*n*-Hexane/EtOAc 1:1 → 7:1) afforded (S_a,*R*)-**11D** (40.1 mg, 72%) as a light brown amorphous solid. $[\alpha]^{20}_D$ +89.7 (*c* 0.5, $CHCl_3$) for 99 % ee. ^{1}H NMR (400 MHz, $CDCl_3$) δ 8.60 (d, *J* = 4.6 Hz, 1H), 7.97 (d, *J* = 8.7 Hz, 1H), 7.89 (d, *J* = 8.2 Hz, 1H), 7.81 (d, *J* = 8.6 Hz, 1H), 7.77 (d, *J* = 7.6 Hz, 1H), 7.51 – 7.43 (m, 1H), 7.43 – 7.32 (m, 2H), 7.10 (d, *J* = 8.5 Hz, 1H), 4.54 (q, *J* = 6.6 Hz, 1H), 2.54 (br s, 1H), 2.00 (s, 3H), 1.47 (d, *J* = 6.5 Hz, 3H). ^{13}C NMR (100 MHz, $CDCl_3$) δ 157.0, 146.8, 140.6, 138.3, 134.8, 133.8, 132.8, 131.1, 129.1, 128.3, 126.6, 125.7, 125.2, 123.3, 123.0, 66.1, 21.6, 18.9. HRMS (ESI) calcd. for $C_{18}H_{18}NO$ (M + H^+) 264.1383 Found 264.1385. HPLC (AS-H column, 90:10 *n*-Hex/*i*-PrOH, 30 °C, 1 mL/min): t_R 4.51 min (minor) and 4.96 min (major).

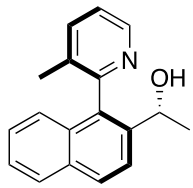

General procedure for the transformation of alcohols (S_a,*R*)-12-15 into azides. Synthesis of azides (S_a,*S*)-16-17.

To a solution of alcohol (S_a,*R*)-**11A, 11D** (~0.1 mmol, 0.2 M) and DPPA (1.5 equivalents) cooled to 0 °C, DPU is added *via* syringe (1.7 equivalents) and stirred for 1 hour. And then warm at 60 °C for 48 hours. The reaction mixture is diluted with ethyl acetate (5 mL) and washed with water (5 mL), brine (3 x 5 mL) and dried over Na_2SO_4, filtrated and concentrated to dryness. The crude was then purified by flash chromatography on silica gel (n-hexane/EtOAc 7:3).

(S)-1-(2-((S)-1-azidoethyl)naphthalen-1-yl)isoquinoline (S_a,S)-13A.

Following the general procedure using (S_a,*R*)-**11A** (0.1 mmol, 30.1 mg, 98% ee),

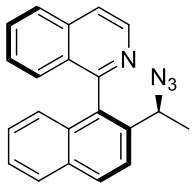

purification by flash chromatography (*n*-Hexane/EtOAc 7:3) afforded (S_a,*S*)-**13A** (72%, 23.2mg) as a beige amorphous solid. $[\alpha]^{20}_D$ +32.7 (*c* 0.5, $CHCl_3$) for 98 % ee. ^{1}H NMR (400 MHz, $CDCl_3$) δ 8.73 (d, *J* = 5.7 Hz, 1H), 8.08 (d, *J* = 8.7 Hz, 1H), 7.97 (d, *J* = 8.3 Hz, 1H), 7.93 (d, *J* = 8.2 Hz, 1H), 7.82 (d, *J* = 5.7 Hz, 1H), 7.76 (d, *J* = 8.7 Hz, 1H), 7.75 – 7.69 (m, 1H), 7.50 – 7.38 (m, 3H), 7.27 (t, *J* = 8.8 Hz, 1H), 6.97 (d, *J* = 8.5 Hz, 1H), 4.26 (q, *J* = 6.7 Hz, 1H), 1.48 (d, *J* = 6.7 Hz, 3H). ^{13}C NMR (100 MHz, $CDCl_3$) δ 158.7, 142.3, 137.7, 136.3, 134.0, 133.0, 132.4, 130.8, 129.8, 128.5, 128.2, 127.9, 127.1, 126.9, 126.7, 126.2, 126.2, 123.3, 120.6, 58.8, 22.1. HRMS (ESI) calcd. for $C_{21}H_{17}N_4$ ($M + H^+$) 325.1448. Found 325.1449. HPLC (IA column, 95:5 *n*-Hex/*i*-PrOH, 30 °C, 1 mL/min): t_R 6.75 min (minor) and 8.66 min (major).

*(S)-2-(2-((S)-1-azidoethyl)naphthalen-1-yl)-3-methylpyridine (S_a,S)-**13D.***

Following the general procedure using (S_a,*R*)-**11D** (0.15 mmol, 40.1 mg, 99% ee), purification by flash chromatography (*n*-Hexane/EtOAc 7:3) afforded (S_a,*S*)-**13D** (84%, 36.7 mg) as a beige amorphous solid. $[\alpha]^{20}_D$ +121.8 (*c* 0.5, $CHCl_3$) for 99 % ee. ^{1}H NMR (400 MHz, $CDCl_3$) δ 8.63 (d, *J* = 4.6 Hz, 1H), 7.98 (d, *J* = 8.7 Hz, 1H), 7.89 (d, *J* = 8.1 Hz, 1H), 7.75 – 7.65 (m, 2H), 7.47 (t, *J* = 7.5 Hz, 1H), 7.40 – 7.30 (m, 2H), 7.10 (d, *J* = 8.5 Hz, 1H), 4.35 (q, *J* = 6.5 Hz, 1H), 2.02 (s, 3H), 1.50 (d, *J* = 6.7 Hz, 3H). ^{13}C NMR (100 MHz, $CDCl_3$) δ 156.7, 147.4, 138.0, 136.3, 135.5, 133.1, 131.3, 129.2, 128.1, 126.7, 126.1, 125.5, 123.2, 122.9, 58.8, 21.8, 18.7. HRMS (ESI) calcd. for $C_{18}H_{17}N_4$ (M + H^+) 289.1448. Found 289.1448. HPLC (OD column, 99:1 *n*-Hex/*i*-PrOH, 30 °C, 1 mL/min): t_R 9.4 min (minor) and 11.7 min (major).

General procedure for the reduction of azides (S_a,*S*)-13A, 13D. Synthesis of amines (S_a,*S*)-14A-14D.

To a stirred solution of azide (S_a,*S*)-**13A-13D** (~0.1 mmol, 0.5 M) in THF, PPh_3 (3 equivalents) was added portionwise and after 5 minutes H_2O (20 equivalents) is added *via* syringe, the reaction mixture is warm to 50 °C, stirred and monitored by TLC analysis for 24h-48 hours until full conversion. The reaction mixture is evaporated to dryness and then the crude is purified by flash chromatography on silica gel (DCM/MeOH 9:1).

*(S)-1-(1-((S)-isoquinolin-1-yl)naphthalen-2-yl)ethanamine (S_a,S)-**14A.***

Following the general procedure using (S_a,*S*)-**13A** (0.07 mmol, 23.2 mg, 98% ee), purification by flash chromatography (DCM/MeOH 9:1) afforded (S_a,*S*)-**14A** (86%, 17.9 mg) as a brown amorphous solid. $[\alpha]^{20}_D$ +31.6 (*c* 0.2, $CHCl_3$) for 98 % ee. ^{1}H NMR (400 MHz, $CDCl_3$) δ 8.72 (d, *J* = 5.7 Hz, 1H), 8.02 (d, *J* = 8.7 Hz, 1H), 7.94 (d, *J* = 8.3 Hz, 1H), 7.89 (d, *J* = 8.2 Hz, 1H), 7.84 (d,

J = 8.7 Hz, 1H), 7.77 (d, *J* = 5.7 Hz, 1H), 7.67 (t, *J* = 7.5 Hz, 1H), 7.45 - 7.36 (m, 3H), 7.23 (t, *J* = 7.6 Hz, 1H), 6.95 (d, *J* = 8.5 Hz, 1H), 3.71 (q, *J* = 6.5 Hz, 1H), 1.98 (br s, 2H), 1.33 (d, *J* = 6.6 Hz, 3H). ^{13}C NMR (100 MHz, $CDCl_3$) δ 159.7, 142.5, 136.2, 133.2, 132.7, 132.5, 130.5, 129.5, 128.7, 127.9, 127.7, 127.0, 126.9, 126.4, 126.1, 125.6, 123.1, 120.2, 48.4, 29.7, 24.4. HRMS (ESI) calcd. for $C_{21}H_{19}N_2$ (M + H^+) 299.1543. Found 299.1547. HPLC* (IA column, 85:15 *n*-Hex/*i*-PrOH, 30 °C, 1 mL/min): t_R 9.32 min (minor) and 12.82 min (major).

*The enantiomeric excess was determined after benzoylation of the amine (*S*$_a$,*S*)-**14A** with benzoyl chloride (1 equivalent) in DCM (~0.6 M) and trimethylamine (5 equivalents) as base at room temperature. The product was purified by preparative TLC (*n*-Hexane/EtOAc 1:1).

*(S)-1-(1-((S)-isoquinolin-1-yl)naphthalen-2-yl)ethanamine (S$_a$,S)-**14D.***

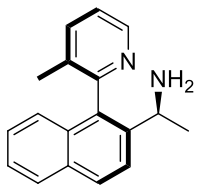

Following the general procedure using (*S*$_a$,*S*)-**13D** (0.12 mmol, 34.6 mg, 99% ee), purification by flash chromatography (DCM/MeOH 9:1) afforded (*S*$_a$,*S*)-**14D** (88%, 30.3 mg) as a brown amorphous solid. $[\alpha]^{20}_D$ -12.8 (*c* 0.5, $CHCl_3$) for >99* % ee. ^{1}H NMR (400 MHz, $CDCl_3$) δ 8.61 (d, *J* = 4.6 Hz, 1H), 7.93 (d, *J* = 8.6 Hz, 1H), 7.85 (d, *J* = 8.1 Hz, 1H), 7.75 (d, *J* = 8.6 Hz, 1H), 7.66 (d, *J* = 7.6 Hz, 1H), 7.41 (t, *J* = 7.4 Hz, 1H), 7.35 – 7.25 (m, 2H), 7.04 (d, *J* = 8.4 Hz, 1H), 3.82 (q, *J* = 6.5 Hz, 1H), 2.00 (s, 3H), 1.84 (s, 2H), 1.32 (d, *J* = 6.5 Hz, 3H). ^{13}C NMR (100 MHz, $CDCl_3$) δ 157.6, 147.2, 142.0, 137.6, 134.3, 132.7, 132.6, 131.6, 128.9, 128.0, 126.3, 125.4, 125.3, 123.0, 122.5, 48.3, 25.0, 18.9. HRMS (ESI) calcd. for $C_{18}H_{19}N_2$ (M + H^+) 263.1543. Found 263.1547. HPLC* (IA column, 85:15 *n*-Hex/*i*-PrOH, 30 °C, 1 mL/min): t_R 7.19 min (minor) and 9.50 min (major).

*The enantiomeric excess was determined after benzoylation of the amine (*S*$_a$,*S*)-**14D** with benzoyl chloride (1 equivalent) in DCM (~0.6 M) and

trimethylamine (5 equivalents) as base at room temperature. The product was purified by preparative TLC (*n*-Hexane/EtOAc 1:1).

General procedure for the hydroarylation of norbornene

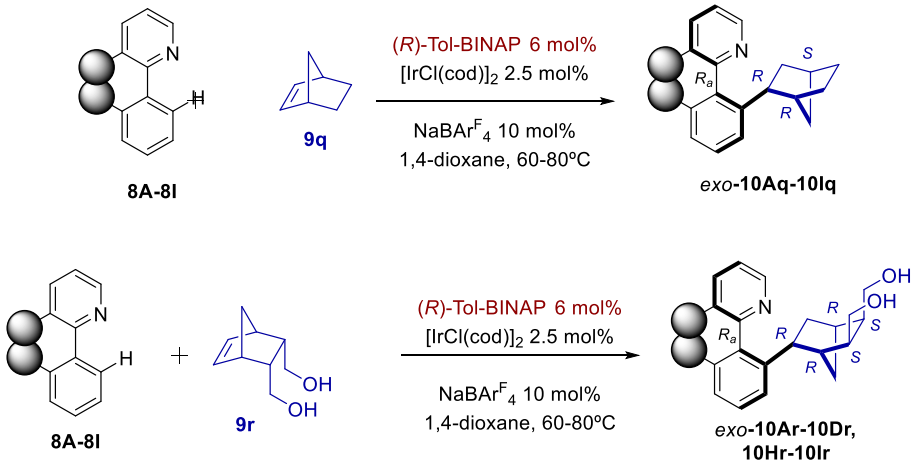

A dried Schlenk tube was charged with [Ir(μ-Cl)(cod)]$_2$ (0.0025 mmol, 1.7 mg) and (*R*)-Tol-BINAP **L12b** (0.006 mmol, 4.1 mg). After three cycles of vacuum-N_2, anhydrous 1,4-dioxane (1 mL) was added and the resulting mixture was stirred at room temperature for 10 minutes. Then, norbornene **9q-9r** (5 equiv.), the corresponding substrate (±)-**8A-8F** and **8H-8i** (0.1 mmol) and $NaBAr^F$ (0.01 mmol, 8.9 mg) were added in this order. The mixture was stirred at 60-80 °C for 24 hours (see Table 4), concentrated to dryness and purified by flash chromatography on silica gel.

Note: For the preparation of the racemic products (HPLC references), the reactions were carried out at 80 °C in 0.1 mmol scale, and using (±)-BINAP (6 mol%)/[Ir(μ-Cl)(cod)]$_2$ *(2.5 mol%) as the catalyst and 5 equiv. of norbornene* ***1q****.*

Yields, solvent used for chromatography purification, and characterization data for the products are as follows:

*(1R)-1-(2-((1R,2R,4S)-bicyclo[2.2.1]heptan-2-yl)-naphthalen-1-yl)isoquinoline (R_a,R,R,S)-**10Aq**.*

Following the general procedure using (±)-**8A** (0.1 mmol, 25.5 mg) and

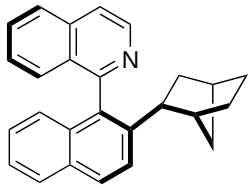

norbornene **2q** (0.5 mmol, 47.1 mg), purification by flash chromatography (toluene → toluene/Et_2O 95:5) afforded (R_a,R,R,S)-**10Aq** (34.8 mg, >99%) as a white foam. $[\alpha]^{20}_D$ −114 (*c* 0.5, $CHCl_3$) for 98 % ee. ^{1}H NMR (400 MHz, $CDCl_3$) δ ^{1}H NMR (400 MHz, Chloroform-*d*) δ 8.73 (dd, *J* = 7.9, 7.5 Hz, 1H), 7.99 – 7.90 (m, 2H), 7.87 (d, *J* = 8.2 Hz, 1H), 7.76 (d, *J* = 5.8 Hz, 1H), 7.71 – 7.63 (m, 2H), 7.45 – 7.34 (m, 3H), 7.20 (dd, *J* = 7.9 Hz, 1H), 6.91 (d, *J* = 8.5 Hz, 1H), 2.30 (dd, *J* = 8.9, 6.3 Hz, 1H), 2.29 – 2.20 (m, 2H), 1.82 – 1.74 (m, 1H), 1.74 – 1.64 (m, 1H), 1.46 – 1.28 (m, 2H), 1.31 – 1.13 (m, 2H), 0.96 – 0.82 (m, 1H), 0.55 – 0.40 (m, 1H). ^{13}C NMR (100 MHz, $CDCl_3$) δ 160.9, 143.5, 142.5, 136.1, 134.4, 132.8, 131.8, 130.2, 128.7, 128.6, 127.7, 127.4, 127.2, 126.9, 126.1, 125.9, 124.9, 124.0, 120.0, 44.5, 42.6, 40.9, 37.2, 36.5, 30.8, 28.1. HRMS (ESI) calcd. for $C_{26}H_{24}N$ ($M + H^+$) 350.1903. Found 350.1899. HPLC (OD column, 99:1 *n*-Hex/*i*-PrOH, 30 °C, 1 mL/min): t_R 16.05 min (minor) and 17.04 min (major).

*Note: The reaction could be carried out at 1 mmol scale following the general procedure using **8A** as the starting material affording* (R_a,R,R,S)-**10Aq** *in >99% (349 mg) and 97.5% ee.*

*((2S,3R,5R)-5-(1-((R)-isoquinolin-1-yl)naphthalen-2-yl)bicyclo[2.2.1]heptane-2,3-diyl)dimethanol (R_a,R,R,R,S,S)-**10Ar**.*

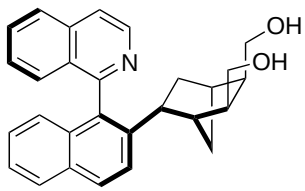

Following the general procedure using **8A** (0.1 mmol, 25.5 mg) and norbornene **9r** (0.5 mmol, 77.1 mg), purification by flash chromatography (EtOAc/MeOH 95:5) afforded (R_a,R,R,R,S,S)-**10Ar** (40.5 mg >99%) as a beige powder. $[\alpha]^{20}_D$ −12.6 (*c* 0.5, $CHCl_3$) for 98 % ee. ^{1}H NMR (400 MHz, $CDCl_3$) δ 8.65 (d, *J* = 5.8 Hz, 1H),

7.99 (d, *J* = 1.8 Hz, 1H), 7.97 (d, *J* = 2.3 Hz, 1H), 7.88 (d, *J* = 8.2 Hz, 1H), 7.82 (d, *J* = 6.0 Hz, 1H), 7.71 (ddd, *J* = 8.2, 6.8, 1.3 Hz, 1H), 7.65 (d, *J* = 8.7 Hz, 1H), 7.43 – 7.36 (m, 2H), 7.34 – 7.29 (m, 1H), 7.21 (ddd, *J* = 8.3, 6.6, 1.3 Hz, 1H), 6.88 (d, *J* = 8.2 Hz, 1H), 3.37 (d, *J* = 7.2 Hz, 2H), 2.71 (t, *J* = 11.0 Hz, 1H), 2.63 (br s, 2H), 2.56 (dd, *J* = 8.6, 6.6 Hz, 1H), 2.33 (s, 1H), 2.08 – 1.94 (m, 3H), 1.94 – 1.86 (m, 1H), 1.80 (tt, *J* = 10.8, 3.8 Hz, 1H), 1.71 – 1.61 (m, 1H), 1.61 – 1.51 (m, 1H), 1.34 (d, *J* = 9.9 Hz, 1H). ^{13}C NMR (100 MHz, $CDCl_3$) δ 160.5, 142.4, 142.1, 136.3, 134.3, 132.5, 131.7, 130.9, 129.0, 128.7, 127.8, 127.7, 127.3, 127.1, 126.4, 125.8, 125.3, 124.4, 120.5, 61.6, 59.3, 47.9, 45.1, 41.4, 40.8, 38.4, 36.6, 33.3. HRMS (ESI) calcd. for $C_{28}H_{28}NO_2$ ($M + H^+$) 410.2115 Found 410.2110. HPLC (AS-H column, 80:20 *n*-Hex/*i*-PrOH, 30 °C, 1 mL/min): t_R 9.75 min (minor) and 14.34 min (major).

*(1R)-1-(2-((1R,2R,4S)-bicyclo[2.2.1]heptan-2-yl)-4-methylnaphthalen-1-yl)isoquinoline (R_a,R,R,S)-**10Bq**.*

Following the general procedure using **8B** (0.1 mmol, 26.9 mg) and

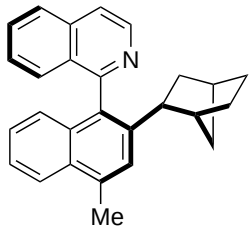

norbornene **1q** (0.5 mmol, 47.1 mg), purification by flash chromatography (toluene → toluene/Et_2O 95:5) afforded (R_a,*R*,*R*,*S*)-**10Bq** (36,3 mg, >99%) as a pale yellow foam. $[\alpha]^{20}_D$ −105 (*c* 0.5, $CHCl_3$) for 95 % ee. ^{1}H NMR (400 MHz, $CDCl_3$) δ 8.72 (d, *J* = 5.7 Hz, 1H), 8.02 (d, *J* = 8.4 Hz, 1H), 7.93 (d, *J* = 8.3 Hz, 1H), 7.75 (d, *J* = 5.8 Hz, 1H), 7.67 (dd, *J* = 8.2, 6.7 Hz, 1H), 7.50 (s, 1H), 7.45 – 7.33 (m, 3H), 7.19 (dd, *J* = 8.5, 6.9 Hz, 1H), 6.92 (d, *J* = 8.5 Hz, 1H), 2.80 (s, 3H), 2.29 – 2.18 (m, 3H), 1.81 (d, *J* = 9.8 Hz, 1H), 1.74 – 1.65 (m, 1H), 1.45 – 1.29 (m, 2H), 1.28 – 1.11 (m, 2H), 0.93 – 0.83 (m, 1H), 0.44 (t, *J* = 10.8 Hz, 1H). ^{13}C NMR (100 MHz, $CDCl_3$) δ 161.2, 143.1, 142.5, 136.1, 134.7, 132.9, 132.7, 130.9, 130.1, 128.8, 127.5, 127.1, 126.8, 126.5, 125.7, 124.8, 124.7, 123.9, 119.8, 44.4, 42.6, 40.8, 37.3, 36.5, 30.9, 28.1, 20.0. HRMS (ESI) calcd. for $C_{27}H_{26}N$ ($M + H^+$) 364.2060. Found 364.2055. HPLC (OD column, 95:5 *n*-Hex/*i*-PrOH, 30 °C, 1 mL/min): t_R 6.99 min (major) and 7.87min (minor).

*((2S,3R,5R)-5-(1-((R)-isoquinolin-1-yl)-4-methylnaphthalen-2-yl)bicyclo[2.2.1]heptane-2,3-diyl)dimethanol (R_a,R,R,R,S,S)-**10Br**.*

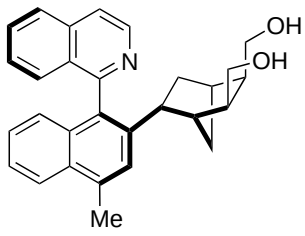

Following the general procedure using **8B** (0.1 mmol, 26.9 mg) and norbornene **9r** (0.5 mmol, 77.1 mg), purification by flash chromatography (EtOAc/MeOH 95:5) afforded *(R_a,R,R,R,S,S)*-**10Br** (32.6 mg, 77%) as a white powder. $[\alpha]^{20}_D$ –20.9 (*c* 0.5, $CHCl_3$) for 89 % ee. ^{1}H NMR (400 MHz, $CDCl_3$) δ 8.66 (d, *J* = 5.7 Hz, 1H), 8.03 (d, *J* = 8.4 Hz, 1H), 7.96 (d, *J* = 8.3 Hz, 1H), 7.80 (d, *J* = 5.7 Hz, 1H), 7.72 – 7.64 (m, 1H), 7.48 – 7.39 (m, 2H), 7.39 – 7.29 (m, 2H), 7.21 (t, *J* = 7.7 Hz, 1H), 6.90 (d, *J* = 8.5 Hz, 1H), 3.36 – 3.24 (m, 2H), 3.22 (br s, 2H), 2.80 (s, 3H), 2.66 (t, *J* = 11.0 Hz, 1H), 2.49 (t, *J* = 7.7 Hz, 1H), 2.26 (s, 1H), 1.98 – 1.85 (m, 4H), 1.79 – 1.69 (m, 1H), 1.66 – 1.57 (m, 1H), 1.56 – 1.46 (m, 1H), 1.37 – 1.21 (m, 1H). ^{13}C NMR (100 MHz, $CDCl_3$) δ 160.8, 142.3, 141.9, 136.3, 135.1, 132.8, 132.7, 130.9, 130.7, 128.9, 127.5, 127.4, 127.1, 126.5, 126.0, 125.2, 125.1, 124.0, 120.3, 61.7, 59.4, 47.8, 45.2, 41.5, 40.8, 38.5, 36.5, 33.3, 20.0. HRMS (ESI) calcd. for $C_{29}H_{30}NO_2$ (M + H^+) 424.2271. Found 424.2264. HPLC (AS-H column, 80:20 *n*-Hex/*i*-PrOH, 30 °C, 1 mL/min): t_R 9.45 min (minor) and 13.94 min (major).

*(1R)-1-(2-((1R,2R,4S)-bicyclo[2.2.1]heptan-2-yl)-4-methoxynaphthalen-1-yl)isoquinoline (R_a,R,R,S)-**10Cq**.*

Following the general procedure using **8C** (0.1 mmol, 28.5 mg) and norbornene **9q** (0.5 mmol, 47.1 mg), purification by flash chromatography (toluene → toluene/Et_2O 95:5) afforded (R_a,R,R,S)-**10Cq** (16.5 mg, 43%) as a beige powder. $[\alpha]^{20}_D$ –147 (*c* 0.5, $CHCl_3$) for 97 % ee. ^{1}H NMR

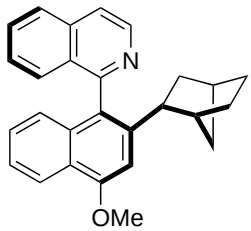

(400 MHz, $CDCl_3$) δ 8.72 (d, *J* = 5.6 Hz, 1H), 8.28 (d, *J* = 8.4 Hz, 1H), 7.92 (d, *J* = 8.3 Hz, 1H), 7.74 (d, *J* = 5.8 Hz, 1H), 7.67 (dd, *J* = 7.5 Hz, 1H), 7.46 (d, *J* = 8.4 Hz, 1H), 7.41 – 7.31 (m, 2H), 7.20 (dd, *J* = 8.6, 6.8 Hz, 1H), 7.00 (s, 1H), 6.86 (d, *J* = 8.5 Hz, 1H), 4.11 (s, 3H), 2.33 – 2.20 (m, 3H), 1.79 (d, *J* = 9.8 Hz, 1H), 1.74 – 1.58 (m, 1H), 1.48 – 1.30 (m, 2H), 1.29 – 1.12 (m, 2H), 0.92 – 0.86 (m, 1H), 0.45 (t, *J* = 10.8 Hz, 1H). ^{13}C NMR (100 MHz, $CDCl_3$) δ 161.1, 155.7, 143.9, 142.4, 136.2, 133.8, 130.2, 129.1, 127.6, 127.2, 126.8, 126.6, 125.6, 124.3, 123.9, 121.6, 119.9, 102.1, 55.5, 44.8, 42.7, 40.9, 37.5, 36.4, 30.9, 28.0. HRMS (ESI) calcd. for $C_{27}H_{26}NO$ (M + H^+) 380.2009. Found 380.2007. HPLC (IA column, 90:10 *n*-Hex/*i*-PrOH, 30 °C, 1 mL/min): t_R 7.95 min (major) and 13.76 min (minor).

*(2S,3R,5R)-5-(1-((R)-isoquinolin-1-yl)-4-methoxynaphthalen-2-yl)bicyclo[2.2.1]heptane-2,3-diyl)dimethanol (R_a,R,R,R,S,S)-**10Cr**.*

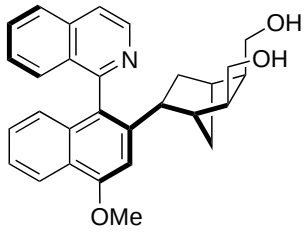

Following the general procedure using **8C** (0.1 mmol, 28.5 mg) and norbornene **9r** (0.5 mmol, 77.1 mg), purification by flash chromatography (EtOAc/MeOH 95:5) afforded *(R_a,R,R,R,S,S)*-**10Cr** (31.5 mg, 72%) as pale greenish powder. $[\alpha]^{20}_D$ –44.1 (*c* 0.5, $CHCl_3$) for 92 % ee. ^1H NMR (400 MHz, $CDCl_3$) δ 8.57 (d, *J* = 5.9 Hz, 1H), 8.29 (d, *J* = 8.4 Hz, 1H), 7.96 (d, *J* = 8.2 Hz, 1H), 7.80 (d, *J* = 5.8 Hz, 1H), 7.69 (t, *J* = 7.4 Hz, 1H), 7.42 – 7.30 (m, 3H), 7.20 (t, *J* = 7.6 Hz, 1H), 6.94 (s, 1H), 6.80 (d, *J* = 8.6 Hz, 1H), 4.10 (s, 3H), 3.36 – 3.24 (m, 2H), 3.14 (br s, 2H), 2.64 (t, *J* = 11.0 Hz, 1H), 2.53 (t, *J* = 7.8 Hz, 1H), 2.28 (s, 1H), 2.03 – 1.88 (m, 3H), 1.85 (d, *J* = 9.9 Hz, 1H), 1.80 – 1.66 (m, 1H), 1.66 – 1.49 (m, 2H), 1.36 – 1.30 (m, 1H). ^{13}C NMR (100 MHz, $CDCl_3$) δ 160.8, 155.9, 142.7, 142.3, 136.4, 133.6, 130.7, 129.1, 127.6, 127.5, 127.1, 127.0, 126.9, 125.6, 124.6, 124.0, 121.8, 120.2, 102.5, 61.9, 59.5, 55.6, 47.8, 45.3, 41.5, 40.8, 38.8, 36.9, 33.6. HRMS (ESI) calcd. for $C_{29}H_{30}NO_3$ (M + H^+) 440.2220. Found 440.2215. HPLC (AS-H column, 80:20 *n*-Hex/*i*-PrOH, 30 °C, 1 mL/min): t_R 9.62 min (minor) and 13.07 min (major).

*(2R)-2-(2-((1R,2R,4S)-bicyclo[2.2.1]heptan-2-yl)naphthalen-1-yl)-3-methylpyridine (R_a,R,R,S)-**10Dq**.*

Following the general procedure using **8D** (0.1 mmol, 21.9 mg) and

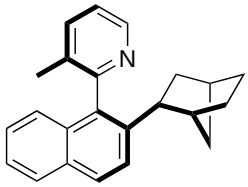

norbornene **9d** (0.5 mmol, 47.1 mg), purification by flash chromatography (toluene → toluene/Et_2O 95:5) afforded (R_a,R,R,S)-**10Dq** (30.1 mg, 96%) as a white foam. $[\alpha]^{20}_D$ –54.3 (*c* 0.5, $CHCl_3$) for 99 % ee. ^{1}H NMR (400 MHz, $CDCl_3$) δ 8.62 (d, *J* = 4.8 Hz, 1H), 7.86 (d, *J* = 8.7 Hz, 1H), 7.83 (d, *J* = 8.2 Hz, 1H), 7.67 (d, *J* = 7.7 Hz, 1H), 7.61 (d, *J* = 8.6 Hz, 1H), 7.38 (t, *J* = 7.5 Hz, 1H), 7.33 – 7.24 (m, 2H), 7.00 (d, *J* = 8.4 Hz, 1H), 2.40 (dd, *J* = 8.9, 6.6 Hz, 1H), 2.33 – 2.26 (m, 2H), 1.98 (s, 3H), 1.81 (d, *J* = 9.8 Hz, 1H), 1.70 – 1.57 (m, 1H), 1.55 – 1.36 (m, 3H), 1.31 – 1.20 (m, 1H), 1.13 – 1.03 (m, 1H), 1.03 – 0.93 (m, 1H). ^{13}C NMR (100 MHz, $CDCl_3$) δ ^{13}C NMR (101 MHz, $CDCl_3$) δ 158.6, 147.1, 142.4, 137.5, 135.6, 132.9, 131.9, 128.2, 127.8, 126.1, 125.2, 124.8, 124.1, 122.3, 44.2, 42.5, 41.0, 37.4, 36.4, 31.3, 28.2, 18.7. HRMS (ESI) calcd. for $C_{23}H_{24}N$ (M + H^+) 314.1903. Found 314.1904. HPLC (OD column, 99:1 *n*-Hex/*i*-PrOH, 30 °C, 1 mL/min): t_R 11.99 min (minor) and 14.18 min (major).

*((2S,3R,5R)-5-(1-((R)-3-methylpyridin-2-yl)naphthalen-2-yl)bicyclo[2.2.1]heptane-2,3-diyl)dimethanol (R_a,R,R,R,S,S)-**10Dr***

Following the general procedure using **8D** (0.1 mmol, 21.9 mg) and

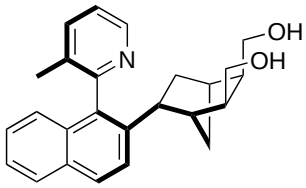

norbornene **9r** (0.5 mmol, 77.1 mg), purification by flash chromatography (EtOAc/MeOH 95:5) afforded *(R_a,R,R,R,S,S)*-**10Dr** (30 mg, 80%) as a white powder. $[\alpha]^{20}_D$ +32.9 (*c* 0.5, $CHCl_3$) for 93 % ee. ^{1}H NMR (400 MHz, $CDCl_3$) δ 8.44 (s, 1H), 7.89 (d, *J* = 8.8 Hz, 1H), 7.84 (d, *J* = 8.1 Hz, 1H), 7.70 (d, *J* = 7.7 Hz, 1H), 7.57 (d, *J* = 8.8 Hz, 1H), 7.44 – 7.36 (m, 1H), 7.35 – 7.25 (m, 2H), 6.96 (d, *J* = 8.6 Hz, 1H), 3.51 (t, *J* = 10.5 Hz, 1H), 3.43 (dd, *J* = 11.2, 3.8 Hz, 1H), 3.32 (t, *J* = 10.7 Hz, 1H), 2.94 (dd, *J* = 11.4, 3.6 Hz, 1H),

2.67 (t, *J* = 7.7 Hz, 1H), 2.37 (br s, 2H), 2.33 (s, 1H), 2.13 (s, 1H), 2.11 – 1.97 (m, 2H), 1.91 (s, 3H), 1.90 – 1.85 (m, 1H), 1.58 (d, *J* = 7.7 Hz, 2H), 1.41 (d, *J* = 10.1 Hz, 1H). ^{13}C NMR (100 MHz, $CDCl_3$) δ 158., 146.8, 141.2, 138.5, 135.3, 133.6, 131.9, 131.5, 128.7, 128.0, 126.6, 125.4, 124.8, 124.4, 122.9, 61.9, 60.2, 47.4, 45.3, 41.7, 40.8, 38.6, 36.3, 33.5, 18.8. HRMS (ESI) calcd. for $C_{25}H_{28}NO_2$ (M + H^+) 374.2115. Found 374.2108. HPLC (IA column, 90:10 *n*-Hex/*i*-PrOH, 30 °C, 1 mL/min): t_R 23.42 min (minor) and 26.16 min (major).

*(2R)-2-(2-((1R,2R,4S)-bicyclo[2.2.1]heptan-2-yl)-4-methylnaphthalen-1-yl)-3-methylpyridine (R$_a$,R,R,S)-**10lq**.*

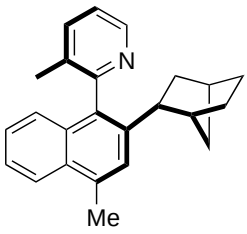

Following the general procedure using **8l** (0.1 mmol, 23.3 mg) and norbornene **9q** (0.5 mmol, 47.1 mg), purification by flash chromatography (toluene → toluene/Et_2O 95:5) afforded (*R$_a$,R,R,S*)-**10lq** (29.1 mg, 89%) as a white foam. $[\alpha]^{20}_D$ –43.5 (*c* 0.5, $CHCl_3$) for 97 % ee. ^{1}H NMR (400 MHz, $CDCl_3$) δ 8.62 (d, *J* = 4.7 Hz, 1H), 7.99 (d, *J* = 8.4 Hz, 1H), 7.65 (d, *J* = 7.7 Hz, 1H), 7.47 – 7.39 (m, 2H), 7.33 – 7.25 (m, 2H), 7.02 (d, *J* = 8.4 Hz, 1H), 2.75 (s, 3H), 2.37 (dd, *J* = 8.9, 7.5 Hz, 1H), 2.33 – 2.24 (m, 2H), 1.98 (s, 3H), 1.84 (d, *J* = 9.8 Hz, 1H), 1.65 (ddt, *J* = 12.4, 6.3, 3.1 Hz, 1H), 1.51 – 1.38 (m, 3H), 1.32 – 1.24 (m, 1H), 1.14 – 1.01 (m, 1H), 0.97 – 0.88 (m, 1H). ^{13}C NMR (100 MHz, $CDCl_3$) δ ^{13}C NMR (101 MHz, $CDCl_3$) δ 158.9, 147.1, 142.0, 137.5, 134.3, 134.0, 133.2, 132.0, 131.1, 125.8(2C), 124.9, 124.7, 124.1, 122.3, 44.2, 42.6, 41.0, 37.5, 36.5, 31.4, 28.3, 20.0, 18.9. HRMS (ESI) calcd. for $C_{24}H_{26}NO$ (M + H^+) 328.2060. Found328.2057. HPLC (IA column, 95:5 *n*-Hex/*i*-PrOH, 30 °C, 1 mL/min): t_R 7.21 min (major) and 9.09 min (minor).

*((2S,3R,5R)-5-(4-methyl-1-((R)-3-methylpyridin-2-yl)naphthalen-2-yl)bicyclo[2.2.1]heptane-2,3-diyl)dimethanol (R_a,R,R,S)-**10Ir**.*

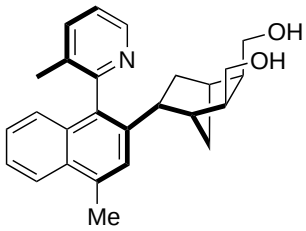

Following the general procedure using **8I** (0.1 mmol, 23.3 mg) and norbornene **9r** (0.5 mmol, 77.1 mg), purification by flash chromatography (EtOAc/MeOH 95:5) afforded *(R_a,R,R,R,S,S)-**10Ir*** (33.5 mg, 86%) as a white foam. $[\alpha]^{20}_D$ +25.7 (*c* 0.5, $CHCl_3$) for 92 % ee. ^{1}H NMR (400 MHz, $CDCl_3$) δ 8.62 (d, *J* = 4.4 Hz, 1H), 7.99 (d, *J* = 8.4 Hz, 1H), 7.69 (d, *J* = 7.7 Hz, 1H), 7.43 (ddd, *J* = 8.2, 6.7, 1.3 Hz, 1H), 7.39 (s, 1H), 7.37 – 7.26 (m, 2H), 7.03 (d, *J* = 8.4 Hz, 1H), 3.54 (t, *J* = 10.3 Hz, 1H), 3.48 (dd, *J* = 10.7, 3.6 Hz, 1H), 3.37 (t, *J* = 10.6 Hz, 1H), 3.05 (br s, 2H), 2.98 (dd, *J* = 11.3, 3.3 Hz, 1H), 2.74 (s, 3H), 2.66 (t, *J* = 7.7 Hz, 1H), 2.34 (s, 1H), 2.17 – 2.13 (m, 1H), 2.15 – 2.01 (m, 2H), 1.93 (s, 3H), 1.93 – 1.88 (m, 1H), 1.64 – 1.57 (m, 2H), 1.42 (d, *J* = 9.9 Hz, 1H). ^{13}C NMR (100 MHz, $CDCl_3$) δ 158.5, 147.23 140.7, 137.9, 134.6, 134.2, 133.3, 131.0, 131.1, 126.1, 125.6, 125.2, 125.0, 124.2, 122.6, 62.12, 60.31, 47.5, 45.5, 41.8, 40.9, 38.7, 36.3, 33.5, 20.0, 18.91. HRMS (ESI) calcd. for $C_{26}H_{30}NO_2$ ($M + H^+$) 388.2271. Found 388.2262. HPLC (IC column, 80:20 *n*-Hex/*i*-PrOH, 30 °C, 1 mL/min): t_R 16.10 min (minor) and 19.06 min (major).

*(2R)-2-(2-((1R,2R,4S)-bicyclo[2.2.1]heptan-2-yl)-4-methoxynaphthalen-1-yl)-3-methylpyridine (R_a,R,R,S)-**10Hq**.*

Following the general procedure using **9H** (0.1 mmol, 24.9 mg) and norbornene **9q** (0.5 mmol, 47.1 mg), purification by flash chromatography (toluene → toluene/Et_2O 95:5) afforded (R_a,R,R,S)-**10Hq** (34.3 mg, >99%) as a white powder. Single crystals suitable for X-ray analysis were obtained by slow evaporation of a solution of (R_a,R,R,S)-**10Hq** in *n*-heptane. $[\alpha]^{20}_D$ –64,4 (*c* 0.5, $CHCl_3$) for >99 % ee. ^{1}H NMR (400 MHz, $CDCl_3$) δ 8.61 (d, *J* = 4.8 Hz, 1H), 8.24 (d, *J* = 8.3 Hz, 1H), 7.65 (d, *J* = 7.6 Hz, 1H), 7.37 (dd, *J* = 8.4, 6.7 Hz, 1H), 7.33 – 7.23 (m, 2H), 6.99 – 6.92 (m, 2H), 4.06 (s, 3H), 2.41 (dd, *J* =

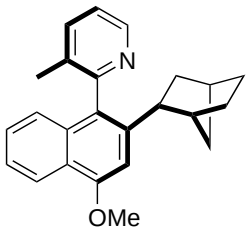

7.8 Hz, 1H), 2.34 – 2.27 (m, 2H), 1.98 (s, 3H), 1.81 (dd, *J* = 9.6, 2.3 Hz, 1H), 1.70 – 1.62 (m, 1H), 1.54 – 1.38 (m, 3H), 1.34 – 1.27 (m, 1H), 1.10 – 1.00 (m, 1H), 0.99 – 0.89 (m, 1H). ^{13}C NMR (100 MHz, $CDCl_3$) δ ^{13}C NMR (101 MHz, $CDCl_3$) δ 158.8, 155.3, 147.1, 142.7, 137.4, 133.4, 132.8, 128.2, 126.6, 124.9, 124.2, 124.0, 122.1, 121.8, 102.1, 102.1, 55.4, 44.5, 42.6, 41.0, 37.6, 36.4, 31.3, 28.1, 18.8. HRMS (ESI) calcd. for $C_{24}H_{26}NO$ (M + H^+) 344.2009. Found 344.2006. HPLC (IA column, 95:5 *n*-Hex/*i*-PrOH, 30 °C, 1 mL/min): t_R 8.62 min (major) and 11.09 min (minor).

((2S,3R,5R)-5-(4-methoxy-1-((R)-3-methylpyridin-2-yl)naphthalen-2-yl)bicyclo[2.2.1]heptane-2,3-diyl)dimethanol (R_α*,R,R,R,S,S)-**10Hr**.*

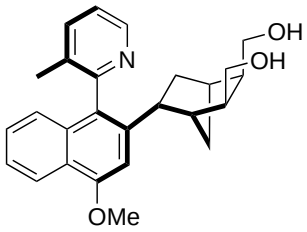

Following the general procedure using **8H** (0.1 mmol, 24.9 mg) and norbornene **9r** (0.5 mmol, 77.1 mg), purification by flash chromatography (EtOAc/MeOH 95:5) afforded *(R_α,R,R,R,S,S)*-**10Hr** (33.5 mg, 83%) as a white powder. $[\alpha]^{20}_D$ +19.2 (*c* 0.5, $CHCl_3$) for 98 % ee. ^{1}H NMR (400 MHz, $CDCl_3$) δ 8.50 (d, *J* = 4.7 Hz, 1H), 8.25 (d, *J* = 8.3 Hz, 1H), 7.71 – 7.64 (m, 1H), 7.39 (ddd, *J* = 8.2, 6.7, 1.3 Hz, 1H), 7.35 – 7.25 (m, 2H), 6.93 (d, *J* = 8.4 Hz, 1H), 6.86 (s, 1H), 4.05 (s, 3H), 3.45 (t, *J* = 10.3 Hz, 1H), 3.40 (br s, 2H), 3.37 (dd, *J* = 10.9, 3.5 Hz, 1H), 3.28 (t, *J* = 10.6 Hz, 1H), 2.90 (dd, *J* = 11.2, 3.3 Hz, 1H), 2.63 (t, *J* = 7.7 Hz, 1H), 2.28 (s, 1H), 2.09 (s, 1H), 2.06 – 1.92 (m, 2H), 1.91 (s, 3H), 1.85 (d, *J* = 9.9 Hz, 1H), 1.56 (d, *J* = 7.7 Hz, 2H), 1.39 (d, *J* = 10.0 Hz, 1H). ^{13}C NMR (100 MHz, CDCl3) δ 158.11, 155.54, 146.72, 141.70, 138.41, 133.96, 132.48, 127.91, 127.01, 124.59, 124.56, 123.98, 122.73, 121.98, 102.33, 61.60, 59.86, 55.45, 47.39, 45.36, 41.45, 40.69, 38.88, 36.56, 33.74, 18.84. HRMS (ESI) calcd. for $C_{26}H_{30}NO_3$ (M + H^+) 404.2220. Found 404.2214. HPLC (IA column, 80:20 *n*-Hex/*i*-PrOH, 30 °C, 1 mL/min): t_R 8.57 min (major) and 11.05 min (minor).

*(1S)-1-(2-((1R,2R,4S)-bicyclo[2.2.1]heptan-2-yl)-6-methylphenyl)isoquinoline (R_a,R,R,S)-**10Eq**.*

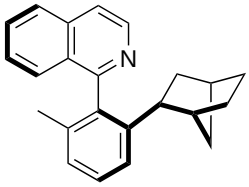

Following the general procedure using **8E** (0.1 mmol, 21.9 mg) and norbornene **9q** (0.5 mmol, 47.1 mg), purification by flash chromatography (toluene → toluene/Et_2O 95:5) afforded (R_a,R,R,S)-**10Eq** (27.4 mg, 88%) as a light brown viscous oil. $[\alpha]^{20}_D$ –89.8 (*c* 0.5, $CHCl_3$) for 94 % ee. ^{1}H NMR (400 MHz, $CDCl_3$) δ 8.64 (d, *J* = 5.8 Hz, 1H), 7.88 (d, *J* = 8.3 Hz, 1H), 7.70 – 7.65 (m, 1H), 7.67 (dd, *J* = 6.5, 1.0 Hz, 1H), 7.52 (dq, *J* = 8.4, 1.0 Hz, 1H), 7.46 (ddd, *J* = 8.3, 6.7, 1.2 Hz, 1H), 7.37 – 7.29 (m, 1H), 7.29 (dd, *J* = 8.0, 1.7 Hz, 1H), 7.14 (dd, *J* = 7.2, 1.1 Hz, 1H), 2.20 – 2.15 (m, 1H), 2.14 – 2.05 (m, 2H), 1.85 (s, 3H), 1.65 (dp, *J* = 9.7, 2.0 Hz, 1H), 1.61 – 1.53 (m, 1H), 1.36 – 1.06 (m, 4H), 0.82 (dddd, *J* = 11.5, 9.0, 4.9, 2.0 Hz, 1H), 0.40 (d, *J* = 1.0 Hz, 1H). ^{13}C NMR (100 MHz, $CDCl_3$) δ 161.7, 146.0, 142.4, 138.1, 136.3, 136.1, 130.1, 128.2, 127.8, 127.2 (2C), 126.9 (2C), 123.0, 119.6, 44.3, 42.4, 40.7, 36.7, 36.6, 30.4, 28.2, 20.0. HRMS (ESI) calcd. for $C_{30}H_{24}NO$ ($M + H^+$) 398.1903. Found 398.1896. HPLC (IG column, 99:1 *n*-Hex/*i*-PrOH, 30 °C, 1 mL/min): t_R 12.63 min (minor) and 14.37 min (major).

(4R)-4-(2-((1R,2R,4S)-bicyclo[2.2.1]heptan-2-yl)naphthalen-1-yl)quinazoline (R_a,R,R,R,S,S)-10Fq

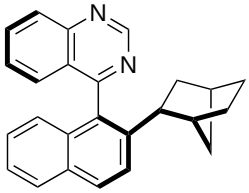

Following the general procedure using **8F** (0.1 mmol, 25.6 mg) and norbornene **9q** (0.5 mmol, 47.1 mg), purification by two sequential flash chromatographies (toluene → toluene/Et_2O 95:5 and DCM → EtOAc) afforded (R_a,R,R,S)-**10Fq** (27.2 mg, 77%) as a white foam. $[\alpha]^{20}_D$ –88,6 (*c* 0.5, $CHCl_3$) for 91 % ee. ^{1}H NMR (400 MHz, $CDCl_3$) δ ^{1}H NMR (400 MHz, Chloroform-*d*) δ 9.53 (s, 1H), 8.19 (d, *J* = 8.5 Hz, 1H), 7.99 (d, *J* = 8.7 Hz, 1H), 7.96 – 7.85 (m, 2H), 7.69 (d, *J* = 8.7 Hz, 1H), 7.50 – 7.36 (m, 3H), 7.26 – 7.14 (m, 1H), 6.90 (d, *J* = 8.5 Hz, 1H), 2.31 – 2.21 (m, 3H), 1.80 (d, *J* = 9.9 Hz, 1H), 1.69 (ddt, *J* = 13.1, 6.8, 3.5 Hz, 1H), 1.46 (ddd, *J* = 12.4, 9.2, 2.5 Hz, 1H), 1.44 – 1.31 (m, 1H), 1.28

– 1.17 (m, 2H), 0.98 – 0.81 (m, 1H), 0.55 – 0.44 (m, 1H). ^{13}C NMR (100 MHz, $CDCl_3$) δ 170.2, 155.1, 150.3, 143.3, 134.1, 131.9, 131.8, 131.6, 129.4, 128.8, 127.9, 127.9, 126.9, 126.5, 125.5, 125.3, 125.3, 123.9, 44.6, 42.7, 41.1, 37.4, 36.5, 30.8, 28.0. HRMS (ESI) calcd. for $C_{25}H_{23}N_2$ (M + H^+) 351.1856. Found 351.1851. HPLC (IA column, 98:2 *n*-Hex/*i*-PrOH, 30 °C, 1 mL/min): t_R 16.44 min (minor) and 18.25 min (major).